

Mono-ubiquitination mediated regulation of KMT5A and its role in prostate cancer



Mahsa Azizyan

Thesis submitted for the degree of Doctor of Philosophy

Solid Tumour Target Discovery Group

Northern Institute for Cancer Research

Faculty of Medical Sciences

Newcastle University

September 2016

Abstract

Abstract: Prostate cancer (PC) is the most common cancer and the second cause of cancer related death in men. Central to this, is the role of the androgen receptor (AR) which acts as a transcription factor, regulating the expression of genes required for normal prostate growth and cancer development. Consequently, the AR remains the primary target for therapeutic intervention. However, these treatments become ineffective, resulting in castrate resistant prostate cancer (CRPC) which generally retains AR expression. The AR interacts with several co-regulatory proteins which can perturb AR-targeted therapies in CRPC. Targeting these co-regulatory proteins to indirectly target the AR signalling cascade may prove beneficial. Recently, our group identified KMT5A as a potential regulator of AR through selective siRNA library screening.

KMT5A is a lysine methyltransferase that mono-methylates histone 4 lysine 20 and non-histone proteins, including p53. Using a relevant *in vitro* CRPC model it was shown that KMT5A acquires AR co-activator activity which is in contrast to androgen sensitive models where KMT5A co-represses AR activity. This highlights the importance of studying KMT5A regulation. KMT5A protein levels are tightly regulated by multiple E3 ligases for cell cycle-dependent poly-ubiquitination-mediated degradation. KMT5A poly-ubiquitination by E3 ligases SCF ^{β -TRCF}, CRL4^{Cdt2} and APC^{Cdh1} promotes degradation in G1, S and late mitosis cell cycle phases, respectively. Moreover, the Skp2 E3 ligase has been suggested to play a role in KMT5A ubiquitination and degradation but direct supporting evidence is currently absent. Additionally, Skp2 is suggested to directly regulate the AR signaling pathway. It is also unknown whether KMT5A could be modified directly by ubiquitination without promoting its degradation. As such, we aimed to investigate KMT5A mono-ubiquitination and the role of Skp2 in regulating KMT5A as well as independently regulating the AR signaling cascade.

Mono-ubiquitinated KMT5A was demonstrated in a panel of PC cell lines. Its existence was further confirmed by performing ubiquitination assays in COS7 cells. Furthermore, the KMT5A C-terminal SET domain was identified as the target for mono-ubiquitination. Moreover, mono-ubiquitinated KMT5A was highly enriched in S phase cells, coincident with extremely low levels of unmodified KMT5A. Mono-ubiquitinated KMT5A was exclusively cytoplasmic and its abundance was greatly enhanced by Skp2, but not associated with protein turnover. Together, this data suggests that cell cycle-dependent KMT5A mono-ubiquitination is an important mechanism to diminish nuclear, unmodified KMT5A levels to facilitate cell cycle progression. Thus, insight for the physiological significance of mono-ubiquitinated KMT5A

may provide a novel therapeutic target to indirectly target the AR. Finally, Skp2 was not found to have a direct effect on AR signaling.

Acknowledgements

Firstly, I would like to sincerely thank my PhD supervisors, Prof Craig Robson and Dr Kelly Coffey for their continuous support and guidance. I am truly grateful for their infinite help and encouragement. I would also like to thank Dr Andrew Filby (Newcastle University flow cytometry core facility unit) for his FACS expertise.

Many thanks to all members of the Solid Tumour Target Discovery group at the NICR both past and present. In particular, I would like express my gratitude to Zainab, Scott and Laura.

This journey would not have been possible without the support of my family. I would like to especially thank my beloved parents who have always stood by me and supported me in every single step of my life. I cannot thank them enough for their endless love, support, encouragement and all the sacrifice they have made. I am truly grateful to my one and only loving brother, Mohammad, who has been my rock. I am so blessed to have such an amazing, kind and caring brother. Finally, no words can convey the love and appreciation I have for the very special person of my life, my beloved husband, Arman. His unconditional love, support, patience and understanding has made it possible for me to complete my PhD degree, whilst we were living in two different countries. I am also blessed to have the kindest father and mother in law and am sincerely grateful for their love and support.

List of presentations

- The role of KMT5A in prostate cancer. Azizyan, M. Coffey, K and Robson, C.N. This poster was presented at the American Association for Cancer Research (AACR) Annual Meeting, New Orleans, USA (2016).
- Mono-ubiquitination mediated regulation of KMT5A and its role in prostate cancer. Azizyan, M. Coffey, K and Robson, C.N. This short thesis talk was presented at the postgraduate cancer research conference, Newcastle University, Newcastle upon Tyne (2016).
- The Skp2-androgen receptor axis in prostate cancer. Azizyan, M. Stevens, S.A. Tan, W.F. Coffey, K and Robson, C.N. This poster was presented at the Androgens conference in London (2014).
- Skp2-mediated stabilisation of KMT5A during AR signalling in castrate resistant prostate cancer. Azizyan, M. Coffey, K and Robson, C.N. This poster was presented at the postgraduate research day, Newcastle University, Newcastle upon Tyne (2014).
- SET8 functions as a co-activator in models of castrate resistant prostate cancer. AlKharaf, D. Azizyan, M. Coffey, K and Robson, C.N. This poster was presented at the Genes and Cancer Meeting, University of Warwick, Coventry (2012).

List of awards

- 2016 The British Association for Cancer Research (BACR) Travel Grant for PhD Students (£900) for attending the AACR 2016.
- 2016 The Faculty of Medical Sciences, Newcastle University Travel Grant for PhD Students (£800) for attending the AACR 2016.
- 2014 Prostate Cancer UK award for submitted abstract “The Skp2-androgen axis in prostate cancer” at the Androgens 2014, London.

Table of Contents

1	Introduction	1
1.1	The structure and function of the prostate	1
1.2	Prostate abnormalities	3
1.2.1	Benign prostatic hyperplasia (BPH).....	3
1.2.2	Prostatic intraepithelial neoplasia (PIN).....	3
1.2.3	Prostate cancer.....	4
1.3	The androgen receptor	8
1.3.1	Androgen receptor structure	8
1.3.2	AR function and mechanism of action	11
1.3.3	Deregulation of AR activity and the mechanism of CRPC development	13
1.4	Ubiquitination.....	17
1.4.1	Process of ubiquitination	17
1.4.2	Ubiquitin function	21
1.5	KMT5A	27
1.5.1	Structure of KMT5A	27
1.5.2	Isoforms of KMT5A.....	28
1.5.3	Function.....	30
1.6	Regulation of KMT5A	38
1.6.1	Transcriptional regulation of KMT5A	39
1.6.2	Post-translational modifications (PTM) of KMT5A	39
1.7	KMT5A and the AR	44
1.8	Hypothesis	46
1.8.1	Aims	46
2	Materials and methods.....	47
2.1	Reagents and antibodies	47
2.2	Mammalian cell culture	48
2.2.1	Reagents	48
2.2.2	Cell lines.....	48

2.2.3	Cell passaging	48
2.2.4	Cell storage and recovery.....	49
2.2.5	Mycoplasma test	49
2.3	Transient DNA transfection	50
2.4	Transient siRNA reverse transfection	52
2.5	Bacterial transformation.....	53
2.6	Protein expression analysis	53
2.6.1	Sodium dodecyl sulphate-polyacrylamide gel electrophoresis (SDS- PAGE)	53
2.6.2	Western blotting.....	54
2.7	Gene expression analysis	55
2.7.1	RNA extraction	55
2.7.2	RNA reverse transcription	55
2.7.3	Quantitative real time PCR	56
2.7.4	Quantitative PCR primers	57
2.8	Luciferase reporter assay	57
2.8.1	Luciferase activity measurement	57
2.8.2	β -galactosidase normalisation assay	58
2.9	Immunoprecipitation (IP).....	58
2.9.1	Native immunoprecipitation	58
2.9.2	Denaturing nickel pull down.....	58
2.10	Cytoplasmic/nuclear extraction.....	59
2.11	Flow cytometry cell cycle analysis	60
2.11.1	Hoechst cell staining and sorting	60
2.11.2	Propidium Iodide (PI) cell staining.....	60
3	Evidence that KMT5A is a mono-ubiquitinated protein and identification of the sites of mono-ubiquitination.....	62
3.1	Introduction.....	62
3.2	Hypothesis.....	63
3.2.1	Aims.....	63

3.3	Specific materials and methods	64
3.3.1	Site-directed mutagenesis	64
3.4	Results	67
3.4.1	Identification of mono-ubiquitinated KMT5A in prostate cancer cell lines	67
3.4.2	Exogenously generated KMT5A exists as both unmodified and mono-ubiquitinated species	68
3.4.3	In vivo ubiquitination assay in COS7 cells confirms KMT5A is mono-ubiquitinated.....	69
3.4.4	Inhibiting KMT5A expression using siRNA does not affect mono-ubiquitinated KMT5A levels.....	71
3.4.5	Mapping of the KMT5A domain for mono-ubiquitination	73
3.4.6	C-terminus of KMT5A is a lysine rich domain.....	75
3.4.7	KMT5A mono-ubiquitination is not specific to a single lysine residue.....	77
3.4.8	Generation and validation of truncated KMT5A C-terminus fragments.....	80
3.4.9	KMT5A C-terminus truncated fragments C3-6 are targeted for mono-ubiquitination.....	82
3.4.10	C-terminus of KMT5A requires amino acids 310-330 for mono-ubiquitination 84	
3.4.11	The single additional lysine, K321, in fragment C3 is not responsible for KMT5A mono-ubiquitination	86
3.4.12	The role of N-terminus KMT5A in KMT5A mono-ubiquitination.....	88
3.4.13	Amino acids 310-330 are required for KMT5A mono-ubiquitination independently of the KMT5A N-terminal domain	91
3.5	Discussion.....	93
4	Investigating the role of mono-ubiquitinated KMT5A and its regulation by Skp2	99
4.1	Introduction	99
4.2	Hypothesis	100
4.2.1	Aims	100
4.3	Results	101
4.3.1	Investigating the cell cycle control of mono-ubiquitinated KMT5A	101

4.3.2	The expression of mono-ubiquitinated KMT5A is cell cycle dependent	103
4.3.3	Mono-ubiquitinated KMT5A expression is associated with cellular confluency 105	
4.3.4	Mono-ubiquitinated KMT5A is cytoplasmic	107
4.3.5	Investigating the role of KMT5A mono-ubiquitination on the cell cycle.....	109
4.3.6	Alteration in KMT5A mono-ubiquitination affects cell proliferation	111
4.3.7	Skp2 is associated with KMT5A mono-ubiquitination.....	113
4.3.8	KMT5A and Skp2 proteins interact	115
4.3.9	Skp2 enhances KMT5A mono-ubiquitination	117
4.3.10	Skp2 does not mediate the mono-ubiquitination of KMT5A C-terminus	119
4.3.11	Investigating the role of the SCF complex in Skp2-mediated mono-ubiquitination of full length KMT5A.....	122
4.3.12	Investigating the role of the SCF complex in Skp2-mediated KMT5A C-terminus mono-ubiquitination.....	125
4.4	Discussion	129
	Cell cycle regulation of KMT5A mono-ubiquitination	129
	Skp2-mediated mono-ubiquitination of KMT5A	133
	Role of Skp2-mediated KMT5A mono-ubiquitination as a coordinator of cell cycle progression	137
5	Investigating the role of Skp2 in androgen receptor signalling in prostate cancer	140
5.1	Introduction.....	140
5.2	Hypothesis.....	141
5.2.1	Aims	141
5.3	Results.....	142
5.3.1	Differential androgenic response of Skp2 protein in LNCaP and LNCaP-AI cell lines	142
5.3.2	Differential effect on Skp2 protein levels in response to increasing androgen concentration in LNCaP and LNCaP-AI cell lines	144
5.3.3	Skp2 response to DHT stimulation is similar in LNCaP and LNCaP-AI cell lines at the transcription level	146

5.3.4	Validation of Skp2 protein depletion using siRNA oligonucleotides	148
5.3.5	Skp2 protein depletion reduces growth of PC cell lines.....	149
5.3.6	Skp2 knockdown causes G1 cell cycle arrest in PC cell lines.....	151
5.3.7	Determining the role of Skp2 in AR-mediated protein expression	152
5.3.8	Assessing the effect of Skp2 depletion on AR-regulated gene expression	154
5.3.9	Skp2 depletion does not affect protein AR levels	156
5.3.10	Skp2 protein forms a complex with the AR	158
5.3.11	Skp2 does not affect AR localisation	159
5.3.12	Skp2 does not influence AR phosphorylation at serine 81	161
5.3.13	Skp2 over-expression does not affect AR transcriptional activity	163
5.4	Discussion.....	165
6	Discussion.....	170
7	References	175

List of figures

Figure 1-1: Diagram representing the anatomy of the human prostate.....	2
Figure 1-2: Schematic diagram of the AR protein.....	10
Figure 1-3: Summary of the AR signalling pathway.	12
Figure 1-4: Process of ubiquitination.....	18
Figure 1-5: Examples of ubiquitin chain linkages.	22
Figure 1-6: Structure of KMT5A isoforms.	29
Figure 1-7: Summary of previous KMT5A findings in regulating the AR in LNCaP and LNCaP-AI cells.....	37
Figure 1-8: Summary of PTMs regulating KMT5A protein levels throughout the cell cycle.	43
Figure 3-1: Identification of a putative mono-ubiquitinated KMT5A form using different anti-KMT5A antibodies.	67
Figure 3-2: Validation of mono-ubiquitinated KMT5A expression using an overexpression system.....	68
Figure 3-3: KMT5A is mono-ubiquitinated <i>in vivo</i>	70
Figure 3-4: KMT5A depletion does not affect mono-ubiquitinated KMT5A level..	72
Figure 3-5: C-terminal domain of KMT5A is targeted for mono-ubiquitination.	74
Figure 3-6: KMT5A C-terminus sequence.	76
Figure 3-7: KMT5A mono-ubiquitination is not abolished by mutating a single lysine residue.	79
Figure 3-8: Truncated deletion mutants of KMT5A C-terminus show a different profile of modified KMT5A levels.	81
Figure 3-9: KMT5A C-terminus fragments C3-C6 undergo mono-ubiquitination.	83
Figure 3-10: Amino acids 310-330 in KMT5A C-terminus are required for KMT5A mono-ubiquitination.	85
Figure 3-11: K321 in KMT5A C-terminus fragment C3 is not the primary ubiquitin acceptor site.	87
Figure 3-12: N-terminus of KMT5A does not alter mono-ubiquitination of C-terminus fragments.....	90
Figure 3-13: N-terminal domain extended fragments maintain the same mono-ubiquitination pattern as C-terminus fragments.	92
Figure 4-1: Mono-ubiquitinated KMT5A is enriched in proliferating cells.	102
Figure 4-2: Mono-ubiquitinated KMT5A oscillation is cell cycle dependent.	104
Figure 4-3: Mono-ubiquitination of KMT5A is elevated in dividing cells.....	106
Figure 4-4: Mono-ubiquitinated KMT5A is exclusively localised in the cytoplasm.	108

Figure 4-5: Transient overexpression of KMT5A truncated mono-ubiquitin deficient and competent truncated derivatives of KMT5A does not affect the cell cycle.	110
Figure 4-6: The ubiquitination status of KMT5A affects cellular proliferation.....	112
Figure 4-7: Mono-ubiquitination of KMT5A is promoted with increasing amounts of Skp2.	114
Figure 4-8: KMT5A and Skp2 are found in a complex.....	116
Figure 4-9: Skp2-mediated ubiquitination of KMT5A does not result in protein turnover. ...	118
Figure 4-10: Skp2 does not promote KMT5A C-terminus mono-ubiquitination.....	121
Figure 4-11: The role of the SCF complex in Skp2-mediated mono-ubiquitination of full length KMT5A.	124
Figure 4-12: The role of the SCF complex in Skp2-mediated mono-ubiquitination of KMT5A C-terminus.	128
Figure 4-13: Proposed model for the role of mono-ubiquitinated KMT5A. Error! Bookmark not defined.	
Figure 5-1: Skp2 protein expression responds differently to androgenic stimulation in LNCaP and LNCaP-AI cells.	143
Figure 5-2: Differential effect on Skp2 protein levels in response to androgen concentration range in the LNCaP and LNCaP-AI cell lines.....	145
Figure 5-3: Androgenic stimulation does not alter Skp2 transcription in LNCaP and LNCaP-AI cell lines.....	147
Figure 5-4: Validation of Skp2 siRNA oligonucleotides.	148
Figure 5-5: Skp2 suppression downregulates cell growth.....	150
Figure 5-6: Skp2 depletion induces G1 cell cycle arrest in PC cell lines.....	151
Figure 5-7: Skp2 depletion differentially affects AR-mediated gene expression.	153
Figure 5-8: Skp2 depletion does not affect classical AR-mediated gene expression.....	155
Figure 5-9: AR level is not altered by Skp2 depletion.	157
Figure 5-10: Skp2 and AR are found in a complex.....	158
Figure 5-11: Skp2 depletion does not alter AR nuclear translocation upon androgenic stimulation.	160
Figure 5-12: AR phosphorylation at serine 81 is not influenced upon Skp2 suppression.....	162
Figure 5-13: Over-expression of Skp2 does not enhance AR transcriptional activity.	164

List of tables

Table 1.1: Reported roles for homogeneous lysine linked ubiquitin chains.	26
Table 2.1: List of primary and secondary antibodies used.	47
Table 2.2: List of plasmids used.	51
Table 2.3: List of siRNA oligonucleotide used. All siRNA oligonucleotides were purchased from Sigma-Aldrich.	52
Table 2.4: Recipes of resolving and stacking gels.	54
Table 2.5: Constituents of the reagent mix for each RT-PCR reaction.	56
Table 2.6: List of qRT-PCR primers used.	57
Table 3.1: Parameters of the PCR cycles.	64
Table 3.2: List of the primers used for the mutagenesis work.	65

List of Abbreviations

ADT	Androgen deprivation therapy
AF-1/2	Activation function 1/2
AFS	Anterior fibromuscular stroma
APC	Anaphase promoting complex
APS	Ammonium persulfate
AR	Androgen receptor
ARE	Androgen response element
AR-FL	Full length androgen receptor
AR-V	Androgen receptor variant
ATP	Adenosine-5'-triphosphate
β -gal	β -galactosidase
BPH	Benign Prostatic Hyperplasia
Cdk	Cyclin dependent kinase
CHIP	Carboxyl-terminus of Hsc70-Interacting protein
CPA	Cyproterone acetate
CRL	Cullin-RING ligase
CRPC	Castrate resistant prostate cancer
CZ	Central zone
DBD	DNA-binding domain
DCC	Dextran-coated charcoal
DDR	DNA damage response
DEPC	Diethylpyrocarbonate
DHT	Dihydrotestosterone
DRE	Digital rectal examination
DUB	Deubiquitinating enzyme
EGFR	Epidermal growth factor receptor
ETS	E twenty-six
FCS	Foetal calf serum
FGFR	Fibroblast growth factor receptor
FM	Full media
FOXA1	Forkhead box protein A1
FSH	Follicle-stimulating hormone
GR	Glucocorticoid receptor
H	Histone
HAT	Histone acetyl-transferase
HBD	Histone binding domain
HDAC1	Histone deacetylase 1
HECT	Homology of the E6AP C terminus
HPRT1	Hypoxanthine phosphoribosyltransferase 1
HSP	Heat shock protein
IGFR	Insulin-like growth factor receptor
IP	Immunoprecipitation
i-set	Insert or Set-1 region
K	Lysine
kDa	Kilo Dalton
KLK2	kallikrein-related peptidase 2
LB	Luria-Bertani
LBD	Ligand binding domain

LCPS	Luciferase count per second
LEF-1	Lymphoid enhancer-binding factor 1
LH	Luteninising hormone
LHRH	Luteninising hormone-releasing hormone
LSD1	Lysine-specific demethylase 1
MDM2	Mouse double minute 2
Me	Methyl group
MMLV	Moloney murine leukaemia virus
MRI	Magnetic resonance imaging
NEDD	Neuronal precursor cell-expressed developmentally down-regulated protein
NLS	Nuclear localisation signal
N/S	Non silencing
NTD	N-terminal domain
PARP	Poly (ADP-ribose) polymerase
PBS	Phosphate buffered saline
PC	Prostate cancer
PCNA	Proliferating cell nuclear antigen
PGS	Protein G sepharose
PHF8	PHD finger protein 8
PI	Propidium iodide
PIN	Prostatic intraepithelial neoplasia
PIP	PCNA interacting peptide
PMSF	Phenylmethanesulfonylfluoride
PPAR- γ	Peroxisome proliferator-activated receptor gamma
PSA	Prostate specific antigen
PTEN	Phosphatase and tensin homolog
PTM	Post-translational modification
PZ	Peripheral zone
qRT-PCR	Real Time quantitative reverse transcription polymerase chain reaction
RBR	RING-between-RING
RING	Really interesting new gene
RNF-6	Ring finger protein 6
RP	Radical prostatectomy
RT	Reverse transcription
RTK	Receptor tyrosine kinases
SAM	S-adenosylmethionine
SDM	Steroid-depleted media
SDS	Sodium dodecyl sulfate
SDS-PAGE	Sodium dodecyl sulfate polyacrylamide gel electrophoresis
SEM	Standard error of the mean
SETD8	SET domain containing (lysine methyltransferase) 8
siRNA	Small interfering RNA
Skp2	S phase kinase-associated protein 2
SPOP	Speckle-type POZ protein
SRC-1	Steroid receptor co-activator 1
SUMO	Small ubiquitin related modifier
TAU	Transcription activation unit
TBS	Tris buffered saline
TBST	Tris buffered saline Tween20 buffer

TEMED	Tetramethylethylenediamine
TIF-2	Transcriptional intermediary factor-2
TMPRSS2	Transmembrane protease serine 2
TR4	Testicular receptor 4
TRUS	Transrectal ultrasonography guided biopsy
TURP	Transurethral resection of the prostate
TZ	Transitional zone
Ub	Ubiquitin
ULM	Ubiquitin-like modifiers
WT	Wild type

1 Introduction

1.1 The structure and function of the prostate

The prostate is an accessory sex gland of the male reproductive system. In healthy adult males, the prostate is slightly larger than a walnut, weighing approximately 25 g. The main function of the prostate is the production of prostatic secretions, responsible for liquefaction of semen which is integral for sperm motility to facilitate fertilisation, therefore it plays an important role in reproduction (Lilja *et al.*, 1989). Androgens are responsible for the growth, development, differentiation and function of the prostate under normal physiological conditions (Huggins and Neal, 1942; Frick and Aulitzky, 1991; Kumar and Majumder, 1995). The biological function of androgens is mediated by their binding to the androgen receptor (AR), a nuclear transcription factor in prostate cells. This leads to activation of the AR and transcription of genes that stimulate growth and survival of prostate cells.

Anatomically, it lies immediately inferior to the bladder, posterior to the pubic symphysis and anterior to the rectum, surrounding the urethra in the pelvic cavity. The prostate consists of four zones: the peripheral zone (PZ), the central zone (CZ), the transitional zone (TZ) and the anterior fibromuscular stroma (AFS) as seen in Figure 1-1. The PZ constitutes approximately 70% of the normal prostate, located at the posterior of the gland and surrounds the distal urethra. It is the main site of prostate cancer (PC) initiation and is felt against the rectum during a physical examination as it is the closest section of prostate to the rectum. The CZ forms 25% of the prostate, with its majority being surrounded by the PZ. The CZ itself surrounds the ejaculatory ducts and is the furthest region from the rectum. Initiation of cancer in this zone is rare, accounting for only 1-5% of cases. The TZ resides in the centre of the prostate and surrounds the urethra proximal to the verumontanum, which is the site where the urethra and the ejaculatory ducts from the testes merge together at a 35° angle. Overall, the TZ accounts for approximately 20% of PC initiation. The prostate is encapsulated by a layer of smooth muscle and fibrous tissue; the AFS, which does not contain any secretory ducts (McNeal, 1981; McLaughlin *et al.*, 2005).

The prostate has a ductal-acinar structure, composed of two major cellular compartments; the glandular epithelial compartment and the fibromuscular stroma, separated from each other by a basement membrane. Three types of epithelial cells reside in the glandular epithelial compartment. Secretory luminal cells are the most abundant, cuboidal in shape and line the inner surface of the ducts. These are differentiated cells which express AR, require androgens for survival and are responsible for the production of prostatic secretions (McNeal, 1988; Shah and Zhou, 2012). The basal cells which generally appear undifferentiated, are androgen-

independent and reside between the basement membrane and luminal cells are presumed to have a protective role (Xin, 2013). Finally, the rare neuroendocrine cells which are sparsely scattered between the luminal and basal cell layers are believed to play a role in regulating the growth, development and secretory function of the prostate through paracrine effects of their neurosecretory products (Noordzij *et al.*, 1995; Huang *et al.*, 2007b). The epithelial compartment is in a dynamic cross-talk with its surrounding stroma. The stroma which is made up of fibroblasts, smooth muscle, nerves, blood vessels and immune cells forms an important part of the machinery that regulates proliferation and differentiation of epithelial cells (Tuxhorn *et al.*, 2001).

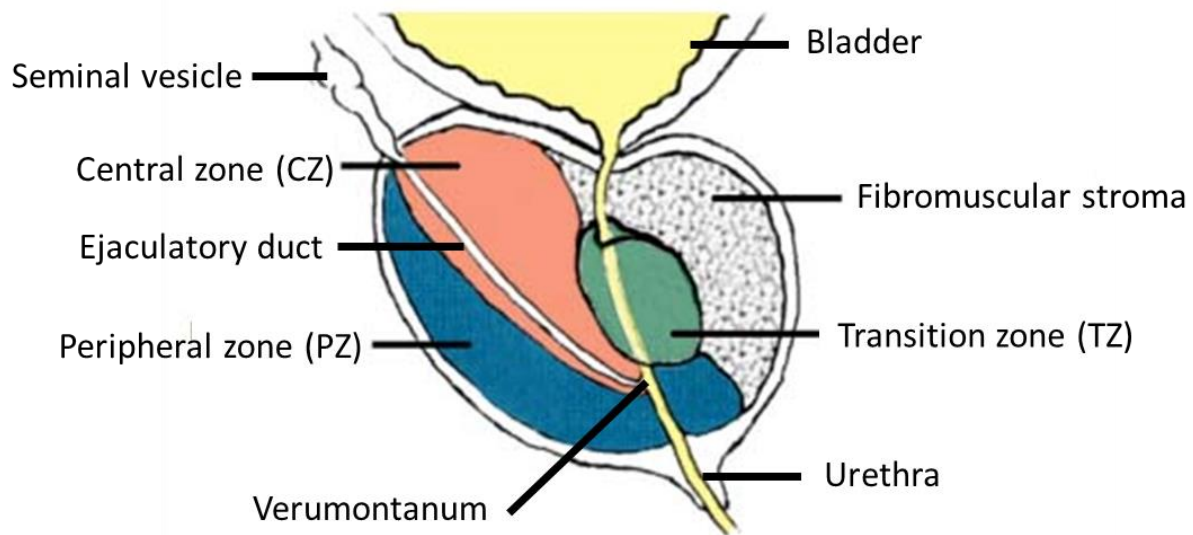


Figure 1-1: Diagram representing the anatomy of the human prostate.

1.2 Prostate abnormalities

1.2.1 Benign prostatic hyperplasia (BPH)

The most common benign proliferative disease of the prostate is BPH, in which there is an increase in the prostate volume due to hyper-proliferation of mainly the stromal compartment and to a lesser extent epithelial cells of the TZ (McNeal, 1990). BPH occurs in ageing men where its incidence increases by 42% and 90% in men between 40-50 years and those over 80 years, respectively (McVary, 2006).

Due to the TZ encapsulating the urethra, BPH causes lower urinary tract complications, partly as a result of mechanical compression on the urethra, including reduced urinary flow and increased frequency of urination, reducing the quality of life. There are different treatment options, depending on the severity of BPH symptoms. In some cases, lifestyle changes such as reduced fluid intake is sufficient to control urinary symptoms (Pinheiro and Martins Pisco, 2012). Alternatively, blocking α_{1A} type of α_1 -adrenoceptors which are commonly expressed in the prostate smooth muscle, cause it to relax, leading to reduced constriction of the urethra and increased urine flow. However, this treatment does not reduce the size of the prostate. Examples of α -adrenergic antagonists include doxazosin and alfuzosin (Bechis *et al.*, 2014). The androgen, dihydrotestosterone (DHT), which is derived from a less active androgen, testosterone, mediates the growth of the prostate. Testosterone is converted to DHT in prostate cells by the membrane-bound enzyme 5 α -reductase (Frick and Aulitzky, 1991). Therefore, 5 α -reductase inhibitors such as finasteride are utilised to block DHT production which reduces prostate proliferation and decreases prostate volume. The combination of these two inhibitors has been shown to be more beneficial. Patients with more advanced symptoms undergo transurethral resection of the prostate (TURP) or laser treatment (Pinheiro and Martins Pisco, 2012).

1.2.2 Prostatic intraepithelial neoplasia (PIN)

PIN is an abnormal proliferation within the lining of prostatic ducts and is sub-divided into low and high-grade (Bostwick, 2000). It is an age-related disease, with high-grade PIN being more frequent in aging men. Patients with high-grade PIN develop PC over a period of 5-10 years. Moreover, as with PC, PIN primarily occurs in the PZ of the prostate and also shares similar genetic alterations, with more than 400 genes with aberrant expression being identified in both PIN and PC (Calvo *et al.*, 2002). Some of these genetic alterations include the loss of tumour suppressors *TP53* and *RBI*, and over-expression of the *MYC* oncogene (Bettendorf *et al.*, 2008). Therefore, PIN is the most established precursor of PC.

In contrast to PC, PIN does not elevate the serum PSA concentration as the surrounding basement membrane and the vasculature remains intact, therefore PSA cannot be secreted into the blood (Ramos *et al.*, 1999). As a result, biopsy is the only detection method. Treatment for PIN include androgen-deprivation therapy such as those utilised in the treatment of PC, however, 5 α -reductase inhibitors have very little effect (Balaji *et al.*, 1999).

1.2.3 Prostate cancer

1.2.3.1 Incidence and risk factors

PC is the most common cancer and the second cause of cancer-related death among men in Western countries. In 2013, there were 47,300 new cases diagnosed in the UK alone, which equates to 130 men every day (Cancer Research UK, last reviewed 17 February 2016). It is estimated that 1 in 8 men develops PC in their lifetime (Prostate Cancer UK).

The incidence of PC increases with age with the highest number of diagnosed patients being men aged 70-74 years (Cancer Research UK). Ethnicity is another considerable risk factor with black men being 3 times more likely to develop the disease in comparison to white men. Family history is also a recognised risk factor where men are twice as likely to be diagnosed with this disease if they have a first-degree relative (father, brother, son) with PC (Brawley *et al.*, 1998a; Brawley *et al.*, 1998b). The susceptibility of developing PC further increases with a history of both breast cancer and PC than PC alone (Thomas *et al.*, 2012). Social and environmental factors including diet, lack of physical activity, heavy smoking, and alcohol consumption have also been associated with increased risk of PC (Hsing and Chokkalingam, 2006).

1.2.3.2 PC initiation and genetic aberrations

The molecular mechanisms leading to the initiation and progression of PC are still an area of ongoing research which has remained incompletely defined due to its complexity. As already alluded to, the incidence of PC is strongly linked to aging and therefore age-related damage is a contributor to the initiation of the disease. This includes accumulation of DNA damage due to increased somatic DNA mutations which increases the probability of a mutation occurring within an oncogene (Hanahan and Weinberg, 2000); as well as, DNA damage caused by DNA telomere shortening as a result of chronic inflammation and oxidative stress (Shen and Abate-Shen, 2010).

Several of the mutations observed in PC are initiated in PIN. For example, the frequent 8q21 allelic loss-of-heterozygosity resulting in reduced expression of the tumour suppressor NKX3.1 is present in 20% of high-grade PIN, 34% of hormone-refractory PC and 78% of metastases (Grasso *et al.*, 2012). Similarly, phosphatase and tensin homolog (PTEN) is found mutated,

while PTEN deletion occurs in over 60% of metastatic prostate tumours. Both these genomic alterations lead to increased PI3K/Akt signalling, which translates into cell survival and proliferation through activating AR signalling independent of ligand-mediated activation of the AR (Feilotter *et al.*, 1998; Feldman and Feldman, 2001). Furthermore, fusion of androgen-regulated transmembrane protease serine 2 (TMPRSS2) and the E twenty-six (ETS) family of transcription factors including ERG, ETV1 and ETV4, is another common genomic aberration. The TMPRSS2-ERG fusion causes the oncogenic ETS transcription factors to be placed under the control of the androgen inducible TMPRSS2 promoter and is associated with tumour progression (Tomlins *et al.*, 2005).

A frequent mutation in primary PC is in the gene encoding Speckle-type POZ protein (SPOP), an E3 ligase, which is mutated in over 10% of primary PC tumours (Barbieri *et al.*, 2012). Moreover, dysregulation of the tumour suppressor p53 is present in 5-10% of primary tumours, but increases to around 50% in metastatic disease (Bettendorf *et al.*, 2008).

1.2.3.3 Symptoms and diagnosis

PC in its early stages is asymptomatic; however symptoms gradually develop and become pronounced as the disease progresses. These symptoms include, but are not limited to, bladder obstruction, dysuria, nocturia, haematuria and impotence. Disease progresses by invading surrounding tissues and metastasises to the lymph nodes, bladder and bone causing bone pain especially in the lower back, hips and upper thighs (Miller *et al.*, 2003).

There is no single and definitive test for PC to date. Initially, serum prostate specific antigen (PSA) is measured and a digital rectal examination (DRE) performed. PSA is an AR-targeted serine protease with increased levels in PC; however, it is not specific to PC cells as inappropriate rise can also be detected in multiple prostatic diseases and following an injury to the prostate (Balk *et al.*, 2003; McCracken *et al.*, 2010).

Following the detection of elevated serum PSA level and prostate abnormalities during DRE, a transrectal ultrasonography (TRUS) guided biopsy is performed to determine the presence of cancer. The sample tissues from the biopsy are analysed and scored using the Gleason system where the sample is given a histological score based on its cellular differentiation. Moreover, the sample is staged which is important in the selection of the appropriate form of therapy (McCracken *et al.*, 2010). Should the outcome of these tests be negative but PC is still suspected based on the initial PSA and DRE results, as well as persistent symptoms, magnetic resonance imaging (MRI) can be used as in addition to the prostate, it visualises tumours. Therefore, further TRUS can be performed to specifically take biopsies from tumours (Heidenreich *et al.*,

2014). However, biopsies are not flawless where a major challenge in PC is distinguishing tumours that are clinically important and likely to metastasise compared to clinically insignificant tumours that will not cause significant symptoms. Therefore, there is a need for identification of novel biomarkers for PC detection that also enables patient stratification into appropriate treatment groups.

1.2.3.4 Treatments

The organ-confined disease, with a low-risk PC are initially not treated but are under watchful waiting or active surveillance whilst the patient remains asymptomatic. The patient is regularly monitored and treatment commences upon the onset of cancer progression. This prevents the unnecessary over-treatment of the disease and its associated side-effects (Klotz, 2013). The confined disease with an intermediate or high risk of progression can be treated surgically by removing the prostate, called radical prostatectomy (RP). Although effective in treating men below the age of 70, this procedure is associated with high risk of complications and unwanted side-effects which influences the quality of life. However, newer surgical techniques such as robot-assisted laparoscopic RP, which is becoming popular, may reduce complication rates. Furthermore, radiotherapy and brachytherapy can be utilised which have a similar progression-free and overall survival rate to that of surgery, but are associated with high risk of toxicity (McCracken *et al.*, 2010; Heidenreich *et al.*, 2014).

The treatment of advanced disease is aimed at prolonging life expectancy and preventing or controlling symptoms. As prostate development depends on the action of androgens and AR-signalling, androgen deprivation therapy (ADT) is used to reduce prostate cell proliferation and survival. ADT can be achieved through a number of mechanisms and works by decreasing AR activity either directly or indirectly through decreasing circulating androgens.

ADT by chemical castration involves the use of luteinising hormone-releasing hormone (LHRH) agonists, such as leuprorelin, which bind to LHRH receptors on gonadotropic cells in the anterior pituitary. This induces the hypothalamic signalling axis, leading to the release of luteinizing hormone (LH) and follicle stimulating hormone (FSH) and subsequent androgen biosynthesis in the testes (Rick *et al.*, 2013). This initially results in elevated serum testosterone levels, often causing bone pain which may be diminished in most cases by co-treatment with anti-androgens (Bublely, 2001). However, overstimulation of the hypothalamic signalling pathways ultimately leads to down-regulation of LHRH receptors, therefore inhibiting testosterone release, resulting in a castrate level of serum testosterone (Rick *et al.*, 2013).

To overcome the testosterone flare, another method of chemical castration using LHRH antagonists such as degarelix, is utilised (Bokser *et al.*, 1990; Rick *et al.*, 2013). These compounds bind LHRH receptors and inhibit them, causing the same outcome as LHRH agonists. Although, a faster response is achieved with LHRH antagonists without the initial flare, currently these drugs are not as long lasting as LHRH agonists (Rick *et al.*, 2013).

ADT is also achieved through direct inhibition of the AR using anti-androgens. The first anti-androgen developed was cyproterone acetate (CPA), which is a steroidal anti-androgen (Goldenberg and Bruchovsky, 1991). Due to patient side-effects caused by the steroidal nature of the compound, non-steroidal AR antagonists including nilutamide, flutamide and the more frequently used, bicalutamide (casodex) were generated. As these compounds do not inhibit testosterone production, they are not associated with erectile dysfunction or loss of bone mineral density. However, they cause other significant side-effects including hot flushes, depressive mood disturbance, cognitive impairment, diminution of muscular strength, increase in body fat, cardiovascular disease and gynecomastia. Anti-androgens prevent the action of adrenal androgens and are used in combination with LHRH agonists to achieve complete androgen blockade (Mottet *et al.*, 2015).

Unfortunately, the ADT eventually fails and the cancer becomes hormone-refractory, called castrate-resistant PC (CRPC). Despite targeting the AR, it becomes aberrantly activated in CRPC through a number of mechanisms which are discussed in Chapter 1.3.3. At this stage, cytotoxic chemotherapeutic agents such as the taxane, docetaxel, which targets the microtubule network, in combination with prednisone are used to delay the progression of symptoms (Yagoda and Petrylak, 1993; Heidenreich *et al.*, 2014).

Second generation AR antagonists, MDV3100 (enzalutamide) and ARN-509, exhibiting a greater affinity for the AR ligand-binding domain (LBD) than casodex were generated for use in metastatic CRPC. They prevent AR nuclear localisation and binding to DNA (Tran *et al.*, 2009). Androgens are further produced through the action of the adrenal gland cytochrome P450 enzyme CYP17 and act to maintain high intratumoural androgen levels despite ongoing castration. Using abiraterone acetate, a CYP17 inhibitor prevents intracellular and adrenal androgen synthesis, thereby leading to a further decrease in circulating testosterone (Barrie *et al.*, 1994).

1.3 The androgen receptor

The AR is a transcription factor, belonging to the nuclear steroid receptor family. The gene encoding the AR is located on Xq11-12 and consists of 8 exons (Lubahn *et al.*, 1988). The exon 1 of AR, which is the largest of AR exons, encodes the entire N-terminal domain (NTD), and exons 2 and 3 encode the cysteine rich DNA-binding domain (DBD). Whilst the 5' region of exon 4 encodes the hinge region of AR, its remaining region along with exons 5-8 encode the ligand-binding domain (LBD) (Kuiper *et al.*, 1989; Brinkmann *et al.*, 1996).

1.3.1 Androgen receptor structure

The AR protein consists of ~ 919 amino acids, generating a protein with a molecular weight of approximately 110 kDa. It has a multi-domain structure, composed of four functional domains: the NTD, the DBD, the hinge region and a carboxyl-terminal LBD (Claessens *et al.*, 2008), demonstrated in Figure 1.2.

The NTD is critical for the transcriptional activity of the AR. It harbours AR transcriptional activation function (AF-1) which contains two transcription activation units 1 and 5 (Tau-1 and Tau-5) required for full ligand-inducible and ligand-independent transcriptional activity, respectively (Jenster *et al.*, 1991; Jenster *et al.*, 1995). Furthermore, the majority of AR phosphorylation sites reside within the NTD (Gioeli *et al.*, 2002). This domain is responsible for interactions with AR co-regulators, such as the steroid receptor co-activator 1 (SRC-1) (Christiaens *et al.*, 2002). In addition, interleukin-6 stimulated STAT3 and MAPK recruitment at the NTD enables activation of the AR in the absence of ligand binding (Ueda *et al.*, 2002).

Moreover, the AR NTD consists of polymorphic glutamine and glycine repeats which have been linked to several disease states as the length of these repeats is inversely correlated with AR transcriptional activity (Chamberlain *et al.*, 1994). For example, impaired spermatogenesis and infertility have been shown to result from decreased AR activity as a result of longer polyglutamine repeats (Tut *et al.*, 1997). Additionally, longer repeats have been associated with a generally lower risk of PC (Buchanan *et al.*, 2004).

The DBD consists of two zinc fingers which function cooperatively to bind AR to the DNA. The first zinc finger composed of a P-box motif, binds to the major groove of DNA at androgen response elements (AREs), ensuring receptor selectivity. The second zinc finger entails a D-box, which stabilises the DNA-AR interactions by binding to the phosphate backbone of DNA and is responsible for DNA-dependent dimerization of AR (Freedman, 1992).

The hinge region links the DBD and LBD of the AR, and encompasses a bipartite AR nuclear localisation signal (NLS). This domain has multiple functions as it is involved in DNA binding,

transcriptional activity and nuclear localisation of the AR (Haelens *et al.*, 2003; Tanner *et al.*, 2004; Haelens *et al.*, 2007). The hinge region is involved in AR nuclear transport through interacting with microtubules as well as exposure of its NLS upon a conformational change induced by ligand binding. The hinge region is subject to post-translational modifications (PTMs) such as acetylation, methylation and phosphorylation. For example, AR methylation at K630 and K632 by the methyltransferase, SET9, has been shown to be required for androgen-mediated AR transcriptional activity (Gaughan *et al.*, 2011; Ko *et al.*, 2011).

The AR binds to its ligand, androgen, through its LBD. In addition, it is involved in interactions with AR co-regulators through its AF-2. Upon ligand binding, this domain undergoes a conformational change, leading to the formation of a surface referred to as Tau-2 that resides in AF-2. This in turn mediates the intramolecular interaction of AR with Tau-1 within the NTD, causing an overall conformational change in the AR (Moras and Gronemeyer, 1998). Moreover, anti-androgens target the LBD to disrupt N/C terminal interactions, recruitment of co-factors and ultimately, AR transcriptional activity (Gao *et al.*, 2005; Korpál *et al.*, 2013).

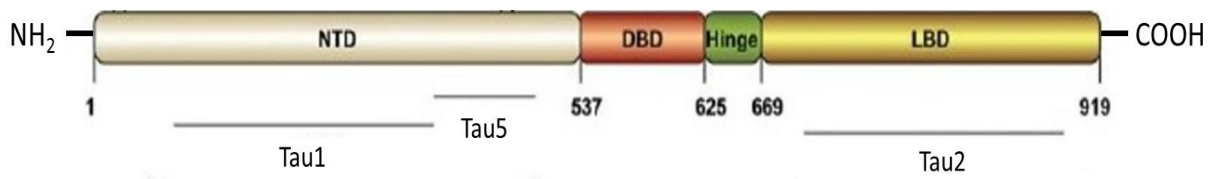


Figure 1-2: Schematic diagram of the AR protein. The diagram demonstrates different domains of the AR protein: N-terminal domain (NTD); DNA-binding domain (DBD), the hinge region and the ligand binding domain (LBD). The key transcription activation units (TAU1, 5 and 2) are also highlighted. The image is taken from Lonergan and Tindall *et al.* (Lonergan and Tindall, 2011).

1.3.2 AR function and mechanism of action

In the absence of ligand, AR is inactive and is present diffusely throughout the cytoplasm in complex with several heat shock protein (HSPs) such as HSP90 and HSP70. Upon ligand binding, AR is activated and undergoes a conformational change leading to its dissociation from the HSPs in an ATP-dependent manner (Smith and Toft, 2008).

The AR then translocates to the nucleus. The ligand-induced conformational changes expose interaction motifs which enables intra N/C terminal interactions of AR, as well as, inter-molecular interactions leading to AR dimerisation. The AR typically homo-dimerises, however, hetero-dimerisation with ER α and testicular receptor 4 (TR4) has also been reported (Bennett *et al.*, 2010).

Once in the nucleus, the AR binds to the DNA at AREs in the enhancer or promoter of its target genes, leading to their transcriptional activation or suppression. Binding of the AR to DNA is facilitated by initially unwinding the chromatin around the ARE in order to make these regions more accessible for the AR to bind. This is generally mediated by FOXA1 pioneer transcription factor which has been shown to bind DNA prior to the AR (Wang *et al.*, 2009).

Following binding to its AREs, the AR recruits a multitude of proteins involved in chromatin remodelling and modification such as the SWI/SNF complex and histone acetyltransferases CBP/p300 and pCAF, respectively. The remodelled chromatin enables AR to recruit the preinitiation complex and mediate the transcription of AR target genes. In addition, the AR recruits a number of co-regulatory proteins which can either enhance or repress its transcriptional activity through various mechanisms (van de Wijngaart *et al.*, 2012). Figure 1-3 summarises the AR activation pathway.

The AR regulates many critical cellular processes required for both the normal prostate growth and development of PC, including proliferation, metabolism, differentiation and apoptosis.

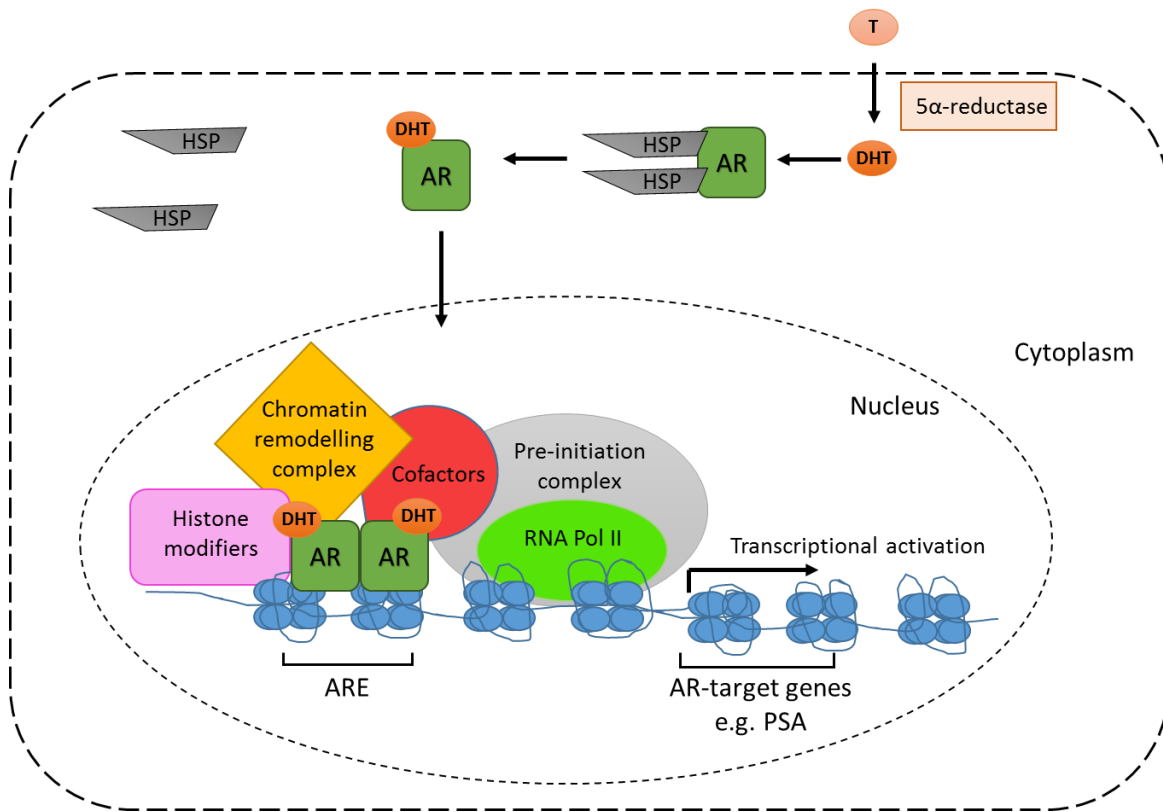


Figure 1-3: Summary of the AR signalling pathway. Diagram is drawn based on information from van de Wijngaart *et al.* and Bennett *et al.* (Bennett *et al.*, 2010; van de Wijngaart *et al.*, 2012). Abbreviations: ARE, androgen responsive element; DHT, dihydrotestosterone; HSP, heat shock protein; RNA pol II, RNA polymerase II. Free testosterone diffuses across the cell membrane into the prostate cell, and is converted to DHT by 5 α -reductase. DHT binds to the AR, induces dissociation of HSPs and activates the AR. The AR enters the nucleus, dimerises and binds to the ARE to transactivate the expression of its target genes leading to increased expression and survival.

1.3.3 Deregulation of AR activity and the mechanism of CRPC development

The AR is a key molecule required for the initiation and development of PC and therefore, AR-targeted therapies have been the mainstay of therapy. However, PC relapses and progresses to its lethal state; the CRPC where AR signalling has been shown to be aberrantly reactivated. Several mechanisms result in aberrant AR signalling which include: AR amplification and sensitisation to low levels of circulating androgens, activating mutations of the AR, generation of ligand-independent AR splice variants, persistent intratumoural androgens, AR activation by other signalling pathways and aberrant interaction with co-regulator proteins.

The amplification of the AR gene is one of the most common genetic alterations in CRPC. This leads to over-expression of the AR protein and ultimately driving increased sensitisation of the AR pathway as it enables sustained cell growth in residual levels of androgen following androgen ablation therapy (Visakorpi *et al.*, 1995; Koivisto *et al.*, 1996).

Mutations of the AR significantly increases in CRPC, where mutations of the NTD are mainly associated with increased AR activity and co-activator interactions in the absence of androgen, whilst mutations of the LBD lead to broadened ligand specificity of the AR. For example a common point mutation, T877A in AR LBD results in increased promiscuity of the receptor (Sack *et al.*, 2001), enabling other non-androgenic steroids (oestrogen and progesterone) and anti-androgens (flutamide, an antagonist of wild-type AR) to bind and activate the AR (Suzuki *et al.*, 1996). Similarly, another point mutation in the LBD, H874Y, has the same effect on AR ligand specificity by causing a conformational change of the AR, leading to enhanced binding with the p160 family of co-activators (Steketee *et al.*, 2002; Duff and McEwan, 2005).

Alternative splicing of the AR, leads to the formation of aberrant AR isoforms lacking the AR LBD. These AR isoforms are able to bind DNA independently of ligand binding and are therefore constitutively active even in the absence of androgen. There are over a dozen AR isoforms that have been identified, with AR-V7 being the most characterised and observed to be up-regulated in patients with relapsed disease following antiandrogen therapy (Dehm *et al.*, 2008; Guo *et al.*, 2009).

In addition to changes in AR structure and levels, alterations in steroid metabolism leading to increased production of AR ligand, DHT, causes sensitisation of the AR signalling pathway post-ADT. Testes are the major source of testosterone production in males. Testosterone is synthesised from cholesterol and then converted into its more potent form, DHT in the prostate. In normal males, testosterone is the primary precursor of DHT. However, in CRPC patients, intratumoural synthesis of DHT can occur through a number of mechanisms such as up-

regulation of enzymes involved in the ‘classical’ DHT production pathway and utilisation of a ‘backdoor pathway’ which enables DHT production from a different precursor, progesterone (Locke *et al.*, 2008). Moreover, an ‘alternative’ pathway contributes to DHT production where androgens produced by the adrenal gland are converted to DHT in the prostate (Chang *et al.*, 2011).

Evasion of the AR blockade by tumours may also be achieved by the up-regulation of the glucocorticoid receptor (GR). The GR belongs to the same class of nuclear steroid receptors (class 1) as AR, where these two receptors have been shown to have overlapping transcriptomes. Therefore, the GR is able to drive gene transcription of AR target genes even in the absence of AR. GR up-regulation promotes tumour resistance to novel AR inhibitors, enzalutamide and ARN-509, with its knockdown leading to sensitisation of cells to these therapies (Arora *et al.*, 2013; Sahu *et al.*, 2013).

The activation of many oncogenic signalling pathways following androgen deprivation and AR inhibition has been implicated in post-transcriptional regulation of the AR and can promote aberrant AR activation independently of ligand binding. For example, the activation of the PI3K/AKT and MAPK pathways by receptor tyrosine kinases (RTKs) such as the insulin-like growth factor receptor (IGFR), epidermal growth factor receptor (EGFR) and fibroblast growth factor receptor (FGFR) which have been shown to be over-expressed in CRPC (Culig *et al.*, 1994; Craft *et al.*, 1999). Furthermore, up-regulation of proteins involved in the DNA damage response (DDR) are also reported in CRPC. The AR has been shown to be activated in response to DNA damage to promote DNA repair and cell survival through the regulation of DDR gene expression programmes. The transcription factor, c-MYB, also involved in the DDR, shares a subset of DDR target genes with the AR. In the absence of the AR, c-MYB dominantly regulates the expression of their common DDR genes, maintaining their high levels to support cell survival (Goodwin *et al.*, 2013; Li *et al.*, 2014b).

Furthermore, the AR is regulated by many co-regulatory proteins, several of which are dysregulated in CRPC. Whilst interactions with its co-activators are enhanced, AR interaction with its co-repressors is decreased leading to sustained AR signalling. The co-regulators of AR modulate AR activity through different mechanisms such as mediating AR PTMs. A large number of these co-regulator proteins are epigenetic enzymes which mediate chromatin remodelling through PTMs of histones. The N-terminal tails of histones undergo PTMs such as acetylation, methylation, ubiquitination and phosphorylation, leading to altered chromatin

structure which in turn affects gene expression without a change in the DNA sequence, termed epigenetics. This indirectly facilitates AR activity by affecting AR-mediated gene transcription.

Examples of epigenetic enzymes include co-activators such as two p160 histone acetyltransferases (HATs), SRC and transcriptional intermediary factor-2 (TIF2), which are frequently shown to be up-regulated in CRPC patients (Gregory *et al.*, 2001). These HAT enzymes recruit a number of general co-activators, CREB binding protein (CBP), p300 and p300/CBP-associating factor (PCAF), all of which possess HAT activity and together acetylate specific lysines on histones H3 and H4. This leads to chromatin relaxation and removal of a physical barrier, thereby promoting the recruitment of the basal transcriptional machinery (Powell *et al.*, 2004). Furthermore, ADT has also been found to increase the expression of p300 and CBP in PC cells (Heemers *et al.*, 2010). Similarly, other HAT enzymes, including the MYST protein family member, Tip60, are elevated in patients with late stage disease and are found to acetylate the AR, leading to increased AR transcriptional activity (Brady *et al.*, 1999; Gaughan *et al.*, 2001; Gaughan *et al.*, 2002).

Methyltransferases are a family of epigenetic enzymes with an evolutionary conserved SET (Suppressor of variegation, Enhancer of Zeste, Trithorax) domain responsible for their catalytic activity. There are 48 SET domain-containing proteins and one SET domain-lacking histone lysine methyltransferase, DOT1L encoded within the human genome. They catalyse the methylation of histones H3 and H4 either on arginine or lysine residues. Moreover, they methylate non-histone proteins ranging from chromatin machinery enzymes to transcription factors, including the AR.

Mis-regulation of methyltransferases and demethylases has been associated with cancer aggressiveness, including in PC. For example, the lysine-specific demethylase 1 (LSD1; also known as BHC110) interacts with the AR and forms a chromatin complex upon androgen stimulation. LSD1 removes the repressive H3K9Me marks and facilitates AR-mediated gene transcription (Metzger *et al.*, 2005). High expression of LSD1 has been associated with PC aggressiveness (Kahl *et al.*, 2006; Metzger *et al.*, 2006).

Another example is SET7/SET9/KMT7, a histone methyltransferase that specifically monomethylates lysine 4 on histone H3 and up-regulates gene transcription (Wang *et al.*, 2001). SET9 was also found to directly methylate the AR which facilitated AR N/C terminal interaction, leading to enhanced AR transcriptional activity. Moreover, SET9 was aberrantly expressed in CRPC (Gaughan *et al.*, 2011; Ko *et al.*, 2011). Additionally, KMT5A (SET8), a specific mono-methyltransferase for lysine 20 on histone H4 has recently been found to be

elevated in PC compared to benign samples (Coffey *et al.*, unpublished data). KMT5A is the focus of this project and will be discussed in detail throughout this chapter.

These co-regulators themselves undergo PTMs which can in turn influence their activity and ultimately AR activity and function. The AR regulates a distinct transcriptional programme in hormone sensitive versus castrate-resistant models of PC, where there is a substantial increase in the number of AR regulated genes involved in cell cycle progression in CRPC (Wang *et al.*, 2009). Therefore understanding the interplay between co-regulators and the AR, but also the mechanisms that modulate the co-regulatory proteins themselves may help in providing novel therapeutics to inhibit AR signalling in CRPC.

1.4 Ubiquitination

Ubiquitination is the process of post-translationally modifying proteins via the covalent conjugation of the highly evolutionary conserved 76 amino acid protein, ubiquitin. Ubiquitin is an abundant protein in mammalian cells which can either be found free or covalently attached to other proteins. Ubiquitination is an important mechanism in many critical regulatory processes including: DNA repair, cell cycle control and the stress response, each requiring a specific type of ubiquitination. The outcome of ubiquitination is diverse ranging from protein degradation by the proteasome to activation of transcription factors. The wide range of signals as a result of ubiquitination depends on the number of ubiquitin molecules that are attached, for example proteins can be mono-ubiquitinated or poly-ubiquitinated, and its configuration which is the way these ubiquitin moieties are conjugated together to form chains (Weissman, 2001). Ubiquitination is a reversible process where ubiquitin can be removed in a hydrolysis reaction by deubiquitinating enzymes (DUBs) (Komander *et al.*, 2009).

1.4.1 Process of ubiquitination

Ubiquitination results in the formation of an iso-peptide linkage between ubiquitin and the acceptor protein. Ubiquitin is ligated through its C-terminal glycine residue to the ϵ -amino group of a lysine in the substrate protein. Moreover, ubiquitin itself consists of 7 lysine residues, each of which can be ligated to other ubiquitin molecules to form different chains of ubiquitin polymers (Vijay-kumar *et al.*, 1987).

The ubiquitination process is an enzymatic cascade which takes place in three stages, summarised in Figure 1-4. Firstly, ubiquitin is activated by an E1 ubiquitin-activating enzyme in an ATP-dependent manner. The activated ubiquitin is then transferred to an ubiquitin-conjugating enzyme (E2) and is finally conjugated to the substrate protein by an ubiquitin-ligase (E3). These enzymes ensure the tight regulation of ubiquitination and the specificity of this process (Ciechanover *et al.*, 1981). So far, two E1 enzymes capable of ubiquitin activation, approximately 40 E2 enzymes and around 600 E3 ligases have been identified to be encoded by the human genome (Villamil *et al.*, 2013).

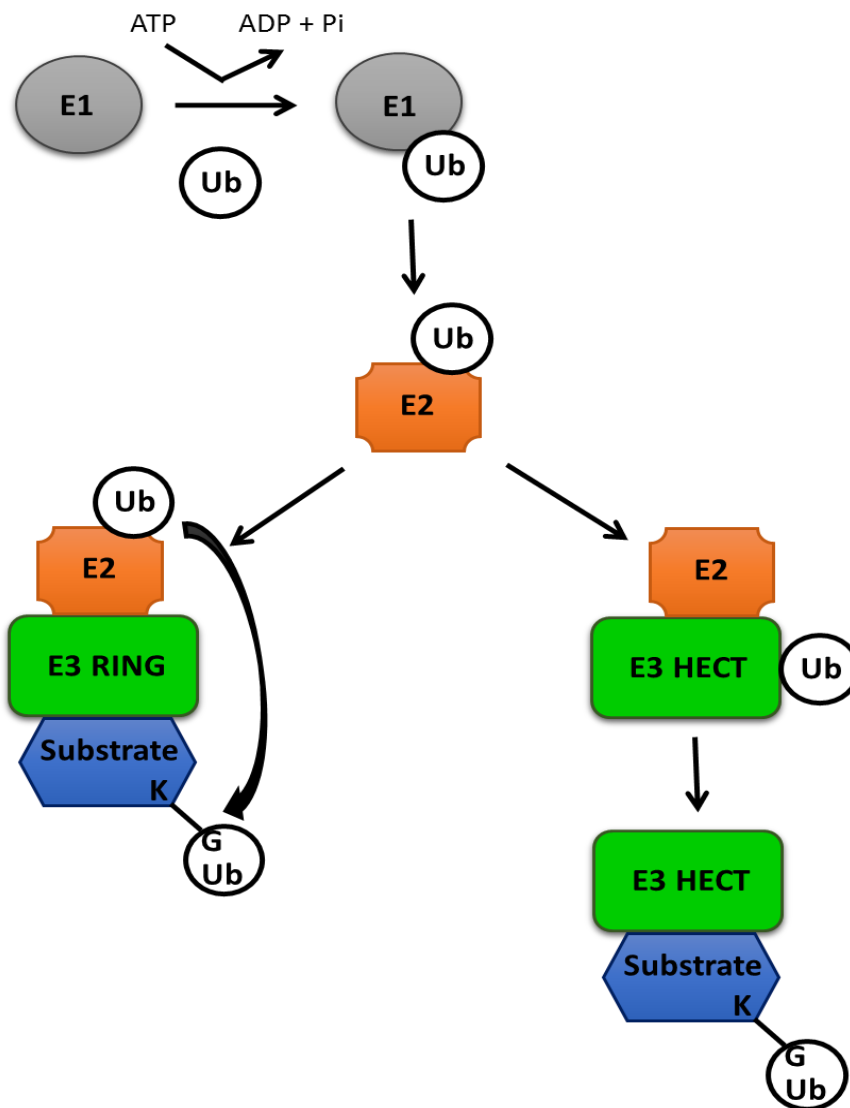


Figure 1-4: Process of ubiquitination. Ubiquitin is activated by an ubiquitin-activating (E1) enzyme using energy from ATP hydrolysis and passed to an ubiquitin-conjugating (E2) enzyme. Ubiquitin is then transferred to a substrate protein, specified by the distinct E3 ligase that binds both the substrate and the E2. E3 ligases may contain really interesting new gene (RING) domains that act as a scaffold to pass ubiquitin from the E2 directly to the substrate protein. Alternatively, homologous to E6-AP carboxy-terminus (HECT) E3 ligases form a covalent bond with ubiquitin itself first and then transfer the ubiquitin onto the substrate. The diagram was drawn independently based on figures from Weissman *et al.* and Kerscher *et al.* (Weissman, 2001; Kerscher *et al.*, 2006). Abbreviations: Ub, ubiquitin; K, lysine; G, glycine.

1.4.1.1 E1 ubiquitin-activating enzymes

In the first stage, ubiquitin becomes activated and ligated to an E1 activating enzyme in an ATP-dependent manner. Ubiquitin activation occurs on the carboxyl group of its C-terminal glycine residue which is ligated to the catalytic cysteine of the E1 active site through thioester linkage to form a thioester-linked E1~Ub conjugate. As a result of ATP and ubiquitin binding, E1 undergoes a conformation change which exposes its ubiquitin-fold domain (UFD) required for binding to E2 (Ciechanover *et al.*, 1981).

There has been eight E1 enzymes identified to date, where only two of them, UBE1 and UBA6 (UBE1L2 or E1-L2), cause ubiquitin activation. In addition to ubiquitin, UBA6 also activates the human leukocyte antigen F-associated transcript 10 (FAT10) (Chiu *et al.*, 2007; Jin *et al.*, 2007; Pelzer *et al.*, 2007). Most of the other E1 enzymes are involved in the activation of ubiquitin-like modifiers (ULM) such as small ubiquitin related modifier (SUMO) and neuronal precursor cell-expressed developmentally down-regulated protein (NEDD) (Groettrup *et al.*, 2008).

1.4.1.2 E2 conjugating enzymes

Following the formation of the thioester-linked E1~Ub conjugate, an E2 docks non-covalently to this complex and the activated ubiquitin is then transferred onto the E2 active site cysteine via a transthioesterification reaction. Loaded E2 enzymes can then either associate with E3 ligases or in a few instances, directly engage with the substrate. Whilst all E2 enzymes interact with an E1 enzyme, they can interact with multiple E3 ligases. Of the approximately 40 E2 enzymes, at least 26 are involved in the transfer of ubiquitin and the remaining transfer ubiquitin-like protein such as SUMO and NEDD8 (Huang *et al.*, 2007a; Lee and Schindelin, 2008).

An example of an E2 enzyme capable of ubiquitin chain initiation is UBE2D2, which lacks specificity for a lysine residue in the substrate protein. On the other hand, UBE2T is an example of a selective E2 enzyme which specifically mono-ubiquitinates its substrate FANCD2. Whilst these E2s can add the first ubiquitin, the E2 enzyme, UBE2S lacks this capability and is instead able to extend lysine 11-specific polyubiquitin chains (Ye and Rape, 2009; Hibbert *et al.*, 2011).

1.4.1.3 E3 ligases

In the final stage of ubiquitination, the E3 enzyme facilitates the ligation of ubiquitin from the active E2 to the substrate protein. The E3 ligase can be a protein or a protein complex and acts as an adaptor as it binds to both the E2 and the substrate. There are three classes of E3 ligases consisting of: really interesting new gene (RING) domain family, the homology to E6AP C terminus (HECT) and the RING-between-RING (RBR) family (Berndsen and Wolberger, 2014; Scheffner and Kumar, 2014).

RING E3 ligases are the largest and diverse family of E3 enzymes. They do not have enzymatic activity and instead mediate the transfer of ubiquitin from the E2 directly to the substrate by simultaneously binding to both components. They commonly function as homomeric or heteromeric complexes by interacting with each other or a related RING protein, respectively (Brzovic *et al.*, 2001; Campbell *et al.*, 2012). Moreover, a subset of E3 ligases, also known as cullin-RING ligases (CRL), are a component of a multi-subunit complex, where E2 and substrate binding occurs on different subunits of the complex, linked together by a cullin-type protein scaffold. In these complexes, substrate recognition and binding is carried out by a variable adaptor protein, forming a bridge between the substrate and the E3 ligase complex. An example is the RING protein RBX1 which is part of the SKP1-CUL1-F-box (SCF) complex (Jackson *et al.*, 2000).

In contrast, HECT containing E3 ligases are a relatively small group of E3 enzymes with 28 members identified in humans thus far. They possess catalytic activity and transfer ubiquitin from E2 on to the substrate by catalysing two distinct reactions. Firstly, a transthioesterification reaction in which ubiquitin is transferred from the E2 active site cysteine onto a cysteine in the HECT domain active site. Secondly, the transfer of ubiquitin from HECT on to a lysine in the substrate (Huibregtse *et al.*, 1995).

The RBR E3 ligases constitute properties of both the RING and HECT E3 families. These enzymes consist of a putative RING domain, followed by an in-between ring (IBR) and a less conserved RING-like domain. Similar to the RING E3s, RBR interacts with the E2~Ub by non-covalent interactions through its first RING domain. Then, as in the HECT E3 ligases, the activated ubiquitin is transferred onto a conserved cysteine in the RING-like domain, prior to being conjugated to the substrate (Wenzel and Klevit, 2012).

1.4.2 Ubiquitin function

Covalent ligation of ubiquitin to the substrate protein causes a diverse range of cellular consequences such as destruction of the substrate by the proteasome, altered substrate activity, localization and affinity to binding partners or other non-proteolytic events. This is due to the vast array of possible ubiquitin chain compositions. Proteins can be modified by a single ubiquitin molecule (mono-ubiquitination) or ubiquitin polymers (poly-ubiquitination). Ubiquitin chains are formed when ubiquitin itself is ubiquitinated through its lysine residues (K6, K11, K27, K29, K33, K48 and K63) or the N-terminal methionine residue (M1). These chains can be homotypic, comprising only a single linkage type i.e. chains are formed using the same lysine residue in each ubiquitin; or heterotypic, containing mixed linkages within the same polymer. Furthermore, heterotypic chains can also be branched i.e. one ubiquitin molecule is ubiquitinated at two or more lysine sites. These chains are poorly characterised (Komander and Rape, 2012). A summary of the different ubiquitin linkages is provided in Figure 1-5.

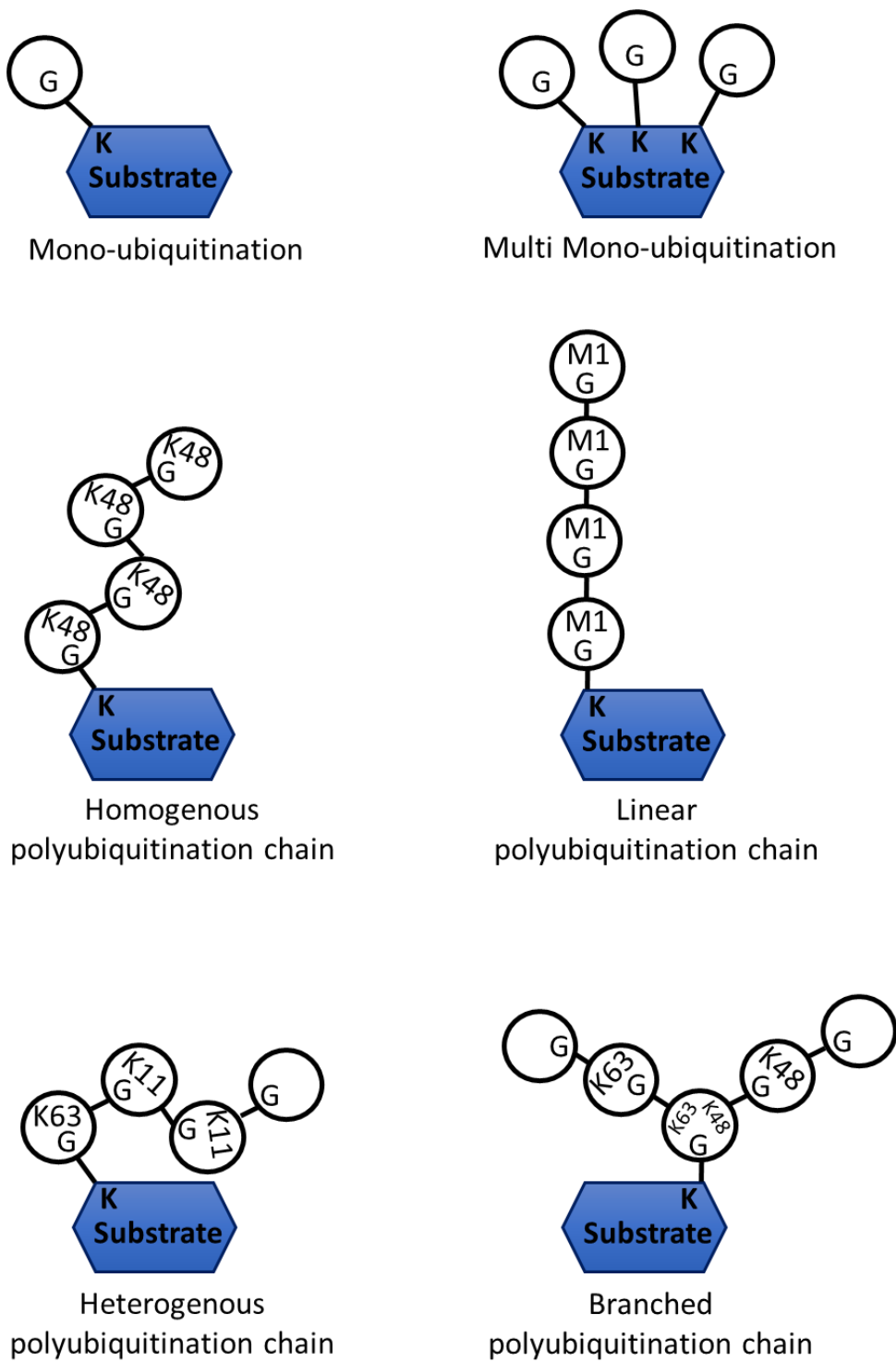


Figure 1-5: Examples of ubiquitin chain linkages. Ubiquitin is represented as the black open circle. G, glycine; K, lysine; M, methionine. The diagram is drawn based on figures from Komander *et al* (Komander and Rape, 2012).

1.4.2.1 Mono-ubiquitination

Mono-ubiquitination is the addition of a single ubiquitin molecule to one lysine in the protein substrate. It regulates proteins through several mechanisms such as: changing stability, subcellular localisation, conformation, activity and interacting partners. Mono-ubiquitination is involved in distinct cellular functions including histone regulation, DNA damage response, endocytosis, and the budding of retroviruses from the plasma membrane. Although mono-ubiquitination is associated with non-proteolytic functions by the proteasome, it has been shown to cause proteasomal-mediated degradation. Moreover, mono-ubiquitination is the first step in the formation of poly-ubiquitin chains. In addition, proteins can be modified by multi mono-ubiquitination, which is the conjugating of a single ubiquitin at several lysine sites in the substrate protein. It can be a signal for internalisation of cell-surface receptors and their subsequent degradation in lysosomes, or recycling to the cell surface. Moreover, it has also been shown to be involved in proteasomal-mediated degradation (Boutet *et al.*, 2007).

1.4.2.2 Poly-ubiquitination

Homotypic chains at all the seven lysine residues of ubiquitin have been shown to be formed *in vivo* (Peng *et al.*, 2003; Xu and Peng, 2006). Each of these linkages have been associated with specific functions, with K-48 linked ubiquitin chains being the best characterised as responsible for elimination of the target protein by the proteasomal degradation system. K-48 and K-11 linked ubiquitin chains are the most abundant linkages (Xu *et al.*, 2009). A summary of the roles for each ubiquitin linkage is described in Table 1.1.

Linkage	Physiological function
K6	<p>K6 linkages increase in response to UV radiation – indirectly associated with DNA damage response although not fully elucidated. Example of E3 ligase assembling K6-linked ubiquitin chain includes the BRCA1–BARD1 heterodimer (Wu-Baer <i>et al.</i>, 2003).</p> <p>Role in promoting protein stabilisation by preventing proteasomal degradation (Shang <i>et al.</i>, 2005).</p> <p>Role in Parkin-mediated mitophagy by modulating cellular localisation. The E3 ligase Parkin is responsible for ubiquitination-mediated destruction of depolarized dysfunctional mitochondria by autophagy (mitophagy). K6-linked chains prevents Parkin localisation to depolarised mitochondria, preventing mitophagy (Durcan <i>et al.</i>, 2015).</p>
K11	<p>Involved in cell cycle control. The APC/C complex assembles the K11-linked ubiquitin chains on proteins involved in mitosis and targets them for proteasomal degradation to mediate mitotic exit and cell cycle progression (Matsumoto <i>et al.</i>, 2010).</p> <p>Implicated in cellular adaptation to hypoxia. The transcription factor HIF-1α is modified by K-11, causing its destabilisation. K11-linkage-specific DUB Cezanne (OTUD7B) promotes the stability and expression level of HIF-1α (Bremm <i>et al.</i>, 2014).</p> <p>Linked to the endoplasmic reticulum-associated degradation (ERAD) pathway (Xu <i>et al.</i>, 2009).</p> <p>Role in cell signalling. TNF-α stimulation and activation of NF-κB requires the addition of K11-linked chains on receptor-interacting protein 1 (RIP1) (Dynek <i>et al.</i>, 2010).</p>
K27	<p>Role in DNA damage response by protein recruitment. RNF168-mediated K27-linked poly-ubiquitination of histone H2A proteins is a major ubiquitin linkage on chromatin following DNA damage, required for the recruitment of several crucial DNA damage response mediators such as 53BP1 and Rap80 at sites of DNA damage (Gatti <i>et al.</i>, 2015).</p> <p>Role in signal transduction and are required for the innate immune response triggered by microbial DNA. For example, AMFR and INSIG1, an E3 ubiquitin ligase complex mediates K27-linked poly-ubiquitination of an essential host immune response protein, STING. This activates a series of downstream signalling, ultimately leading to activation of the interferon regulatory factor-3 (IRF3) and/or NF-κB signalling pathways (Wang <i>et al.</i>, 2014).</p>

Linkage	Physiological function
K29	<p>Role in protein stabilisation. K29 linked ubiquitin of β-catenin enhances its stability leading to up-regulation of the Wnt signalling pathway (Hay-Koren <i>et al.</i>, 2011).</p> <p>Role in cell signalling. Axin, a component of the Wnt signalling pathway is involved in destruction of β-catenin. The E3 ligase, Smurf, mediates K29-linked poly-ubiquitination of Axin and prevents its interaction with Wnt co-receptors LRP5/6, thereby represses Wnt/β-catenin signalling (Fei <i>et al.</i>, 2013).</p> <p>Signals for lysosomal destruction. The E3 ligase, AIP4 is a negative regulator of the Notch pathway. It mediates K29-linked poly-ubiquitination of the positive regulator of the Notch pathway, Deltex, and targets for lysosomal degradation (Chastagner <i>et al.</i>, 2006).</p>
K33	<p>Role in inhibition of T-cell antigen receptor (TCR) signalling. K33-linked poly-ubiquitination of T-cell receptor-ζ prevents it from undergoing phosphorylation resulting in inhibition of downstream signal transduction (Huang <i>et al.</i>, 2010).</p> <p>Role in inhibition of AMP-activated protein kinase (AMPK)-related protein kinase signalling. K33-linked ubiquitination of AMPK-related kinases, NUAK1 and MARK4, may inhibit their phosphorylation by the LKB1-tumour suppressor kinase and prevent their activation (Al-Hakim <i>et al.</i>, 2008).</p> <p>Role in post-Golgi protein trafficking. Attachment of non-degradable K33-linked ubiquitin chains onto coronin7 (Crn7) by the E3 ligase Cul3–KLHL20, promotes Crn7 recruitment to the trans-Golgi network (Yuan <i>et al.</i>, 2014).</p>
K48	<p>Targets proteins for destruction by the proteasome (Chau <i>et al.</i>, 1989).</p>
K63	<p>Role in activating the NF-κB signalling by enabling protein-protein interactions to facilitate signal transductions (Conze <i>et al.</i>, 2008). Involved in activation of the T-cell receptor pathway. NF-κB activation by T- and B-cell receptors in response to antigen-receptor stimulation is mediated through K63-linked poly-ubiquitination of an essential NF-κB modulator, NEMO (Zhou <i>et al.</i>, 2004).</p> <p>Role in protein trafficking, including endocytosis of cell-surface receptors by endosomal and vacuolar sorting complexes (Lauwers <i>et al.</i>, 2009; MacDonald <i>et al.</i>, 2012).</p> <p>Role in the control of protein synthesis through activation of ribosomes at specific points in the cell cycle (Spence <i>et al.</i>, 2000). Moreover, K63 ubiquitination is increased in response to oxidative stress which serves to stabilize the ribosome complex and polysomes, thereby promoting protein synthesis and cellular viability (Silva <i>et al.</i>, 2015).</p> <p>Important in DNA damage response. K63 poly-ubiquitination of histone H2A by the E3 ligase RNF8 following DNA damage is required for the recruitment of 53BP1 and BRCA1 (Huen <i>et al.</i>, 2007). Moreover, K63-linked chains on FANCG following DNA interstrand crosslinks enables the recruitment of the BRCA1</p>

	complex and the formation of Rad51 foci at the damage site. This initiates the homologous recombination repair pathway (Zhu <i>et al.</i> , 2015).
--	--

Table 1.1: Reported roles for homogeneous lysine linked ubiquitin chains.

In addition to the canonical lysine linked ubiquitin chains, ubiquitin can be ligated to protein substrates via its N-terminal methionine (M1) and forms a linear ubiquitin chain. This is assembled by the RBR E3 ligase complex, linear ubiquitin chain assembly complex (LUBAC) (Kirisako *et al.*, 2006). Ubiquitin M1 linkages are pivotal in inflammatory and immune responses by regulating the activation of the transcription factor NF- κ B. As such they have an important role in the immune and inflammatory responses (Iwai and Tokunaga, 2009; Ikeda *et al.*, 2011).

1.5 KMT5A

The KMT5A protein, also known as SET8 and PR-SET7, is a member of the SET domain family of lysine methyltransferases. It is located on chromosome 12q24.31, encoding a 393 amino acid protein with a molecular weight of approximately 42 kDa. KMT5A specifically mono-methylates histone 4 on lysine 20 (H4K20Me1), and is the sole mono-methyltransferase responsible for this histone modification in higher eukaryotes (Couture *et al.*, 2005; Xiao *et al.*, 2005). It recognises the sequence RHRK²⁰VLRDN within H4 N-terminus (Yin *et al.*, 2005). Moreover, it mono-methylates a number of non-histone proteins including p53. As such, KMT5A plays a key role in maintaining genome integrity, gene transcription and cell cycle progression through regulating higher-order chromatin structure either directly or indirectly, modulating the expression of genes that are important for DNA synthesis and in the G1-S phase transition.

1.5.1 Structure of KMT5A

The structure of KMT5A is divided into two functional domains: the SET or enzymatic domain located at the C-terminus and the N-terminal histone binding domain (Yin *et al.*, 2005; Yin *et al.*, 2008). As already alluded to, KMT5A's enzymatic activity is restricted to the addition of one methyl group from the co-factor, S-adenosylmethionine (SAM), to the side-chain nitrogen of lysine 20 on H4. Moreover, KMT5A exhibits greater enzymatic activity towards nucleosomal H4 over either histone octamer or H4 polypeptide (Fang *et al.*, 2002; Nishioka *et al.*, 2002).

This has been shown following the determination of the structure of KMT5A SET domain by crystallographic studies. For example, the active site of KMT5A, where it accommodates the amino group of its substrate is a small pocket, is only capable of housing a mono-methylated lysine compared to other H4K20 methyltransferases, Suv4-20h1 and Suv4-20h2, which have a more open active site and catalyse di- and tri-methylation (Xiao *et al.*, 2005). Furthermore, an evolutionary conserved tyrosine residing in the active site of KMT5A ensures methylation is terminated after the conjugation of one methyl group by forming hydrogen bonds with the mono-methylated lysine of the substrate. Moreover, part of the KMT5A specificity is governed by an array of contacts with the surrounding residues, in particular the histidine residue flanking K20 in H4. This residue is recognised by KMT5A and contributes to the complete formation of KMT5A's lysine-access channel which connects the substrate and cofactor binding sites and as a result enables efficient enzymatic activity (Couture *et al.*, 2005; Xiao *et al.*, 2005).

The insert or Set-1 region (i-set) is a region approximately in the middle of the SET domain which is responsible for mediating the enzyme's interactions with its substrate. Recently, it was reported that KMT5A binds the nucleosome through multivalent interactions mediated by c-terminal (s-set) and n-terminal (n-set) flanking regions of i-set. Subsequently, this was proposed to enable KMT5A to recognise the nucleosome architecture in addition to individual elements in its substrate (Girish *et al.*, 2016).

In contrast to the C-terminal domain, the N-terminal region of KMT5A-related proteins, as well as, KMT5A isoforms share low sequence homology with the exception of a conserved region containing a Cdk phosphorylation consensus sequence and a D-box destruction motif recognised by the APC/C ubiquitin ligase complexes (Wu *et al.*, 2010). Although, the structure of KMT5A N-domain has not been resolved to date, it has been speculated to have a floppy structure and play a role in stabilising the interaction of KMT5A with the nucleosome. Consistently, using deletion mutants, immunostaining and imaging techniques, Yin demonstrated that the KMT5A N-domain truncation mutant was always located in the nucleus and was responsible for binding to H4 N-terminal (Yin *et al.*, 2008).

1.5.2 Isoforms of KMT5A

There are three isoforms of KMT5A which all share the same C-terminus, but differ in their N-terminal sequence. Two of the isoforms were identified by Abbas in U2OS cells (a human osteosarcoma derived cell line) as Set8a and Set8b following their observation of KMT5A protein running as a doublet on SDS-PAGE (Abbas *et al.*, 2010).

Set8a is reported to consist of 352 amino acids and correspond to the heavier and slower-migrating KMT5A band. Set8b is composed of 322 amino acids and is a splice variant of Set8a, which is generated as a result of missing amino acids 10-40 within exon 2 of KMT5A. Furthermore, Set8b was shown to be functional *in vivo* and more abundant than Set8a (Abbas *et al.*, 2010). Although not stated by the group, Set8a and Set8b have a molecular weight of approximately 39 and 36 kDa. Moreover, the largest isoform of KMT5A is a 393 amino acid long protein with a molecular weight of approximately 42 kDa. This isoform differs to Set8a by a sequence of 41 amino acids extended in its N-terminus and an alternative sequence in amino acids 42-57 (Figure 1.6, information from UniProt and NCBI websites).

Most of the studies have numbered KMT5A residues based on the 352 amino acid long protein. The 42 kDa isoform is the observed form of KMT5A by our group and is consistent with the molecular weight stated by the anti-KMT5A antibody datasheets. Therefore, KMT5A residues have been numbered based on the 393 amino acid long protein in this work.

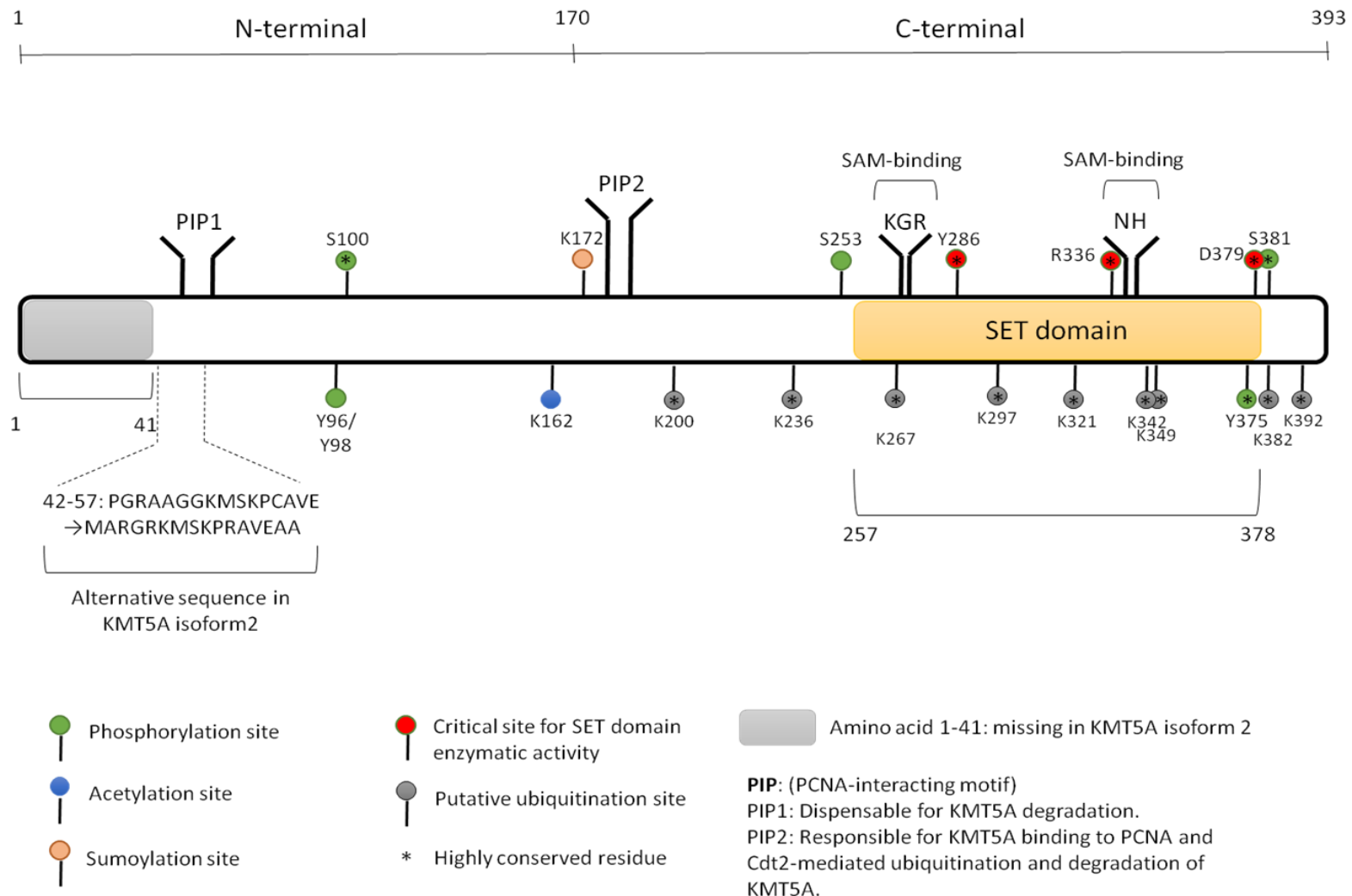


Figure 1-6: Structure of KMT5A isoforms. The diagram is drawn based on information from UniProt, Abbas *et al* (Abbas *et al.*, 2010), Wang *et al* (Wang *et al.*, 2015) and Wu and Rice (Wu and Rice, 2011).

1.5.3 Function

KMT5A mediates its function primarily through mono-methylating H4K20. The methylation status of H4K20 contributes to chromosome behaviour and it can undergo further methylation to become di- and tri-methylated by distinct methyltransferases, Suv4-20h1 and Suv4-20h2, respectively (Schotta *et al.*, 2004). The single methyl group can also be removed from H4K20Me1 by demethylase, PHF8, whilst no demethylase for H4K20Me2/3 has been identified (Liu *et al.*, 2010; Qi *et al.*, 2010). Each degree of methylation is uniquely distributed throughout the genome. Whilst H4K20Me2 is widely present on chromatin, H4K20Me1 and H4K20Me3 are less abundant (Pesavento *et al.*, 2008; Yang *et al.*, 2008). Furthermore, they each have distinct functions for example, H4K20Me1 is associated with chromatin condensation processes (Trojer *et al.*, 2007) and has a role in both the activation and repression of gene transcription (Barski *et al.*, 2007). H4K20Me2 is involved in the DNA repair pathway by guiding DNA repair proteins to DNA strand breaks (Sanders *et al.*, 2004; Botuyan *et al.*, 2006). Finally, H4K20Me3 is enriched in pericentromeric heterochromatin and is correlated with transcriptional repression (Schotta *et al.*, 2004) where global loss in its level are associated with tumourigenesis (Fraga *et al.*, 2005). However, KMT5A-mediated mono-methylation of H4K20 is the first step and the primary substrate required for the formation of subsequent methylation states (Oda *et al.*, 2009).

The enzymatic activity of KMT5A is essential for viability. Its biological importance was demonstrated to be critical during embryonic development in *Drosophila*, where *KMT5A* null mutation leading to its complete loss-of-function caused lethality at the third instar larval stage (Karachentsev *et al.*, 2005). This was further demonstrated using *KMT5A* knockout mouse model in which loss of KMT5A led to embryonic lethality at the four-cell stage of embryogenesis. However, restoring KMT5A function by microinjection of mRNA encoding the wild-type, but not its catalytically-dead form into the two-cell embryo rescued its development (Oda *et al.*, 2009). Therefore, KMT5A has a critical role in regulating the genomic integrity, DNA-based processes and the development of eukaryotic cells.

1.5.3.1 Cell cycle progression

KMT5A and H4K20Me1 levels are under precise regulation during the cell cycle. Their levels change dynamically, being most abundant during G2/M phase and absent in S phase of the cell cycle. This fluctuation reflects the essential role of KMT5A-mediated H4K20Me1 in regulating higher-order chromatin structure and subsequently the proper progression of the cell cycle. The impact of KMT5A loss on cell cycle progression has been extensively studied in mammalian cells using mainly knockdown approaches in transformed cells, as well as, a knockout and a conditional knockout mouse and *Drosophila* models with contrasting conclusions.

In accordance with KMT5A and H4K20Me1 demonstrating high levels in mitosis, *KMT5A* null mutation in *Drosophila* neuroblasts led to the formation of abnormal chromosomes, defective in chromosome condensation and separation during mitosis. These neuroblasts also exhibited delayed progression through early stages of mitosis and decreased S phase population (Sakaguchi and Steward, 2007). Similarly, conditional inactivation of the *KMT5A* gene in mouse embryonic stem (ES) cells caused decondensation of chromosomes during mitosis and accumulation of cells in G2/M phase of the cell cycle, as well as delayed S phase progression. Detailed analysis using cell cycle arrest experiments revealed that cell cycle progression was disturbed in the following S phase and G2/M phase when cells had undergone a single round of mitosis without KMT5A protein, which was when H4K20Me1 levels started to decrease, suggesting cell cycle defects are due to reduced H4K20Me1 levels rather than KMT5A protein *per se* (Oda *et al.*, 2009). Furthermore, similar observations were made with transient depletion of KMT5A in HEK293 cells, which caused cell cycle arrest at G2 with subsequent increased G2/M population and global decondensation of chromosomes (Houston *et al.*, 2008). The failure of chromosome compaction could be linked to either of the H4K20Me1-binding proteins, L3MBTL1 or condensin 2, which are both involved in chromatin compaction (Trojer *et al.*, 2007).

In contrast, although cell cycle was impaired with KMT5A knockdown, it was shown to be due to delayed S phase progression by causing defective replication fork activity and origin firing rather than slowed mitotic progression in U2OS human osteosarcoma cells (Jørgensen *et al.*, 2007; Tardat *et al.*, 2007). Moreover, KMT5A was hypothesised to have other substrates than H4K20 during S phase to promote S phase progression (Tardat *et al.*, 2007).

Collectively, KMT5A has a critical role maintaining genomic stability, either through having a role in accurate completion of DNA replication or mitosis, and potentially links these two processes together.

1.5.3.2 DNA replication

As already alluded to, despite the very low levels of KMT5A and H4K20Me1 during S phase (Oda *et al.*, 2009), KMT5A-mediated H4K20Me1 generation has been shown to be critical for DNA replication. Firstly, studies of several well-characterised human replication origins, which are discrete chromosomal sites where genome duplication initiates, including *Top1*, *MCM4*, *LaminB2* and *β -globin* genes (Goren *et al.*, 2008; Miotto and Struhl, 2008; Miotto and Struhl, 2010) showed a transient increase in H4K20Me1 by KMT5A. This event preceded the onset of DNA-replication licensing at the end of mitosis (Tardat *et al.*, 2010), a critical process responsible for activation of replication origins that starts towards the end of mitosis, continues through to G1 and terminates in S phase (Remus and Diffley, 2009).

Secondly, although KMT5A is highly unstable during S phase, inhibiting KMT5A proteasomal-mediated degradation leads to its stabilisation and is found to localise at sites of active replication (Tardat *et al.*, 2007), where it interacts with PCNA (Proliferating cell nuclear antigen) through its PCNA-interacting motif (PIP domain) (Jørgensen *et al.*, 2007; Huen *et al.*, 2008). Furthermore, physiological expression of KMT5A resistant to CRL4^{Cdt2}-mediated ubiquitination and degradation during S phase leads to maintained H4K20Me1 and DNA re-replication exemplified by cells with a larger nuclear volume and >4n DNA content, which occurred dependent on the catalytic activity of KMT5A (Abbas *et al.*, 2010; Tardat *et al.*, 2010). Moreover, inhibiting PCNA and CRL4^{Cdt2}-mediated KMT5A degradation leads to disappearance of H4K20Me1 at replication origins and prevents origin licensing (Tardat *et al.*, 2010).

Finally, as discussed previously, progression through S phase is delayed upon loss of KMT5A catalytic activity accompanied by reduced numbers of active origins in S phase (Jørgensen *et al.*, 2007; Tardat *et al.*, 2007). Consistent with having a positive role in replication licensing, KMT5A silencing impairs the chromatin loading of CDC6, MCMs and ORC2 which are components of the pre-replicative complex (pre-RC), a multi-protein complex that is recruited at origins to make them competent for replication. Furthermore, artificial targeting of a catalytically active KMT5A to an origin-free locus in the genome promotes H4K20Me1 and recruitment of the pre-RC components (Tardat *et al.*, 2010).

In addition to KMT5A mediated H4K20Me1 creating an environment for origin firing as one of the mechanisms for facilitating DNA replication, H4K20Me1 may affect the status of H4 acetylation which also modulates replication licensing. In this case, another H4 modifying enzyme, HBO1 which acetylates H4 at origins in G1 phase and induces replication licensing is

found at origins enriched with H4K20Me1 during mitosis (Iizuka *et al.*, 2006; Miotto and Struhl, 2008; Miotto and Struhl, 2010). In contrast to KMT5A, HBO1 level is stable throughout the cell cycle and does not cause DNA re-replication if overexpressed (Iizuka *et al.*, 2006; Miotto and Struhl, 2008). Therefore, a DNA replication model modulated by a cascade of H4 modifications has been proposed in which a burst of KMT5A-mediated H4K20Me1 in mitosis is followed by increased acetylation of H4 at K5, K8 and K12 during G1 phase. The degradation of KMT5A through PCNA and CRL4^{Cdt2} dependent mechanisms and its removal from the origins at the onset of S phase then ensures DNA replication occurs once in each cell cycle (Brustel *et al.*, 2011).

Moreover, KMT5A regulation of DNA replication can be through transcriptional regulation of E2F-1 target genes that are important for DNA synthesis and in the G1-S phase transition (Abbas *et al.*, 2010; Liu *et al.*, 2010). Consistently, KMT5A has been shown to repress E2F-target genes by directly docking to L3MBTL1 (lethal 3-malignant brain tumour like protein 1) at E2F target gene promoters (Trojer *et al.*, 2007; Kalakonda *et al.*, 2008).

1.5.3.3 DNA damage and repair

A large number of studies have shown that mammalian cells lacking KMT5A undergo extensive DNA damage. For example, a massive spontaneous DNA damage was induced in mouse ES cells with complete loss of KMT5A function (Oda *et al.*, 2009), as detected by an increase in γ -H2AX, a well-established marker for DNA double strand breaks (DSBs) (Pilch *et al.*, 2003). Interestingly, unlike mouse ES cells, there was no major change in the level of γ -H2AX, as well as the 53BP1 DNA repair protein in KMT5A^{-/-} embryos which did not survive past the eight-cell stage, suggesting DNA damage is not necessarily responsible for lethality in these embryos (Oda *et al.*, 2009). Similar to mouse ES cells, substantial DNA damage was observed in HEK293 and U2OS cells lacking KMT5A. This led to activation of the DNA damage response via ATM and ATR kinase-mediated pathways, two critical DNA damage checkpoints, followed by p53-dependent DNA damage response (DDR) (Jørgensen *et al.*, 2007; Tardat *et al.*, 2007; Houston *et al.*, 2008). The spontaneous DNA damage upon KMT5A inhibition also led to sensitisation of breast cancer cells to DNA damage (Yu *et al.*, 2013). Consistently, in an unbiased siRNA screen to identify proteins important in maintaining genome stability through modulating the DDR, KMT5A depletion led to increased γ -H2AX in HeLa cells (Paulsen *et al.*, 2009).

The DNA damage caused by KMT5A depletion was dependent on cells undergoing DNA replication. Furthermore, this damage was suppressed with depletion of Rad51, a key regulator

of the homologous recombination pathway, which is a pathway that plays an important role in the DDR during DNA replication (Jørgensen *et al.*, 2007). Recruitment of 53BP1, a critical component of mammalian DDR that is involved in the initial sensing and signalling of DNA strand breaks and is pivotal in determining non-homologous end joining (NHEJ)-directed repair (Ward *et al.*, 2006; Panier and Boulton, 2014), was speculated to be disrupted upon KMT5A depletion, as an underlying mechanism for the DNA damage induction. However, this was refuted by Jørgensen (Jørgensen *et al.*, 2007) as KMT5A depletion did not influence the recruitment of 53BP1 at DNA DSBs, and was bound to H4K20Me2 (Jørgensen *et al.*, 2007). On the other hand, although H4K20Me2 was an important determinant in 53BP1 binding at DSBs, KMT5A-mediated H4K20Me1 was shown to be the upstream event required for *de novo* H4K20Me2 by Suv4-20 and efficient NHEJ-directed repair. Moreover, recruitment of KMT5A at DSBs was mediated by NHEJ Ku70 protein (Tuzon *et al.*, 2014). In line with this, NHEJ-directed repair was severely impaired in KMT5A-depleted cells, concurrent with accumulated unrepaired DSBs (Houston *et al.*, 2008; Oda *et al.*, 2009). Interestingly, KMT5A levels were shown to be a determinant of the DDR pathway as KMT5A depletion severely impaired the NHEJ-directed repair, whilst the HDR was significantly enhanced.

Although loss of KMT5A robustly induces DNA damage which has been attributed to genomic instability as a result of defective DNA replication and mitosis, degradation of KMT5A is required to enable DNA repair. KMT5A was shown to be recruited to sites of laser-induced DNA damage and bound chromatin through docking to PCNA. The CRL4^{Cdt2} complex then ubiquitinated and degraded KMT5A. This mechanism restricts the presence of KMT5A on chromatin after DNA damage in order to relax the chromatin to enable access of DNA repair pathway proteins. In line with KMT5A destruction following DNA damage, a proteomics study conducted global ubiquitin profiling in whole-cell lysates to identify DNA damage-regulated ubiquitination sites and revealed KMT5A is ubiquitinated at 11 lysine residues, all of which were residing in the KMT5A C-terminal domain. KMT5A ubiquitination was induced in response to UV and ionizing radiation which marked KMT5A for proteasomal degradation as the lysine sites could only be detected in the presence of the proteasomal inhibitor, MG132 (Elia *et al.*, 2015).

1.5.3.4 Gene regulation/ Transcription

The role of KMT5A and its mark, H4K20Me1 in regulating gene transcription is controversial. Earlier studies found KMT5A is enriched within transcriptionally repressed chromatin (Fang *et al.*, 2002; Nishioka *et al.*, 2002). Consistently, H4K20Me1 was shown to have a putative role in X chromosome inactivation, where in combination with histone H3 lysine 27 tri-methylation

(H3K27Me3) marked the beginning of X inactivation in mouse ES cells (Kohlmaier *et al.*, 2004). Furthermore, detailed analysis using ChIP-chip experiments on a large subset of the genome in HeLa cells revealed KMT5A is preferentially enriched within gene bodies of specific genes. The expression of these H4K20Me1-enriched genes was upregulated upon loss of KMT5A and H4K20Me1 (Congdon *et al.*, 2010). Moreover, H4K20Me1 is shown to localise at repressed E2F-target genes. Stable expression of KMT5A inhibited the transcription of various E2F1-regulated genes including cyclin E2, cyclin A2, CDC25A, geminin, MCM7 and Cdt1, as well as histone genes H2A, H2B, H3 and H4 where full repression was dependent on KMT5A catalytic activity (Abbas *et al.*, 2010). KMT5A also repressed a subset of p53 target genes, described in Chapter 1.5.3.5.

Deposition of H4K20Me1 by KMT5A is suggested to repress transcription by directly promoting chromatin compaction (Lu *et al.*, 2008; Oda *et al.*, 2009), or indirectly through the recruitment of the repressor protein L3MBTL1 (Trojer *et al.*, 2007). Indeed, L3MBTL1 preferentially binds mono- and di-methylated forms of H4K20 (Li *et al.*, 2007; Min *et al.*, 2007). Moreover, the transcription of endogenous H4K20Me1-associated genes including *RUNX1* and *c-myc* were up-regulated with the loss of H4K20Me1 and subsequent depletion of L3MBTL1 (Trojer *et al.*, 2007; Sims and Rice, 2008). Additionally, loss of PHF8 and the subsequent elevation in H4K20Me1 level leads to increased L3MBTL1 binding which causes increased repression of E2F-controlled genes (Liu *et al.*, 2010).

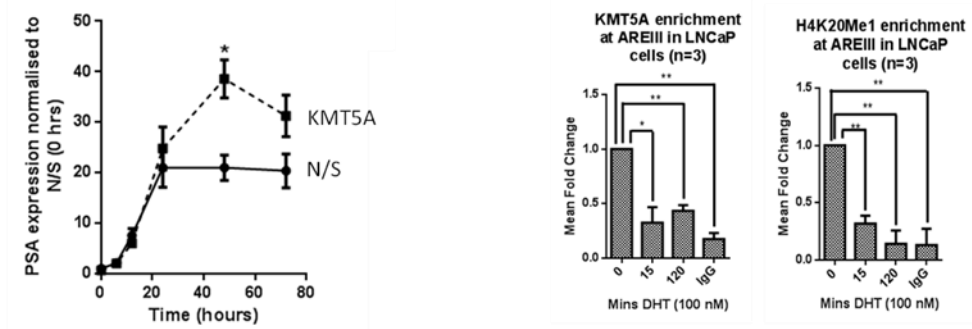
In contrast, H4K20Me1 enrichment has also been detected in active promoters, where it overlaps with RNA polymerase II (RNA pol II) (Talaszi *et al.*, 2005) and transcribed regions which suggested it as a marker of transcription elongation (Vakoc *et al.*, 2006), implicating a role in activating transcription. Consistently, a genome-wide ChIP analysis in human T lymphocytes found H4K20Me1 is associated with gene activation as it was found downstream of transcription start sites (TSS) of active genes (Barski *et al.*, 2007). This was further supported as H4K20Me1 was one of the histone modifications highly correlated with active transcription (Wang *et al.*, 2008b).

In line with a role in activating transcription, gene-specific studies have also provided evidence for H4K20Me1 positively regulating gene transcription. For example, KMT5A-mediated H4K20Me1 at the PARP γ gene causes an up-regulation of PARP γ to promote adipocyte differentiation (Wakabayashi *et al.*, 2009). Furthermore, KMT5A was shown to be required for ER α -mediated gene expression through deposition of H4K20Me1. In MCF7 cells, H4K20Me1 level was elevated at the ER- α target gene promoter, TFF1, upon receptor activation. On the

other hand, this enrichment was almost abolished in KMT5A depleted MCF7 cells. Interestingly, KMT5A interacting partners differed at various regions of the TFF1 gene. Whilst KMT5A and ER α were co-occupied only at TFF1 promoter, KMT5A was then found to co-occupy with pol II only at TFF1 coding regions, consistent with a role in both transcriptional initiation and elongation (Li *et al.*, 2011a). Similarly, H4K20Me1 and KMT5A were enriched at Wnt target genes upon Wnt stimulation. The activation of Wnt signalling led to the recruitment of KMT5A into the β -catenin/TCF4 transcription complex, required to activate Wnt-mediated gene transcription in both mammalian cells and zebrafish; therefore, suggested to act as a co-activator (Li *et al.*, 2011b). Interestingly, KMT5A was discovered to act as a dual transcriptional regulator at TWIST-target genes, E-cadherin and N-cadherin. TWIST which is a pivotal transcription factor in promoting epithelial-mesenchymal transition (EMT) leading to metastasis, interacts with KMT5A. Whilst this interaction causes suppression of the epithelial marker, E-cadherin, it activates the transcription of the mesenchymal marker, N-cadherin (Yang *et al.*, 2012).

Importantly, KMT5A is also found to interact with the AR and through deposition of H4K20Me1, activate the transcription of an AR-target gene, *PSA*, in the androgen dependent PC cell line model, LNCaP. Further, stimulation of AR signalling by DHT led to enriched KMT5A and H4K20Me1 at the *PSA* promoter (Yao *et al.*, 2014). The role of KMT5A in regulating the AR has also been extensively studied in the Solid Tumour Target Discovery (STTD) group by Dr Kelly Coffey, who has demonstrated KMT5A exhibits differing functions towards the AR between models of androgen dependent and independent PC. KMT5A knockdown experiments in the LNCaP PC cell line representative of androgen sensitive PC led to an increase in the AR regulated genes, *PSA* and *TMPRSS2* at the mRNA and protein levels. In contrast, this led to a reduction in AR regulated genes in the CRPC model, LNCaP-AI cells, as well as other drug-resistant PC cell lines. Furthermore, KMT5A and H4K20Me1 were enriched at inactive androgen-responsive genes which were lost upon AR activation in LNCaP cells whereas, they were enriched at AR-responsive genes upon AR activation in LNCaP-AI cells. This suggests that KMT5A acts as a co-repressor in LNCaP cells but an activator in LNCaP-AI cells (Figure 1.7, Coffey *et al.*, unpublished data).

LNCaP (model of androgen-sensitive PC): *KMT5A* acts as an AR repressor



LNCaP-AI (model of CRPC): *KMT5A* acts as an AR activator

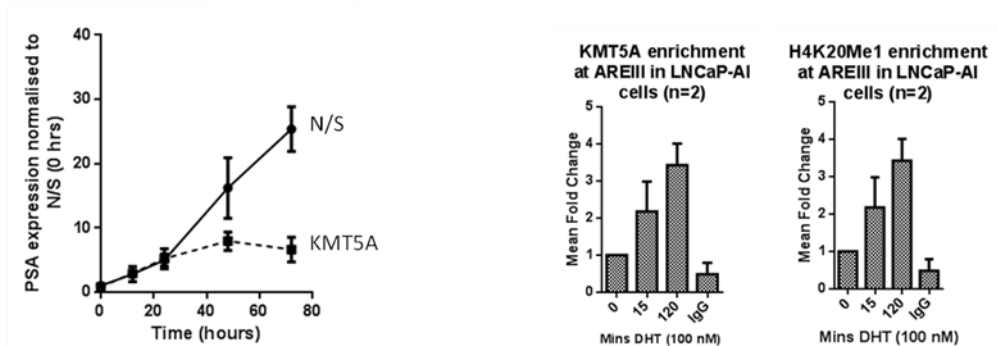


Figure 1-7: Summary of previous *KMT5A* findings in regulating the AR in LNCaP and LNCaP-AI cells (Coffey et al, unpublished data).

1.5.3.5 Non-histone proteins

In addition to histone methylation, *KMT5A* has been shown to methylate non-histone proteins, with the most archetypal substrate being p53. *KMT5A* methylates p53 at lysine 382 (K382) and causes repression of the highly responsive p53-target genes, *PUMA* and *p21*. *KMT5A* prevents p53-mediated transcriptional activation of these genes by inhibiting p53 binding at gene promoters. However, *KMT5A* did not influence weaker p53-responsive genes such as *Bax* and *NOXA*. Negative regulation of p53 function by *KMT5A* was further demonstrated as *KMT5A* and p53K382Me1 were decreased with DNA damage whereas *KMT5A* knockdown led to enhanced p53 activity and increased apoptosis. However, *KMT5A*-mediated mono-methylation of p53 at K382 is suggested to be more complex than just acting as a switch for p53 activity, as it positively regulates the expression of the DNA repair gene, *GADD45*. It was therefore speculated that whilst p53 activity is dampened under normal conditions, *KMT5A*-mediated mono-methylation causes it to be predisposed to specific cellular stress signals, perhaps milder cellular insults. This would enable activation of p53-dependent DNA repair without causing cell death (Shi *et al.*, 2007).

As well as directly regulating p53 function, KMT5A negatively modulates the pro-apoptotic activity of the p53-Numb interaction. Numb is involved in promoting apoptosis and its pro-apoptotic function mainly depends on p53, which is mediated through their interaction with each other in the nucleus, causing p53 stabilisation. However, KMT5A methylates the p53-interacting domain of Numb at two lysine residues, K158 and K163. This prevents the binding of p53 and Numb, leading to increased p53 ubiquitination and degradation. This interaction however, was not influenced by KMT5A-mediated p53 mono-methylation at K382 (Dhami *et al.*, 2013).

Moreover, PCNA undergoes methylation at K248 by KMT5A which is mediated through interaction with the PIP motif of KMT5A. This leads to stabilisation of the PCNA protein by protecting PCNA from ubiquitination and degradation. Furthermore, methylation enhances the binding of PCNA with FEN1, a structure-specific nuclease with both 5' flap endonuclease and 5'-3' exonuclease activities (Lieber, 1997). FEN1 is recruited to DNA replication loci during S phase in a methylated-PCNA, interaction-dependent manner and is responsible for RNA primer removal during Okazaki fragment processing, as well as participating in DNA base excision repair (Chen *et al.*, 1996; Zheng *et al.*, 2007). Inhibiting PCNA methylation abrogates its co-localisation with FEN1, retards Okazaki fragment maturation, DNA replication and induces DNA damage. As FEN1 deregulation has been associated with cancer and the fact that methylated PCNA promotes increased cell growth, together with observed overexpression of KMT5A and PCNA in various cancers, means abnormal interaction between PCNA and FEN1 may cause carcinogenesis (Takawa *et al.*, 2012).

Recently, a screening experiment conducted by Dr Fabio Pittella Silva (Memorial Sloan Kettering Cancer Centre, USA), with the aim of identifying novel KMT5A substrates revealed that almost half of the substrates identified are cytoplasmic proteins. This highlights the important role of KMT5A and suggests many other, as yet un-identified signalling pathways that KMT5A regulates (personal communication).

1.6 Regulation of KMT5A

KMT5A protein expression is under tight regulation in a cell cycle-dependent manner, being at its highest level in G2/M, declines in G1 and is absent during S phase (Rice *et al.*, 2002; Yin *et al.*, 2008; Oda *et al.*, 2010). This is also reflected in the level of H4K20Me1 which follows a similar oscillation pattern throughout the indicated cell cycle phases (Oda *et al.*, 2009). KMT5A level is primarily regulated by post-translational modifications (PTM). However, there is evidence of KMT5A regulation at the transcriptional level, where its deregulation has been

associated with the onset and outcome of various cancers. In addition to its protein level, KMT5A localisation and activity are also directly regulated by PTMs. It is speculated that, KMT5A is subject to additional, as yet unidentified modifications which may in turn influence its function.

1.6.1 Transcriptional regulation of KMT5A

KMT5A fluctuations have also been observed at the mRNA level, however it does not correlate well with the dynamic changes in KMT5A protein throughout the cell cycle (Rice *et al.*, 2002). Additionally, ectopically expressed KMT5A from a constitutively active promoter exhibits similar protein levels as endogenous KMT5A during the cell cycle (Oda *et al.*, 2010).

Interestingly however, KMT5A gene transcription has been indicated to play a role in lineage development and maintenance. In adipogenesis, the peroxisome proliferator activated receptor γ (PPAR γ) protein, a pro-adipogenic transcription factor regulates KMT5A gene expression. PPAR γ -mediated up-regulation of KMT5A is required for differentiation of pre-adipocytes into differentiated adipocytes. Subsequently, KMT5A-mediated H4K20Me1 at PPAR γ gene enhances PPAR γ transcription, where they work in a positive feedback loop to facilitate terminal adipocyte differentiation (Wakabayashi *et al.*, 2009). However, it is not shown whether KMT5A mRNA levels correlated with its protein levels. In addition, using skin-specific KMT5A knockout mouse models, it was shown that KMT5A is a transcriptional target of c-Myc and is essential in mediating Myc-induced proliferation and differentiation of skin (Driskell *et al.*, 2012).

In addition, KMT5A is subject to post-transcriptional regulation by microRNAs (miRNAs). These are a class of noncoding small RNAs that bind to the 3' untranslated region (3'UTR) of target mRNA by complementary base pairing, leading to degradation of the mRNA and translational repression (Bartel, 2004). KMT5A was found to be negatively regulated by miRNA-7, which degraded KMT5A mRNA and subsequently inhibited H4K20Me1 in breast cancer cell lines. Repression of KMT5A by miRNA-7 led to suppression of EMT and invasion of breast cancer cells (Yu *et al.*, 2013).

1.6.2 Post-translational modifications (PTM) of KMT5A

KMT5A is regulated through multiple PTMs including acetylation, phosphorylation, sumoylation and ubiquitination. These modifications have a diverse range of effects on KMT5A including modulating KMT5A stability, structure, cellular localisation and interacting partners. Whilst ubiquitination has been shown to be responsible for maintaining KMT5A protein level under control, acetylation and sumoylation are involved in modulating KMT5A activity rather

than its protein levels (Spektor *et al.*, 2011). Phosphorylation however, is reported to regulate both the expression level and enzymatic activity, as well as, localisation of KMT5A (Yin *et al.*, 2008). The dynamic regulation of KMT5A throughout the cell cycle depends on the orchestrated regulation of these PTMs and their cross-talk to ensure timely cell cycle progression. A summary of PTMs regulating KMT5A protein level is provided in Figure 1.8. The aim of this project is to further elucidate how KMT5A is regulated by a type of ubiquitin conjugation: mono-ubiquitination.

1.6.2.1 Phosphorylation

Phosphorylation of KMT5A modulates its protein stability by regulating KMT5A ubiquitination as many ubiquitin ligases either require phosphorylation or dephosphorylation of their substrate prior to their recognition. Additionally, phosphorylation can directly influence the enzymatic activity of KMT5A.

A KMT5A orthologue has been shown to be phosphorylated in *X. laevis* specifically during mitosis (Stukenberg *et al.*, 1997). KMT5A protein sequence contains a consensus sequence S-P-X-K/R which is highly conserved and is recognised by the Cdk1-cyclin B complex for phosphorylation. KMT5A was subsequently shown to be phosphorylated by this kinase complex at serine 100 (S100) during prophase to early anaphase. This phosphorylation event inhibits KMT5A ubiquitination and proteasomal-mediated proteolysis by the anaphase-promoting complex, APC^{Cdh1}, leading to stabilisation of KMT5A during mitosis. Moreover, it leads to removal of KMT5A from mitotic chromosomes without altering KMT5A enzymatic activity. The extrachromosomal KMT5A is then rapidly dephosphorylated by the Cdc14 phosphatase which enables KMT5A ubiquitination and subsequent proteasomal degradation by the APC^{Cdh1} complex during late mitosis (Wu *et al.*, 2010).

Recently, KMT5A has been reported to be phosphorylated by casein kinase 1 (CK1) on serine 253 (S253). CK1-mediated phosphorylation promotes KMT5A ubiquitination and its destruction by the SCF ^{β -TRCP} complex, leading to KMT5A reduction (Wang *et al.*, 2015).

1.6.2.2 Ubiquitination

KMT5A ubiquitination has been extensively studied and several ubiquitin ligases are shown to down-regulate the abundance KMT5A protein. Some of these ligases are suggested to work synergistically to tightly regulate KMT5A stability through ubiquitination-mediated proteasomal degradation at different stages of the cell cycle, which is essential for both the compaction of mitotic chromosomes and for the control of replication origins.

The CRL4^{Cdt2} ubiquitin ligase complex has been shown to be a master regulator of cell cycle progression, through ubiquitin-mediated degradation of its substrates, the replication initiation protein Cdt1 (Arias and Walter, 2005; Abbas *et al.*, 2008) and the Cdk inhibitor p21 (Abbas *et al.*, 2008; Kim *et al.*, 2008; Nishitani *et al.*, 2008), whose expression are incompatible with DNA replication. The CRL4^{Cdt2} also governs KMT5A levels during S phase and in response to DNA damage (Abbas *et al.*, 2010; Centore *et al.*, 2010; Oda *et al.*, 2010; Jørgensen *et al.*, 2011).

The ubiquitination and degradation of KMT5A by the CRL4^{Cdt2} complex requires the binding of KMT5A to PCNA via the PIP degron (Havens and Walter, 2009). KMT5A consists of two PIP boxes, PIP box 1 (amino acids 51-58) and PIP box 2 (amino acids 178-185), where PIP box 2 has been shown to be responsible for KMT5A binding to PCNA and in turn Cdt2 as mutations of critical residues within this region disrupts these interactions and causes KMT5A stabilisation. On the other hand, KMT5A with mutations in PIP box 1 is still able to interact with PCNA and is dispensable for KMT5A degradation (Abbas *et al.*, 2010). Therefore, KMT5A suppression during S phase is dependent on proteasome activity, KMT5A PIP2 degron and its interaction with both PCNA and Cdt2. Interestingly, although KMT5A PIP mutant degradation was delayed in replicating cells (S phase), it was not abolished even in the presence of Cdt2 knockdown. It was therefore suggested that during S phase, there are additional mechanism(s) which contribute to KMT5A destruction independently of PIP degron and Cdt2 mechanisms (Centore *et al.*, 2010).

Moreover, KMT5A undergoes ubiquitination and degradation by the APC^{Cdh1} ligase complex during late mitosis. This complex binds to KMT5A through a D-box destruction motif to perform its ubiquitination function. Although, there was a modest change in KMT5A transcription during the cell cycle which could partially account for the fluctuations in KMT5A protein level in this study, it was suggested that due to the short half-life of the KMT5A protein, KMT5A is predominantly regulated at the protein level (Wu *et al.*, 2010).

In addition, KMT5A is reported to undergo ubiquitination and degradation by the SCF^{Skp2} E3 ligase complex during G1 to S transition phase. This multi-component E3 complex recognises and interacts with its substrates via its modular F-box component, Skp2. Additionally, the activity of the SCF complex is regulated by the abundance of Skp2 protein. A number of tumour suppressor proteins, including the cell cycle inhibitors, p27 and p21 are destructed by the SCF^{Skp2}. As a consequence, cells are induced to undergo G1-S transition and mitosis. Therefore, Skp2 plays a crucial role in cell cycle progression. Consistently, elevated Skp2 expression is frequently observed in various cancer types such as breast and prostate carcinomas. The ability

of Skp2 to degrade KMT5A is based on the findings that KMT5A protein expression is suppressed as cells exit G1 to enter S phase and that Skp2 silencing leads to elevated KMT5A protein level during the same phase (Yin *et al.*, 2008). Similarly, Skp2 has been suggested to destabilise KMT5A, though outside of the chromatin context. This is because whilst UV treatment led to KMT5A suppression in wild-type MEFs, it was unable to down-regulate KMT5A in Skp2^{-/-} MEFs in the whole-cell extracts. However, in the chromatin-bound fraction, KMT5A stabilisation was only subtle upon Skp2 knockout after UV treatment (Oda *et al.*, 2010). Therefore, it was suggested that KMT5A stability is regulated through two independent pathways, one being Cdt2 and the other Skp2. However, the major limitation of Oda and Yin's work is the lack of demonstrating Skp2 direct ubiquitination of KMT5A and whether Skp2-mediated ubiquitination does indeed cause KMT5A destruction by the proteasome. Conversely, Abbas *et al* demonstrated that the SCF^{Skp2} complex does not play a role in KMT5A regulation as knockdown of the SCF complex subunit, Cullin 1 (CUL1) did not influence KMT5A degradation in U2OS cells (Abbas *et al.*, 2010).

Recently, β -TRCP, an F-box protein was found to interact with KMT5A using mass spectrometry. It was subsequently shown that the SCF ^{β -TRCP} E3 ligase complex targets KMT5A for poly-ubiquitination in a CK1 δ -dependent phosphorylation on S253 during G1 phase of the cell cycle. This complex is activated by DNA-damaging agents and also contributes to ultraviolet-induced KMT5A poly-ubiquitination and degradation in the same manner. The regulation of KMT5A by the SCF ^{β -TRCP} complex is independent of the PIP degron and CRL4^{Cdt2} mechanisms as KMT5A PIP mutant which is protected from Cdt2-mediated ubiquitination and destruction, is efficiently ubiquitinated and degraded by co-expression of CK1 δ and SCF ^{β -TRCP}. Moreover, generation of KMT5A ^{Δ PIP/S253A} mutant which is resistant to destruction by both Cdt2 and β -TRCP ligases led to a more stable form of KMT5A. The F-box protein, Skp2, however was reported to have no effect on KMTA levels (Wang *et al.*, 2015), in contrast to work by Yin and Oda (Yin *et al.*, 2008; Oda *et al.*, 2010).

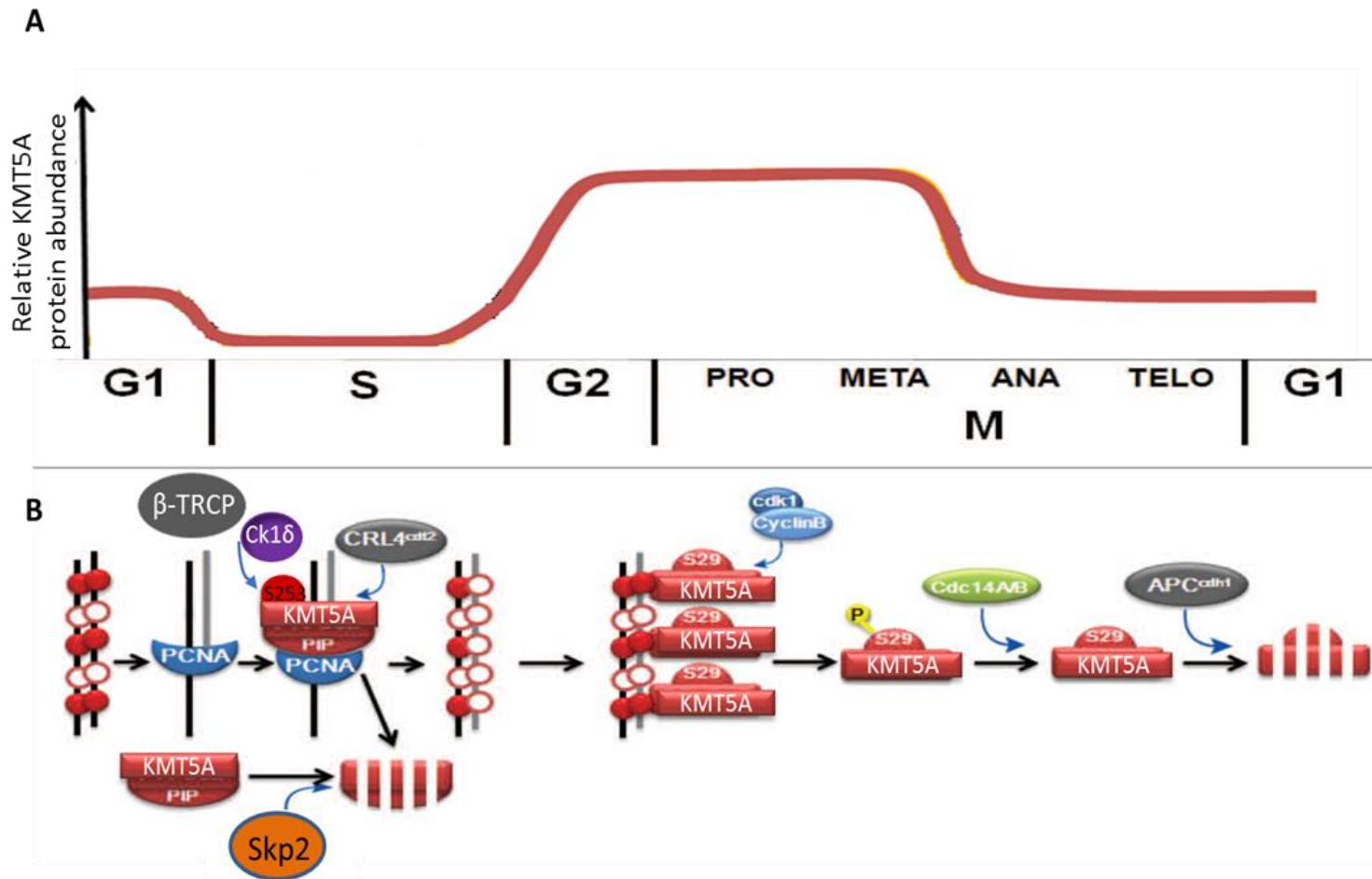


Figure 1-8: Summary of PTMs regulating KMT5A protein levels throughout the cell cycle. (A) Relative abundance of KMT5A protein level during each phase of the cell cycle. (B) Model of KMT5A protein level regulation by various enzymes. During G1, KMT5A resides at specific loci resulting in H4K20Me1 (closed red circles). In this phase, KMT5A is phosphorylated at S253 by Ck1 δ which targets it for ubiquitination and degradation by β -TRCP. KMT5A is degraded at the G1-S border by the CRL4^{Cdt2} complex in a PIP-domain and PCNA dependent manner. Skp2 is suggested to degrade extra-chromosomal KMT5A. The Cdk1/Cyclin B complex phosphorylates the chromatin-bound KMT5A on serine 29 (S29) leading to its stabilisation during mitosis, enabling KMT5A to carry out its function on mitotic chromosomes. KMT5A is then dephosphorylated by Cdc14A/B which facilitates its degradation by the APC^{Cdh1} complex. Image adapted from Wu and Rice (Wu and Rice, 2011).

1.7 KMT5A and the AR

As already discussed, KMT5A is the sole mono-methyltransferase for H4K20, as well as regulating an array of non-histone proteins. It therefore plays a vital role in regulating chromatin-based processes and other cellular pathways. Deregulation of KMT5A activity has been associated with a number of cancers, including PC. The initiation and progression of PC is regulated by a key transcription factor, the AR. The activity of the AR itself is modulated by a plethora of regulatory proteins.

KMT5A was identified as a potential regulator of the AR from selective siRNA library screening in the PC cell line LNCaP, which was undertaken by members of the STTD group. Following its identification, KMT5A was taken forward for extensive validation across a number of PC cell lines including LNCaP, LNCaP-AI, LNCaP-casodex resistant (LNCaP-CdxR) and LNCaP-MDV3100 resistant (LNCaP-MDV3100R). Subsequently, KMT5A was found to act as a functional repressor of AR in LNCaP cells which represent the androgen-dependent stage of PC. However, KMT5A exhibited differing functions towards the AR in LNCaP-AI cells representative of a more aggressive castration-resistant PC and in a number of other drug-resistant PC cell lines, in which KMT5A switched to act as an AR co-activator. Although the underlying mechanism(s) responsible for the opposing role of KMT5A in AR modulation has remained largely unclear, it was demonstrated that KMT5A participates in the ability of the AR to bind to chromatin by regulating AR phosphorylation. This suggests that deregulated KMT5A activity may in turn enhance the activity of the AR. Indeed, KMT5A is over-expressed in different types of cancer and cancer cell lines including bladder cancer, non-small cell lung carcinoma (NSCLC), small cell lung carcinoma (SCLC), chronic myelogenous leukaemia, hepatocellular carcinoma, pancreatic cancer (Takawa *et al.*, 2012) and PC (Coffey *et al.*, unpublished data). Whilst, high expression of KMT5A is positively correlated with poor overall and disease free survival in breast cancer patients (Yang *et al.*, 2012; Liu *et al.*, 2016), low expression is associated with decreased susceptibility to epithelial ovarian cancer and longer survival time (Song *et al.*, 2009; Wang *et al.*, 2012). Moreover, as a positive regulator of EMT in association with TWIST, KMT5A expression has been shown to promote breast cancer metastasis. Consistently, inhibiting KMT5A expression suppressed EMT and invasion of breast cancer cells. Additionally, KMT5A suppresses p53-dependent transcriptional activation in cancer cells by monomethylating p53 at lysine 382. Furthermore, recently, KMT5A has been identified as a druggable target in Neuroblastoma. KMT5A ablation using either genetic or pharmacological approaches, inhibited tumour xenograft growth and extended murine survival. The significant survival advantage observed in these pre-clinical xenograft

Neuroblastoma models was shown to be due to the activation of the p53 canonical pathway. As such KMT5A is emerging as a promising clinical target.

The activity of KMT5A is primarily regulated through PTMs to maintain precise levels of KMT5A throughout the cell cycle, where ubiquitination plays a vital role. Moreover, KMT5A is reported to undergo dynamic cellular localisation in a cell cycle dependent manner. KMT5A ubiquitination and degradation by a number of ubiquitin ligases has been extensively studied and it is becoming evident that multiple ubiquitin ligases target KMT5A through different mechanisms. However, as ubiquitination is known to cause a number of outcomes, it is not known whether KMT5A undergoes any other type of ubiquitination which could modulate KMT5A other than causing its destruction.

1.8 Hypothesis

The overall hypothesis of this thesis is that PTMs of KMT5A could in turn either directly or indirectly modulate AR activity. The identification of novel PTMs regulating KMT5A could be exploited to indirectly target the AR in CRPC.

1.8.1 Aims

- Investigate whether KMT5A is modified by other forms of ubiquitination, specifically mono-ubiquitination
- Identify the site of KMT5A mono-ubiquitination
- Determine whether KMT5A mono-ubiquitination is subject to cell cycle control
- Investigate the effect of mono-ubiquitinated KMT5A on cell cycle
- Determine the role of Skp2 in KMT5A ubiquitination
- Investigate the role of Skp2 in AR signalling

2 Materials and methods

2.1 Reagents and antibodies

Routinely used chemicals were molecular or analytical grade and were purchased from either Sigma-Aldrich or Fisher Scientific unless otherwise stated. A list of antibodies used is listed in Table 2.1.

Antibody	IgG clone type	Host	Manufacturer	Catalogue number
AR-N20	Polyclonal	Rabbit	Santa Cruz biotechnology	sc-816
ATAD2	Polyclonal	Rabbit	Sigma-Aldrich	Kind gift from Dr Steven Darby (Newcastle University)
Flag	Monoclonal	Mouse	Sigma-Aldrich	F3165
KMT5A	Monoclonal	Rabbit	Cell Signalling	2996
KMT5A	Monoclonal	Mouse	Abcam	ab3798
KMT5A	Polyclonal	Rabbit	Santa Cruz biotechnology	sc-135009
Mouse Immunoglobulin Fraction (Normal) Negative Control	-	Mouse	Millipore	12-371
p27 (c-19)	Polyclonal	Rabbit	Santa Cruz biotechnology	sc-528
PARP1/2 (H-250)	Polyclonal	Rabbit	Santa Cruz biotechnology	sc-7150
PSA (H117)	Monoclonal	Mouse	BioGenex	MU014-UCE
pSer10 H3	Polyclonal	Rabbit	Millipore	06-570
Rabbit anti-mouse immunoglobulins HRP conjugate	Polyclonal	Rabbit	Dako	P0260
Rabbit Immunoglobulin Fraction (Normal) Negative Control	-	Rabbit	Dako	X0903
Skp2 (8D9)	Monoclonal	Mouse	Invitrogen	32-3300
Swine anti-rabbit immunoglobulins HRP conjugate	Polyclonal	Swine	Dako	P0217
α -tubulin	Monoclonal	Mouse	Sigma-Aldrich	T9026

Table 2.1: List of primary and secondary antibodies used.

2.2 Mammalian cell culture

2.2.1 Reagents

All cell culture plastic-ware was purchased from Corning. RPMI-1640 growth media with HEPES modification and foetal calf serum (FCS) was from Sigma. Dextran-coated charcoal (DCC) treated FCS was from Thermo Scientific. L-glutamine and trypsin were obtained from Sigma Aldrich.

2.2.2 Cell lines

All cell lines were purchased from the American Type Culture Collection (ATCC). All cell lines except LNCaP-AI were maintained in RPMI-1640 supplemented with 1% L-glutamine (20 mM) and 10% FCS, termed as full media (FM). LNCaP-AI was maintained in RPMI-1640 supplemented with 1% L-glutamine (20 mM) and 10% DCC, termed as steroid depleted FCS media (SDM). All cells were grown in a humidified 5% CO₂ incubator (Sanyo) at 37 °C.

COS7: These kidney-derived cells were from the African green monkey, *Cercopithecus aethiops*.

HEK293T: These cells were derived from the human embryonic kidney. COS7 and HEK293T cell lines are suitable for transfections and were utilised for overexpression studies due to the ease with which they can be transfected and high levels of exogenous protein expression.

LNCaP: Lymph node carcinoma of the prostate (LNCaP) cell line was derived from a metastatic site of the left supraclavicular lymph node of a 50 year old Caucasian male in 1980 (Horoszewicz *et al.*, 1980). LNCaP cells are AR positive and are sensitive to androgens. They are a model of hormone sensitive PC.

LNCaP-AI: LNCaP-Androgen-Independent (LNCaP-AI) were derived from the serial passage of LNCaP cells under androgen depleted conditions, in SDM media. LNCaP-AI cells are AR positive and sensitive to androgens; however, these cells are independent of androgens for growth. They are a model of androgen-independent PC.

2.2.3 Cell passaging

Cells were grown in flasks and were sub-cultured when reaching approximately 70% confluency. Culture media was removed and cells were washed with phosphate buffered saline (PBS). Cells were then trypsinised in the presence of 1x trypsin and left to incubate at 37 °C, 5% CO₂ until the cells detached. Once detached, cells were resuspended in sufficient fresh growth medium to neutralise the trypsin and placed into an appropriate tissue culture flask, or seeded as required.

2.2.4 Cell storage and recovery

Sub-confluent cells were trypsinised as in Chapter 2.2.3 and resuspended in sufficient fresh growth medium. The suspension was centrifuged at 300 g for 5 minutes and the supernatant was removed. The cells were then resuspended in freezing media (10% DMSO, 10% FCS diluted in FM) and 1 mL was aliquoted into cryovials at a density of $2-5 \times 10^6$ cells/mL. The cells were initially frozen at -80°C overnight before being transferred to liquid nitrogen for long-term storage.

For recovery, frozen cells were immediately thawed in a 37°C water bath. Once thawed, cells were gently transferred into 10 mL pre-warmed FM and centrifuged at 300 g for 5 minutes. Pelleted cells were then resuspended in fresh growth medium and left to reattach in a T25 flask. They were subsequently passaged as in 2.2.3.

2.2.5 Mycoplasma test

All cell lines were routinely subjected to mycoplasma testing using Mycoalert mycoplasma detection kit (Cambrex, East Rutherford, USA) at the Northern Institute for Cancer Research. One mL of culture media in which cells were grown for at least 48 hours was removed and sent for testing by Dr Liz Matheson.

2.3 Transient DNA transfection

Cells were plated at appropriate numbers depending on the size of the dish being used so that they were 50-60% confluent after 24 hours. The following day, transfection cocktail was prepared by mixing RPMI-1640 + 1% glutamine (20 mM), termed basal media (BM), with optimized amount of plasmid DNA. Lipofectamine (TransIT-LT1 Transfection Reagent, GeneFlow) was added at a ratio of 2:1 lipofectamine to DNA. The cocktail was incubated at room temperature for 30 minutes to allow lipid-DNA complexes to form. Plasmid DNA concentrations were balanced with the corresponding empty vector. The mixture was then added to cells in a drop-wise manner and incubated for 48 hours at 37 °C and 5% CO₂. All plasmid DNAs used for transient DNA transfection are listed in Table 2.2.

Subsequent KMT5A point mutants and C-terminus truncation mutations were generated in house by site directed mutagenesis (Aglient Technologies) using pSG5-Flag-KMT5A WT and pSG5-Flag-KMT5A C-terminus as a template, respectively. See Chapter 3.3.1 for more details.

Construct	Source
pFLAG-AR	Professor Ralf Janknecht (Oklahoma University)
pARE3-luc	Generated by members of the STTD group as described in (Brady et al., 1999)
pCMV- β -gal	Generated by members of the STTD group as described in (Brady et al., 1999)
pcDNA3-Flag-Cul1	Professor Meloche Sylvain (Université de Montréal)
pcDNA3-HA-Rbx1	Professor Meloche Sylvain (Université de Montréal)
pcDNA3-HA-Skp1	Professor Meloche Sylvain (Université de Montréal)
pcDNA3-Flag-Skp2	Professor Neil Perkins (Newcastle University)
p-LRR-Skp2	Professor Hui-Kuan Lin (The University of Texas)
pSG5-Flag-KMT5A WT	Professor Judd Rice (University of Southern California)
pSG5-Flag-KMT5A C-terminus	Professor Judd Rice (University of Southern California)
pSG5-Flag-KMT5A N-terminus	Professor Judd Rice (University of Southern California)
pSG5-Flag-KMT5A K205R	Generated in house
pSG5-Flag-KMT5A K234R	Generated in house
pSG5-Flag-KMT5A K236R	Generated in house
pSG5-Flag-KMT5A K245R	Generated in house
pSG5-Flag-KMT5A K267R	Generated in house
pSG5-Flag-KMT5A K297R	Generated in house
pSG5-Flag-KMT5A K321R	Generated in house
pSG5-Flag-KMT5A K342R	Generated in house
pSG5-Flag-KMT5A K349R	Generated in house
pSG5-Flag-KMT5A C1	Generated in house
pSG5-Flag-KMT5A C2	Generated in house
pSG5-Flag-KMT5A C3	Generated in house
pSG5-Flag-KMT5A C4	Generated in house
pSG5-Flag-KMT5A C5	Generated in house
pSG5-Flag-KMT5A C6	Generated in house
pSG5-Flag-KMT5A C3 K321R	Generated in house
pSG5-Flag-KMT5A N-C1	Generated in house
pSG5-Flag-KMT5A N-C2	Generated in house
pSG5-Flag-KMT5A N-C3	Generated in house

Table 2.2: List of plasmids used.

2.4 Transient siRNA reverse transfection

Reverse transfection was used to introduce small interfering RNA (siRNA) to the cells in order to silence the gene of interest. A list of the siRNA oligonucleotide sequences, including the negative non-silencing control, are provided in Table 2.3. Transfection cocktail was prepared by mixing Lipofectamine™ RNAiMAX (Invitrogen) with basal media and the siRNA (50 µM stock) to give a final concentration of 25 nM siRNA per well. The mixture was added to the wells and incubated at room temperature for 30 minutes to allow sufficient time for lipid-RNA complexes to form. Meanwhile, cells were diluted in the appropriate volume, type of media and concentration depending on their proliferation rate. They were then added to the wells containing the siRNA transfection cocktail, mixed gently and incubated at 37 °C, 5% CO₂ for 72 hours.

In case of DHT treatment to stimulate the cells following siRNA knockdown, cells were simultaneously starved and siRNA treated in SDM. After 72 hours, existing SDM was replaced with freshly prepared SDM containing 10 nM DHT, unless otherwise stated, and incubated for various time periods.

Target	siRNA Sequence 5'-3'
KMT5A-1	CCAUGAAGUCCGAGGAACA
KMT5A-2	CAGGAAGAGAACUCAGUUA
Non-silencing	UUCUCCGAACGUGUCACGU
Skp2-1	AAGGGAGUGACAAAGACUUUG
Skp2-2	GAGGAGCCCGACAGTGAGA
Skp2-3	GUGAUAGUGUCAUGCUIAA

Table 2.3: List of siRNA oligonucleotide used. All siRNA oligonucleotides were purchased from Sigma-Aldrich.

2.5 Bacterial transformation

This procedure was performed under sterile conditions using aseptic techniques, autoclaved plastic-ware and Luria-Bertani (LB) medium.

Plasmids were propagated by transforming NEB 5-alpha competent *Escherichia coli* (*E.coli*) (New England BioLabs). Briefly, 1 μ L of plasmid was mixed with 25 μ L of bacteria and incubated on ice for 20 minutes. Bacteria were then heat shocked by placing in a 42 °C water bath for 90 seconds and then back on ice for 5 minutes. One mL of LB medium (10 g/L tryptone, 5 g/L yeast extract, 10 g/L NaCl) was added and bacteria were incubated at 37°C while shaking at 200 rpm for 1 hour. The transformation mixture was spread on LB agar plates containing ampicillin (50 ng/mL) and incubated at 37 °C overnight. Successful bacterial transformation with the plasmid DNA will result in resistance to plasmid-derived antibiotic gene (ampicillin resistance), and formation of colonies on LB agar containing ampicillin. Bacteria without the plasmid DNA will lyse.

A single bacterial colony was picked and inoculated into 10 mL ampicillin-containing LB medium and shaken at 200 rpm at 37 °C for approximately 6 hours. The starter culture was then added to 200 mL LB medium, supplemented with ampicillin and incubated overnight while shaking at 200 rpm at 37 °C. The plasmid DNA was purified using the Endo-free plasmid maxi kit (Invitrogen) performed according to the manufacturer's instructions. DNA quality and yield was determined using a NanoDrop® ND-1000 UV-Vis Spectrophotometer.

2.6 Protein expression analysis

2.6.1 Sodium dodecyl sulphate-polyacrylamide gel electrophoresis (SDS- PAGE)

Cell lysates were prepared by adding SDS sample buffer (0.125 M Tris, pH 6.8, 2% (w/v) SDS, 10% (v/v) glycerol, 10% (v/v) β -mercaptoethanol and 0.01% (w/v) bromophenol blue) directly to cultured cells washed in PBS or any other sample which was analysed by SDS-PAGE and immunoblotting. The samples were boiled at 100 °C for 10 minutes to ensure proteins were denatured and loaded into wells of polyacrylamide gels. Gels were prepared using Bio-Rad gel casting apparatus according to Table 2.4. Separation buffer (2X) consisted of: 375 mM Tris-HCL, pH 8.8 and 0.1% SDS. Stacking buffer (2X) was comprised of: 125 mM Tris-HCL, pH 6.8 and 0.1% SDS.

First a resolving gel was poured and allowed to set, followed by the addition of a lower percentage stacking gel on the top, in which a well comb was inserted. Electrophoresis was carried out at 180-200 V for approximately 45 minutes in 1x running buffer (25 mM Tris-HCL,

190 mM glycine, 0.1% SDS). A protein marker, Spectra™ Multicolor Broad Range Protein Ladder (Thermo Fisher Scientific) was run alongside the samples to mark molecular weight.

Ingredient	10% resolving gel	5% stacking gel
30% Acrylamide	3.33 mL	0.83 mL
2X separation buffer	5 mL	-
2X stacking buffer	-	2.5 mL
Tetramethylethylenediamine (TEMED)	10 µL	5 µL
10% ammonium persulfate (APS)	100 µL	50 µL
dH ₂ O	1.67 mL	1.67 mL
Total volume	10.1 mL	5.1 mL

Table 2.4: Recipes of resolving and stacking gels.

2.6.2 Western blotting

Proteins separated by electrophoresis were transferred to Hybond-C nitrocellulose membrane (GE Healthcare) in transfer buffer (25 mM Tris-HCl pH 8.3, 190 mM glycine, 10% methanol) using a Bio-Rad Transfer system at 100 V for 60 minutes on ice, or at 30 V overnight at room temperature. Membrane with transferred proteins was blocked in 5% non-fat milk (Marvel) in TBS (0.5 M NaCl, 0.02 M Tris-HCl, pH 7.5) for 60 minutes at room temperature. After washing the membrane twice in TTBS (0.5 M NaCl, 0.02 M Tris-HCl, 0.001% Tween-20, pH 7.5) for 5 minutes, it was incubated overnight at 4 °C with appropriate primary antibody diluted in 1% milk (Marvel) in TTBS to reduce non-specific antibody binding. The membrane was then washed twice with TTBS for 5 minutes to remove unbound primary antibody before being incubated with appropriate horseradish peroxidase (HRP)-conjugated secondary antibody (Dako) diluted in 1% milk-TTBS for 1 hour at room temperature. The membrane was then washed twice in TTBS for 10 minutes and once in TBS. Visualisation of HRP-conjugated immune complexes was achieved using ECL reagent (GE Healthcare) which was washed over the membrane for 1 minute and exposed to X-ray film (Fuji Film) and developed using an automated developer. A list of primary and secondary antibodies used are provided in Table 2.1.

2.7 Gene expression analysis

All RNA work was performed using pipette barrier tips (Scientific Laboratory Supplies Ltd).

2.7.1 RNA extraction

The adherent cells grown as a monolayer in 6 well plates was washed with ice cold PBS before being lysed directly in the culture dish by adding 500 μ L of Trizol and incubated for 5 minutes at room temperature to permit complete dissociation of the nucleo-protein complex. The homogenised sample was transferred to an Eppendorf tube and 250 μ L of chloroform was added. Samples were mixed vigorously for 15 seconds and incubated at room temperature for 10 minutes, followed by centrifugation at 12,000 x g for 15 minutes at 4 °C. The mixture separates into a lower red phenol-chloroform phase, an interphase, and a colourless upper aqueous phase which contains RNA exclusively. The aqueous phase was carefully transferred into a fresh tube and RNA was precipitated by adding 250 μ L propan-2-ol. Samples were incubated at room temperature for 30 minutes, followed by centrifugation at 12,000 x g for 10 minutes at 4 °C. The supernatant was completely removed and the RNA pellet was washed with 75% ethanol and centrifuged at 7500 x g for 5 minutes at 4 °C. The RNA pellet was air-dried and resuspended in an appropriate volume of Diethylpyrocarbonate (DEPC) treated water and heated to 55 °C for 10 minutes.

RNA concentration and purity was determined using a NanoDrop® ND-1000 UV-Vis Spectrophotometer. The integrity of the sample was assessed by the 260/280 ratio (the ratio of absorbance at 260nm and 280 nm). The optimal 260/280 ratio for RNA is 2.0.

2.7.2 RNA reverse transcription

Reverse transcription of mRNA to cDNA was carried out using the MMLV reverse transcription kit (Promega) according to the manufacturer's protocol. Briefly, 1 μ g of isolated RNA was mixed with DEPC water to a final volume of 12.7 μ L, and incubated at 65 °C for 5 minutes to denature the RNA secondary structures. The RNA samples were then incubated at 37 °C for 1 hour with 7.3 μ L of Moloney Murine Leukaemia Virus (MMLV) master-mix containing: 4 μ L 5x MMLV reaction buffer, 2 μ L 4 mM dNTP mix (dGTP, dATP, dCTP and dTTP), 1 μ L 50 μ g/mL Oligo-dT15 and 0.3 μ L MMLV reverse transcriptase enzyme. The samples were further incubated for 5 minutes at 95 °C to inactivate the MMLV-RT enzyme and the resulting cDNA was stored at -20 °C until required.

2.7.3 Quantitative real time PCR

Quantitative real time PCR (qPCR) was carried out using the Platinum® SYBR® Green qPCR SuperMix-UDG w/ROX (Invitrogen), and was performed in the 384-well plate ABI 7900HT thermocycler (Applied Biosystems). The absolute quantification method was used to determine gene expression levels in the unknown samples which required the generation of a standard curve for each gene under investigation. A standard curve was generated using a sample which is known to express the gene of interest and was serially diluted to include 5 concentrations. To control for PCR contamination, a sample with no template cDNA was included.

A total reaction volume of 10 µL, containing 8 µL reaction cocktail (according to Table 2.5) and 2 µL cDNA was dispensed respectively in each well of a MicroAmp® 384-well plate (Life Technologies). A list of PCR primers used is provided in Table 2.7. The plate was then sealed with Applied Biosystems® MicroAmp® Optical Adhesive Film (Life Technologies). The reactions were achieved under the following PCR conditions: 95 °C for 10 minutes, 95 °C for 15 seconds and 60 °C for 1 minute over 40 cycles. The data was analysed using Sequence Detection System software (SDS) version 2.3 (Applied Biosystems). The detector used was SYBR and ROX was applied as a passive reference. The expression levels of each gene was then normalised to the housekeeping gene Hypoxanthine phosphoribosyltransferase 1 (HPRT1).

Reagent	Volume added per well
SYBR Green	5 µL
dH ₂ O	2.2 µL
Forward primer	0.4 µL
Reverse primer	0.4 µL
cDNA	2 µL
Total volume	10 µL

Table 2.5: Constituents of the reagent mix for each RT-PCR reaction.

2.7.4 Quantitative PCR primers

The primer sequences were either obtained from the published literature or designed using the Primer-BLAST program and were verified for target specificity using NCBI BLAST:Basic Local Alignment Search Tool. All primers were purchased from Sigma-Aldrich. The primers were resuspended in nuclease-free water and used at a concentration of 2.5 μ M in the reaction cocktail to give a final concentration of 0.1 μ M.

Gene	Forward primer sequence	Reverse primer sequence
<i>AR</i>	CATGTGGAAGCTGCAAGGTCT	TCTGTTCCCTTCAGCGGC
<i>PSA (KLK3)</i>	GGTGCATTACCGGAAGTGGAT	TGGTCATTTCCAAGGTTCCAA
<i>KLK2</i>	AGCATCGAACCAGAGGAGTTCT	TGGAGGCTCACACACCTGAAGA
<i>TMPRSS2</i>	CTGCTGGATTTCCGGGTG	TTCTGAGGTCTTCCCTTTCTCCT
<i>ATAD2</i>	GGAATCCCAAACCACTGGACA	GGTAGCGTCGTCGTAAAGCACA
<i>HPRT1</i>	TTGCTTTCCTTGGTCAGGCA	AGCTTGCGACCTTGACCATCT

Table 2.6: List of qRT-PCR primers used.

2.8 Luciferase reporter assay

2.8.1 Luciferase activity measurement

HEK293T cells were seeded into 24-well plates in 1 mL SDM and incubated for at least 24 hours to ensure seeding down and sufficient starvation of cells. Once the cells were approximately 70% confluent, they were transfected with the plasmid constructs as in Section 2.3 and incubated for a further 24 hours. The cells were then stimulated with 10 nM DHT for 24 hours. Upon completion of the assay in the 24-well plates, cells were washed with PBS before being lysed in 50 μ L of 1 x lysis buffer (Promega) at 37 $^{\circ}$ C for 10 minutes followed by a freeze-thaw cycle. The plates were then scraped, the lysate mixed and 10 μ L of each sample was transferred into a well of an opaque flat-bottomed 96-well plate to be analysed using a FLUOstar Omega microplate reader (BMG LABTECH). The injector adds 50 μ L of Luciferase Assay Reagent (Promega) per well and the well was read immediately to determine the luciferase counts per second (LCPS). The plate is advanced to the next well and the process is repeated until all wells are read. Each reading was normalised to its corresponding β -galactosidase absorbance (Chapter 2.8.2).

2.8.2 *β-galactosidase normalisation assay*

In order to account for variations in transfection efficiency and cell numbers, β -galactosidase activity was measured, where a constant amount of pCMV- β -galactosidase (β -gal) was added to each transfection reaction. An equal amount of cell lysate (10 μ L) as in Chapter 2.8.1 was incubated with 10 μ L of β -gal assay substrate (2 mM MgCl₂, 100 mM β -mercaptoethanol, 1.33 mg/mL o-nitrophenyl- β -D-galactopyranoside (ONPG) and 100 mM sodium phosphate buffer, pH 7.3) at room temperature in a clear 96 well flat-bottomed plate (Corning) until the mixture turned yellow. The reaction was terminated by adding 50 μ L of 1 M Na₂CO₃ and absorbance at 415 nm was measured using a 96-well model 680 plate reader (Bio-Rad).

2.9 Immunoprecipitation (IP)

2.9.1 *Native immunoprecipitation*

Cells were plated in 90 mm dishes at appropriate numbers depending on their proliferation rate and grown to 90% confluency in FM. Cells were washed and collected by scraping into ice-cold PBS. They were then centrifuged at 12,000 rpm for 10 minutes at 4 °C before being resuspended in 1 mL lysis buffer (50 mM Tris pH 7.5, 150 mM NaCl, 0.2 mM Na₃VO₄, 1% NP-40 alternative, 1 mM PMSF, 1mM Dithiothreito (DTT), protease inhibitor cocktail tablet (Roche)) for 1 hour with agitation at 4 °C. Cellular debris were removed by centrifuging the lysed cells at 14,000 rpm for 3 minutes and collecting the supernatant. At this point, 100 μ L of supernatant was taken as an input sample and 30 μ L Protein G Sepharose (PGS; GE Healthcare) was added to the remaining 900 μ L supernatant which was pre-cleared for 4 hours at 4 °C.

PGS was removed after centrifugation at 14,000 rpm for 3 minutes and the supernatant was split into two equal volumes and each incubated with the appropriate antibodies overnight at 4 °C. Endogenous or ectopically expressed protein of interest was immunoprecipitated using the appropriate antibody and an equivalent amount (2 μ g) of normal IgG was used as a negative control. PGS was added the following day for 1 hour at 4 °C to immunoprecipitate the antibody-protein complexes. The beads were then collected by centrifugation at 14,000 rpm for 5 minutes and washed once with 1 mL IP wash A (PBS, 350 mM NaCl, 0.2% Triton) and twice with 1 mL IP wash B (PBS, 0.2% Triton). PGS was resuspended in SDS loading buffer containing 10% β -mearcaptoethanol for Western analysis.

2.9.2 *Denaturing nickel pull down*

Cells were seeded in 90 mm dishes and were grown to 80% confluency at the time of collection. Cells were collected by scraping into 1 mL ice-cold PBS and 100 μ L was removed, centrifuged and the pellet was used as an input sample. The remaining 900 μ L was centrifuged at 2,000 rpm

at 4 °C for 10 minutes. PBS was removed and cells were lysed by resuspending them in a denaturing lysis buffer (6 M guanidine-HCl, 0.1 M Na₂HPO₄/NaH₂PO₄, 0.01 M Tris-HCl, pH 8, 5 mM imidazole, 10 mM β-mercaptoethanol) and mixed gently on a shaker for 1 hour at 4 °C. Fifty μL of Ni-NTA agarose beads (Qiagen) were added to samples followed by overnight incubation at 4 °C. Histidine (His) tagged proteins bind to the nickel ions through their His tag with high affinity and form a complex. To pull down the complexes, samples were centrifuged the following day and the supernatant discarded. Ni-NTA agarose beads were washed with several denaturing IP wash buffers in the following order: buffer 1 (6 M guanidinium-HCl, 0.1 M Na₂HPO₄/NaH₂PO₄, 0.01 M Tris-HCl, pH 8, 10 mM β-mercaptoethanol), buffer 2A (8 M Urea, 0.1 M Na₂HPO₄/NaH₂PO₄, 10 mM β-mercaptoethanol, 0.01 M Tris, pH 8), buffer 2B (8 M Urea, 0.1 M Na₂HPO₄/NaH₂PO₄, 10 mM β-mercaptoethanol, 0.01 M Tris, pH 6.3, 0.2% (v/v) Triton X-100), and buffer 2C (8 M Urea, 0.1 M Na₂HPO₄/NaH₂PO₄, 10 mM β-mercaptoethanol, 0.01 M Tris, pH 6.3, 0.1% (v/v) Triton X-100), where beads were resuspended in each of the wash buffers and rotated for 5 minutes at room temperature. They were then centrifuged at 12,000 rpm for 5 minutes and the supernatant was removed before resuspending in the next wash buffer. To elute the complexes, Ni-NTA agarose beads were resuspended in elution buffer (200 mM imidazole, 0.1 M Na₂HPO₄/NaH₂PO₄, 0.15 M Tris-HCl, pH 6.7, 10 mM β-mercaptoethanol, 30% (v/v) glycerol, 5% (w/v) SDS) and mixed by rotating on a wheel for 20 minutes. The supernatant was collected after centrifugation to which SDS loading buffer containing 10% β-mercaptoethanol was added. Samples were then analysed by Western blotting.

2.10 Cytoplasmic/nuclear extraction

Nuclear and cytoplasmic extracts were generated using the NE-PER™ extraction kit (Thermo Scientific) according to the manufacturer's protocol. Briefly, cells were harvested by trypsinisation, pelleted by centrifugation at 300 g for 5 minutes, and washed with PBS. Cell pellets were then resuspended in 200 μl CER I solution, vortexed vigorously and incubated on ice for 5 minutes. Eleven μl CER II solution was added, vortexed and incubated on ice for 1 minute to allow cell membrane disruption. The lysed cells were vortexed briefly again and centrifuged at 16,000 g for 10 minutes. The supernatant which is the cytoplasmic extract was then immediately transferred to a new pre-chilled tube. The remnant nuclear pellet was washed with PBS prior to being lysed in 100 μl NER solution, vortexed and incubated on ice for 10 minutes. This was repeated for a total of 40 minutes, followed by a final 10 minutes centrifugation at 16,000 g. All centrifugations were carried out at 4 °C. The nuclear extract was transferred to a new pre-chilled tube.

2.11 Flow cytometry cell cycle analysis

2.11.1 Hoechst cell staining and sorting

Hoechst is an exclusive DNA-binding dye which is taken up passively by live cells and preferentially binds to A-T base regions of the DNA. The amount of DNA present in a cell based on its phase of the cell cycle at a particular time determines the amount of Hoechst binding and in turn its fluorescence. This enables live cells to be specifically separated into different phases of the cell cycle (G0/G1, S and G2/M) based on DNA content analysis. Propidium Iodide (PI) was added to exclude dead cells.

Exponentially growing cells were harvested by trypsinisation, trypsin was then deactivated, and cells were counted with a haemocytometer, after which 20×10^6 cells were centrifuged at 300 g for 5 minutes. The supernatant was removed and the cells were resuspended in 10 mL culture medium containing 20 $\mu\text{g/mL}$ (stock 1 mg/mL) Hoechst 33342 (Sigma-Aldrich). The samples were then incubated in the dark at 37 °C for 45 minutes, while gently shaken every 10 minutes. After incubation, cells were resuspended in their existing Hoechst-containing medium at a concentration of 10×10^6 cells/mL and transferred into FACs tubes (BD Biosciences) for sorting. Immediately prior to sorting, PI was directly added to the samples which were subsequently analysed using BD FACS Aria Fusion. The sorted cells were collected into FACs tubes containing 250 μL FBS, before being pelleted at 300 g for 5 minutes and resuspended in SDS-sample buffer. Cells were sorted based on the amount of DNA by defining three regions (G0/G1, S and G2/M) for sorting. Hoechst 33342 excitation took place with the UV laser at 350 nm and emission collected at 450/50 nm. PI was excited at 560 nm and emission collected at 610/20 nm. Live cells were collected by gating out PI positive cells. They were ensured to be single cells by gating out doublets and clumps using a dot plot showing Hoechst parameters area vs height and area vs width. All data analysis was carried out using FlowJo software.

2.11.2 Propidium Iodide (PI) cell staining

PI is another fluorescent dye that also binds DNA and is taken up in cells with permeabilised cell membrane. Cells were seeded in a 6-well plate and upon completion of the experiment, both culture media and trypsinised cells were collected in FACs tubes (BD Biosciences). The cells were pelleted at 300 g for 5 minutes, and washed once with PBS. They were then resuspended in 100 μL citrate buffer (0.25 M sucrose, 40 mM sodium citrate, pH 7.6), 400 μL DNA staining/ lysis buffer (20 $\mu\text{g/mL}$ PI, 0.5% NP-40, 0.5 mM EDTA) and 10 μL RNase A (stock 10 mg/mL). Following gentle mixing, the cells were incubated at 4 °C for 45 minutes in the dark. Samples were analysed using a BD FACsCalibur to quantify PI binding, capturing 10,000 events per sample. Data acquisition was performed using CellQuest software. Single

cells were only gated in a FL2-W vs FL2-A plot, excluding cell aggregates/ debris. All data analysis was carried out using Cyflogic software.

3 Evidence that KMT5A is a mono-ubiquitinated protein and identification of the sites of mono-ubiquitination

3.1 Introduction

As the AR remains active in advanced and relapsed disease, targeting the AR remains a valid therapeutic target. Deregulation of AR regulators is one of the underlying mechanisms of AR activity in advanced disease (Abeshouse *et al.*, 2015). Therefore, targeting AR regulators to indirectly target AR activity is important. KMT5A has been identified as a novel regulator of the AR by our group (Coffey *et al.*, unpublished data). Interestingly, KMT5A was found to regulate AR activity in an opposing manner in models of androgen sensitive disease compared to castrate resistant disease. Therefore, KMT5A regulation itself is important which can in turn influence AR activity.

KMT5A is primarily regulated through post-translational modifications in a cell cycle dependent manner. Ubiquitination-mediated proteasomal degradation plays a key role in the regulation of KMT5A protein stability and activity. Under physiological conditions, as well as in response to DNA damage, KMT5A is tightly controlled and maintained at low levels by the CRL4^{Cdt2} complex during G1-S transition phase of the cell cycle. CRL4^{Cdt2} binds to KMT5A-bound chromatin in a PCNA-dependent manner, mediating KMT5A poly-ubiquitination and its subsequent proteasomal degradation (Abbas *et al.*, 2010; Centore *et al.*, 2010; Oda *et al.*, 2010). Furthermore, the SCF ^{β -TRCP} complex poly-ubiquitinates KMT5A and marks it for degradation by the proteasome during G1 phase (Wang *et al.*, 2015). Moreover, KMT5A is targeted for poly-ubiquitination and proteasomal-mediated proteolysis by the APC^{Cdh1} complex during late mitosis, to maintain low levels of KMT5A in late mitosis and G1 phases of the cell cycle (Wu *et al.*, 2010). Although, poly-ubiquitination of KMT5A and its degradation by the proteasome has been extensively studied, it is not known whether KMT5A could be modified directly by ubiquitination allowing it to carry out a specific function before being subjected to further ubiquitination and degradation. For example, SETDB1, a histone methyltransferase that trimethylates H3K9 and contributes to euchromatic gene silencing is required to undergo mono-ubiquitination as this modification is essential for its catalytic activity (Sun and Fang, 2016).

In a number of studies there has been a higher molecular weight KMT5A band observed in Western blots with KMT5A-directed antibodies, which has either been reported to be a non-specific band without much investigation, or completely ignored and in most cases not even acknowledged, despite being present in some published figures. The higher molecular weight KMT5A band can be observed in some of the work by Tardat, Houston, Sims, Abbas, Centore,

Congdon, Jorgensen and Dulev et al (Tardat *et al.*, 2007; Houston *et al.*, 2008; Sims and Rice, 2008; Abbas *et al.*, 2010; Centore *et al.*, 2010; Congdon *et al.*, 2010; Jørgensen *et al.*, 2011; Dulev *et al.*, 2014). Our group, which has been studying the role of KMT5A in regulating the AR signalling in disease progression to CRPC, also observed the same slow migrating KMT5A band in Western blots. This band has a molecular weight of approximately 50 kDa, which is a molecular weight equivalent to the predicted molecular weight of KMT5A (42 kDa) conjugated to a single ubiquitin (8 kDa), suggesting the possibility of a mono-ubiquitinated form of KMT5A.

3.2 Hypothesis

KMT5A is predominantly mono-ubiquitinated and this alteration generates a physiologically relevant form of modified KMT5A.

3.2.1 Aims

- To determine and confirm the presence of mono-ubiquitinated KMT5A in cell line models
- Identify the site(s) of mono-ubiquitination

3.3 Specific materials and methods

3.3.1 Site-directed mutagenesis

Site-directed mutagenesis was performed using the QuikChange II XL Site-Directed Mutagenesis Kit (Agilent Technologies) according to the manufacturer's instructions. It was used to create ubiquitination-deficient mutants of KMT5A at individual lysine sites, where the lysine of interest has been substituted with arginine in the full-length KMT5A construct. Furthermore, deletion mutants of the C-terminus KMT5A were created by replacing the amino acid of interest with a stop codon.

Briefly, oligonucleotide primers (Table 3.2) containing the desired mutation were designed to have a melting temperature (T_m) of $\geq 78^\circ\text{C}$ based on the formula below:

$$T_m = 81.5 + 0.41 (\%GC) - (675/N) - \% \text{ mismatch}$$

Where N is the primer length in bases and values for GC% and % mismatch are whole numbers.

The pSG5-Flag KMT5A WT or pSG5-Fag KMT5A C-terminus plasmids were used as a template for single lysine mutants and deletion mutants, respectively. The reactions then underwent 18 cycles of PCR as in Table 3.1.

Cycles	Temperature ($^\circ\text{C}$)	Time (secsnds)
1	95	60
18	95	50
	60	50
	68	480
	68	420

Table 3.1: Parameters of the PCR cycles.

Mutation	Primer direction	Sequence 5'-3'
K205R	Forward	GGGGGCCTGTCTGCCCTTGATGGGCTT
	Reverse	AAGCCCATCAAGGGCAGACAGGCCCCC
K234R	Forward	GAAGGAGCTCCAGGAGGAGCAAAGCCGAGCTG
	Reverse	CAGCTCGGCTTTGCTCCTCCTGGAGCTCCTTC
K236R	Forward	GCTCCAGGAAGAGCAGAGCCGAGCTGCAGTC
	Reverse	GACTGCAGCTCGGCTCTGCTCTTCCTGGAGC
K245R	Forward	GCTGCAGTCTGAAGAAAGGAGAAGAATAGATGAATTGATTG
	Reverse	CAATCAATTCATCTATTCTTCTCCTTTCTTCAGACTGCAGC
K267R	Forward	GACCTCATCGATGGCAGAGGCAGGGGTGTGATTG
	Reverse	CAATCACACCCCTGCCTCTGCCATCGATGAGGTC
K297R	Forward	GAGCCTCCCGTTTCCTGGCGTCGGTGATC
	Reverse	GATCACCGACGCCAGGAAACGGGAGGCTC
K321R	Forward	GCATCCACGCAGTAGGTTCTGCTCAGATACTGAAAAT
	Reverse	ATTTTCAGTATCTGAGCAGAACCTACTGCGTGGATGC
K342R	Forward	GACTGATCAATCACAGCAGATGTGGGAACTGCCAAAC
	Reverse	GTTTGGCAGTTCCCACATCTGCTGTGATTGATCAGTC
K349R	Forward	GGAAGTCCAAACCAGACTGCACGACATCG
	Reverse	CGATGTCGTGCAGTCTGGTTTGGCAGTTCC
C1 truncation	Forward	GCAAAGCCGAGCTGCAGTCTTAAGAAAGGAAAAGAATAGATG
	Reverse	CATCTATTCTTTTCCTTTCTTAAGACTGCAGCTCGGCTTTGC
C2 truncation	Forward	CTGAAAATAGTACATGTATCAGCCCGTGGAAGGGTC
	Reverse	GACCCTTCCACGGGCTGATACATGTACTATTTTCAG
C3 truncation	Forward	GCGTGGATGCAACTAGATAGACAAATCGCCTAGG
	Reverse	CCTAGGCGATTTGTCTATCTAGTTGCATCCACGC
C4 truncation	Forward	CAGCAAATGTGGGAACTGACAAACCAAACTGCACGAC
	Reverse	GTCGTGCAGTTTGGTTTGTGAGTTCCCACATTTGCTG
C5 truncation	Forward	CATCGCGGCTGGGTAGGAGCTCCTGTA
	Reverse	TACAGGAGCTCCTACCCAGCCGCGATG
C6 truncation	Forward	GCAAGGCTTCCATTTAAGCCCACCCGTGGC
	Reverse	GCCACGGGTGGGCTTAAATGGAAGCCTTGC

Table 3.2: List of the primers used for the mutagenesis work.

Following PCR, samples were treated with *Dpn I* restriction enzyme and incubated at 37 °C for 1 hour to digest the methylated and hemi-methylated parental, non-mutated DNA template. The end product was transformed into NEB 5-alpha competent *E.coli* under ampicillin selection (50 ng/mL) (Chapter 2). Subsequently, up to 3 colonies were picked for propagation and were miniprepmed using GenElute™ Mammalian Genomic DNA Miniprep Kit (Sigma-Aldrich). The purified plasmids were subject to Sanger sequencing (Beckman Coulter Genomics) to confirm successful mutagenesis.

3.4 Results

3.4.1 Identification of mono-ubiquitinated KMT5A in prostate cancer cell lines

Consistently, a distinct high molecular weight band of KMT5A has been observed when Western blotting for KMT5A by our group. This is a persistent band of 50 kDa which has not been described previously to be a modified form of KMT5A. As native KMT5A is a 42 kDa protein in the absence of any post-translational modifications, and ubiquitin is an 8 kDa peptide, this higher molecular weight species may represent a mono-ubiquitinated form of KMT5A.

To investigate the presence of this putative mono-ubiquitinated KMT5A form, a panel of PC cell lines were tested. The cells were grown in their native media and whole cell lysates were collected for Western blot analysis using an anti-KMT5A antibody from Cell Signalling. Unmodified, native KMT5A (42 kDa) was found to be present in all the cell lines, though to varying degrees. Interestingly, the higher molecular weight KMT5A band at 50 kDa was also present, except in the DU145 cell line. The putative mono-ubiquitinated KMT5A band appeared to be a prevalent form of the total KMT5A as the ratio of the two bands were approximately equal as shown in Figure 3.1A. In order to exclude the fact that the 50 kDa band was due to non-specific binding of this particular antibody, a smaller panel of PC cell lines were tested with a different anti-KMT5A antibody purchased from Santa Cruz. As seen in Figure 3.1B, the same higher molecular weight KMT5A species was present at 50 kDa and the unmodified KMT5A at 42 kDa, as expected.

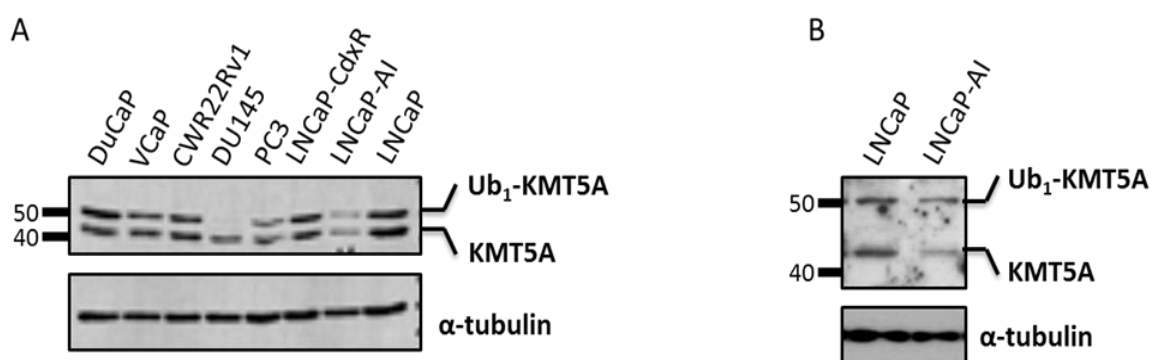


Figure 3-1: Identification of a putative mono-ubiquitinated KMT5A form using different anti-KMT5A antibodies. Western blot analysis of endogenous KMT5A expression and the loading control α -tubulin in a panel of PC cell lines grown in their native media. All sample were collected with SDS sample buffer and two different anti-KMT5A antibodies used were from (A) Cell Signalling and (B) Santa Cruz. This is a representative image of multiple repeats.

3.4.2 Exogenously generated KMT5A exists as both unmodified and mono-ubiquitinated species

There are two isoforms of KMT5A, produced by alternative splicing. (Abbas *et al.*, 2010). The larger isoform is 42 kDa, which we describe as the unmodified form of KMT5A. The second isoform is around 3 kDa smaller as it lacks the first 41 amino acids in the KMT5A N-terminus. Having demonstrated unmodified KMT5A and its larger, putatively representing mono-ubiquitinated form at 50 kDa endogenously, we wished to determine whether the larger KMT5A was also evident from a plasmid construct encoding the 42 kDa KMT5A. A third anti-KMT5A antibody (Abcam) was used alongside one of the antibodies (Cell Signalling) in the previous section 3.4.1, to examine KMT5A expression. Consistently, the higher molecular weight 50 kDa KMT5A form was observed when KMT5A was overexpressed in COS7 cells, though at a smaller ratio relative to the unmodified KMT5A (Figure 3.2A) when compared to the PC cell lines. Anti-KMT5A antibodies from Cell Signalling and Abcam, Figure 3.2A and B respectively, were both able to detect the higher molecular weight KMT5A form with a consistent band position for both antibodies. As three different anti-KMT5A antibodies recognising different regions of KMT5A were able to detect the 50 kDa KMT5A band, it was considered satisfactory to describe it as a genuine KMT5A product. The Cell Signalling anti-KMT5A antibody worked more robustly and was therefore used for the rest of the work, unless mentioned otherwise.

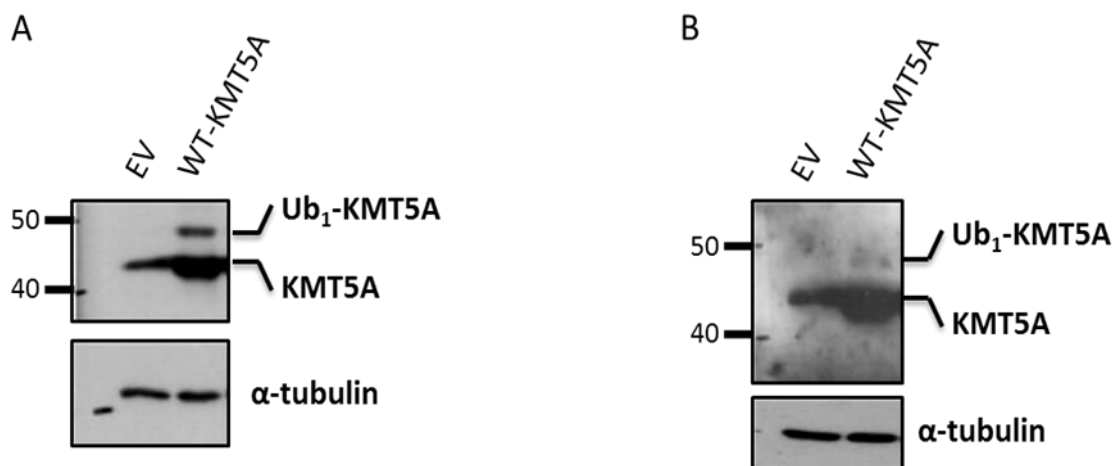


Figure 3-2: Validation of mono-ubiquitinated KMT5A expression using an overexpression system. Western blots of KMT5A and the loading control α -tubulin after COS7 cells were transfected with 500 ng control empty vector (EV) or pSG5-FLAG KMT5A WT plasmid vectors for 48 hours prior to cell lysis using SDS sample buffer. Anti-KMT5A antibodies from Cell Signalling (A) and Abcam (B) were used to test KMT5A expression.

3.4.3 In vivo ubiquitination assay in COS7 cells confirms KMT5A is mono-ubiquitinated

In order to confirm the high molecular weight band at 50 kDa is a mono-ubiquitinated form of KMT5A, an ubiquitination assay using polyhistidine pull down technique was performed in COS7 cells which overexpressed His-tagged ubiquitin (His-Ub) and Flag-KMT5A. In this assay, the histidine tag binds to nickel cations immobilised onto agarose beads (Ni-NTA beads), and captured proteins had undergone covalent modification by exogenously expressed His-Ub under denaturing conditions. Following pull down of His-tagged ubiquitinated proteins from the cell lysate, they were eluted off the beads and the resultant sample was analysed by Western blotting with anti-KMT5A antibody to detect ubiquitinated KMT5A. Figure 3-3 3.3 demonstrates that the polyhistidine pull down was very specific as only the ubiquitinated-modified forms of KMT5A were pulled down. Results showed that, the addition of His-Ub leads to the formation of the higher molecular weight band at 50 kDa which confirms it is mono-ubiquitinated KMT5A as this band was absent when KMT5A or His-Ub were overexpressed alone (Figure 3.3). Moreover, additional higher molecular weight products, likely representing poly-ubiquitinated KMT5A were also apparent as seen by the upward mobility shift of KMT5A, a typical pattern of protein poly-ubiquitination. KMT5A mono-ubiquitination and consequently its poly-ubiquitination were markedly enhanced when the proteasome inhibitor, MG132, was added which further validates these are genuinely ubiquitinated species of KMT5A as they are stabilised upon inhibiting the proteasome, in line with the current literature. Furthermore, there are other heavier products of multi-ubiquitinated KMT5A formed with the addition of Ub, such as the distinct bands around 60 and 70 kDa regions which could correspond to di- and tri-ubiquitinated KMT5A. Alternatively, they could also be mono-ubiquitination at two and three different lysine residues, respectively. For this work, we concentrated on the single mono-ubiquitination of KMT5A as this is the prominent band in PC cell lines.

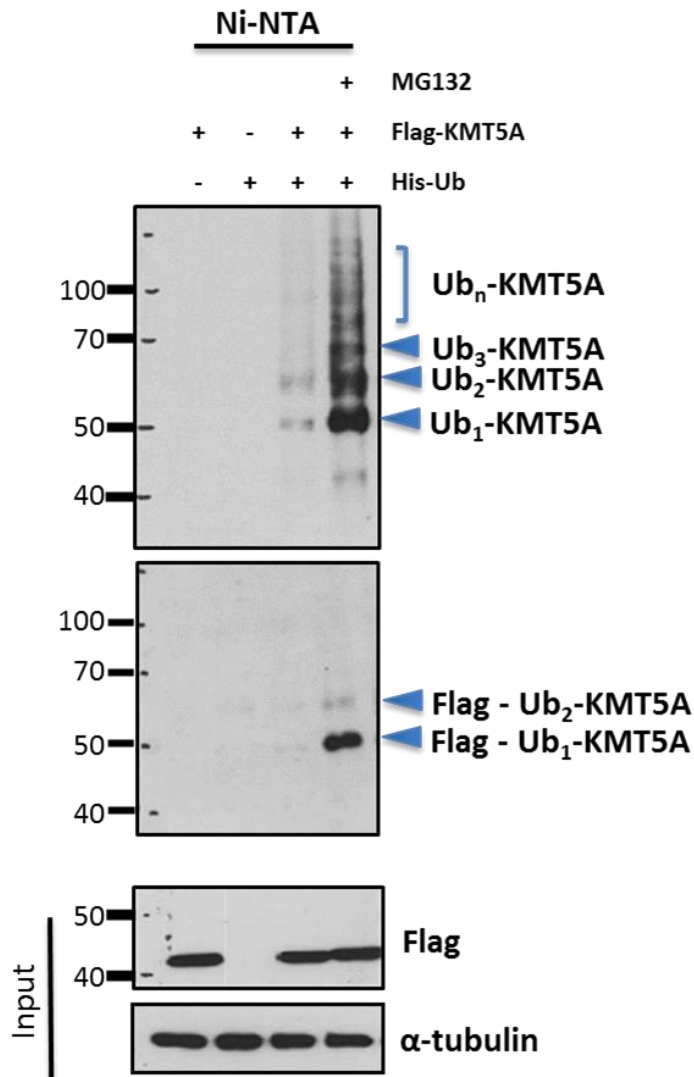


Figure 3-3: KMT5A is mono-ubiquitinated *in vivo*. COS7 cells were transfected with the indicated plasmids for 48 hours. Cells were then subjected to 20 μ M MG132 treatment in the final 16 hours, where indicated. *In vivo* ubiquitination assay using Ni-NTA (nickel beads) was then performed to pull down ubiquitinated proteins. The resultant samples were subject to Western analysis following the addition of SDS sample buffer. Anti-KMT5A and anti-flag antibodies were used to detect pulled down ubiquitinated KMT5A products. This is a representative blot of at least 3 independent experiments.

3.4.4 Inhibiting KMT5A expression using siRNA does not affect mono-ubiquitinated KMT5A levels

Mono-ubiquitination is known to have non-proteolytic functions such as regulating protein stability. Therefore, it was hypothesised that inhibiting the expression of unmodified KMT5A should not influence mono-ubiquitinated levels of KMT5A. As such, KMT5A was depleted using two independent siRNA oligonucleotides that target the KMT5A C-terminus, as this domain is shared across the two isoforms of KMT5A. This also further validates the 50 kDa band is not due to KMT5A isoforms. As KMT5A was found to function in an opposing manner between the two PC cell lines, LNCaP and LNCaP-AI, both cell lines were taken forward for investigation.

Figure 3.4 demonstrates that KMT5A is efficiently depleted with both siRNA oligonucleotides compared to the non-silencing (N/S) control. However, mono-ubiquitinated KMT5A levels remained unchanged following KMT5A knockdown across the two PC cell lines tested, indicating mono-ubiquitination causes stabilisation of KMT5A. Interestingly, di-ubiquitinated KMT5A levels were markedly reduced following inhibition of KMT5A expression. This however may not be a direct consequence of KMT5A knockdown, which will be discussed later. Moreover, persistence of the 50 kDa band after targeting the C-terminus of KMT5A using siRNA, further confirms KMT5A isoforms do not play a role in this phenomenon.

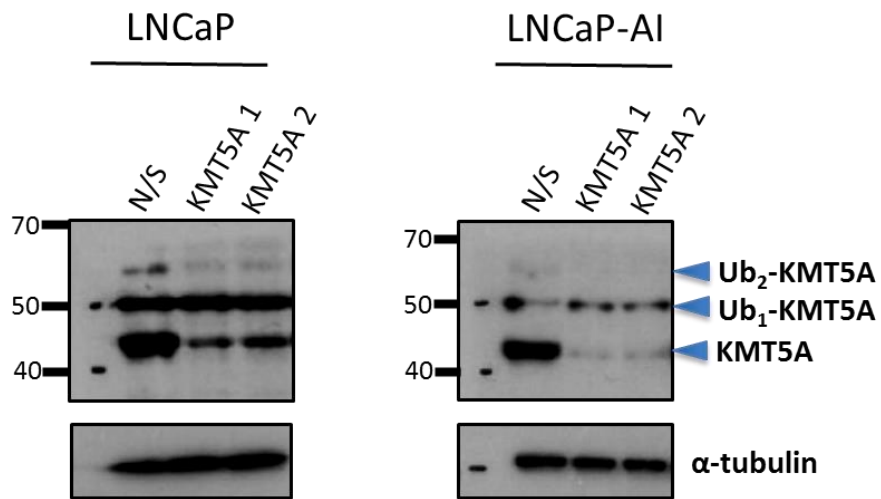


Figure 3-4: KMT5A depletion does not affect mono-ubiquitinated KMT5A level. PC cell lines were reverse transfected with 25 nM non-silencing (N/S) or KMT5A siRNA for 96 hours, in their native growth medium. Post-transfection, cells were lysed with SDS sample buffer to be analysed by Western blotting for KMT5A expression and the loading control α -tubulin.

3.4.5 Mapping of the KMT5A domain for mono-ubiquitination

Having provided strong evidence that mono-ubiquitinated KMT5A exists, we then sought to determine which domain(s) of KMT5A is targeted for mono-ubiquitination. Figure 3.5 A shows a schematic representation of full-length KMT5A and its defined regions, including the catalytic SET domain. To this end, plasmid constructs encoding KMT5A N or C-terminus (Figure 3-5A) were overexpressed alone or in combination with His-Ub, in COS7 cells and KMT5A levels were assessed by Western blotting (Figure 3-5B).

Overexpression of KMT5A C-terminus construct alone led to the expression of unmodified C-terminus fragment and a heavier band, the equivalent weight of a mono-ubiquitinated C-terminus form, as marked on Figure 3-5B, right panel. Addition of Ub enhanced the level of this heavier C-terminus product, in keeping with the full length KMT5A findings. Similarly, KMT5A N-terminus construct was overexpressed and an anti-KMT5A antibody from Abcam which recognises the N-terminus region of KMT5A was used for Western blotting. Unfortunately, this antibody which is currently the only anti-KMT5A antibody available against the N-terminus domain of KMT5A did not detect any protein bands, despite extensive testing. This antibody has also proved difficult and unreliable for Western blotting when tested by a former member of the lab working on KMT5A, and has not been used in any of the publications so far. Instead, the KMT5A N-terminus was detected using an anti-flag antibody which detected the correct molecular weight protein of ~ 15 kDa. However, in our hands the anti-flag antibody only detects unmodified KMT5A N-terminus efficiently and is not consistent in detecting its modified products. As KMT5A C-terminus entails the larger section of KMT5A, containing all the conserved lysine residues, we decided to continue our investigations with the assumption that the C-terminus KMT5A contains the lysine(s) responsible for mono-ubiquitination.

3.4.6 C-terminus of KMT5A is a lysine rich domain

Before commencing our mutagenesis work to identify the site(s) of mono-ubiquitination in KMT5A C-terminus, it was required to closely study the information available on its lysine residues. KMT5A protein consists of 37 lysine residues, of which 25 of them are located in its C-terminus. There are a number of lysine residues in this domain which are highly conserved, including K236, K267, K342 and K382 which are conserved across human, mouse, rat, zebrafish and chicken species (Figure 3.6). Moreover, K245 and K255 are conserved in three and four of the indicated species, respectively. Additionally, K172 which is another highly conserved lysine, is responsible for KMT5A sumoylation (Spektor *et al.*, 2011).

A number of KMT5A lysine residues have been identified as positive hits for sites of ubiquitination by various mass spectrometry studies; though, no confirmatory validation work has been carried out. All of these predicted lysines are located in the C-terminus of KMT5A which include K236, K245, K255, K267, K342 and K382. Furthermore, in a quantitative proteomics study, carrying out global profiling of ubiquitination, acetylation and phosphorylation sites in proteins regulated by the DNA damage response, the same lysine residues except K382 were identified to be sites of ubiquitination for subsequent degradation of KMT5A. Moreover, additional lysine residues, K260, K275, K297, K298, K349 and K39 were also identified as sites of ubiquitination (Elia *et al.*, 2015).

Considering the information available, it was decided to initially carry out mutagenesis to generate full-length KMT5A point mutants at each of the single lysine residues for the six following lysines: K236, K245, K255, K267, K342 and K382.

180 190 200
 QKSEAAEPPK TPPSSCDSTN AAIAKQALKK
 210 220 230 240 250
 PIK GKQAPRK KAQGKTQQNR KLTD FYPVRR SSRKSKAELQ SEERKRIDEL
 260 270 280 290 300
 IESGKEEGMK IDLIDGKGRG VIATKQFSRG DFVVEYHGDL IEITDAKKRE
 310 320 330 340 350
 ALYAQDPSTG CYMYFQYLS KTYCVDATRE TNRLGRLINH SKCGNCQTKL
 360 370 380 390
 HDIDGVPHLI LIASRDIAAG EELLYDYGDR SKASIEAHPW LKH

Figure 3-6: KMT5A C-terminus sequence. All the lysines in the C-terminus have been highlighted in different colours. Blue: sumoylation site; red: lysines conserved across human, mouse, zebrafish, chicken and rat; green: lysines conserved across 3 or more of the species including human. The orange boxed region is the defined SET domain.

3.4.7 KMT5A mono-ubiquitination is not specific to a single lysine residue

We next assessed whether the lysine residues K236, K245, K255, K267, K342 or K382 located in the C-terminus could be the site of KMT5A mono-ubiquitination. We chose these positions because these lysines were highly conserved, predicted and some of them previously shown to be sites of ubiquitination. Wild-type full-length KMT5A template was used to generate the single point mutations using site-directed mutagenesis, replacing lysine with an arginine at the indicated positions. Once KMT5A mutants were generated and verified by DNA sequencing the plasmid constructs were overexpressed in COS7 cells, cell lysates were prepared and subjected to Western blot to assess mono-ubiquitinated KMT5A levels. However, mutating a single lysine at a time at any of these positions did not abolish KMT5A mono-ubiquitination (data not shown). As a result, we continued to individually mutate the remainder of the lysine residues in KMT5A C-terminus, including the identified sumoylation site at K172, and found no detectable change in KMT5A mono-ubiquitination (data not shown). Although, some of the KMT5A mutants including K205R, K234R, K236R, K245R, K267R, K297R, K321R, K342R and K349R showed a small change in the level of mono-ubiquitinated KMT5A; but, nothing that was significant. Thus, overexpression of these mutants was repeated and samples were subjected to Western blotting. The different KMT5A plasmid constructs expressed the unmodified KMT5A protein at different levels, which was not due to loading differences as the total protein content of the cells, assessed by α -tubulin levels (data not shown) was similar. Hence, it was difficult to determine changes in the mono-ubiquitination levels of the mutant constructs compared to wild-type KMT5A. Therefore, serial dilution of samples was carried out to achieve equivalent levels of unmodified KMT5A in mutants, as well as, wild-type KMT5A. Regrettably, no appreciable reduction in KMT5A mono-ubiquitination was evident upon repeating the overexpression (Figure 3.7).

While the site-directed mutagenesis work was being conducted using full-length KMT5A, mass spectrometry was carried out using partially purified KMT5A C-terminus. This was based on the assumption that KMT5A C-terminus contains the site(s) of mono-ubiquitination for reasons previously described (Chapter 3.4.5 and 3.4.6), in turn reducing noise by eliminating the lysine residues in KMT5A N-terminus. For this purpose, Flag-tagged C-terminus KMT5A was co-expressed with His-Ub at 1 μ g each in three 90 mm dishes, in COS7 cells. After 48 hours incubation, ubiquitinated forms of KMT5A C-terminus were separated from the cell lysate using Ni-NTA beads (Chapter 2.9.2) where we attempted to generate a concentrated sample. The sample was resolved by SDS-PAGE and sent to the Newcastle University protein and proteome analysis facility run by Dr Achim Treumann and his staff. They then excised the

region of our gel where mono-ubiquitinated KMT5A C-terminus was predicted to resolve and analysed this by MS. Unfortunately, no signal was detected which was thought to be due to the low concentration of material. In a follow up meeting with Dr Treumann, we were advised to generate a much higher concentrated sample which was not within the scope of the project at that time. Consequently, mass spectrometry work was terminated.

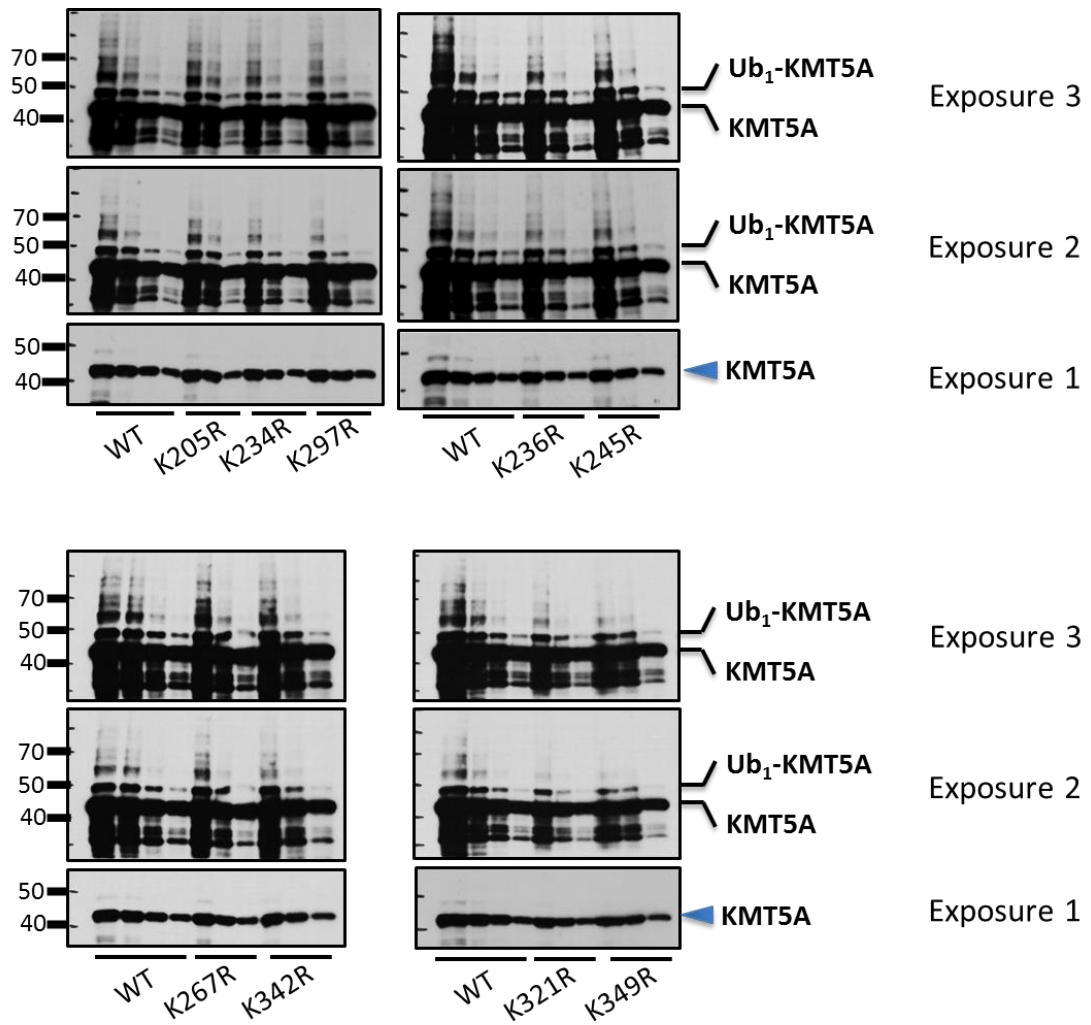


Figure 3-7: KMT5A mono-ubiquitination is not abolished by mutating a single lysine residue. A representative blot of some of the mutagenesis work. Site-directed mutagenesis was performed on full-length wild-type KMT5A. KMT5A was mutagenised to generate a single point mutation, replacing lysine with an arginine, for each lysine individually in KMT5A C-terminus. The following lysine to arginine mutants are shown: K205R, K234R, K236R, K245R, K267R, K297R, K321R, K342R and K349R. Wild-type (WT) or mutant KMT5A constructs were overexpressed in COS 7 cells at 0.5 μ g for 48 hours. Cells were lysed using SDS sample buffer, samples serially diluted and subjected to Western blotting. Different exposures are shown, exposure 1 being the shortest and exposure 3, the longest.

3.4.8 *Generation and validation of truncated KMT5A C-terminus fragments*

As our attempts in identifying the site(s) of KMT5A mono-ubiquitination did not yield any lysine residue that markedly abrogates mono-ubiquitination through mutagenesis of each lysine individually in KMT5A C-terminus, we next sought to determine the region in KMT5A C-terminus that is targeted for mono-ubiquitination.

Therefore, we created a series of KMT5A truncated mutants derived from the C-terminus of KMT5A. These mutants were generated by introducing a stop codon at selected sites using site-directed mutagenesis. We initially focused on creating KMT5A C-terminus truncations as our assumption was that mono-ubiquitination occurs in the C-terminal domain of KMT5A (Chapter 3.4.5 and 3.4.6). Further, all our earlier mutagenesis work was conducted on the lysines located in KMT5A C-terminus (Chapter 3.4.7). Therefore, we aimed to eliminate any interference from the KMT5A N-terminus, though the lysines in the N-domain should not play a role in KMT5A mono-ubiquitination.

Six truncated C-terminal domain fragments were generated, C1 being the smallest (not shown) and C6 the largest, as shown schematically in Figure 3.8A and Figure 3.9A. The smallest fragment (C1) was made long enough to ensure it contains the important arginine, R230, required for anti-KMT5A antibody binding. For each deletion construct, three clones were selected for propagation and the subsequent overexpression in COS7 cells as before. As demonstrated in Figure 3.8B, for all the truncations, the three clones were successfully expressed and were all of the predicted molecular weight. Although it is difficult to clearly distinguish the bands on this blot, it is clear that each fragment displays a different banding pattern.

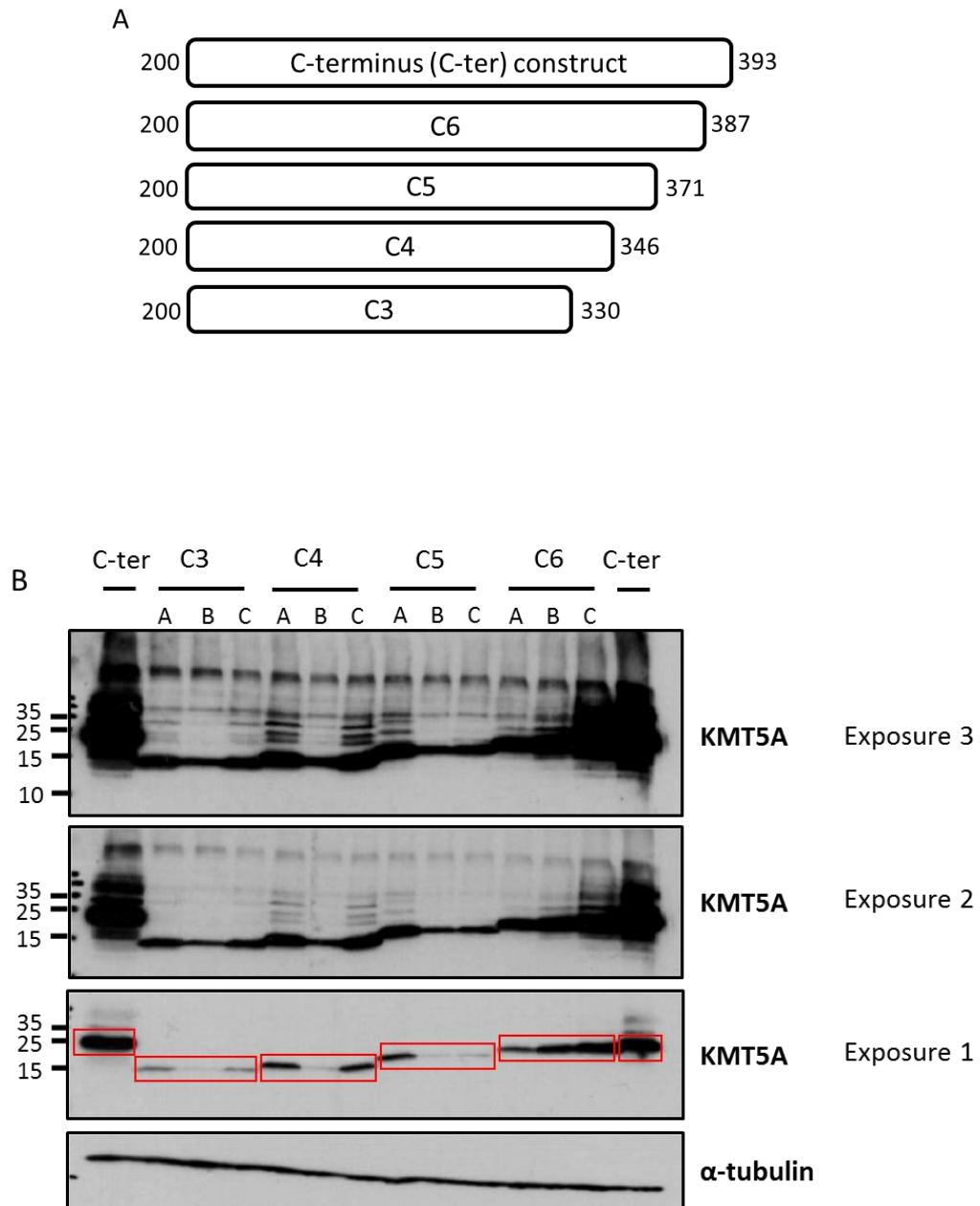


Figure 3-8: Truncated deletion mutants of KMT5A C-terminus show a different profile of modified KMT5A levels. (A) Schematic diagram of KMT5A C-terminus truncated fragments created by introducing a stop codon in different regions of KMT5A C-terminus by site-directed mutagenesis. All the truncated forms were derived from full-length KMT5A C-terminus plasmid. (B) The constructs, C-terminus (200-393) and its derivatives, C3 to C6 were overexpressed at 0.5 μ g in COS7 cells. Following 48 hours incubation, cell lysates were generated by lysing cells in SDS sample buffer and analysed by Western blotting for KMT5A and the loading control α -tubulin. For each fragment, three independent constructs were generated, A-C. Red boxes display unmodified KMT5A.

3.4.9 KMT5A C-terminus truncated fragments C3-6 are targeted for mono-ubiquitination

In order to further analyse the KMT5A C-terminus fragments, a representative construct was selected for each of the three independent constructs available for each fragment. The samples were again analysed by Western blotting and this time loaded to ensure equal level of unmodified KMT5A was achieved.

Results showed that unmodified C-terminus (200-393) and its mono-ubiquitinated form were expressed consistently as before. All other fragments were also expressed at the correct predicted molecular weight in their unmodified forms (Figure 3.9). Interestingly, truncating the C-terminus to C2 abolished KMT5A mono-ubiquitination, as well as higher molecular weight forms of ubiquitinated KMT5A C-terminus. Whereas, mono-ubiquitination was retained in the larger C3 truncated KMT5A C-terminus. Further, mono-ubiquitination was retained for the other larger truncated deletion mutants, C4-C6. Surprisingly, although present, mono-ubiquitinated levels markedly declined when larger C-terminal fragments of KMT5A were expressed (compare C3 to C4-C6). As seen in Figure 3.9, fragment C3 displayed the highest proportion of its mono-ubiquitinated form, and other ubiquitinated products such as its di-ubiquitin form were also evident, which were even stronger than the KMT5A C-terminus (200-393).

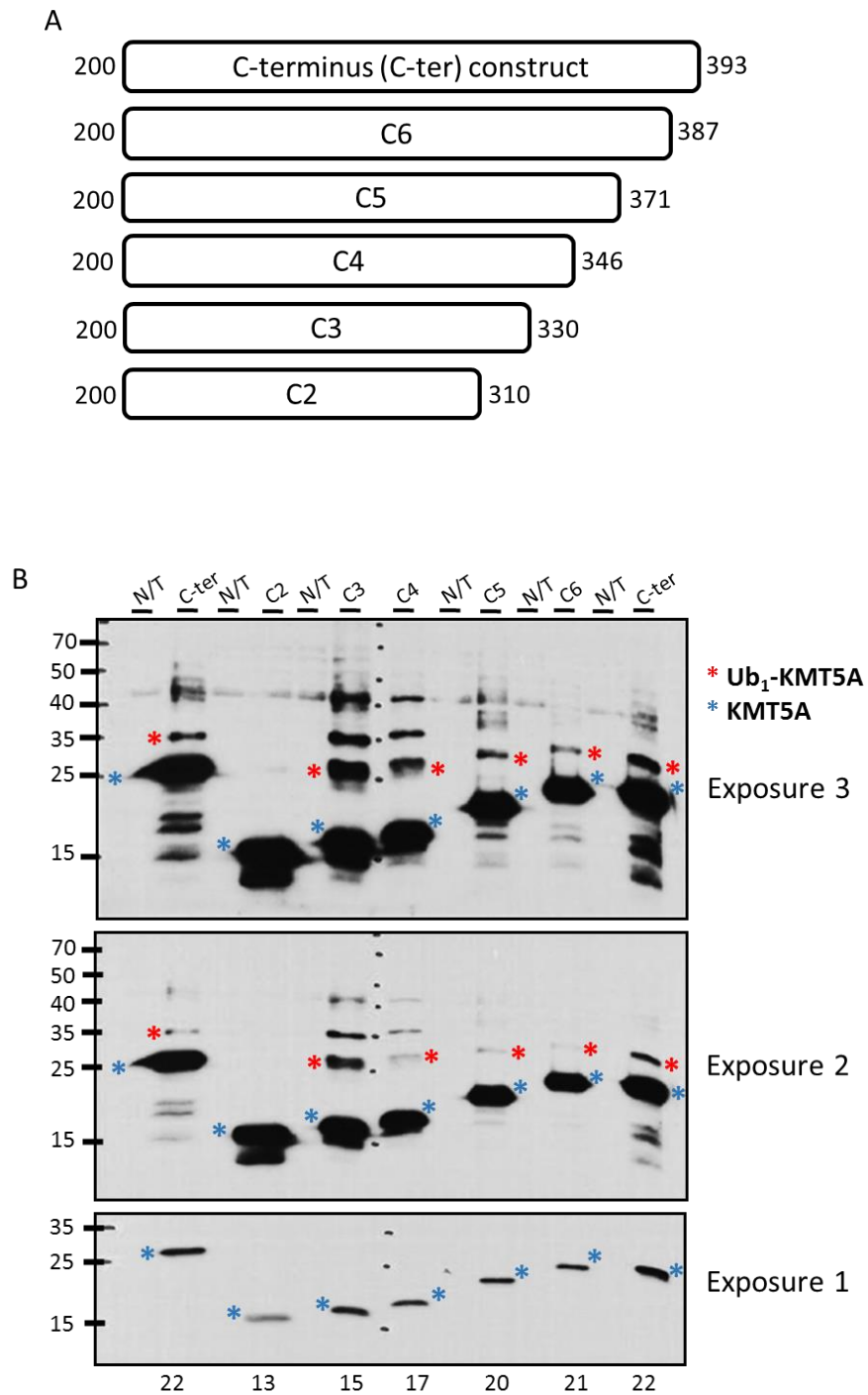


Figure 3-9: KMT5A C-terminus fragments C3-C6 undergo mono-ubiquitination. (A) Schematic diagram of truncated KMT5A C-terminus fragments, including C2. (B) Western blot analysis against KMT5A, assessing mono-ubiquitinated levels of representative constructs for each of the truncations compared to KMT5A C-terminus (200-393), with different exposures (exposure 1-3). N/T: non-transfected.

3.4.10 C-terminus of KMT5A requires amino acids 310-330 for mono-ubiquitination

To determine if the truncated KMT5A C-terminus fragments are indeed altered by mono-ubiquitin conjugation, *in vivo* ubiquitination assays using Ni-NTA beads was performed for fragments C2-C4 in COS7 cells. Only three of the fragments were selected for validation as we were specifically interested in the region responsible for mono-ubiquitination of KMT5A, which appears to be located between C2 and C3 (Chapter 3.4.9).

For this purpose, KMT5A C-terminus fragments were overexpressed either in the absence or presence of His-Ub. Following pull down of ubiquitinated proteins modified by exogenous His-Ub using the Ni-NTA beads, samples were subjected to Western blot analysis to assess mono-ubiquitination of the fragments. Figure 3.10 clearly demonstrates that C3 undergoes mono-ubiquitination when overexpressed in combination with His-Ub whereas it fails to become ubiquitinated when expressed alone. In addition, C3 was also heavily di-ubiquitinated and poly-ubiquitinated, in keeping with the banding pattern as apparent in Figure 3.9.

Similarly, fragment C4 was also mono-ubiquitinated, but the degree of ubiquitination appeared to be at a much smaller proportion relative to the level of unmodified C4 when compared to C3. However, C4 mono-ubiquitination was more abundantly expressed (Figure 3.9B) than what is demonstrated in this particular Western blot as the input shows considerably lower α -tubulin levels (Figure 3.10). In contrast, C2 was not modified by mono-ubiquitination and no other forms of ubiquitination were evident, which is consistent with the data in Chapter 3.4.9. As KMT5A mono-ubiquitination was abolished by truncating KMT5A C-terminus to the smaller fragment C2 and subsequently restored upon extending the C-terminus to fragment C3, it implies that the primary site of KMT5A mono-ubiquitination is located in the region between these two fragments.

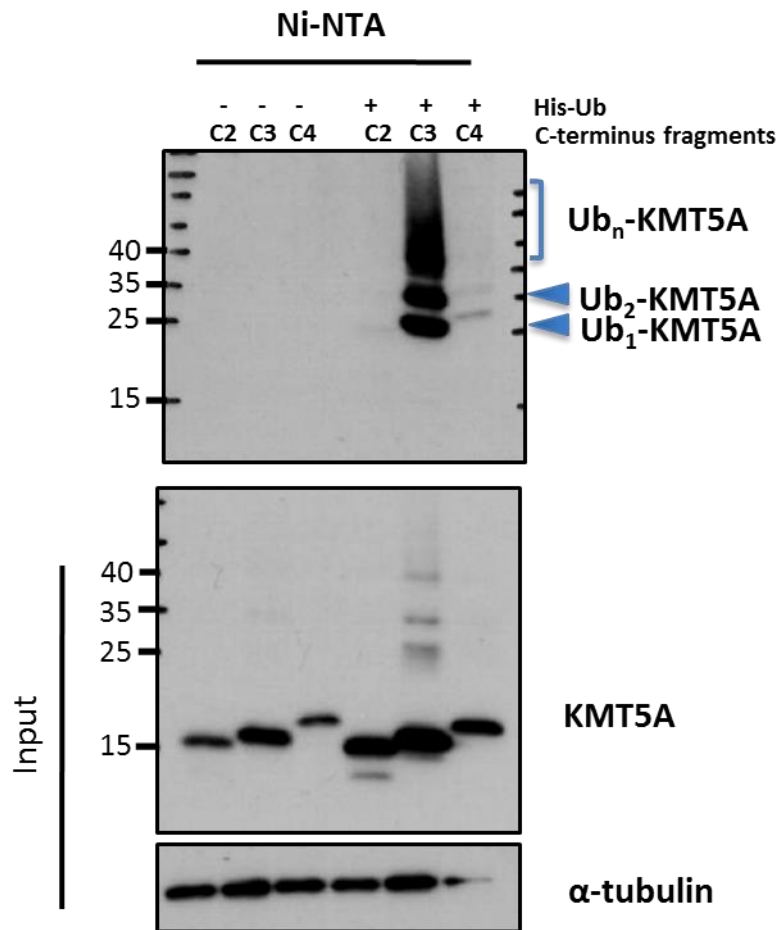


Figure 3-10: Amino acids 310-330 in KMT5A C-terminus are required for KMT5A mono-ubiquitination. *In vivo* ubiquitination assays were performed in COS7 cells transfected with the indicated plasmids for 48 hours. Subsequently, samples were mixed with SDS sample buffer and subjected to Western blotting for KMT5A and the loading control α -tubulin.

3.4.11 The single additional lysine, K321, in fragment C3 is not responsible for KMT5A mono-ubiquitination

Having determined the region of KMT5A undergoing mono-ubiquitination, we then sought to identify the lysine residue(s) that is being modified. As seen in Chapter 3.4.10, the region being responsible for KMT5A mono-ubiquitination is the section between C2 and C3 of KMT5A C-terminus. Analysis of the amino acid sequence in this section revealed there is only one lysine, K321, different between these two fragments which is located in C3 (Figure 3.11A), suggesting K321 is the primary ubiquitin acceptor site in KMT5A.

To test whether K321 is the lysine responsible for KMT5A mono-ubiquitination, the KMT5A C-terminus fragment C3 construct was mutagenised at K321 to generate a single point mutation, replacing lysine with an arginine (K321R) using site-directed mutagenesis, as before. Three independent constructs were generated as seen in Figure 3.11B which were overexpressed in COS7 cells and then mono-ubiquitinated KMT5A levels were assessed by Western blotting.

Non-ubiquitinated, unmodified KMT5A fragment C3 mutagenised at K321 (C3 K321R) was expressed at the expected molecular weight, in line with wild-type fragment C3 (C3 WT). Unfortunately, mutagenesis at K321 was found not to cause any change in the levels of the mono-ubiquitinated form of KMT5A C3 (C3 K321R) when compared to wild-type C3 (C3 WT). In contrast to the earlier indication (Chapter 3.4.10), this result indicates that the site of KMT5A mono-ubiquitination does not lie in the section between C2 and C3 of KMT5A C-terminus. As a result, we have identified a region in KMT5A C-terminus which is required for KMT5A mono-ubiquitination.

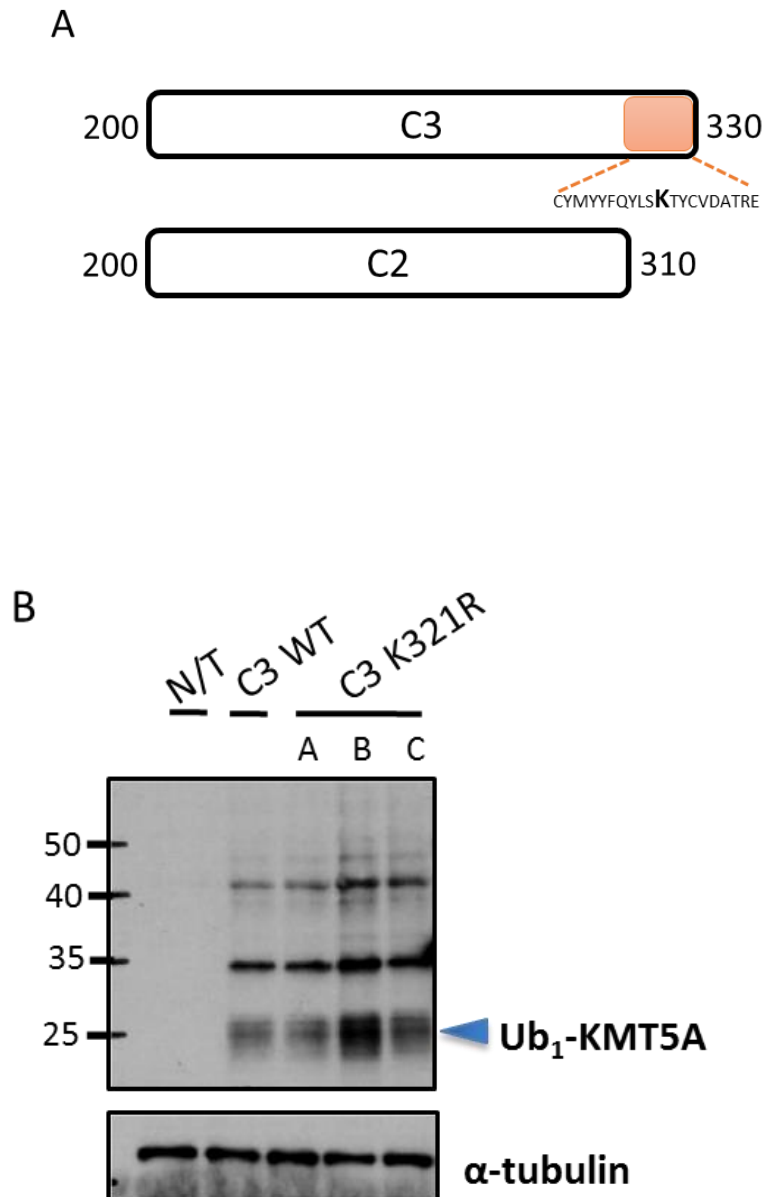


Figure 3-11: K321 in KMT5A C-terminus fragment C3 is not the primary ubiquitin acceptor site. (A) Schematic diagram of KMT5A C-terminus fragments C2 and C3. The orange box represents the extended amino acid sequence, comprising the only additional lysine, K321, which is missing in C2. **(B)** KMT5A C-terminus fragment 3 was mutagenised at K321 by site-directed mutagenesis. The constructs were overexpressed in COS7 cells. Following 48 hours post-transfection, cell lysates were collected using SDS sample buffer and analysed by Western blotting for KMT5A and the loading control α -tubulin. N/T: non-transfected.

3.4.12 The role of N-terminus KMT5A in KMT5A mono-ubiquitination

Having demonstrated and validated the reasons for investigating the site(s) of mono-ubiquitination in KMT5A C-terminus, we wanted to rule out the possibility that our results could have been influenced by the absence of the KMT5A N-terminus. Furthermore, although the site(s) of mono-ubiquitination was not identified, we had KMT5A C-terminus truncated constructs that were mono-ubiquitin competent and mono-ubiquitin deficient which could be utilised for investigating the functional analysis of the mono-ubiquitinated form of KMT5A. However for functional analysis, a better representative of full-length KMT5A is required, rather than working with C-terminus truncations only.

Therefore new KMT5A truncated deletion constructs were generated to include the KMT5A N-terminal domain, extended to include the C-terminus deleted fragments (C1, C2 and C3) generated in Chapter 3.4.8. Site-directed mutagenesis was performed on full-length wild-type KMT5A construct with the same primers, which were used to generate C-terminus fragments, to introduce a stop codon at the same sites in KMT5A C-terminus as performed previously (Figure 3.12A). Following overexpression of the new constructs in COS7 cells, and their analysis by Western blotting, three constructs for each of the KMT5A fragments (fragments N-C1, N-C2 and N-C3) were expressed at the expected molecular weight in their unmodified forms. Figure 3.12B clearly demonstrates a different profile of bands for each of the newly created fragments, where there were more of the higher molecular weight bands of KMT5A fragment N-C3, as well as, increased amounts of them. However, there were fewer bands for fragment N-C2 and even less for fragment N-C1, despite the higher protein expression level of their unmodified forms compared to fragment N-C3. The C-terminus fragment C1 (41 amino acids in length; aa 200-240, Chapter 3.4.8) which was previously derived from the KMT5A C-terminus (200-393) construct, could not be resolved on Western blotting due to its very small size of 5 kDa; hence, not presented on earlier western blots. Although, KMT5A C-terminus fragment C1 was not expected to be mono-ubiquitinated as it is a shorter version of fragment C2 which was demonstrated to not be subject to mono-ubiquitination, it is included in this section as an additional mono-ubiquitin deficient form of KMT5A which can now be resolved due to its larger size by the addition of the KMT5A N-terminus.

As we expected, the inclusion of the N-terminus did not alter the mono-ubiquitination pattern of KMT5A C-terminus fragments, as the new fragment N-C2 failed to undergo any mono-ubiquitination. In contrast, the new fragment N-C3 was subject to mono-ubiquitination (Figure 3.12B), in keeping with KMT5A C-terminus truncated deletion mutants (Figure 3.10). Even though there were bands present for fragments N-C1 and N-C2 which may appear to be mono-

ubiquitinated forms, their molecular weight was not equivalent to any ubiquitin conjugated product. However, we cannot completely rule out the absence of fragments N-C1 and N-C2 mono-ubiquitination, as it is difficult to judge from this Western blot, but if there is any mono-ubiquitination of these fragments it is very low compared to fragment N3, and possibly due to background non-specific mono-ubiquitination of other lysine residues.

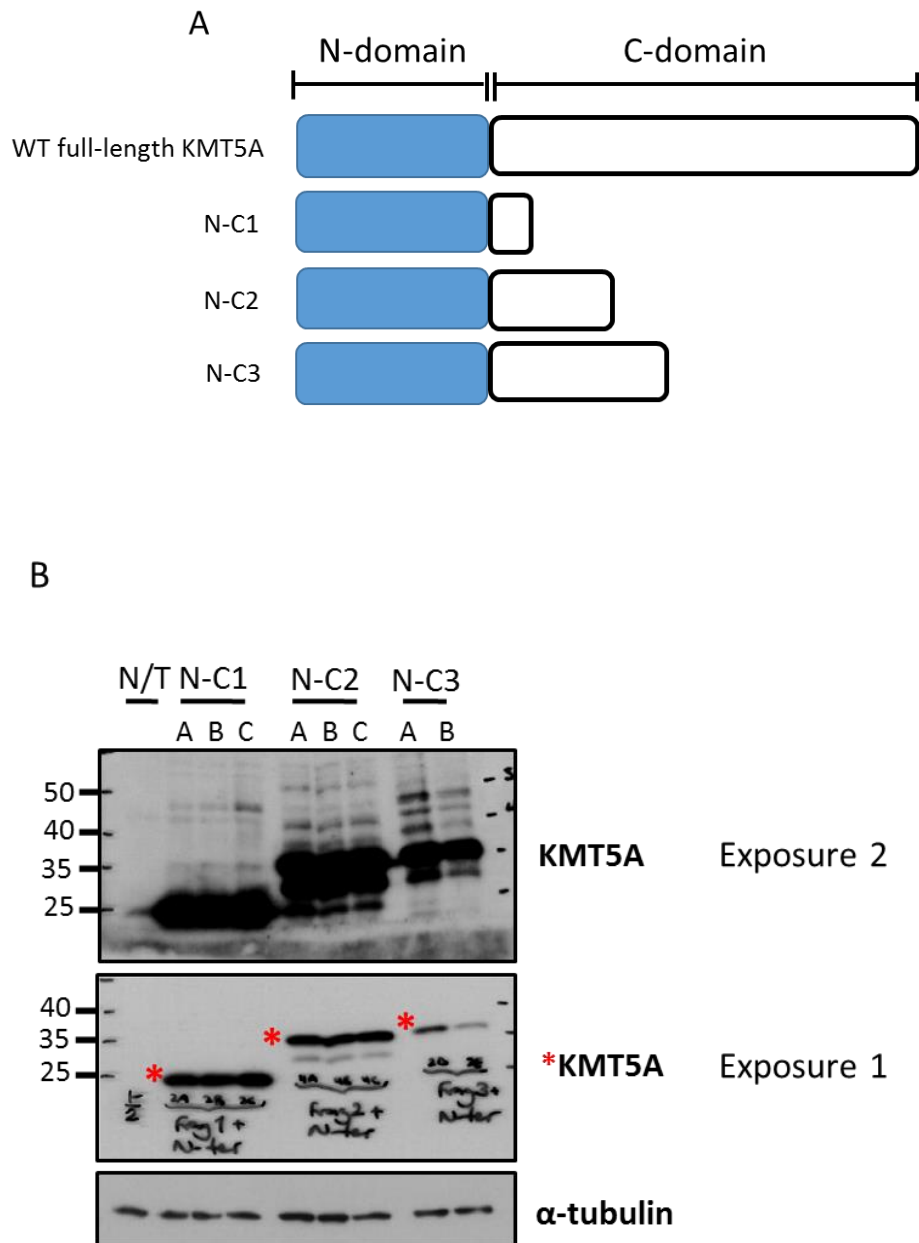


Figure 3-12: N-terminus of KMT5A does not alter mono-ubiquitination of C-terminus fragments. (A) Schematic diagram of truncated C-terminus fragments containing the KMT5A N-domain. (B) The wild-type full length KMT5A construct was used as a template to generate the same truncated C-terminus fragments with the additional N-terminal domain. Site-directed mutagenesis was carried out to introduce a stop codon using the same primers as in section 3.4.8, and three constructs (A-C) was generated for each fragment. The constructs were subsequently overexpressed in COS7 cells for 48 hours. SDS sample buffer was used to lyse the cells and samples were analysed by Western blotting for KMT5A and α -tubulin as the loading control. N/T: non-transfected.

3.4.13 Amino acids 310-330 are required for KMT5A mono-ubiquitination independently of the KMT5A N-terminal domain

Given the consistent pattern of mono-ubiquitination for KMT5A fragments in the presence of the KMT5A N-terminus, ubiquitination assays were used to confirm the attenuated ability of the new fragments N-C1 and N-C2 to be modified by mono-ubiquitin conjugation relative to the new fragment N3 to undergo this modification. In line with our previous findings for KMT5A C-terminus truncated mutants, the new fragment N-C3 was demonstrated to be mono-ubiquitinated, as well as di- and poly-ubiquitinated; whereas, fragments N-C1 and N-C2 remained unmodified (Figure 3.13). This further validated our initial data that the lysine(s) modified by mono-ubiquitination does not reside in the KMT5A N-terminus and that the region between C2 and C3 is critical for ubiquitination.

Interestingly, there was an additional band formed in fragment N-C3, as indicated on the Western blot (Figure 3.13). This band is possibly an ubiquitinated product of fragment N-C3 with an additional post-translational modification as its molecular weight is greater than a mono-ubiquitinated form but lower than a di-ubiquitinated product of this fragment.

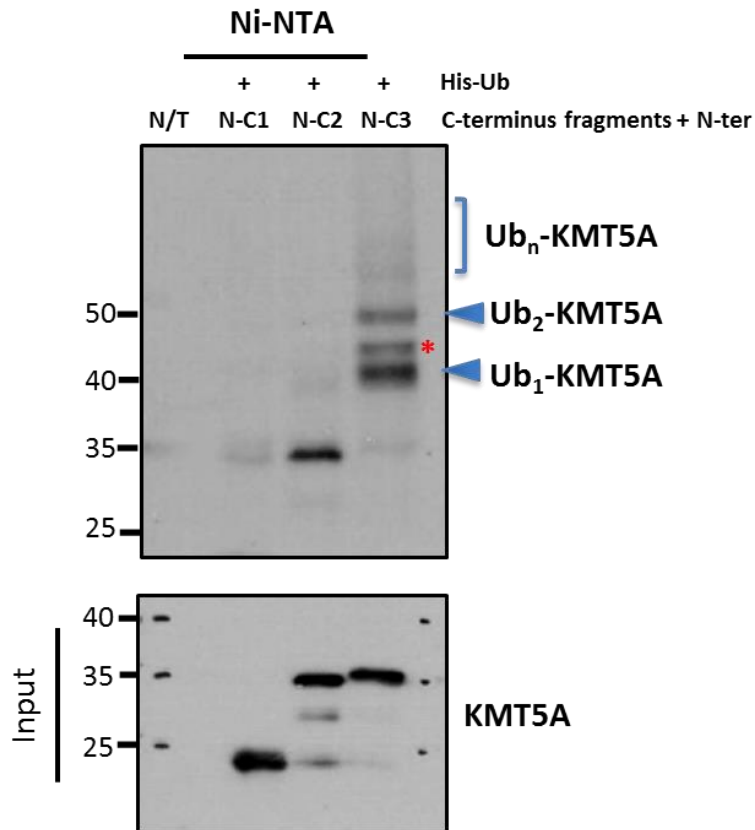


Figure 3-13: N-terminal domain extended fragments maintain the same mono-ubiquitination pattern as C-terminus fragments. *In vivo* ubiquitination assay in COS7 cells following 48 hours of transfection with the indicated plasmids. Western blotting was performed for KMT5A and the loading control, α -tubulin. N/T: non-transfected. The red asterisk indicates a poly-ubiquitinated KMT5A product with an additional post-translational modification.

3.5 Discussion

Whilst considerable attention has been directed to KMT5A poly-ubiquitination and its degradation by the proteasome as a crucial mechanism in controlling KMT5A activity during the cell cycle, no studies have investigated the presence of mono-ubiquitinated KMT5A as a prominent post-translational modification. This significance is backed up by the lack of studies in investigating an abundant form of KMT5A with a higher molecular weight, indicative of a mono-ubiquitinated KMT5A. In this chapter, various methods were utilised to provide evidence for the existence of mono-ubiquitinated KMT5A.

The data presented in this chapter revealed the existence of mono-ubiquitinated KMT5A in a panel of PC cell lines which were expressed at different levels. Notably, the level of endogenous mono-ubiquitinated KMT5A was similar to unmodified KMT5A levels for each cell line, except for DU145 cells which did not show detectable mono-ubiquitinated KMT5A (Figure 3.1). This could be due to these cells being devoid of an enzyme to mono-ubiquitinate KMT5A or it is possible that KMT5A is ubiquitinated and eliminated rapidly in DU145 cells, making it below the detection limit of our system. It would be interesting to investigate KMT5A mono-ubiquitination in DU145 cells following KMT5A over-expression. Mono-ubiquitinated KMT5A was further shown to be present when expressed from a plasmid in a different cellular background, using COS7 cells (Figure 3.2). Interestingly, despite the high expression level of unmodified KMT5A, the level of mono-ubiquitinated KMT5A was much lower, in contrast to the PC cell lines. The extent of this post-translational modification could therefore be cell-type specific possibly caused by the expression level of protein(s) responsible for mono-ubiquitinating KMT5A or deubiquitinating enzymes (DUBs) which remove ubiquitin moieties from proteins. Furthermore, it could be due to the proteins that modulate the activity of the E3 responsible for KMT5A mono-ubiquitination or the corresponding DUB. Additionally, it may partly be due to the difference in the cell cycle distribution of the cells at the time of collection, which will be discussed further in Chapter 4.

The Western-based ubiquitination assays performed using COS7 cells confirmed full-length KMT5A is mono-ubiquitinated (Figure 3.3). Furthermore, inhibiting proteasomal-mediated degradation by MG132 treatment led to a dramatic stabilisation of KMT5A, forming multi-ubiquitinated KMT5A products, namely di- and tri-ubiquitinated KMT5A as seen by their distinct bands (Figure 3.3). Interestingly, the mono-ubiquitinated form of KMT5A was predominant over any of the poly-ubiquitinated KMT5A forms, indicating KMT5A is stabilised upon mono-ubiquitin conjugation. Therefore, this could be the underlying reason for observing mono-ubiquitinated

KMT5A as a prominent form in PC cell lines. Similarly, mammalian apurinic/apyrimidinic endonuclease (APE1), an essential DNA repair regulatory protein has been inferred to be stabilised in a similar manner (Busso *et al.*, 2009).

The C-terminal domain of KMT5A represents two thirds of the protein and comprises many of the evolutionary conserved lysines. Moreover, it contains the catalytic SET domain of KMT5A which must be tightly regulated. In addition to altering protein stability, mono-ubiquitination regulates the function of the protein substrate, leading to either increased or decreased activity. Interestingly, SETDB1 tri-methylase activity has been shown to be positively regulated by mono-ubiquitination of its evolutionary conserved lysine, K867, located in its SET insertion (i-set) domain (Sun and Fang, 2016). As already discussed in Chapter 1.5.2, the SET domain of human methyltransferases is flanked by distinctive sub-domains at its N and C termini, n-SET and c-Set, respectively. These sub-domains are separated by a considerably variable i-set region which acts as a substrate docking platform, whilst the majority of its invariant residues are associated most directly with the active site (Xiao *et al.*, 2003). As mono-ubiquitination played such a crucial role in the activity of SETDB1, sequence alignment of human SETDB1 and KMT5A was performed to determine whether the i-set sequence or the sequence flanking the mono-ubiquitinated lysine (K867) in SETDB1 is common with that of KMT5A or is it similar to the region between KMT5A C2 and C3 required for KMT5A mono-ubiquitination. However, there were no similarities found. Although, no evidence has been provided by this body of work, KMT5A enzymatic activity could also be subject to a similar regulation, all of which suggests that the C-terminus is targeted for mono-ubiquitination.

In an effort to identify the site(s) of KMT5A mono-ubiquitination, site-directed mutagenesis was used to substitute the lysine of interest with an arginine. Six different lysine residues, located in KMT5A C-terminus, previously identified as putative ubiquitination sites in a mass spectrometry study (Kim *et al.*, 2011), were selected and individually mutagenised. The fact that these lysines were evolutionary conserved among different species, implied that some of them might have an important role in KMT5A regulation other than mediating its poly-ubiquitination and degradation. However, these lysines were found not to be responsible for KMT5A mono-ubiquitination as the mono-ubiquitinated levels of KMT5A were not affected upon their mutagenesis. Subsequently, all the remaining lysine residues in KMT5A C-terminus were individually mutagenised (25 lysines in total), but none of the single point mutations caused an apparent change in mono-ubiquitination of KMT5A (Figure 3.7). This suggested that either these lysines are not the primary site for accepting

a single ubiquitin moiety or that there is a compensatory mechanism whereby mono-ubiquitination can take place on alternative lysines following mutation of the primary site, with the “alternative hypothesis” being reported by many other studies (Ju and Xie, 2006; Demuc *et al.*, 2009; Li *et al.*, 2014c; Ray *et al.*, 2014). However, an alternative speculation is that KMT5A is mono-ubiquitinated at multiple lysine residues, where the di- and tri-ubiquitinated KMT5A products visualised on Western blotting could actually be mono-ubiquitin conjugations at two or three different lysine residues, respectively. This suggests, there are more than one primary lysine site in KMT5A undergoing mono-ubiquitin conjugation. As a result, it was not possible to find a major mono-ubiquitin acceptor site as mutating individual lysine did not prevent mono-ubiquitin conjugation at the other lysines available.

To study this further in the future and to confirm our speculation it would be useful to use a mutant ubiquitin containing no lysines (K0-Ub), which would only allow for mono-ubiquitination, in our ubiquitination assays. As K0-Ub is unable to form ubiquitin chains, the level of mono-, di- and tri-ubiquitin KMT5A should not be affected relative to wild-type ubiquitin, should those forms of KMT5A be mono-ubiquitination at multiple lysines.

Interestingly, mono-ubiquitinated KMT5A persisted after KMT5A knockdown in PC cell lines which further suggests it is a more stable form of KMT5A and hence its prevalence in PC cell lines; whereas the di-ubiquitinated KMT5A was found to be depleted, (Figure 3.4). Mono-ubiquitination of KMT5A represents the transition between unmodified and di-ubiquitinated (assuming chain formation) KMT5A forms where its latter form could be more susceptible to becoming further poly-ubiquitinated and degraded. However, proteasomal degradation of ubiquitinated proteins has been reported to require four or more ubiquitin molecules in the poly-ubiquitin chain conjugated to the substrate protein (Pickart, 2000; Pickart and Fushman, 2004). In addition to the canonical lys48-linked poly-ubiquitination and proteolysis by the proteasome, multiple mono-ubiquitination at different sites has also been shown to signal for protein degradation by the proteasome (Boutet *et al.*, 2007; Dimova *et al.*, 2012). This may account for depletion of di-ubiquitinated KMT5A, and the absence or undetectable endogenous levels of these higher molecular weight forms (Figure 3.4), further supporting speculation of KMT5A being mono-ubiquitinated at multiple lysine residues. Additionally, it helps to explain the stabilisation of mono-, di- and tri-ubiquitinated KMT5A products upon MG132 treatment, indicating multiple mono-ubiquitinated forms of KMT5A could potentially be targeted for degradation (Figure 3.3). However, it does not explain why di-ubiquitinated KMT5A forms are only depleted with KMT5A knockdown. It would be of great

value to perform cycloheximide experiments to follow the stability of the unmodified, mono- and di-ubiquitinated KMT5A forms in some of the PC cell lines.

In the current work, mass spectrometry analysis was also used to identify the lysine residue(s) that can be mono-ubiquitinated in KMT5A. Unfortunately, our first attempt was not successful and indicated that a much larger amount of material was required. This would have involved scaling up the work at a level that was no longer practical.

Whilst the specific lysine(s) undergoing mono-ubiquitin conjugation remains unknown, it was possible to apply an alternative strategy to localise a region of KMT5A being mono-ubiquitinated. Firstly, a series of truncations were made from the larger KMT5A C-terminus fragment and subsequently assessed for their ability to become mono-ubiquitinated. This system enabled a region in KMT5A which is required for its mono-ubiquitination to be defined. The inability of the shortened fragment C2 of KMT5A C-terminus to be mono-ubiquitinated (or di-, tri-ubiquitinated) whilst the slightly lengthened fragment C3 of KMT5A was efficiently mono-ubiquitinated (and also di- and poly-ubiquitinated) highlights a short region within the C-terminal KMT5A that is important for KMT5A mono-ubiquitination, Figure 3.9. Interestingly, KMT5A C-terminus fragment C3 was modified to the greatest extent compared to the longer fragments including the KMT5A C-terminus (Figure 3.9). De-stabilisation of mono-ubiquitinated KMT5A as the C-domain gets longer could be due to degradation as more lysines are available for ubiquitination, or de-ubiquitination. For example, the longer fragments may include peptide binding sequence for protein partners involved in KMT5A turnover, or possibly introduce a phosphorylation site required for de-ubiquitination as there are reports of phosphorylation-dependent de-ubiquitination (Ramachandran *et al.*, 2016).

The fact that K321 is the sole additional lysine present in fragment C3 compared to fragment C2, and appears to be responsible for the formation of higher molecular weight KMT5A products, may conflict with initial speculation that KMT5A is mono-ubiquitinated at multiple lysines. Furthermore, this may suggest the detected di- and tri-ubiquitinated forms of KMT5A are chains of ubiquitin rather than multiple mono-ubiquitin additions in the protein. However, mono-ubiquitination of C3 may lead to a conformational change in KMT5A C-terminus that exposes other lysine residues for further mono-ubiquitination at multiple sites.

As K321 was the only lysine in the amino acid stretch between fragments C2 and C3, it was thought that K321 is the primary ubiquitin acceptor site in KMT5A. Therefore, K321 was mutated in

KMT5A C-terminus background, but it failed to abolish KMT5A mono-ubiquitination (Figure 3.11). This could have been due to the fact that KMT5A fragment C3 is mono-ubiquitinated at multiple sites, whereby mutating K321 does not affect mono-ubiquitin conjugation occurring at other available lysines, in line with our initial speculation. Additionally, it may mean that the peptide sequence (aa 310-330) contains an important recognition sequence for an associated protein partner that is involved with KMT5A mono-ubiquitin conjugation, whilst the site of mono-ubiquitination may lie somewhere else in the KMT5A C-terminus. Alternatively, a phosphorylation event may be required for KMT5A to become mono-ubiquitinated, as many ubiquitination events are preceded by phosphorylation (Fuchs *et al.*, 1996; Tsvetkov *et al.*, 1999; Chernov *et al.*, 2001). However, analysis of KMT5A phosphorylation sites using available online software in this stretch of amino acids did not reveal any strong consensus phosphorylation sites. In contrast to these speculations, K321 could potentially be the primary mono-ubiquitin acceptor site in KMT5A, but due to promiscuity of the ubiquitination sites in KMT5A, other lysines may act as backup ubiquitin acceptor sites and compensate for the loss of K321. Similarly, the same problem has been reported by other studies investigating the site of mono-ubiquitination in various proteins. As an example, Han *et al.*, (2016), Li *et al.*, (2014) and Ray *et al.*, (2014) identified the site of mono-ubiquitination in survival motor neuron (SMN), ovarian tumour domain-containing ubiquitin aldehyde binding protein 1 (Outb1) and signal transducers and activator of transcription-3 (STAT3), respectively, by mass spectrometry; whilst, they failed to identify the same site using site-directed mutagenesis where the authors speculated the alternative lysine hypothesis to be the underlying reason.

Assessment of the role of KMT5A N-terminus in the mono-ubiquitination pattern of KMT5A C-terminus fragments was consistent with our notion that the C-domain of KMT5A is solely targeted for mono-ubiquitination. The newly created truncated fragments that included the N-terminal domain of KMT5A retained the same mono-ubiquitination pattern as the C-terminal constructs. The N-terminus-containing fragments, N-C1 and N-C2 failed to be ubiquitinated whereas fragment N-C3 underwent mono-ubiquitination (Figure 3.12 and 3.13). It is important to note that both fragments C3 and N-C3 were more abundantly expressed, regardless of the presence or absence of the KMT5A N-terminus than the other generated longer fragments. Although, the site(s) of mono-ubiquitination is almost certainly not located in KMT5A N-terminus, this region may still contribute to the level of KMT5A mono-ubiquitination through providing stability, binding site and other post-translational modifications which positively or negatively regulate mono-ubiquitin conjugation of KMT5A. Other post-translational modifications, in particular phosphorylation,

could underlie the presence of an additional ubiquitinated KMT5A form in the ubiquitination assay for the N-terminal domain containing fragment N-C3, (Figure 3.13). The important contribution of alternative post-translational modifications within the KMT5A N-terminus has previously been demonstrated by Wu et al., (Wu *et al.*, 2010) showing that de-phosphorylation of KMT5A at serine 100 promotes KMT5A ubiquitination by the APC^{Cdh1} complex. To investigate this further it would be possible to mutate consensus phosphorylation sites in the N-terminal domain of C-terminal deleted constructs and monitor the degree of mono-ubiquitination.

To continue the work in identifying the site of mono-ubiquitination, it would be of significant value to generate a set of KMT5A deletion constructs where the extreme C-terminus adjacent to the stop codon is retained, whilst regions back towards the N-terminus are progressively added. Similarly, the short peptide between fragments C2 and C3 could be expanded out in both C and N terminal directions. Moreover, the lysine residues on the surface of KMT5A can be identified using structural information, and a mutant KMT5A with all these lysines knocked out generated. The mutated lysines could then be reintroduced one at a time to monitor the re-appearance of mono-ubiquitinated KMT5A.

In summary, this body of work suggests the presence of mono-ubiquitinated KMT5A as a novel post-translational modification has been demonstrated and validated which has not been previously reported. The region of KMT5A important to enable mono-ubiquitination was shown to be localised within its C-terminus, specifically, amino acids 310-330. This could either be required for KMT5A mono-ubiquitination, or may contain important lysine residues responsible for mono-ubiquitin conjugation in KMT5A. However, the specific lysine site(s) undergoing mono-ubiquitination, and the underlying mechanism for KMT5A to be modified by mono-ubiquitin linkage remains unknown and warrants further investigations.

4 Investigating the role of mono-ubiquitinated KMT5A and its regulation by Skp2

4.1 Introduction

KMT5A plays an important role in an array of biological processes, by regulating the mono-methylation of histone H4K20 and non-histone proteins. More importantly, KMT5A has been shown to be a co-activator of the AR in CRPC, enhancing AR transcriptional activity. As KMT5A level, and in turn its activity, are under tight cell cycle regulation through post-translational modifications, and having demonstrated the dominant existence of mono-ubiquitinated KMT5A in PC cell lines in Chapter 3, it was hypothesized that regulatory mechanisms of KMT5A could be exploited to indirectly target the AR. Whilst, much effort has been made to understand the role unmodified KMT5A plays in many cellular processes and the functional consequences of its fluctuating levels during the cell cycle, nothing is known about the role of mono-ubiquitinated KMT5A. Therefore, the first aim of this chapter is to characterize the role of mono-ubiquitinated KMT5A.

In addition to previously characterized ubiquitination-mediated degradation of KMT5A by the SCF ^{β -TRCP}, CRL4^{Cdt2} and APC^{Cdh1} complexes during G1, S phase and mitosis, respectively, Skp2 has also been suggested to play a role in ubiquitinating KMT5A for proteasomal degradation (Abbas *et al.*, 2010; Centore *et al.*, 2010; Oda *et al.*, 2010; Wu *et al.*, 2010; Wang *et al.*, 2015). Skp2 is the F-box component of the SCF complex (Skp1-Rbx1-Cul1- F-Box) and functions as an E3 ligase (Schulman *et al.*, 2000). Skp2 regulates an array of downstream substrates and as such is essential in modulating several cellular functions such as cell cycle proliferation, cellular senescence, DNA repair and signal transductions (Carrano *et al.*, 1999; Sutterlüty *et al.*, 1999; Frescas and Pagano, 2008; Lin *et al.*, 2010). Moreover, Skp2 is also involved in regulating epigenetic events by targeting chromatin modifying enzymes in PC (Lu *et al.*, 2015).

Substantial evidence demonstrated that Skp2 plays a critical role in the tumourigenesis of various cancers including PC. Skp2 levels have been shown to be increased in PIN, suggesting induction of Skp2 is an early event in cellular transformation (Yang *et al.*, 2002). Moreover, Skp2 is dramatically elevated in PC, where increased copy number of *Skp2* gene has been reported in metastatic prostate tumours (Robbins *et al.*, 2011). Importantly, Skp2 protein levels are inversely correlated with recurrence-free survival (Yang *et al.*, 2002).

Despite the identification of many of the Skp2 substrates, there is emerging evidence of additional substrates. For example KMT5A has been suggested to be a target of Skp2 for ubiquitination and destruction by the proteasome (Yin *et al.*, 2008). However, no direct evidence has been published to confirm this to date. Therefore, the role of Skp2 in regulating KMT5A is understudied and remains elusive. As such, the second aim of this chapter is to investigate the role of Skp2 in regulating KMT5A.

4.2 Hypothesis

Firstly, based on the fact that post-translational modifications of KMT5A are under cell cycle regulation, it is hypothesised that the underlying mechanism regulating KMT5A mono-ubiquitination is cell cycle dependent.

Secondly, due to the dominant existence of mono-ubiquitinated species of KMT5A in PC cell lines as shown in the previous chapter, it is hypothesised that mono-ubiquitinated KMT5A has an important role in the cell.

Thirdly, Skp2 is a well-known cell cycle regulator, responsible for G1-S transition of the cell cycle through ubiquitination and degradation of the cell cycle inhibitor, p27 (Carrano *et al.*, 1999; Sutterlüty *et al.*, 1999). KMT5A has also been extensively shown to regulate cell cycle progression; whereby, it is degraded when cells are transitioning from G1 to S phase of the cell cycle. In this regard, it is predicted that Skp2 modulates KMT5A through ubiquitination.

4.2.1 Aims

- Investigate the cell cycle control of KMT5A mono-ubiquitination
- Determine mono-ubiquitinated KMT5A cellular localisation
- Determine the effect of mono-ubiquitinated KMT5A on the cell cycle
- Establish the role of Skp2 in KMT5A ubiquitination

4.3 Results

4.3.1 *Investigating the cell cycle control of mono-ubiquitinated KMT5A*

Given that post-translational modifications of KMT5A are strongly modulated depending on the cell cycle stage, we sought to investigate whether the regulation of mono-ubiquitination itself is subjected to the same regulatory mechanism. For this purpose, exponentially growing LNCaP and LNCaP-AI cell lines were sorted according to their cell cycle phase using Hoechst staining as described in Chapter 2.11.1. LNCaP and LNCaP-AI cell lines were chosen as it was initially thought mono-ubiquitinated KMT5A could be differentially regulated between these two cell lines as a possible underlying mechanism for KMT5A's opposing manner in regulating the AR.

Asynchronous cells were sorted into the different cell cycle phases after placing tight gates for each phase to prevent as much contamination as possible by excluding the collection of cells in other phases of the cell cycle, shown in Figure 4.1A. The separation system of cells was validated using the mitotic marker, phosphorylated serine 10 on histone 3 (pS10-H3), which was shown to be significantly enriched in the G2/M sorted pool of the cells compared to the mixed population, as of expected (Figure 4.1B).

Consistent with the reported KMT5A expression levels, unmodified KMT5A was expressed at very low levels in the G0/G1 population of cells, which was further reduced in the S phase; whereas, it was expressed at very high levels in the G2/M phase of the cell cycle (Figure 4.1B). Thus, unmodified KMT5A level was used as an internal control for the system as its levels reflected that of the published literature. Interestingly, mono-ubiquitinated KMT5A was found to be enriched in the S phase sorted population of cells for both LNCaP and LNCaP-AI (Figure 4.1B). Although at first sight, mono-ubiquitinated KMT5A levels appeared to be similar across the different phases of the cell cycle, it became evident that despite the very low levels of unmodified KMT5A in S phase, mono-ubiquitinated KMT5A is expressed to a similar extent as in other phases of the cell cycle, in particular G2/M, where the unmodified KMT5A is at its highest level. It is therefore apparent that the ratio of modified : unmodified KMT5A varies dramatically between the different cell cycle phases with the highest ratio of mono-ubiquitinated KMT5A : unmodified KMT5A being evident in S phase. This observation is in keeping with our hypothesis that mono-ubiquitination of KMT5A occurs in a cell cycle dependent manner.

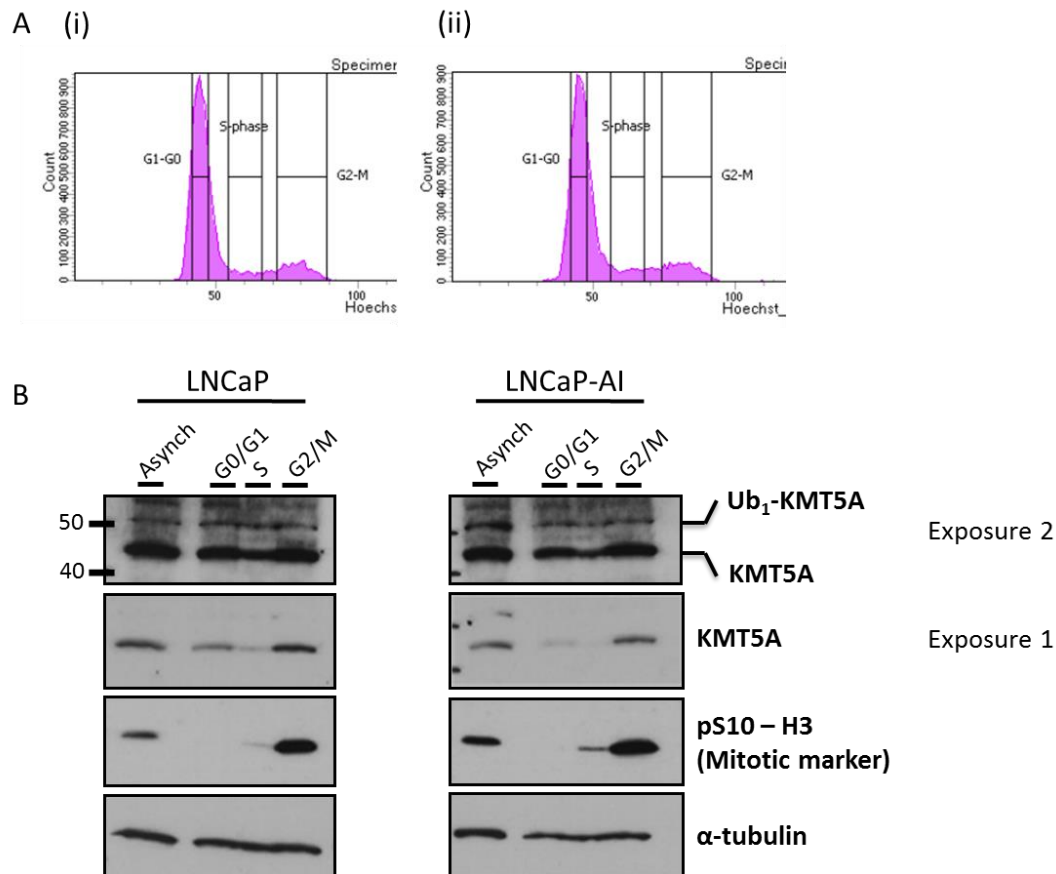


Figure 4-1: Mono-ubiquitinated KMT5A is enriched in proliferating cells. Exponentially growing LNCaP and LNCaP-AI cell lines were stained with Hoechst at 20 $\mu\text{g}/\text{mL}$ for 40 minutes at 37 $^{\circ}\text{C}$ in the dark. For each cell line, the asynchronous (Asynch) population was sorted into the different cell cycle phases using flow cytometry. **(A)** LNCaP **(i)** and LNCaP-AI **(ii)** were separated into G0/G1, S and G2/M. The histograms demonstrate the cell cycle distribution of cells and the vertical lines define the gates to isolate cells in the indicated phases of the cell cycle. Data was analysed using FlowJo software. **(B)** Western blot analysis was performed for each of the sub-populations after being re-suspended in SDS sample buffer for KMT5A, the mitotic marker, pS10-H3, and loading control α -tubulin. This blot is a representative of three independent repeats.

4.3.2 The expression of mono-ubiquitinated KMT5A is cell cycle dependent

Having demonstrated and validated a robust cell sorting system, we aimed to extend our data to assess the level of KMT5A mono-ubiquitination in cells transitioning from G1 to S, and then from S to G2 phases of the cell cycle. The experiment was performed as before but only in the LNCaP cell line, as no difference in KMT5A mono-ubiquitination was observed between the LNCaP and LNCaP-AI tested in Chapter 4.3.1, and might be the same in LNCaP-AI cells.

Figure 4.2A demonstrates that the levels of unmodified KMT5A throughout the cell cycle confirms the data in the previous section and is in line with the literature, where KMT5A is expressed at low levels in G0/G1. Upon transition of cells from G1 to S phase (G1>S), unmodified KMT5A levels declined rapidly and is at its lowest level during S phase. However, as cells transitioned from S to G2 (S>G2), unmodified KMT5A expression significantly increased and reached its peak in mitosis. In a striking contrast, mono-ubiquitin conjugated KMT5A is at its highest level in S phase, despite the very small pool of unmodified KMT5A present, suggesting that mono-ubiquitinated KMT5A is the abundant form of total KMT5A in this phase of the cell cycle. On the other hand, mono-ubiquitinated KMT5A levels declined rapidly as cells exited the S phase and progressed into the G2/M phase of the cell cycle; whereby, mono-ubiquitinated KMT5A is at its lowest expression level despite the large pool of unmodified KMT5A.

The unmodified and mono-ubiquitinated KMT5A bands on this Western blot were quantified using densitometry and data presented as a line graph, demonstrates the ratio of mono-ubiquitinated KMT5A to its unmodified form for the corresponding cell cycle phases (Figure 4.2B). Interestingly, it became evident that unmodified and mono-ubiquitinated KMT5A levels are inversely correlated in all the phases of cell cycle, with the highest ratio of mono-ubiquitinated KMT5A to unmodified KMT5A in S phase (Figure 4.2C).

Moreover, Skp2 expression was also investigated as a potential regulator of KMT5A. As already alluded to, KMT5A has been suggested to be regulated by Skp2, although there is a lack of detailed studies to confirm this. Skp2 expression was shown to be consistent with other studies, where, it is almost undetectable in G0/G1, suddenly increased as cells transitioned from G1 to S phase and rose even further during S phase. Its levels then appears to be maintained throughout the remaining phases (Figure 4.2B).

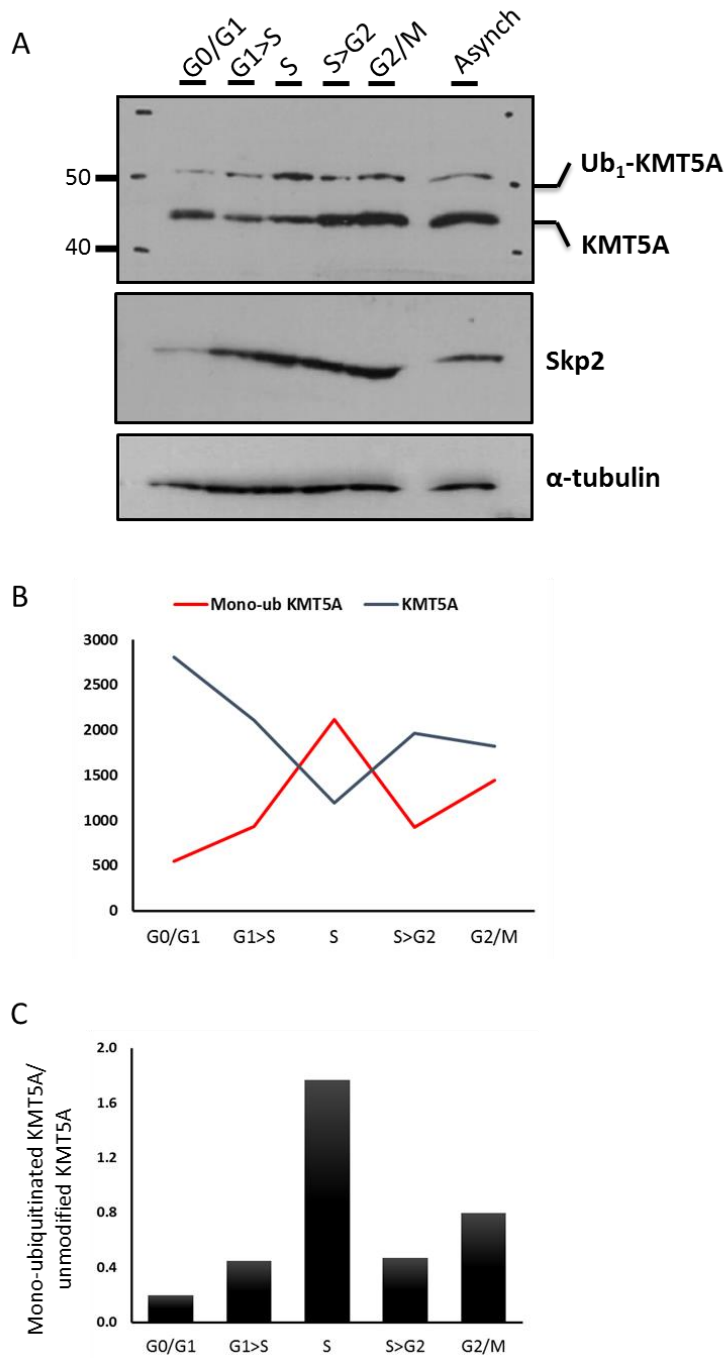


Figure 4-2: Mono-ubiquitinated KMT5A oscillation is cell cycle dependent. Exponentially growing LNCaP cells were stained with Hoechst at 20 $\mu\text{g}/\text{mL}$ in the dark. Following 40 minutes incubation at 37 $^{\circ}\text{C}$, the cells were sorted into the respective cell cycle phases using flow cytometry. (A) The retrieved cells were lysed with SDS sample buffer and subject to Western analysis for KMT5A, Skp2 and the loading control, α -tubulin. (B) Densitometry was used to quantify the unmodified and mono-ubiquitinated KMT5A bands, and the absolute values represented graphically. (C) The ratio of mono-ubiquitinated KMT5A to unmodified KMT5A using the raw densitometry data.

4.3.3 Mono-ubiquitinated KMT5A expression is associated with cellular confluency

During the course of these experiments it was observed that the level of mono-ubiquitinated KMT5A was influenced with the confluency of cells for different experiments that were performed. As the relative proportion of mono-ubiquitinated KMT5A was found to be enriched in S phase where LNCaP cells are in a proliferative state, it suggested that KMT5A mono-ubiquitination is affected by cellular confluency. Sub-confluent cells are actively dividing and colonising the available space and are thus in a more proliferative state. Conversely, growth slows and ceases when cells are over confluent, entering quiescence. Therefore, it was hypothesised that sub-confluent cells express higher levels of mono-ubiquitinated KMT5A.

To test this hypothesis, LNCaP cells were seeded at different densities and grown for 48 hours in FM, after which three different confluences were chosen (30%, 50% and 80-90%) as seen in Figure 4-3A. Western blot analysis revealed that sub-confluent cells at 30% and 50%, which are rapidly dividing as confirmed by the expression level of mitotic marker pS10-H3, exhibited higher levels of KMT5A mono-ubiquitination. However, upon becoming highly confluent at 80-90%, the level of mono-ubiquitinated KMT5A modestly declined, Figure 4-3B.

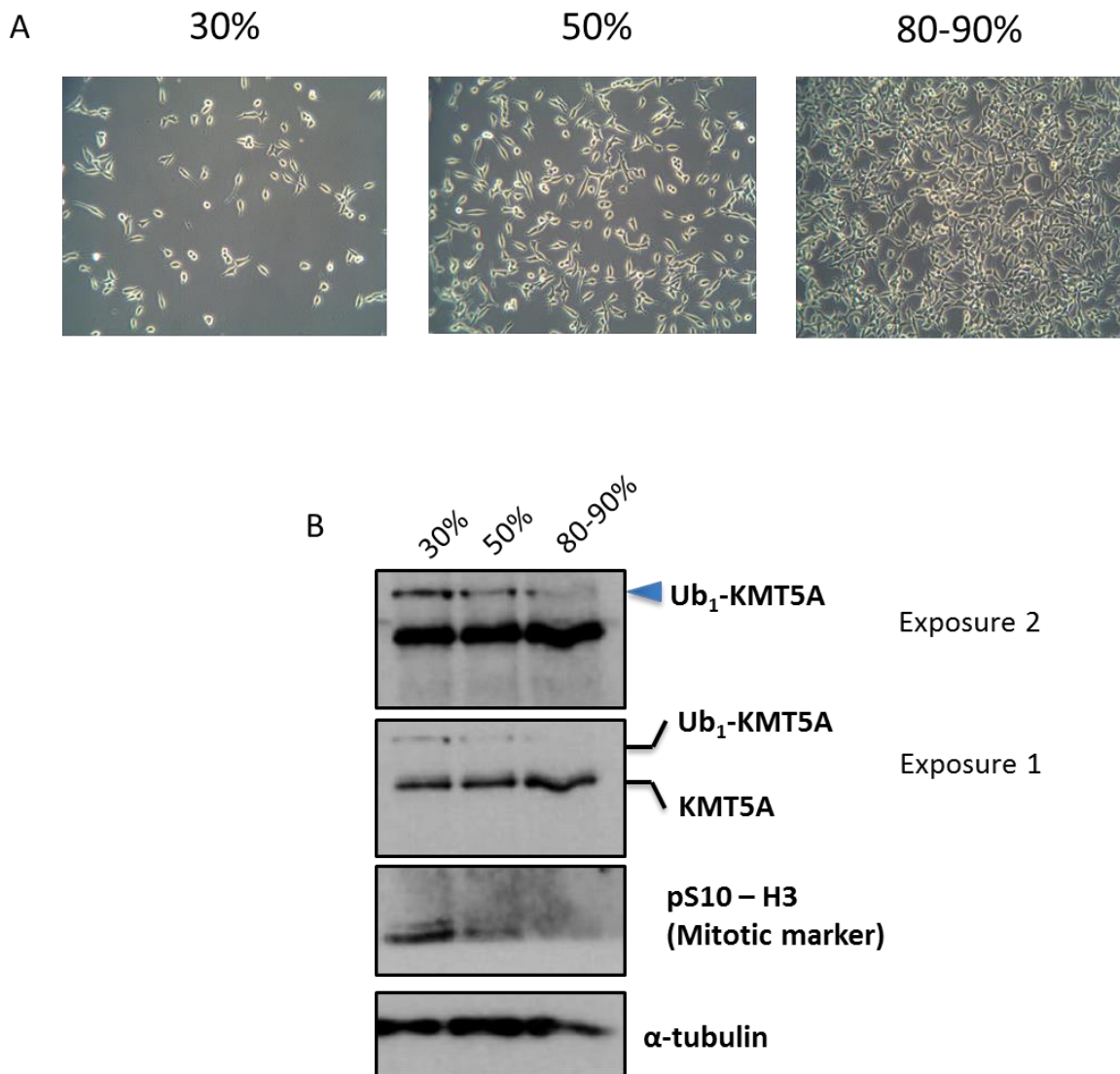


Figure 4-3: Mono-ubiquitination of KMT5A is elevated in dividing cells. LNCaP cells were seeded at different cellular densities and left to grow for 48 hours in FM. **(A)** The cells were assessed for their confluency using microscopy and images were taken for the following confluencies, 30, 50 and 80-90%. **(B)** The indicated cell confluencies were collected for Western blotting for KMT5A, mitotic marker pS10-H3 and the loading control, α -tubulin. This is a representative blot of two independent repeats.

4.3.4 *Mono-ubiquitinated KMT5A is cytoplasmic*

Mono-ubiquitination regulates the cellular localisation of proteins (Grompe and D'Andrea, 2001; Li *et al.*, 2003; van der Horst *et al.*, 2006). Many groups have demonstrated KMT5A to be mainly in the nucleus due to its role in maintaining genome integrity and chromatin structure. KMT5A mobilisation between cellular compartments has only been reported by Yin *et al* (2008) who showed KMT5A distribution varies greatly between cells, and is cell cycle dependent. In order to address the localization of mono-ubiquitinated KMT5A, cellular fractionation was carried out on LNCaP cells which were grown in FM, followed by Western blot analysis.

The efficiency of the cellular fractionation was visualised using the nuclear protein PARP and the cytoplasmic protein α -tubulin and confirmed there was relatively little contamination between the nuclear and cytoplasmic samples (Figure 4.4A). Unmodified KMT5A was present in equal quantities in the chromatin fraction, nucleus and the cytoplasm, whereas mono-ubiquitinated KMT5A was found exclusively in the cytoplasm (Figure 4.4A). This observation suggested that mono-ubiquitination of KMT5A could either result in its nuclear export or restrict its entry into the nucleus.

To further elucidate that mono-ubiquitin conjugation is responsible for the cytoplasmic localisation of mono-ubiquitinated form of KMT5A, cellular fractionation was performed using the mono-ubiquitin competent KMT5A truncated fragments N-C2 and N-C3 that were overexpressed in COS7 cells. As expected, KMT5A fragment N-C3 which undergoes mono-ubiquitin conjugation, showed mono-ubiquitinated KMT5A is located almost exclusively in the cytoplasm, although small amounts could be observed in the nucleus following longer exposures (Figure 4.4B). Furthermore, unmodified KMT5A was present in both the nucleus and cytoplasm in an approximate 50/50 ratio, as seen with endogenous unmodified KMT5A's distribution in the LNCaP cells (Figure 4.4A) In contrast, KMT5A fragment N-C2 which is not modified by mono-ubiquitination, only expressed the unmodified form of KMT5A, which exhibited the same distribution pattern as unmodified KMT5A fragment N-C3 and endogenous KMT5A (Figure 4.4A and B). It is important to note, that the higher molecular weight bands present on the Western blot for KMT5A N-C2, do not correspond to any mono-ubiquitinated form as they have too high a molecular weight to be a mono-ubiquitin conjugated N-C2 product, and are therefore non-specific binding. Collectively, the data suggests mono-ubiquitin conjugation is responsible for mono-ubiquitinated KMT5A cytoplasmic accumulation.

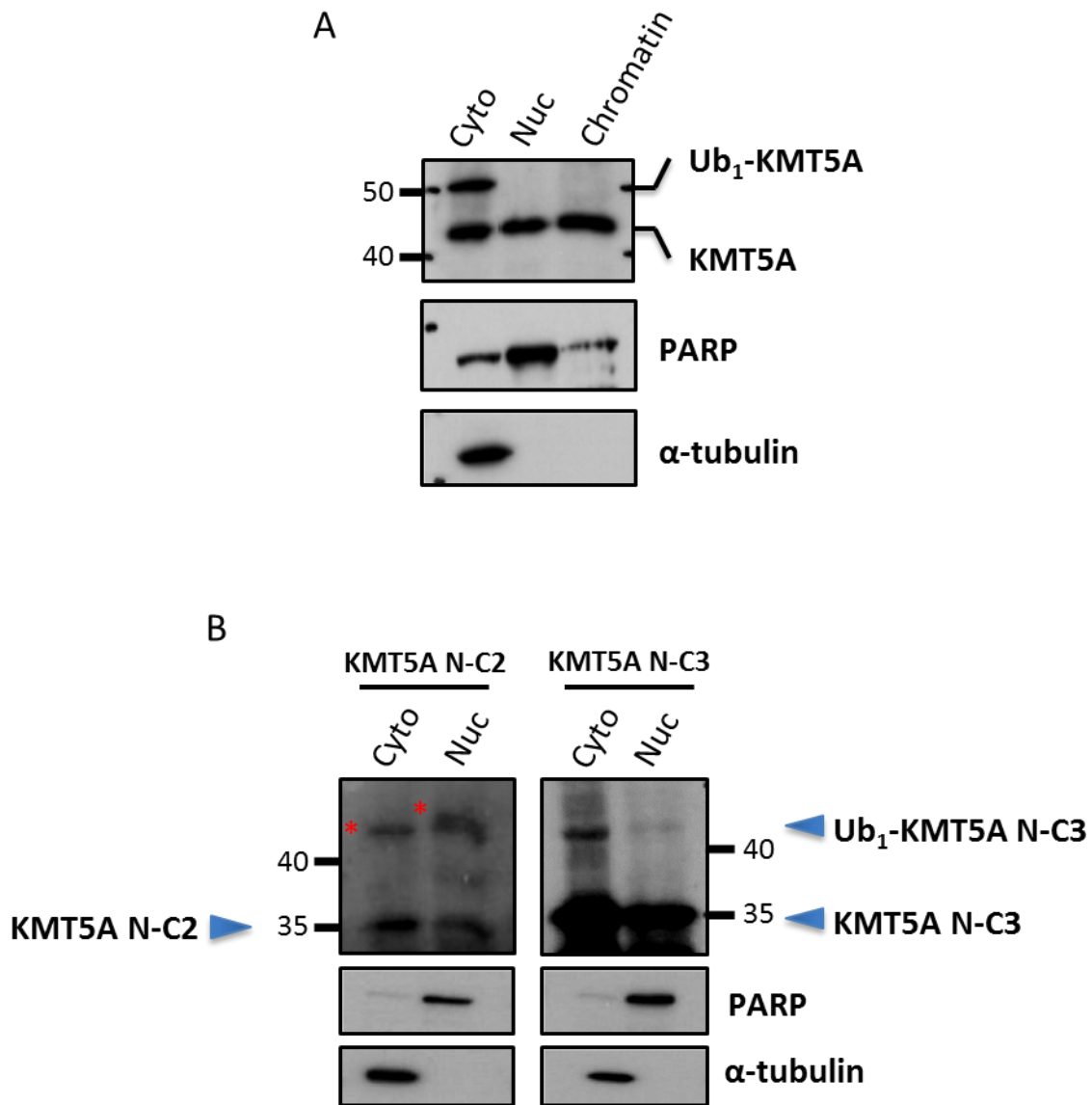


Figure 4-4: Mono-ubiquitinated KMT5A is exclusively localised in the cytoplasm. (A) LNCaP cells were subjected to cellular fractionation, followed by Western blot analysis for endogenous KMT5A, cytoplasmic marker α -tubulin and nuclear marker PARP. (B) COS7 cells overexpressing the mono-ubiquitin deficient (fragment N-C2) and mono-ubiquitin competent (fragment N-C3) KMT5A constructs were subject to cellular fractionation, followed by Western blot analysis for KMT5A, cytoplasmic marker α -tubulin and nuclear marker PARP. Asterisk indicates non-specific binding.

4.3.5 Investigating the role of KMT5A mono-ubiquitination on the cell cycle

KMT5A plays a crucial role in cell cycle progression, where KMT5A knockdown and overexpression studies demonstrate mild to dramatic cell cycle disturbances depending on the experimental conditions (Abbas *et al.*, 2010; Centore *et al.*, 2010). The enzymatic activity of KMT5A has been reported to be a negative regulator of DNA replication and cellular proliferation, hence the degradation of KMT5A in S phase (Centore *et al.*, 2010). However, an opposite role for mono-ubiquitinated KMT5A is suggested by its accumulation in proliferative cells. Importantly though, despite the accumulation of mono-ubiquitinated KMT5A in S phase, it was then found to be exclusively residing in the cytoplasm, suggesting indeed that KMT5A is incompatible with DNA replication. Therefore, the biological relevance of oscillating mono-ubiquitinated KMT5A expression during the cell cycle was investigated.

To this end, COS7 cells were transfected with mono-ubiquitin deficient (fragments N-C1 and N-C2) and mono-ubiquitin-competent (fragment N-C3) KMT5A fragments. Following 48 hours post-transfection, PI based flow cytometry was performed to determine any cell cycle profile changes. However, analysis of the data did not show any alterations in the cell cycle profile of cells overexpressing the mutant forms of KMT5A compared to non-transfected COS7 cells (Figure 4.5). As in some studies, KMT5A overexpression-mediated changes have been observed with longer expression time points as compared to 48 hours used in our experiment, it was considered such changes on the cycle and proliferation require longer KMT5A overexpression. Due to time constraints, this experiment was performed only once, but if it was to be repeated, constructs should be overexpressed for longer time points and also include the full-length, wild-type KMT5A as a positive control. Furthermore, as the transient transfection efficiency in COS7 cells is expected to be around 50-70% it would be important to separate only those cells expressing the constructs for further analysis. This could be achieved by co-transfecting an identifiable marker-containing plasmid, such as GFP and sorting cells by flow cytometry prior to Western blotting.

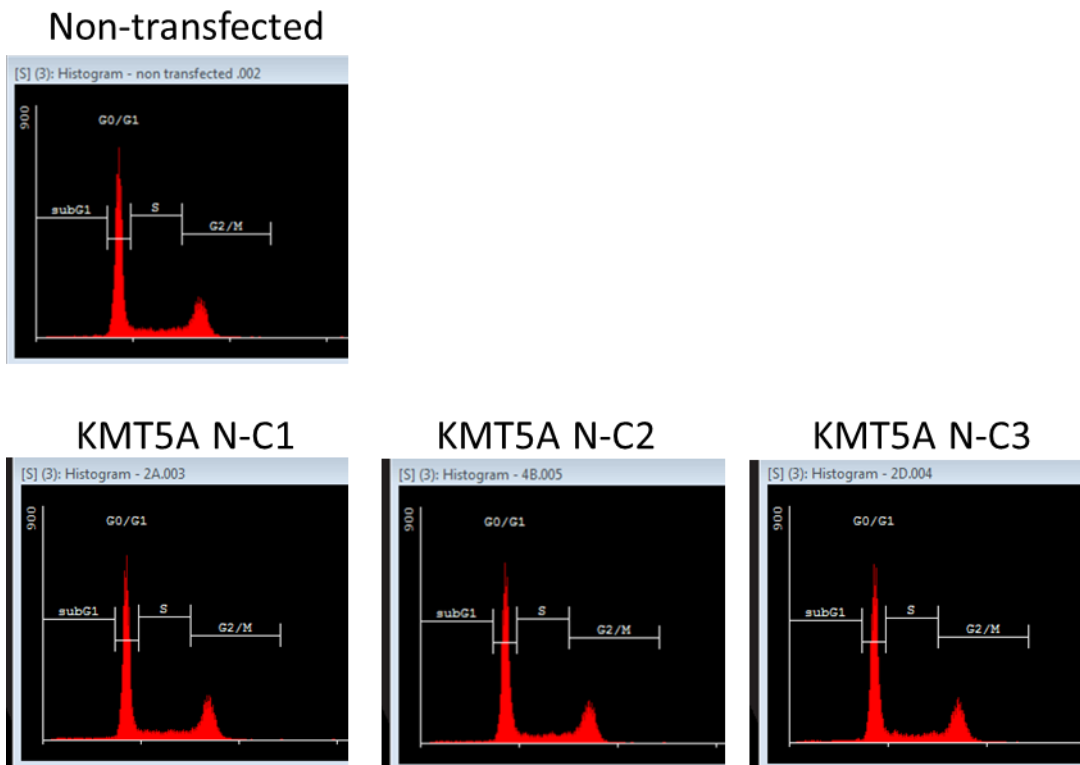


Figure 4-5: Transient overexpression of KMT5A truncated mono-ubiquitin deficient and competent truncated derivatives of KMT5A does not affect the cell cycle. COS7 cells were transfected with KMT5A mono-ubiquitin deficient (fragments N-C1 and N-C2) and mono-ubiquitin competent (fragment N-C3) constructs. Non-transfected COS7 cells were only treated with the LT-1 cocktail without any plasmid. Following 48 hours incubation in FM, the cells were subjected to cell cycle analysis subsequent to flow cytometry using propidium iodide. Data was analysed using Cyflogic software for 10,000 cells. This experiment was conducted once.

4.3.6 Alteration in KMT5A mono-ubiquitination affects cell proliferation

In order to elucidate the role of KMT5A mono-ubiquitination on cell cycle progression, cell proliferation rates were examined. COS7 cells were transfected with full-length wild-type KMT5A and its truncation mutants, fragments N-C2 and N-C3, in a 6-well plate for 48 hours. Then the cells were trypsinised and seeded out in a 96-well plate and left to grow for six days in the IncuCyte system (Essen Bioscience), measuring dynamic alterations in cellular confluence over this time period. This approach was conducted to firstly, enable efficient transfection of the constructs and secondly, allow sufficient time for KMT5A overexpression-mediated effects to take place. As mono-ubiquitinated KMT5A was found to be at its highest level in proliferating cells despite the very low levels of unmodified KMT5A, as well as the data strongly supporting mono-ubiquitination being responsible for the cytoplasmic localisation of mono-ubiquitinated KMT5A, it was predicted that mono-ubiquitin deficient KMT5A fragment N-C2 would reduce proliferation rate compared to wild-type KMT5A. This was suggested because N-C2 cannot undergo mono-ubiquitination or at least efficient mono-ubiquitination for it to be excluded from the nucleus. However, mono-ubiquitin competent KMT5A fragment N-C3, which is modified by mono-ubiquitination is able to localise to the cytoplasm and should therefore not have a significant effect on proliferation compared to wild-type KMT5A.

Interestingly, the overexpression of KMT5A N-C2 caused a reduction in cell proliferation compared to wild-type KMT5A. Conversely, KMT5A N-C3 overexpression increased proliferation in comparison to wild-type KMT5A (Figure 4.6). Although it is promising that this observation supports the hypothesis and is consistent with previously published data with regards to the negative role of KMT5A on cell proliferation, further experimental optimisation is required. For example, cell density should be optimized to ensure sufficient cells are seeded to enable them to reach the logarithmic phase of cell growth earlier than the 3 days achieved in this initial experiment. Such a delay may affect transfected KMT5A expression levels and any effects that KMT5A may have had on the rate of proliferation.

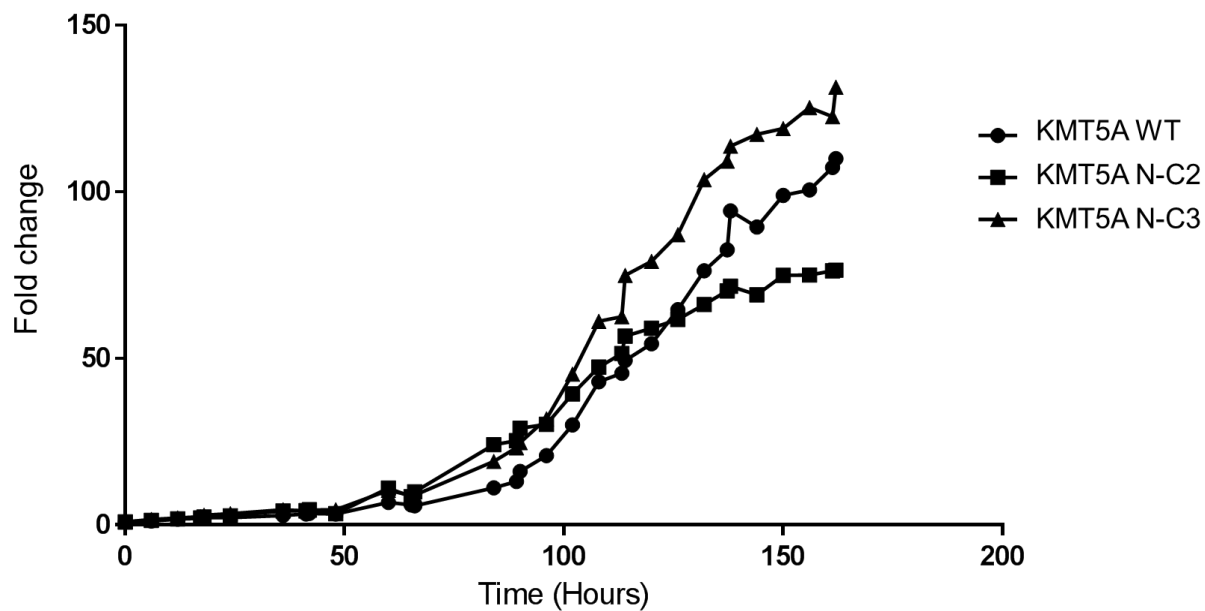


Figure 4-6: The ubiquitination status of KMT5A affects cellular proliferation. COS7 cells were transfected with wild-type KMT5A and its truncated mutants in a 6-well plate. 48 hours post-transfection, the cells were trypsinised, seeded in a 96-well plate and left to grow for 6 days in the IncuCyte system (Essen Bioscience), analysing the cellular confluency of wells every 4 hours. This experiment was performed once.

4.3.7 *Skp2 is associated with KMT5A mono-ubiquitination*

Skp2 plays an important role in cell cycle progression where it is responsible for driving G1 to S phase transition via ubiquitination of the cell cycle inhibitor, p27, to result in its subsequent proteasomal destruction. Skp2 has been suggested to play a secondary role to the CRL^{Cdt2} complex in KMT5A ubiquitination and proteasomal mediated degradation (Centore *et al.*, 2010); however, there is insufficient evidence to confirm this to date. Moreover, KMT5A is mainly ubiquitinated at the G1-S transition (Yin *et al.*, 2008; Centore *et al.*, 2010), and unmodified KMT5A levels declined rapidly at this stage of the cell cycle whilst Skp2 expression was found to be significantly upregulated (Figure 4.2A). Therefore, the role of Skp2 in regulating KMT5A was investigated.

In order to determine the role of Skp2 in regulating KMT5A, a constant amount of KMT5A was co-expressed with increasing amounts of Skp2 in COS7 cells, as increasing the levels of Skp2 is expected to result in increased levels of KMT5A destruction via higher level of ubiquitination. The whole cell lysates were collected for Western blot analysis. Interestingly, mono-ubiquitinated KMT5A was found to be significantly upregulated with higher concentrations of Skp2 at 1 µg and 2 µg (Figure 4-7, lanes 5 and 6), with lower concentrations of 0.1, 0.2 and 0.5 µg causing a clear but modest increase (Figure 4-7, lanes 2-4). In contrast, poly-ubiquitination of KMT5A was not affected at these lower Skp2 concentrations, and was only markedly upregulated at higher concentrations of Skp2. However, it would have been prudent to include an MG132 treatment arm to determine the poly-ubiquitination pattern of KMT5A.

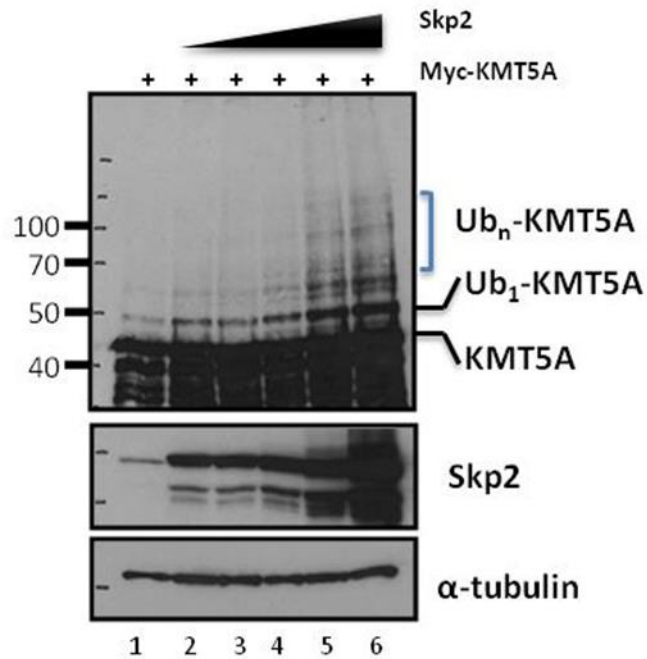


Figure 4-7: Mono-ubiquitination of KMT5A is promoted with increasing amounts of Skp2. COS7 cells were co-transfected with a constant amount of KMT5A plasmid and an increasing amount of Skp2 plasmid (0.1, 0.2, 0.5, 1 and 2 μg). All the reactions were balanced with appropriate empty vector. Western blot analysis of the cell lysates was carried out 48 hours post-transfection for KMT5A, Skp2 and the loading control, α-tubulin.

4.3.8 KMT5A and Skp2 proteins interact

Skp2 is a crucial component of the SCF^{Skp2} E3 ubiquitin ligase complex. As well as providing specificity, Skp2 is responsible for recruiting the substrates to the complex to allow ubiquitin transfer from the ubiquitin activated E2 enzyme. As Skp2 was found to cause an increase in KMT5A mono-ubiquitination (Figure 4-7) it indicated that these two proteins may come into direct contact with each other. To address this theory, HEK293T cells were transfected with equal amounts of Myc-KMT5A and Skp2, and anti-Skp2 antibody mediated immunoprecipitation was performed according to Chapter 2.9.1 to determine whether KMT5A protein could be co-precipitated.

KMT5A was detected by Western blotting following Skp2 pull down compared to control lanes, IgG and the antibody control only (Figure 4.8A). To further confirm this interaction, a reciprocal immunoprecipitation was performed with anti-Myc antibody mediated immunoprecipitation of KMT5A. Similarly, Skp2 was determined to interact with KMT5A (Figure 4.8B). Therefore, Skp2 and KMT5A interact supporting the theory that Skp2 has the potential to post-translationally modify KMT5A.

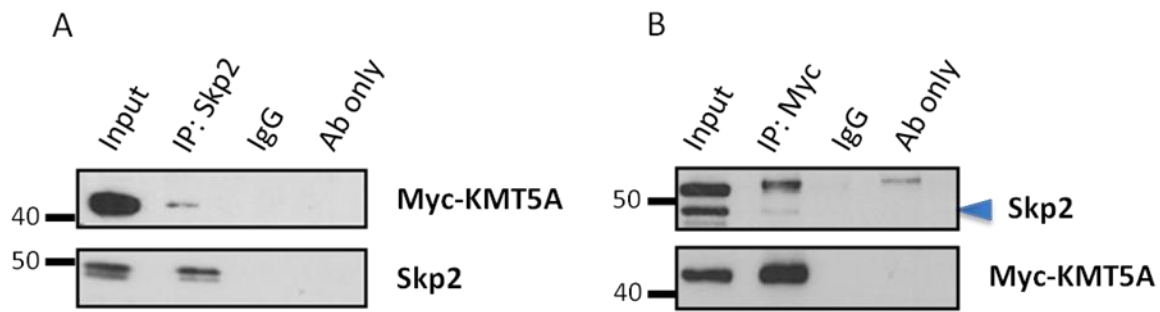


Figure 4-8: KMT5A and Skp2 are found in a complex. HEK293T cells were transfected with equal amounts of Myc-KMT5A and Skp2 for 48 hours. Cells were lysed in non-denaturing conditions and pre-cleared with excess protein G sepharose (PGS) for 4 hours to remove proteins that bind PGS non-specifically. **(A)** Skp2 or **(B)** KMT5A (Myc) was immunoprecipitated overnight with 2 μ g of the appropriate antibody and negative control IgG. The following day, antibody bound complexes were isolated after incubation with PGS for 1 hour. Western blot analysis was then conducted.

4.3.9 *Skp2 enhances KMT5A mono-ubiquitination*

As an interaction between Skp2 and KMT5A has been confirmed (Figure 4.8), the ability of Skp2 to promote mono-ubiquitin conjugation of KMT5A was tested by performing *in vivo* ubiquitination assays using Ni-NTA beads in COS7 cells, under denaturing conditions. As maximal KMT5A mono-ubiquitination and poly-ubiquitination was observed with 1 µg of Skp2 (Chapter 4.3.7), this amount was used in these ubiquitination assays. COS7 cells overexpressing His-Ub, Flag-KMT5A and Flag-Skp2 were subjected to denaturing polyhistidine pull down (Chapter 2.9.2) followed by Western blot analysis.

Figure 4.9 demonstrates that the addition of Skp2 alone significantly increased KMT5A mono-ubiquitination and leads to KMT5A stabilisation, as seen by the stronger smearing pattern (lane 6 versus 4). As MG132 inhibits the proteasome, thereby preventing degradation of proteins, Skp2-mediated ubiquitinated KMT5A was expected to be stabilised following MG132 treatment. Unexpectedly, combining Skp2 overexpression with MG132 treatment did not cause any further stabilisation of KMT5A (lanes 6 and 7). This observation suggests that ubiquitinated products of KMT5A generated by Skp2 are not targeted for proteasomal degradation.

Interestingly, treatment with MG132 in the absence of Skp2 was sufficient to inhibit KMT5A degradation. However, MG132-mediated stabilisation of KMT5A occurred to a greater extent and also affected heavier multi-ubiquitinated KMT5A products than Skp2 overexpression alone (lane 6 versus 5), indicating Skp2 is mainly involved in promoting KMT5A mono-ubiquitination. Interestingly, the presence of Skp2 prevented the stabilisation effect of MG132 on KMT5A, as heavier poly-ubiquitinated forms of KMT5A are present at a lower level with combined Skp2 overexpression and MG132 treatment than MG132 treatment alone (lane 7 versus 5). Overall, the data suggests that Skp2 mainly mediates mono-ubiquitination of KMT5A rather than poly-ubiquitination.

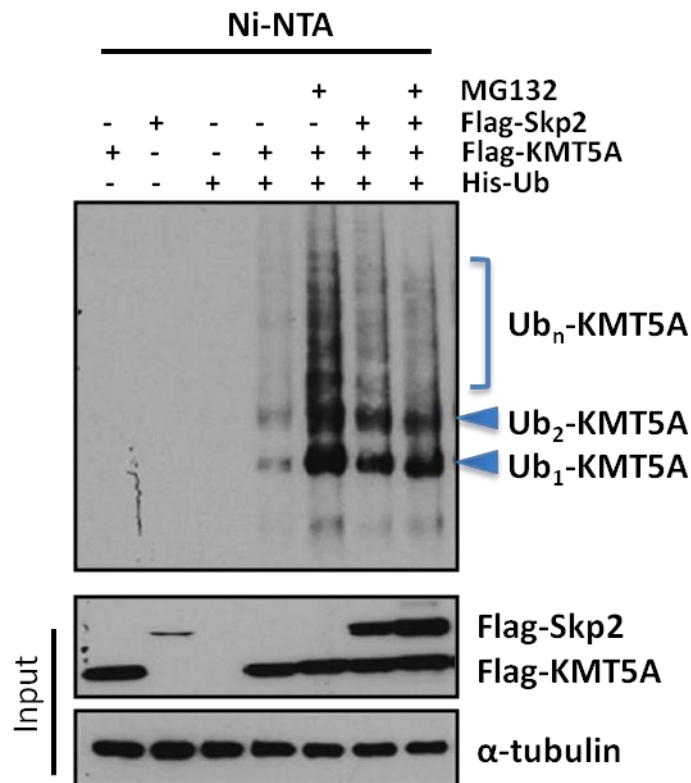


Figure 4-9: Skp2-mediated ubiquitination of KMT5A does not result in protein turnover. COS7 cells were transfected with the indicated constructs for 48 hours. All reactions were balanced with the appropriate empty vector. MG132 at 20 μ M was added where indicated in the final 16 hours. *In vivo* ubiquitination assays were then performed under denaturing conditions using Ni-NTA beads to immunoprecipitate ubiquitinated proteins. Western blotting was carried out on input and immunoprecipitated samples for KMT5A, Skp2 and α -tubulin as the loading control.

4.3.10 *Skp2 does not mediate the mono-ubiquitination of KMT5A C-terminus*

Having provided evidence that Skp2 significantly elevates mono-ubiquitination of full length KMT5A (Figure 4.9), and that the site(s) of mono-ubiquitination is located in KMT5A C-domain (Figure 3.7), the ability of Skp2 to mono-ubiquitinate KMT5A C-terminus was tested. For this purpose, a constant amount of KMT5A C-terminus and His-Ub constructs were co-expressed with an increasing amount of either WT-Skp2 or a catalytically-dead truncated form of Skp2 obtained from Dr Lin (The University of Texas) (Xu *et al.*, 2015). After 48 hours of transfection, cell lysates were collected for Western blot analysis.

The addition of Ub leads to increased mono-ubiquitination of KMT5A C-terminus (Figure 4-10A, lane 3 versus 2), similar to full length KMT5A observations (Figure 4-9). However, co-expression of WT-Skp2 at lower concentrations did not further affect C-terminus mono-ubiquitination, whereas at higher concentrations Skp2 caused a clear reduction of this modification (Figure 4-10A, lanes 4 – 6), in contrast to full length KMT5A findings. The decrease in mono-ubiquitination of C-terminus however could be due to the reduced total KMT5A C-terminus levels, suggesting Skp2 is causing its degradation at higher concentrations. A truncated form of Skp2 that is missing its C-terminal leucine-rich domain (LRR-Skp2) was also utilised in this experiment as a negative control. Skp2 binds to its protein substrates through its LRR domain and recruits them to the SCF complex (Zhang *et al.*, 1995; Sutterlüty *et al.*, 1999). As KMT5A was found to be in complex with Skp2, the LRR-Skp2 protein should not be able to interact with KMT5A and therefore, compromise Skp2 function in ubiquitinating KMT5A; hence, it is called the E3 ligase-dead Skp2 form by Dr Lin and also in this work. However, catalytically-dead mutant Skp2 (LRR-Skp2) showed a strong ability in enhancing mono-ubiquitination of KMT5A C-terminus (Figure 4-10A, lanes 7-9) which was not expected as it should not be able to bind KMT5A to mediate its ubiquitination. Although similarly to the WT-Skp2, increased expression of catalytically-dead Skp2 construct also reduced the level of KMT5A C-terminal mono-ubiquitination.

Given the reduction in total KMT5A C-terminus level upon co-expression of WT-Skp2, we wanted to determine if WT-Skp2 caused C-terminal domain proteolysis. To this end, COS7 cells were transfected with a constant amount of KMT5A C-terminus and His-Ub, and increasing amounts of WT-Skp2 either in the absence or presence of MG132. As in part A, addition of Ub led to an upregulation of mono-ubiquitinated KMT5A C-terminus (Figure 4-10B, lane 3 versus 2), with Skp2 not influencing the level of mono-ubiquitination (Figure 4-10B, lanes 4-6 versus 3). Co-

treatment with MG132 in the presence of Skp2 expression did not cause any stabilisation of KMT5A C-terminus, suggesting it is not degraded by Skp2.

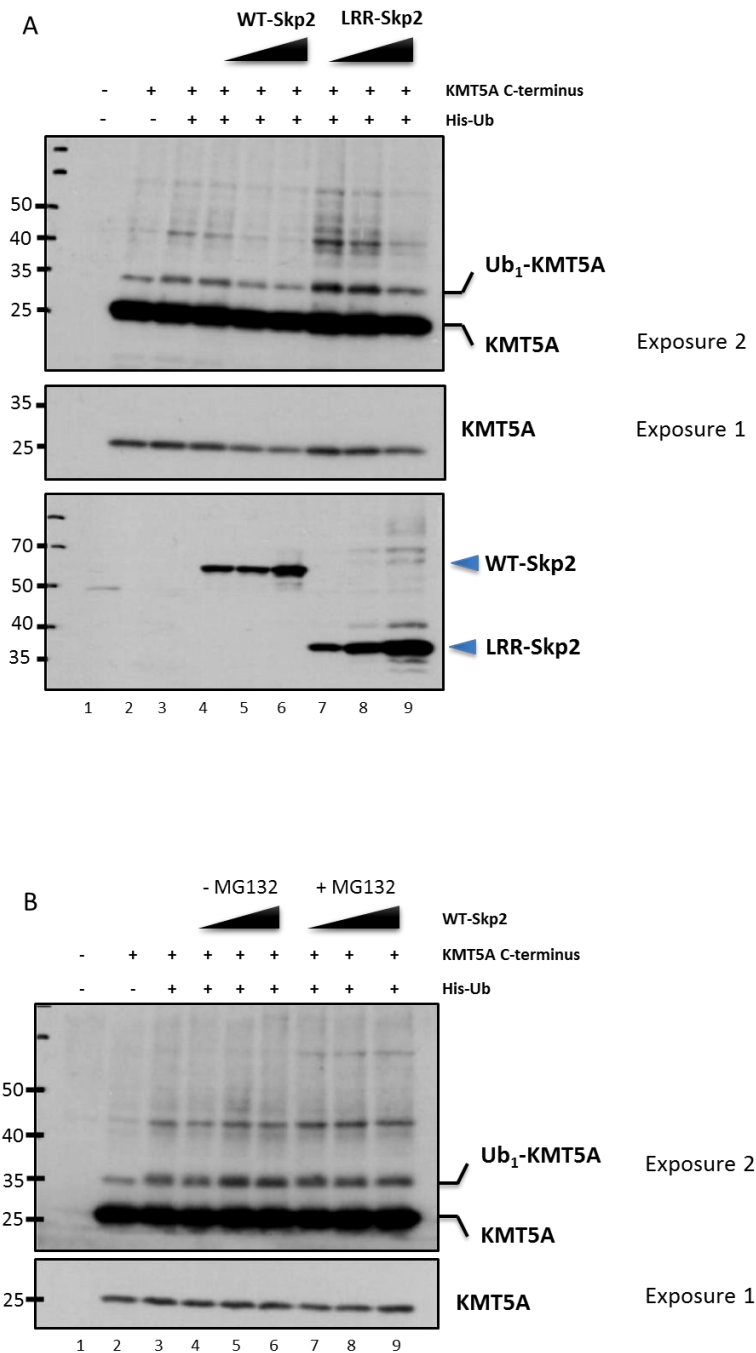


Figure 4-10: Skp2 does not promote KMT5A C-terminus mono-ubiquitination. (A) COS7 cells were transfected with a constant amount of KMT5A C-terminus and His-Ub with increasing amount of either wild-type Skp2 (WT-Skp2) or ligase-dead Skp2 (LRR-Skp2). After 48 hours incubation, cell lysates were generated using SDS sample buffer and subjected to Western blot analysis for KMT5A and Skp2. (B) KMT5A C-terminus was co-expressed with an increasing amount of WT-Skp2 in COS7 cells. MG132 was added in the final 16 hours of the 48 hour incubation period, where indicated. The cells were lysed using SDS sample buffer and analysed by Western blotting. All reactions were balanced using appropriate empty vector.

4.3.11 Investigating the role of the SCF complex in Skp2-mediated mono-ubiquitination of full length KMT5A

Skp2 is the F-box component of the SCF ubiquitin E3 ligase complex, which works in complex with the other SCF components, S-Phase Kinase-Associated Protein 1 (Skp1), Cullin 1 (Cul1), and a Ring-Box 1 (Rbx1/Roc1). As already mentioned, the F-box protein, Skp2, determines the specificity of the complex as it recognises and targets specific substrates to the SCF complex for ubiquitination and proteasomal-mediated degradation. Skp2 was found to mainly mediate KMT5A mono-ubiquitination in preference to poly-ubiquitination, which did not cause protein turnover (Figure 4-9). Hence, to ensure that the inability of Skp2 to cause turnover was because the other components of the SCF complex were not over-expressed alongside Skp2, it is important to address the SCF components relating to Skp2 function.

As such, an *in vivo* ubiquitination assay using Ni-NTA beads under denaturing conditions (Chapter 2.9.2) was performed, in COS7 cells to determine KMT5A ubiquitination in the absence and presence of exogenous SCF complex by over-expressing all the components of the complex at the same ratio. Western blot analysis of the input samples indicated that addition of WT-Skp2 alone and in combination with its SCF complex elevates KMT5A mono-ubiquitination (Figure 4.11, lanes 3 and 5 versus 2). However, analysis of the immunoprecipitated ubiquitinated proteins revealed that firstly, Skp2 overexpression alone leads to an increase in the mono-ubiquitination and poly-ubiquitination of KMT5A compared to its basal levels (Figure 4.11, lanes 2 versus 3), as also observed previously. Secondly however, the level of KMT5A mono-ubiquitination was not noticeably altered when the SCF components were expressed in combination with WT-Skp2, as compared to Ub overexpression alone (Figure 4.11, lane 5 versus 2). Furthermore, reconstituting the SCF complex actually attenuated Skp2-mediated KMT5A mono-ubiquitination in comparison to WT-Skp2 overexpression alone (Figure 4.11, lane 5 versus 3), bringing the mono-ubiquitination and also poly-ubiquitination down to basal levels, which might suggest the intact exogenous SCF complex is promoting KMT5A poly-ubiquitination for degradation.

As also seen previously, the catalytically-dead truncated Skp2 (LRR-Skp2) caused a greater mono-ubiquitination of KMT5A than WT-Skp2 in the absence of the SCF components (Figure 4.11, lane 4 versus 3), which was not expected. Moreover, both the WT-Skp2 and LRR-Skp2 were heavily ubiquitinated when over-expressed without the SCF components (Figure 4.11, lanes 3 and 4). On the other hand, LRR-Skp2 no longer caused an upregulation in KMT5A mono-ubiquitination upon

co-expression with all the SCF components (Figure 4.11, lane 6 versus 4), and did not change the level of mono-ubiquitination of KMT5A relative to the basal level in the absence of SCF components (Figure 4.11, lane 6 versus 2). It is important to note, that co-expression of the SCF components significantly suppressed the ubiquitination of both WT-Skp2 and LRR-Skp2.

There are obvious limitations with this particular experiment in that unmodified KMT5A has been immunoprecipitated when only the ubiquitinated proteins modified by exogenous His-Ub were the target of Ni-NTA beads pull down. This could be due to a technical error in this experiment or the unmodified KMT5A sticking directly to Ni-NTA beads. Moreover, as the stoichiometry of the SCF complex and any possible interaction is unknown, comprehensive optimisation experiments with varying amounts of the complex components should be carried out to obtain conditions where the SCF complex performs at its maximal activity.

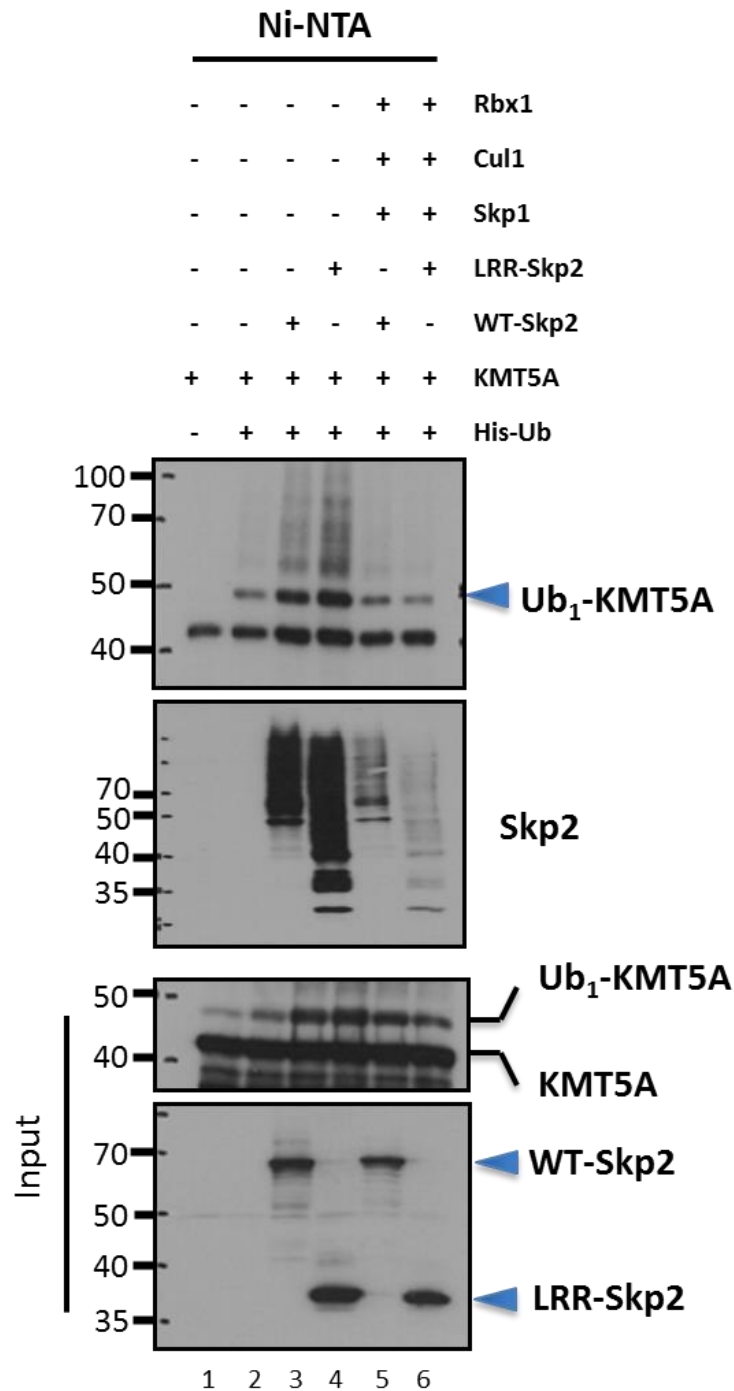


Figure 4-11: The role of the SCF complex in Skp2-mediated mono-ubiquitination of full length KMT5A. COS7 cells were transfected with the indicated plasmids for 48 hours. All reactions were balanced with the appropriate empty vector. Denaturing *in vivo* ubiquitination assay with Ni-NTA beads was then performed, followed by Western blot analysis for KMT5A and Skp2.

4.3.12 Investigating the role of the SCF complex in Skp2-mediated KMT5A C-terminus mono-ubiquitination

As Skp2 alone promotes the mono-ubiquitin conjugation of full length KMT5A, but not the C-terminal fragment, it was questioned whether the presence of the SCF components could facilitate Skp2-mediated mono-ubiquitination of KMT5A C-terminus. Again, *in vivo* ubiquitination assay using Ni-NTA beads under denaturing conditions was employed in COS7 cells overexpressing the indicated constructs, and KMT5A C-terminus mono-ubiquitination was assessed with Skp2 alone or in combination with its SCF complex.

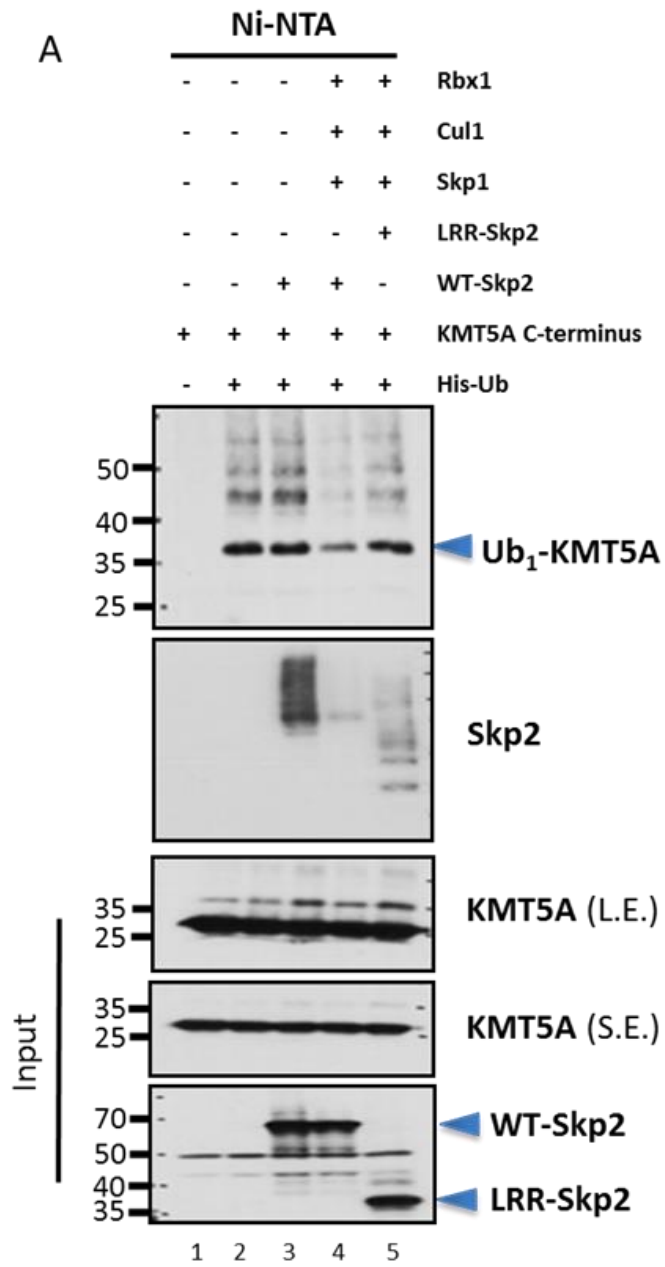
Firstly, KMT5A C-terminus ubiquitination pattern observed in Figure 4.12A, lane 2 is similar to the full length KMT5A (Figure 4.9), with distinct bands forming which correspond to mono-, di-, tri and poly-ubiquitinated forms of KMT5A C-terminus (Figure 4.12A). Secondly, similar to the whole cell lysate observations in Chapter 4.2.10, co-expression of WT-Skp2 did not cause an obvious change in mono-ubiquitinated KMT5A C-terminus (Figure 4.12A, lane 3 versus 2). Thirdly, upon co-expression of the SCF components with WT-Skp2 a clear suppression of C-terminus mono-ubiquitination and poly-ubiquitination was observed (Figure 4.12A, lane 4 versus 3), with its levels becoming even lower than basal mono-ubiquitinated levels (Figure 4.12A, lane 4 versus 2) and of mutant Skp2-mediated mono-ubiquitination (Figure 4.12A, lane 5 versus 4) which was unexpected. This may suggest the ubiquitinated KMT5A C-terminus products are being targeted for degradation by the proteasome. Finally, the catalytically dead mutant Skp2 (LRR-Skp2) did not alter basal mono-ubiquitination levels of the KMT5A C-terminus (Figure 4.12A, lane 5 versus 2).

As the expression of WT-Skp2 when combined with the SCF components led to a significant reduction in C-terminus mono-ubiquitination and poly-ubiquitination, it was considered it may be due to disturbing the stoichiometry of the complex. As optimising the concentration of each of the SCF components is a comprehensive task and not the aim of this project, different SCF components were overexpressed at the same concentration whilst increasing the concentration of WT-Skp2 in the ubiquitination assay. Similar to data shown in Chapter 4.2.10, Ub expression caused the formation of mono-ubiquitinated C-terminus (Figure 4.12B). Interestingly, the basal mono-ubiquitination level of the C-domain was modestly decreased in the presence of the SCF complex when no Skp2 was overexpressed (Figure 4.12B, lane 3 versus 2). Upon reintroducing Skp2 at lower concentrations, mono-ubiquitination was increased back to basal levels (Figure 4.12B, lanes

4 and 5 versus 2). However, higher concentrations of Skp2 caused a clear reduction in C-terminus KMT5A mono-ubiquitination (Figure 4.12B, lanes 7-8 versus 4-5).

There are again similar problems with this particular repeat, as also observed in Chapter 4.2.11, in that unmodified KMT5A C-terminus is immunoprecipitated, despite the Ni-NTA beads only targeting ubiquitinated proteins which have undergone modification by the His-Ub.

Overall, elucidating the role of the SCF complex in Skp2-mediated mono-ubiquitination of full length KMT5A and its C-terminus proved difficult as there were discrepancies in the level of KMT5A mono-ubiquitination and poly-ubiquitination between experiments. Unfortunately, no firm conclusions could be drawn from some of the *in vivo* polyhistidine pull down ubiquitination assays for various reasons, including for example the immunoprecipitation of the unmodified form of KMT5A. Moreover, there was a large amount of cell death observed following the transfection of cells with a large amount of plasmid DNA required to accommodate the overexpression of all the SCF components.



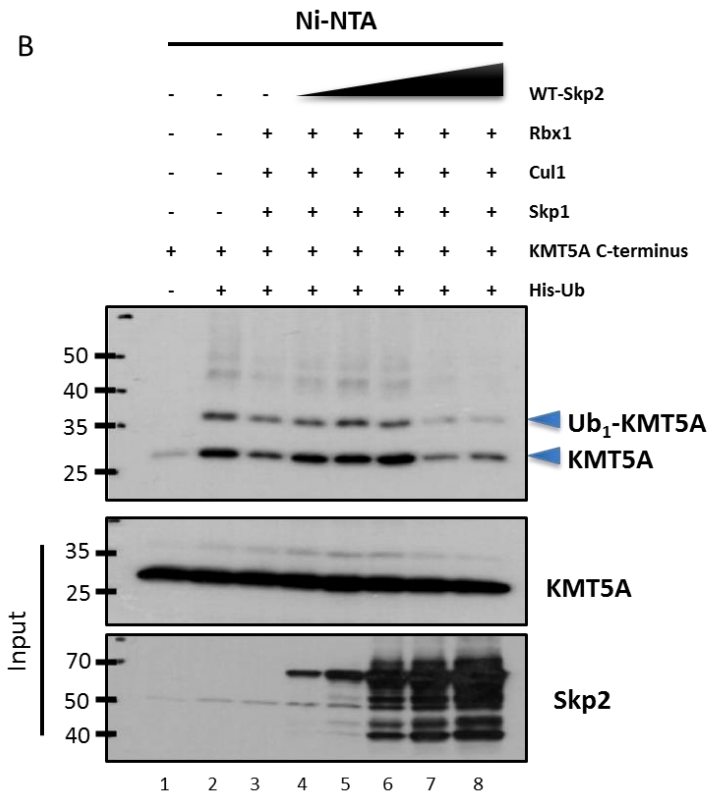


Figure 4-12: The role of the SCF complex in Skp2-mediated mono-ubiquitination of KMT5A C-terminus. (A and B) Denaturing *in vivo* ubiquitination assays using Ni-NTA beads performed in COS7 cells transfected with the indicated plasmids. (L.E.) and (S.E.) denotes long and short exposure, respectively.

4.4 Discussion

Cell cycle regulation of KMT5A mono-ubiquitination

KMT5A plays a critical role in maintaining genome integrity and ensuring cell cycle progression. As such, its activity is under tight cellular control, mainly through regulation of its expression level during the cell cycle by post-translational modifications. This has mainly been shown to be via the poly-ubiquitination of KMT5A by the SCF ^{β -TRCP}, CRL4^{Cdt2} and APC^{Cdh1} complexes in G1, S and late mitosis phases of the cell cycle, respectively (Centore *et al.*, 2010; Oda *et al.*, 2010; Wu *et al.*, 2010; Wang *et al.*, 2015). Published work to date has concentrated on determining KMT5A activity in its unmodified form which is shown to be incompatible with DNA replication. This study has demonstrated that mono-ubiquitinated KMT5A is a dominant form of post-translationally modified KMT5A in the cell lines that were tested, yet nothing is known about its function and underlying mechanism(s) of action. The initial aims of this chapter were therefore to determine whether KMT5A mono-ubiquitination, similar to its poly-ubiquitination, is under the control of cell cycle regulation, and to establish the role mono-ubiquitinated KMT5A may have on cell cycle progression.

Work by several groups has shown KMT5A protein level varies greatly throughout the cell cycle. Specifically, it is transiently expressed at its highest levels during early mitosis, reduces as cells exit mitosis and enter G1, declines rapidly as cells transition from G1 to S phase and is further suppressed to undetectable levels during the S phase (Figure 1.6). Reassuringly, similar observations were seen in prostate cancer cell lines that were used in this study (Figure 4.2A). Furthermore, upon investigation of mono-ubiquitinated KMT5A a striking contrast to its unmodified levels was observed. Mono-ubiquitinated KMT5A levels were found to peak during S phase of the cell cycle. Conversely, as cells exit the S phase to transition into G2 phase and further progress into the G2/M phase, mono-ubiquitinated KMT5A declined sharply, despite high levels of unmodified KMT5A (Figure 4.2A). Therefore mono-ubiquitinated KMT5A protein levels exhibit a cell cycle-dependent oscillation which is inversely correlated with the unmodified KMT5A fluctuations during the cell cycle.

Importantly, the significant rise in KMT5A mono-ubiquitination in S phase is concomitant with DNA synthesis and corresponds to a highly proliferative state. This was further confirmed by demonstrating mono-ubiquitinated KMT5A is most abundant in actively dividing, low confluency cells as compared to the less proliferative, high confluency cells (Figure 4.3). This suggested that

mono-ubiquitination of KMT5A is promoted during cell proliferation. Interestingly, this observation is in contrast to the suppressive role of unmodified KMT5A on DNA replication and cell growth, hence KMT5A poly-ubiquitination and degradation in S phase and mitosis.

To assess the biological significance of mono-ubiquitinated KMT5A, mono-ubiquitin deficient and competent KMT5A truncated fragments N-C1 and N-C2 which were generated in Chapter 3.4.12, were utilised to determine any cell cycle changes due to the presence of mono-ubiquitinated KMT5A. However, overexpression of these constructs did not influence the cell cycle profile of COS7 cells compared to non-transfected cells (Figure 4.5). There are different reports on the effect of KMT5A overexpression on the cell cycle, all of which show cell cycle defects, though to varying degrees depending on the level of KMT5A expression. For instance, similar to the data here, Abbas *et al* (Abbas *et al.*, 2010) showed that whilst wild-type KMT5A transduction did not influence cell proliferation, KMT5A PIP mutant that is a stable form of KMT5A which is resistant to the CRL4^{Cdt2}-mediated proteolysis, inhibited cell proliferation after cells underwent two rounds of cell division. Furthermore, the KMT5A PIP mutant caused re-replication, induced apoptosis and arrested cells at the G2/M phase of the cell cycle, all of which was dependent on KMT5A enzymatic activity (Abbas *et al.*, 2010). Moreover, Centore *et al* (Centore *et al.*, 2010) showed DNA synthesis was reduced, cell proliferation decreased gradually, and the ATR checkpoint response was activated upon constitutive expression of wild-type KMT5A. However, the overexpressed wild-type KMT5A was rapidly degraded in this study. Again this was addressed by using the stable KMT5A PIP mutant which caused dramatic effects including a significant loss in replicating cells, proliferation and induction of a prominent G2 arrest, which were dependent on the catalytic activity of KMT5A (Centore *et al.*, 2010). Therefore, the rapid degradation of exogenous wild-type KMT5A has hindered research into this area. This could also be one of the underlying reasons for the lack of any apparent alteration in the cell cycle following overexpression of our KMT5A mutants in COS7 cells, however the percentage transfection efficiency under these conditions also needs to be considered. Although we expected the mono-ubiquitin deficient form of KMT5A (fragment N-C2) to be stable compared to its mono-ubiquitin competent form (fragment N-C3), as it does not undergo mono-ubiquitination and therefore should not be subject to poly-ubiquitination. Nonetheless, as already mentioned, complete lack of ubiquitination of KMT5A fragment N-C2 is not likely, as there are other lysines available which can potentially be modified by ubiquitin conjugation; hence, leading to poly-ubiquitination and degradation. Moreover, all the KMT5A C-truncated fragments contain the PIP degron that is required for ubiquitination and degradation by

the CRL4^{Cdt2} complex, and can therefore be subject to this mode of destruction. Therefore, investigating the stability of the KMT5A fragments is required.

As already alluded to, all studies to date have shown KMT5A's effect on the cell cycle is dependent on its enzymatic activity (Jørgensen *et al.*, 2007; Abbas *et al.*, 2010; Centore *et al.*, 2010; Jørgensen *et al.*, 2011). As we have truncated KMT5A from the C-terminal end the region comprising the SET domain responsible for KMT5A catalytic activity has been partially deleted. Moreover, the two critical residues for enzymatic activity, Arg 336 and Asp 379, are missing in these KMT5A fragments. Mutation of these two residues and inactivation of KMT5A's enzymatic activity has been demonstrated to alleviate the inhibitory effects of the stable KMT5A PIP mutant on cell proliferation (Abbas *et al.*, 2010). The KMT5A truncated fragments generated therefore lack the essential enzymatic activity required for normal proliferation which could account for their lack of impact on the cell cycle observed in this Chapter (Figure 4.5). However, despite all these possibilities, mono-ubiquitinated KMT5A was shown to be exclusively located in the cytoplasm (Figure 4.4). As a result, any potential direct effect mono-ubiquitinated KMT5A may have is not expected to be due to its enzymatic activity on nuclear H4K20, which is the substrate through which KMT5A is shown to affect the cell cycle.

Moreover, cells were shown to require two rounds of the cell cycle to be completed for KMT5A overexpression-mediated effects to take place. Therefore cell proliferation with COS7 cells overexpressing the KMT5A mutants was assessed using the IncuCyte system. Interestingly, mono-ubiquitinated KMT5A fragment N-C3 overexpression led to enhanced cell proliferation compared to wild-type KMT5A; whilst, mono-ubiquitin-deficient KMT5A fragment N-C2 led to a reduction in proliferation (Figure 4.6), suggesting mono-ubiquitination of KMT5A positively regulates cell proliferation. Although this approach allowed prolonged KMT5A overexpression to take effect on cell proliferation, the KMT5A constructs overexpressed could have been substantially degraded before cells reached their exponential growth due to the small numbers seeded in this experiment, and may have undermined the data.

Additionally, the truncated KMT5A fragments may lack other critical residues or motifs that contribute to KMT5A function. In order to more accurately elucidate the effect of mono-ubiquitinated KMT5A on cellular proliferation and its consequences in a more physiological setting, it would be desirable to perform these experiments in PC cell lines using full-length KMT5A mutant constructs. A commonly used technique in generating a mono-ubiquitinated

protein mimetic could be utilised, where a direct, in-frame fusion of an ubiquitin sequence with the N-terminus (Haglund *et al.*, 2003; van der Horst *et al.*, 2006) or C-terminus (Terrell *et al.*, 1998; Li *et al.*, 2003) of wild-type protein results in a constitutive mono-ubiquitinated form of the protein being expressed. In order to further stabilise mono-ubiquitinated KMT5A, further mutation to remove or inactivate the PIP degron responsible for KMT5A destruction by the CRL4^{Cdt2} complex could be conducted to prevent the rapid degradation, as reported. Stably expressing PC cell lines with the resultant construct could then be utilised as a more appropriate physiological model.

The association of the inhibitory effect of KMT5A's enzymatic activity on DNA replication and proliferation is consistent with KMT5A nuclear-cytoplasmic shuttling during the cell cycle. Post-translational modifications have been shown to regulate KMT5A localisation in addition to its stability and activity. Wu *et al* (Wu *et al.*, 2010) demonstrated phosphorylation of KMT5A at serine 100 causes chromatin disassociation, preventing it from mono-methylating H4K20. Moreover, Yin *et al* (Yin *et al.*, 2008) showed dramatic changes in KMT5A distribution during the cell cycle, whereby the newly synthesized KMT5A in S phase was excluded from the nucleus and exported into the cytoplasm throughout S phase. Upon reaching G2 phase, KMT5A was removed from the cytoplasm as it re-entered the nucleus. This was shown using a single living cell imaging technique but the underlying mechanism leading to KMT5A localisation remained unknown. However, as this technique did not distinguish between unmodified and modified KMT5A, it is not known which form(s) of KMT5A was being translocated in their observations. Interestingly, although in contrast to its unmodified form, mono-ubiquitinated KMT5A was enriched in proliferating cells (Figure 4.3), it was later found to reside in the cytoplasm (Figure 4.4). This finding is therefore consistent with DNA replication being incompatible in the presence of KMT5A and suggests mono-ubiquitination is a potential mechanism to promote the absence of KMT5A in the nucleus when the cell is proliferating. Mono-ubiquitination is reported to signal for protein localisation for many different proteins. For example, low levels of Mdm2 have been shown to induce mono-ubiquitination of p53 without dramatically affecting its stability and led to the nuclear export of p53 (Li *et al.*, 2003). Interestingly, mono-ubiquitinated KMT5A was found exclusively in the cytoplasm, unlike unmodified KMT5A which was present in the chromatin, nucleus and cytoplasm (Figure 4.4). From this, several speculations can be made: firstly, KMT5A may undergo mono-ubiquitination in the cytoplasm and lead to its interaction with a cytoplasmic protein which retains mono-ubiquitinated KMT5A in this compartment. Secondly, KMT5A is mono-ubiquitinated in its nuclear localisation sequence (NLS) in the cytoplasm which prevents it from entering the nucleus,

as shown for the tumour suppressor, BAP1 protein (Mashtalir *et al.*, 2014). However, there are no reports of a NLS in KMT5A and no classical NLS was found upon manual inspection of the KMT5A amino acid sequence. Although, cNSL mapper online software predicted a putative non-classical NLS within KMT5A C-terminus consisting of three lysine sites (data not shown). A third more likely alternative is that KMT5A is mono-ubiquitinated in the nucleus, which then signals for its nuclear export. This may be mediated by a KMT5A conformational change exposing its nuclear export sequence (NES), causing its export into the cytoplasm. Again, there are no reports of a NES in KMT5A and we did not find a classical NES in KMT5A amino acid sequence. However, two different online software programmes, LocNES and NetNES predicted different regions in KMT5A to comprise a NES. Alternatively, export of mono-ubiquitinated KMT5A may be facilitated through interaction with other ubiquitin-binding proteins. It is important to note that the lack of mono-ubiquitinated KMT5A detection in the nuclear compartment does not mean it is not present at all. Mono-ubiquitination of KMT5A in the nucleus may result in its extremely rapid exclusion and hence extremely low nuclear levels that are not detected in our Western blots.

Collectively, the data strongly suggests mono-ubiquitination of KMT5A during S phase leads to its nuclear export, to maintain low levels of KMT5A in the nucleus. To test this further, ubiquitin-mediated fluorescence complementation could be utilised to monitor ubiquitination in living cells (Fang and Kerppola, 2004). In this technique, the amino terminal part of a fluorescent protein, e.g. YFP is tagged to ubiquitin, and the carboxyl terminal portion of YFP is attached to the protein of interest, in this case KMT5A. Following co-transfection of the constructs and the covalent attachment of ubiquitin-N-terminal-YFP to KMT5A, YFP complementation is achieved resulting in a fluorescent signal. Distribution of mono-ubiquitinated KMT5A and its levels could be monitored during the cell cycle in real time. It is further speculated that, de-ubiquitination of mono-ubiquitinated KMT5A in G2 phase can enable it to re-enter the nucleus. This speculation is supported by the requirement of unmodified KMT5A in G2/M phase of the cell cycle and localisation of KMT5A into the nucleus during this phase by Yin *et al.* as discussed earlier (Yin *et al.*, 2008). In summary, the data has demonstrated mono-ubiquitination of KMT5A is under the cell cycle control and mono-ubiquitination regulates the cellular distribution of KMT5A.

Skp2-mediated mono-ubiquitination of KMT5A

In the next part of the work, the role of Skp2 E3 ligase was investigated in ubiquitinating KMT5A. Multiple E3 ligases have thus far been shown to precisely regulate KMT5A protein levels

throughout the cell cycle, each functioning through a different mechanism to ensure efficient poly-ubiquitination and degradation of KMT5A. The CRL4^{Cdt2} complex specifically recognises KMT5A that is bound to PCNA on chromatin during S phase and therefore poly-ubiquitinates and degrades KMT5A, as well as its other substrates, in a replication-coupled manner. CRL4^{Cdt2}-mediated destruction of KMT5A in S phase is required to prevent H4K20Me1 deposition and premature chromatin compaction in replicating cells, ensuring proper DNA replication and entry into mitosis. The KMT5A level then increases and peaks in early mitosis to modulate chromatin compaction. Furthermore, the APC^{Cdh1} complex targets KMT5A that has undergone dephosphorylation on serine 100 by the Cdc14 phosphatase and has dissociated from chromatin. Moreover, the SCF ^{β -TRCP} complex has been shown to poly-ubiquitinate KMT5A in a phosphorylation-dependent manner at serine 253 by CK1 during G1 (Figure 1.6).

In addition, Skp2 has been suggested to play a role in regulating KMT5A through proteolytic degradation during S phase. Skp2 is a positive regulator of the cell cycle and is frequently overexpressed in PC. Skp2 accumulates during G1-S transition and poly-ubiquitinates the cell cycle inhibitor p27 for proteasomal degradation. Whilst Skp2 knockdown has been reported to lead to increased KMT5A levels during S phase by Yin et al (Yin *et al.*, 2008), it was recently reported to not affect KMT5A stability by Wang et al (Wang *et al.*, 2015). However, despite these observations, no detailed study have investigated the role of Skp2 in ubiquitinating KMT5A.

We identified Skp2 as a novel KMT5A-associated protein. The association of KMT5A and Skp2 was confirmed by co-immunoprecipitation analysis using HEK293T cells expressing exogenous KMT5A together with Skp2 (Figure 4.8). However, the interaction may not be direct and other factor(s) may mediate KMT5A-Skp2 interaction. Over-expression of Skp2 increased KMT5A mono-ubiquitination. This was demonstrated using *in vivo* ubiquitination assay in COS7 cells, where Skp2 significantly up-regulated KMT5A mono-ubiquitination. In addition, Skp2 also caused a modest increase in KMT5A poly-ubiquitination, though to a much lesser extent than of mono-ubiquitination without using MG132 to inhibit the proteasome (Figure 4.9). This indicated that Skp2-mediated mono-ubiquitination of KMT5A is not involved in protein turn over. This was supported when treatment with MG132 did not affect Skp2-mediated KMT5A mono-ubiquitination, as well as poly-ubiquitination, suggesting these products are not targeted for proteasomal degradation (Figure 4.9). This is in contrast to the established role of Skp2 as an E3 ligase which has been shown to ubiquitinate its substrates for proteolysis by the proteasome.

Furthermore, it conflicts with Yin *et al.* (Yin *et al.*, 2008) who suggested Skp2 plays a role in KMT5A poly-ubiquitination and degradation during S phase of the cell cycle as Skp2 knockdown in HeLa cells during G1-S transition caused an up-regulation in KMT5A expression. However, Yin *et al.*, (2008) does not undermine our observations as the role of Skp2 is not investigated in any detail, and lacks the use of appropriate ubiquitination assays. Similar to Yin *et al.*, work by Oda *et al.* (Oda *et al.*, 2010) suggests a similar role for Skp2 in KMT5A regulation as KMT5A was shown to be upregulated in Skp2^{-/-} compared to wild type MEFs following exposure to UV treatment. KMT5A stabilisation however was markedly enhanced in the whole cell extracts compared to the chromatin-bound fraction. This suggested that in addition to the CRL4^{Cdt2}-mediated poly-ubiquitination and degradation, KMT5A is subject to destruction through CRL4^{Cdt2}-independent mechanisms. Additionally, the stable KMT5A PIP mutant that is resistant to CRL4^{Cdt2}-mediated proteolysis during S phase was observed to be degraded, although at a slower rate than wild-type KMT5A which further indicates KMT5A is targeted by two independent pathways when cells are replicating their DNA.

Interestingly, despite MG132's ability to dramatically stabilise KMT5A which led to the formation of higher molecular weight KMT5A poly-ubiquitinated products, further inclusion of Skp2 caused a clear reduction in MG132-mediated poly-ubiquitination of KMT5A. Moreover, the degree of Skp2-mediated poly-ubiquitination was significantly lower than of MG132-mediated poly-ubiquitination of KMT5A (Figure 4.9). This further suggests that Skp2-mediated mono-ubiquitination of KMT5A causes KMT5A stabilisation on its own. Poly-ubiquitination of proteins requires the conjugation of four or more ubiquitin molecules in order to signal for their proteasomal degradation (Deveraux *et al.*, 1994), which could explain why Skp2 does not induce KMT5A degradation. This implies that Skp2 may primarily affect KMT5A localisation and/or activity rather than stability, indicating a unique role for Skp2 in KMT5A regulation. Although evidence supporting Skp2-mediated mono-ubiquitination is currently lacking, new substrates for Skp2 are emerging where Skp2 is shown to be involved in regulating their function. For example, Skp2 has recently been shown to poly-ubiquitinate LKB1 through non-proteolytic K63-linked ubiquitination, thereby modulating LKB1 activity to impact cancer cell survival under energy stress (Lee *et al.*, 2015). The fact that Skp2 attenuated the ability of MG132 to cause KMT5A poly-ubiquitination could also be attributed to Skp2-mediated mono-ubiquitination of KMT5A which may subsequently impact the accessibility of KMT5A for other ligases that promote KMT5A poly-ubiquitination and degradation. There are 25 lysine residues in the KMT5A C-terminus that are

potential sites to ubiquitination. Treatment with MG132 may favour ubiquitination of KMT5A at lysine sites that favour protein turnover but once Skp2 is added at maximal level to saturate the system, the equilibrium may be pushed towards Skp2-mediated KMT5A mono-ubiquitination which is a more stable form. Alternatively, Skp2 may regulate E3 ligases that target KMT5A for poly-ubiquitination and degradation. Consistent with this idea, Lu *et al* (2014) demonstrated Skp2 indirectly inhibits K63-linked ubiquitination of JARID1B via E3 ubiquitin ligase TRAF6 (Lu *et al.*, 2015). E2-ubiquitin-conjugating enzymes determine the linkage specificity of poly-ubiquitination chains. As Skp2 was shown to up-regulate KMT5A mono-ubiquitination, it would be interesting to identify the E2-ubiquitin-conjugating enzymes responsible for mediating Skp2 function.

Skp2 primarily enhanced KMT5A mono-ubiquitination at lower concentrations whilst promoted poly-ubiquitination at higher concentrations, suggesting Skp2 level may control the ratio of KMT5A mono-ubiquitination to poly-ubiquitination. Skp2 expression was elevated during G1-S transition, which further increased in S phase. This may in turn result in mainly KMT5A mono-ubiquitination early in the transition phase when Skp2 levels are low and then poly-ubiquitination of KMT5A as Skp2 levels further rise. Such a dual ubiquitination mechanism has been reported for BAP1 and MDM2-mediated ubiquitination of p53, where the *in situ* concentration of MDM2 is a critical factor in determining the ratio of p53 mono-ubiquitination to its poly-ubiquitination (Li *et al.*, 2003). However, requirement of an additional co-factor in facilitating Skp2-mediated poly-ubiquitination of KMT5A cannot be excluded, as complete poly-ubiquitination of mono-ubiquitinated p53 has been demonstrated to require p300 as an E4 ligase (Shi *et al.*, 2009).

Despite significantly elevating full-length KMT5A mono-ubiquitination, Skp2 was unable to increase C-terminal KMT5A fragment mono-ubiquitination above basal mono-ubiquitination levels (Figure 4.10). This could be a consequence of disrupting KMT5A-Skp2 interaction if Skp2 requires interaction with the KMT5A N-terminus. Alternatively, a post-translational modification on the N-terminus may facilitate Skp2-mediated mono-ubiquitination of full-length KMT5A. Although, there is no known consensus sequence for Skp2 substrates, Skp2 is known to recognise its substrates in a phosphorylation-dependent manner. The cross-talk between phosphorylation and ubiquitination has been demonstrated by Wu *et al* (2010) who showed KMT5A phosphorylation at serine 100 caused KMT5A stabilisation by preventing its degradation by the APC^{Cdh1} complex.

Subsequently, de-phosphorylation of the same site leads to APC^{Cdh1}-mediated poly-ubiquitination and degradation of KMT5A during late mitosis (Wu *et al.*, 2010).

Having determined that Skp2 alone was capable of promoting KMT5A mono-ubiquitination, we sought to elucidate whether the SCF complex plays a role in this regulation. Unlike Skp2 alone, further addition of the SCF complex caused a reduction in KMT5A mono-ubiquitination (Figure 4.11). This may be a consequence of disrupting the proportion of individual components of the SCF complex which will subsequently undermine the overall balance of the system, affecting the outcome of the whole complex. In this study we examined different concentrations of Skp2 in combination with constant amounts of the core SCF components. However, we did not consider the contribution of endogenous level of each SCF core component in the experiments, which may have impacted the results. Of note, in the majority of published studies, the role of Skp2 in ubiquitinating its substrates has been investigated without including the SCF components.

The ligase-dead mutant Skp2 we had available as a negative control for Skp2 function, did not function as expected. This truncated form promoted increased mono-ubiquitination of full-length and C-terminus KMT5A. However, being truncated, it may fail to act within the SCF complex as its binding to the SCF components may be attenuated. Alternatively, it could still bind other proteins, recruiting them to SCF complex promoting aberrant activity. Additionally, both WT-Skp2 and mutant Skp2 were heavily ubiquitinated when expressed without the SCF components. However, when expressed in combination with the SCF components, their ubiquitination was significantly reduced, indicating the SCF complex, probably when bound to Skp2, protects Skp2 from excessive ubiquitination.

Role of Skp2-mediated KMT5A mono-ubiquitination as a coordinator of cell cycle progression

Based on the data collected in this thesis and reported elsewhere, a model is proposed for the role of mono-ubiquitinated KMT5A in the G1-S transition, summarised in Figure 4.13.

During G1-S transition and throughout S phase of the cell cycle, KMT5A that is bound to the chromatin becomes poly-ubiquitinated and subsequently degraded by the CRL4^{Cdt2} complex in a PIP degron- and PCNA-dependent manner, to prevent H4K20Me1 deposition and thereby enable DNA replication and timely cell cycle progression. During S phase, as new KMT5A is re-synthesised, it undergoes mono-ubiquitination in the nucleus, signaling for its cytoplasmic translocation. As poly-ubiquitination is a time-consuming and energy-consuming event, it is

speculated that mono-ubiquitination-mediated exclusion of nuclear KMT5A could be an additional mechanism to facilitate its rapid removal from the nucleus during S phase to ensure KMT5A levels are kept at a minimum level. Skp2 upregulation in S phase would promote this process by primarily mediating KMT5A mono-ubiquitination. Therefore, KMT5A mono-ubiquitination plays a role in regulating the levels of KMT5A and consequently is important in maintaining the genome integrity and proper cell cycle progression. Mono-ubiquitinated KMT5A may then undergo de-ubiquitination to facilitate KMT5A re-entering the nucleus during G2/M, and its histone methylase activity being required for mitotic chromatin compaction and progression of the cell cycle. Some of the mono-ubiquitinated KMT5A may also undergo further ubiquitination for degradation by the proteasome. The APC^{Cdh1} complex then degrades KMT5A as cells exit mitosis and the SCF ^{β -TRCP} continues the destruction in G1, to ensure the cell has minimal levels of KMT5A as it enters the S phase.

As mono-ubiquitination is not only a pre-requisite for degradation, once mono-ubiquitinated KMT5A is in the cytoplasm, it may have additional roles by interacting with other proteins and in turn modulating their activity. In support of this speculation, novel substrates of KMT5A are currently under investigation and it has been shown that almost half of the substrates identified are cytoplasmic proteins (personal communication with Dr Fabio Pittella Silva, Memorial Sloan Kettering Cancer Centre). Therefore, it is concluded that mono-ubiquitination of KMT5A and its export into the cytoplasm may have biological relevance as an additional mechanism to the CRL4^{Cdt2}-mediated nuclear destruction of KMT5A during S phase. Moreover, due to the prevalence of mono-ubiquitinated KMT5A in the PC cell lines tested, and the fact that mono-ubiquitination exerts non-proteolytic effects on the protein of interest, mono-ubiquitinated KMT5A must have important additional, as-yet-unidentified roles through regulating proteins residing in the cytoplasm.

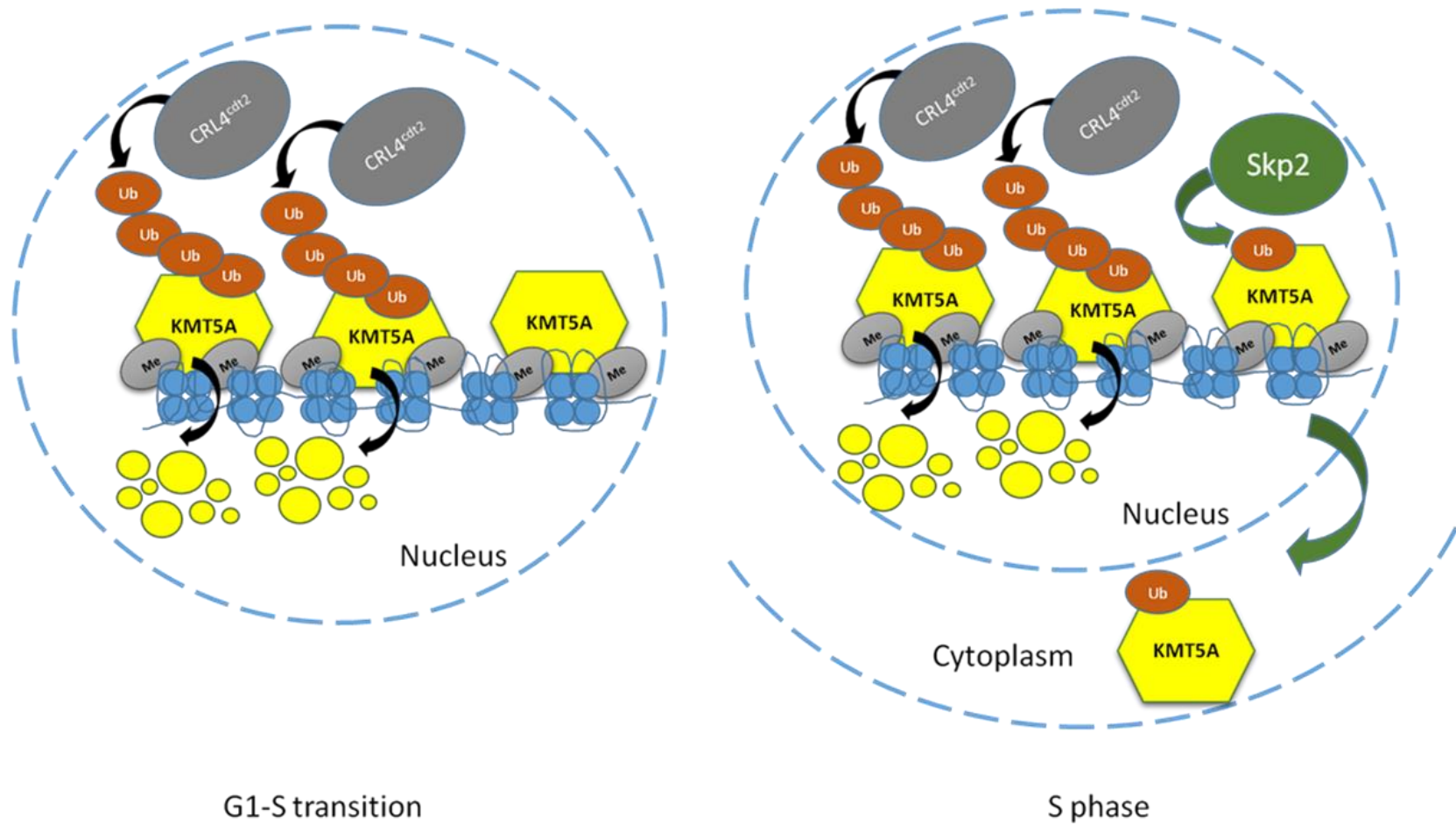


Figure 4-13: Proposed model for the role of mono-ubiquitinated KMT5A. During G1-S transition, KMT5A that is bound to the chromatin is targeted by the CRL4^{Cdt2} complex for poly-ubiquitination and proteasomal mediated degradation. As cells progress into the S phase, newly synthesised and/or remaining KMT5A are primarily subjected to mono-ubiquitination by Skp2 and targeted for cytoplasmic localisation. The diagram is independently drawn based on information from (Yin *et al.*, 2008; Oda *et al.*, 2009).

5 Investigating the role of Skp2 in androgen receptor signalling in prostate cancer

5.1 Introduction

As previously described in Chapter 4, Skp2 is an E3 ubiquitin ligase which positively regulates cell cycle progression by promoting G1-S transition. This is primarily mediated through ubiquitination and degradation of its substrate, the cyclin-dependent kinase inhibitor, p27 (Carrano *et al.*, 1999; Sutterlüty *et al.*, 1999). Skp2 is overexpressed in various types of cancers, including colorectal carcinoma, oral epithelial carcinoma, lymphomas, breast cancer and PC where its upregulation is inversely correlated with p27 protein levels (Catzavelos *et al.*, 1997; Porter *et al.*, 1997; Gstaiger *et al.*, 2001; Hershko *et al.*, 2001; Latres *et al.*, 2001). Specifically, Skp2 has been shown to play a role in the development of prostate cancer with elevated Skp2 expression being observed in premalignant prostate lesions, indicating deregulation of Skp2 is an early event in transformation, and even higher levels are evident in metastasis. In addition, Skp2 level is correlated with tumour stage, histological grade and recurrence in prostate cancer. Therefore, the oncogenic roles of Skp2 make it a promising target for therapeutic intervention and potentially a useful prognostic biomarker (Yang *et al.*, 2002; Ben-Izhak *et al.*, 2003).

Although the role of Skp2 in prostate tumourigenesis is well established, the molecular mechanism(s) by which Skp2 regulates tumour growth has not been fully elucidated. In addition to p27, Skp2 regulates a variety of downstream effectors in cellular processes, both dependent and independent of its E3 ligase complex. Skp2 has been reported to cross-talk with a broad spectrum of signalling cascades such as phosphatidylinositol 3-kinase (PI3K)/Akt, AR, PTEN and p27 in prostate cancer, which is believed to result in its critical role in prostate tumourigenesis (Mamillapalli *et al.*, 2001; Yang *et al.*, 2002; Van Duijn and Trapman, 2006). More recently, Skp2 has been shown to play a role in epigenetic events by regulating histone modification enzymes, such as JARID1B/KDM5B, a histone demethylase responsible for H3K4 tri- and di-methylation. Aberrant elevation of H3K4Me3 is reported to contribute to prostate cancer development and its progression to CRPC, which is positively regulated by Skp2 through inhibition of JARID1B activity (Lu *et al.*, 2015).

The role of Skp2 in regulating the AR directly, and the modulation of Skp2 by the AR signalling however has been controversial and remains unclear. Skp2 expression has been shown to be upregulated upon activation of the AR signalling cascade; whilst Skp2 functioned downstream of the AR and promoted cell proliferation without altering AR level and activity (Wang *et al.*, 2008a). In contrast, Skp2 has also been demonstrated to be negatively regulated by the AR

signalling cascade (Jiang *et al.*, 2012; Kokontis *et al.*, 2014). Furthermore, more contradictory data has revealed that Skp2 negatively regulates AR activity by targeting the AR for poly-ubiquitination and destruction by the proteasome (Li *et al.*, 2014a). The lack of consistency is partly due to the complexity of AR signalling and also the many pathways in which Skp2 is involved, which can consequently influence the AR signalling cascade. Importantly, there are some shortcomings with each of these reports, in that they are not sufficiently detailed, failing to investigate alternative PC cell lines which differ in their sensitivity to androgens, are limited to investigating one AR-regulated gene and either lack Skp2 protein or mRNA expression data.

In Chapter 4, Skp2 was shown to promote KMT5A mono-ubiquitination which was not associated with protein turnover. Although, a potential Skp2-mono-ubiquitinated KMT5A axis may exist in the modulation of AR signalling, Skp2 may affect KMT5A and AR regulation independently of each other. Hence, the overall aim of this chapter is to independently investigate the role of Skp2 in AR regulation, by performing experiments in androgen-dependent and independent cell lines.

5.2 Hypothesis

Skp2 regulates PC cell growth and survival either directly or indirectly of the AR signalling cascade.

5.2.1 Aims

- Determine the androgenic regulation of Skp2
- Determine whether Skp2 modulates AR activity
- Investigate the underlying mechanism of Skp2-mediated AR regulation by assessing AR localisation and phosphorylation status

5.3 Results

5.3.1 Differential androgenic response of Skp2 protein in LNCaP and LNCaP-AI cell lines

A number of reports have described the involvement of androgen and the AR in regulating Skp2 either at the protein or mRNA level. However, these studies mostly contradict each other (Wang *et al.*, 2008a; Pernicová *et al.*, 2011; Jiang *et al.*, 2012; Kokontis *et al.*, 2014; Li *et al.*, 2014a). This may be partly due to the difference in cell lines used to investigate Skp2 levels, for example androgen dependent and independent cells have been investigated. Consequently, androgenic regulation of Skp2 remains unclear. In order to address this in both the androgen-dependent and androgen-independent states of PC, the parental LNCaP androgen-sensitive cell line and its castrate-resistant derivative, LNCaP-AI cell line were used to investigate Skp2 response to androgenic stimulation. To this end, LNCaP and LNCaP-AI cells were grown in steroid-deprived conditions by using dextran-coated charcoal stripped serum media, before being subjected to androgenic stimulation with 10 nM DHT for various time points.

In the androgen-dependent LNCaP cell line, DHT stimulation markedly induced the protein expression of the AR-regulated gene, PSA, used as a positive control. The AR protein expression also increased upon activating the AR signalling with 10 nM DHT, as expected (Figure 5.1). Furthermore, DHT treatment led to the upregulation of Skp2 protein levels which was only apparent at 48 hours post androgenic stimulation. This was in contrast to PSA which was acutely elevated after 8 hours and continued to rise with longer DHT treatments up to 48 hours. This suggested that androgenic regulation of Skp2 occurs at the post-translational level or could be a secondary effect of androgen-AR signalling.

However, in the androgen-independent cell line, LNCaP-AI, PSA protein could not be detected. These cells express significantly lower levels of PSA, where Western blotting is frequently not sensitive enough to detect such minute PSA levels. Similar to the LNCaP cells however, the AR expression was enhanced with 10 nM DHT stimulation. In contrast, DHT stimulation did not upregulate Skp2 in the LNCaP-AI, and even seemed to cause a subtle down-regulation at 48 hours post DHT treatment. Therefore Skp2 protein expression was found to respond differentially in response to DHT treatment in LNCaP and LNCaP-AI cell lines.

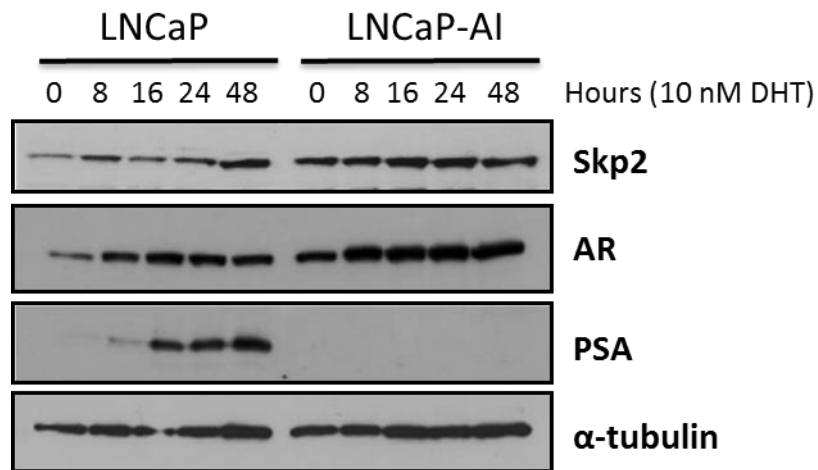


Figure 5-1: Skp2 protein expression responds differently to androgenic stimulation in LNCaP and LNCaP-AI cells. LNCaP and LNCaP-AI cells were cultured in steroid-depleted media (SDM) for 72 hours before being treated with 10 nM DHT for the indicated time points. Cell lysates were collected with SDS sample buffer and analysed by Western blotting for AR, Skp2, PSA and the loading control, α -tubulin. This is a representative blot of three independent repeats.

5.3.2 Differential effect on Skp2 protein levels in response to increasing androgen concentration in LNCaP and LNCaP-AI cell lines

Skp2 has been previously reported to be under dual modulation by androgens at sub-physiological compared to physiological and supra-physiological concentrations (Jiang *et al.*, 2012). As shown in Figure 5.1, Skp2 responds in an opposing manner to androgenic stimulation between LNCaP and LNCaP-AI cell lines. To further confirm this observation, a range of DHT concentrations was used to stimulate both cell lines over 48 hours. Western blot analysis for the LNCaP cell line treated with androgens revealed Skp2 protein levels clearly increased at both 10 and 100 nM DHT and more subtly at 1 nM DHT. However, it remained unchanged at sub-physiological DHT levels of 0 - 0.1 nM in LNCaP cells. In addition, PSA levels showed similar expression kinetics at these DHT concentrations, although no PSA could be detected at sub-physiological concentrations of DHT. Conversely, in the LNCaP-AI cell line it was observed that Skp2 protein expression was suppressed by 10 and 100 nM DHT treatment, but sub-physiological DHT concentrations did not affect Skp2 levels (Figure 5.2A). Interestingly, the changes in Skp2 level in response to DHT concentration mirrors that of AR expression.

The difference in Skp2 regulation is interesting between these two cell lines, as LNCaP-AI cell line is derived from parental LNCaP cells following continuous growth in steroid-depleted conditions to model androgen-independent disease. As LNCaP and LNCaP-AI cells are normally cultured in FM and SDM, respectively, it was decided to examine Skp2 expression in both cell lines in FM and SDM (Figure 5.2B). Consistently, Skp2 protein expression was markedly down-regulated in LNCaP cells upon culturing them in SDM. However, Skp2 protein levels did not obviously alter in the LNCaP-AI cells following their growth in the different culture media (Figure 5.2). This could be due to FM not containing sufficiently high levels of androgens that would lead to Skp2 suppression, or other factors such as some growth hormones that are removed in charcoal-treated media may prevent Skp2 down-regulation following LNCaP-AI growth in full media. Overall, the data clearly demonstrates that Skp2 is regulated by androgen in LNCaP cells but in LNCaP-AI cells this mechanism is different and Skp2 protein expression is diminished by high androgen concentrations. This suggests that during the changes which occurs in LNCaP to transition from an androgen dependent to an androgen independent state, the regulation of Skp2 by the androgenic pathway is altered.

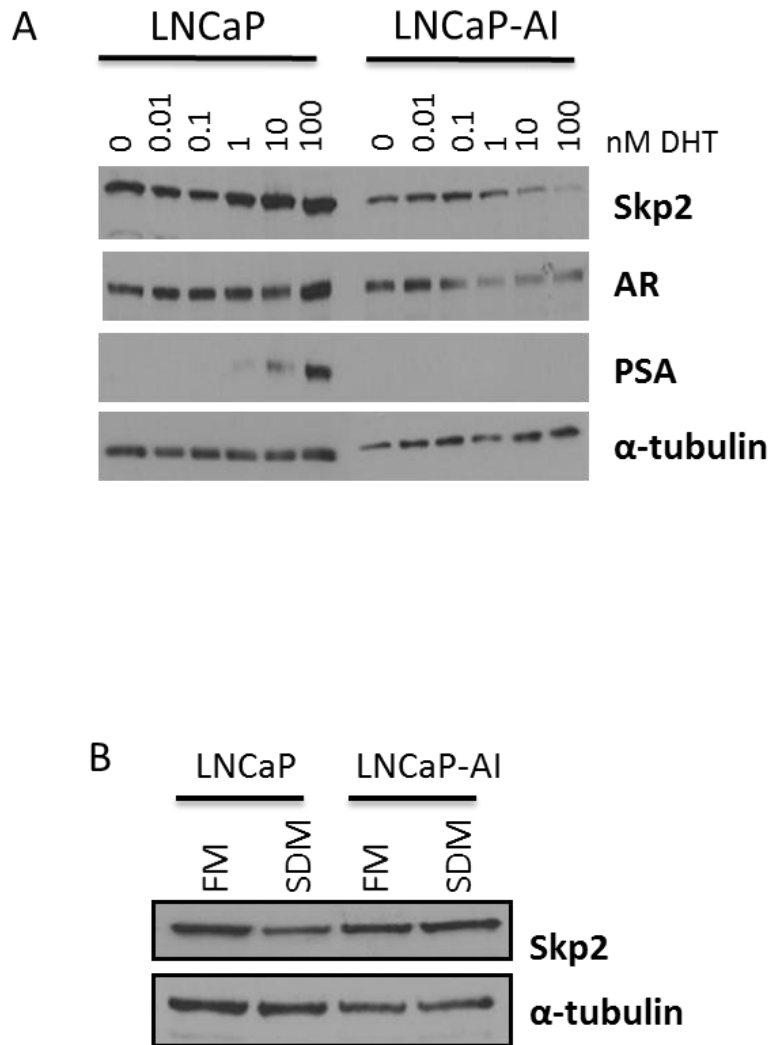


Figure 5-2: Differential effect on Skp2 protein levels in response to androgen concentration range in the LNCaP and LNCaP-AI cell lines. Western blot analysis of AR, Skp2, positive control PSA and the loading control, α -tubulin for (A) LNCaP and LNCaP-AI cells cultured in steroid-depleted media (SDM) and treated with increasing concentration of DHT for 48 hours before being subject to Western blot analysis and (B) LNCaP and LNCaP-AI cells grown in either in FM or SDM prior to collection for Western blot.

5.3.3 Skp2 response to DHT stimulation is similar in LNCaP and LNCaP-AI cell lines at the transcription level

It was then sought to determine whether the changes observed in the Skp2 protein level were also evident at the transcriptional level in both LNCaP and LNCaP-AI cell lines. In order to investigate this, the effect of 10 nM DHT treatment on Skp2 transcription in LNCaP and LNCaP-AI cell lines was examined. QRT-PCR was undertaken to determine mRNA levels of Skp2, with PSA included as a positive control of an androgen regulated gene, following androgen deprivation of the cell lines for 72 hours and subsequent stimulation with 10 nM DHT for various time points. AR mRNA expression was also examined over this time period in both cell lines.

In the LNCaP cells, PSA up-regulation was induced by 4.2 fold at 8 hours after DHT stimulation and was sustained for at least a further 16 hours (Figure 5.3). However, in contrast to its protein levels, the AR expression was not altered at the transcriptional level, except after 48 hours where there was a small down-regulation, possibly due to the over-activation of AR signalling which has been reported to suppress AR expression. Nonetheless, consistent with the AR protein and mRNA expression data, androgenic stimulation causes stabilisation of the AR protein by binding to the AR (Bennett *et al.*, 2010). In contrast to the protein level, Skp2 mRNA levels were found to be unaffected with DHT treatment. Similarly, in the LNCaP-AI cells, PSA mRNA expression was induced following 8 hours DHT treatment, as expected. Although the reason for its observed small decrease at 24 hours is unclear. Of note, the PSA mRNA level in LNCaP-AI cells is approximately two orders of magnitude lower than that found in the LNCaP cells, consistent with difficulties observed in detecting PSA protein in LNCaP-AI cells by western analysis (Figure 5.1). Conversely, the AR mRNA in LNCaP-AI cells increased following 16 and 24 hours DHT stimulation and was further elevated at 48 hours by 1.9 fold. Interestingly, similar to LNCaP cells, the Skp2 mRNA remained unaltered even at 48 hours DHT treatment (Figure 5-3). Therefore, the data implies androgenic regulation of Skp2 is not a primary event and Skp2 is not directly regulated by androgen-AR signalling.

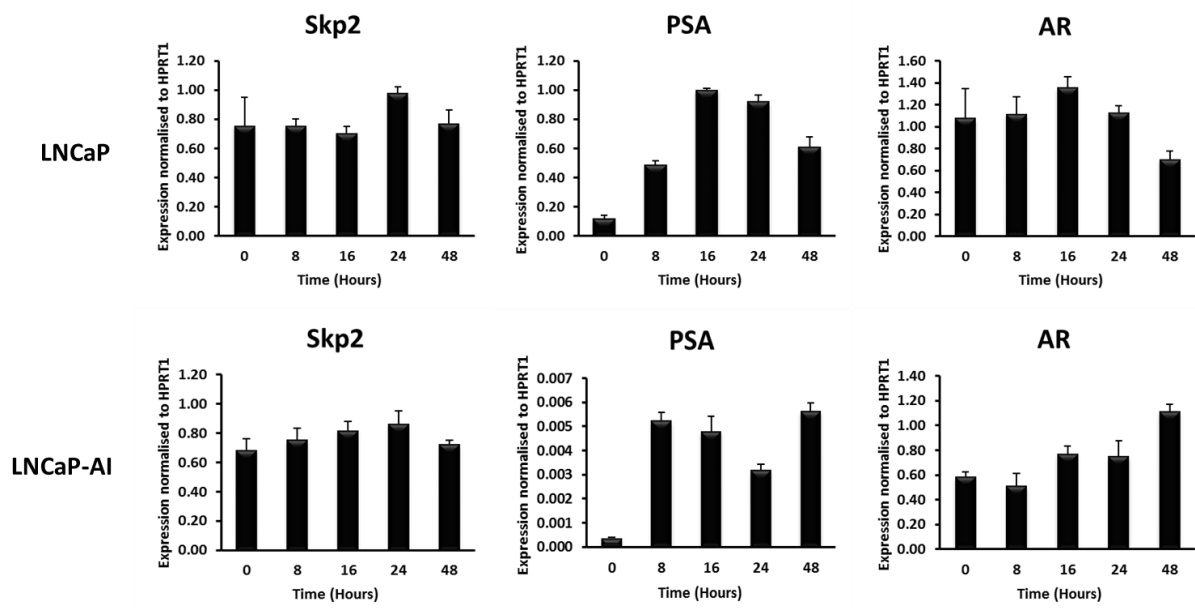


Figure 5-3: Androgenic stimulation does not alter Skp2 transcription in LNCaP and LNCaP-AI cell lines. Quantitative RT-PCR demonstrating the effect of 10 nM DHT treatment on Skp2, PSA and AR relative to the control gene, HPRT1. LNCaP and LNCaP-AI cells were grown in steroid-depleted media (SDM) prior to stimulation with 10 nM DHT for the indicated time points and subject to gene expression analysis for one repeat, n=1.

5.3.4 Validation of Skp2 protein depletion using siRNA oligonucleotides

Having determined Skp2 is not a direct downstream effector of the androgen-AR signalling cascade, it was questioned whether there was any role for Skp2 in regulating AR signalling, as Skp2 is frequently upregulated in CRPC, concomitant with re-activation of AR signalling (Yang *et al.*, 2002; Nguyen *et al.*, 2011; Robbins *et al.*, 2011). For this purpose, three Skp2 siRNA oligonucleotides were tested for their efficiency in LNCaP and LNCaP-AI cell lines grown in their native media to deplete Skp2 protein. Following 72 hours siRNA treatment, Skp2 and its substrate, p27, protein levels were tested.

Figure 5.4 demonstrates that all three Skp2 siRNA oligonucleotides, and additionally the pool (P) of combined Skp2 siRNAs, resulted in a significant suppression of Skp2 protein to almost undetectable levels compared to the non-silencing control. Consistent with Skp2 depletion, p27 used as the positive control was markedly up-regulated, as expected.

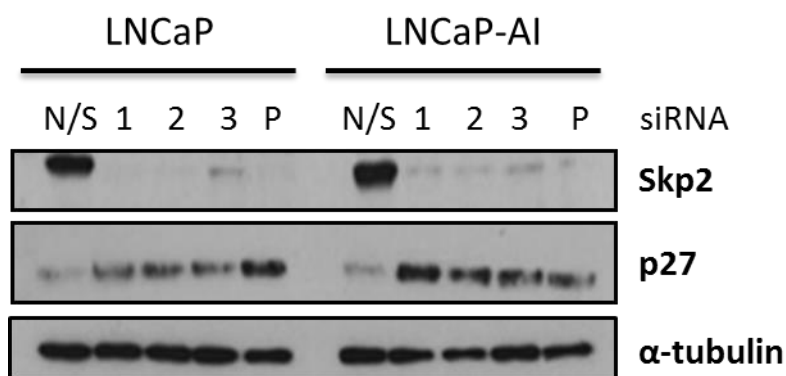


Figure 5-4: Validation of Skp2 siRNA oligonucleotides. LNCaP and LNCaP-AI cells grown in their native culture media were reverse-transfected with one of three Skp2 siRNA oligonucleotides, a combined pool of the three Skp2 siRNAs (P), or non-silencing (N/S) control siRNA at 25 nM. After 72 hours incubation, cell lysates were generated using SDS sample buffer and Western blot performed for Skp2, the positive control p27 and loading control α -tubulin. This is a representative blot of multiple independent repeats.

5.3.5 Skp2 protein depletion reduces growth of PC cell lines

Given the role of Skp2 in promoting cell cycle transition and the impact of its depletion on p27 levels, cell growth was then examined following Skp2 silencing using Skp2 siRNA 3, in LNCaP and LNCaP-AI cell lines. To this end, siRNA-mediated Skp2 knockdown was performed in a 6-well plate for 72 hours with the PC cells being cultured in their native growth media for the course of the experiment. Following this, the cells were trypsinised, seeded in wells of a 96-well plate and left to grow. Growth of cells was monitored in the incucyte system over a period of 5.5 – 6.0 days, measuring confluency every 6 hours.

In keeping with its role in promoting cell growth, Skp2 suppression led to reduced cell growth in both the LNCaP and LNCaP-AI cell lines, inhibiting cell proliferation by approximately fifty per cent (Figure 5.5).

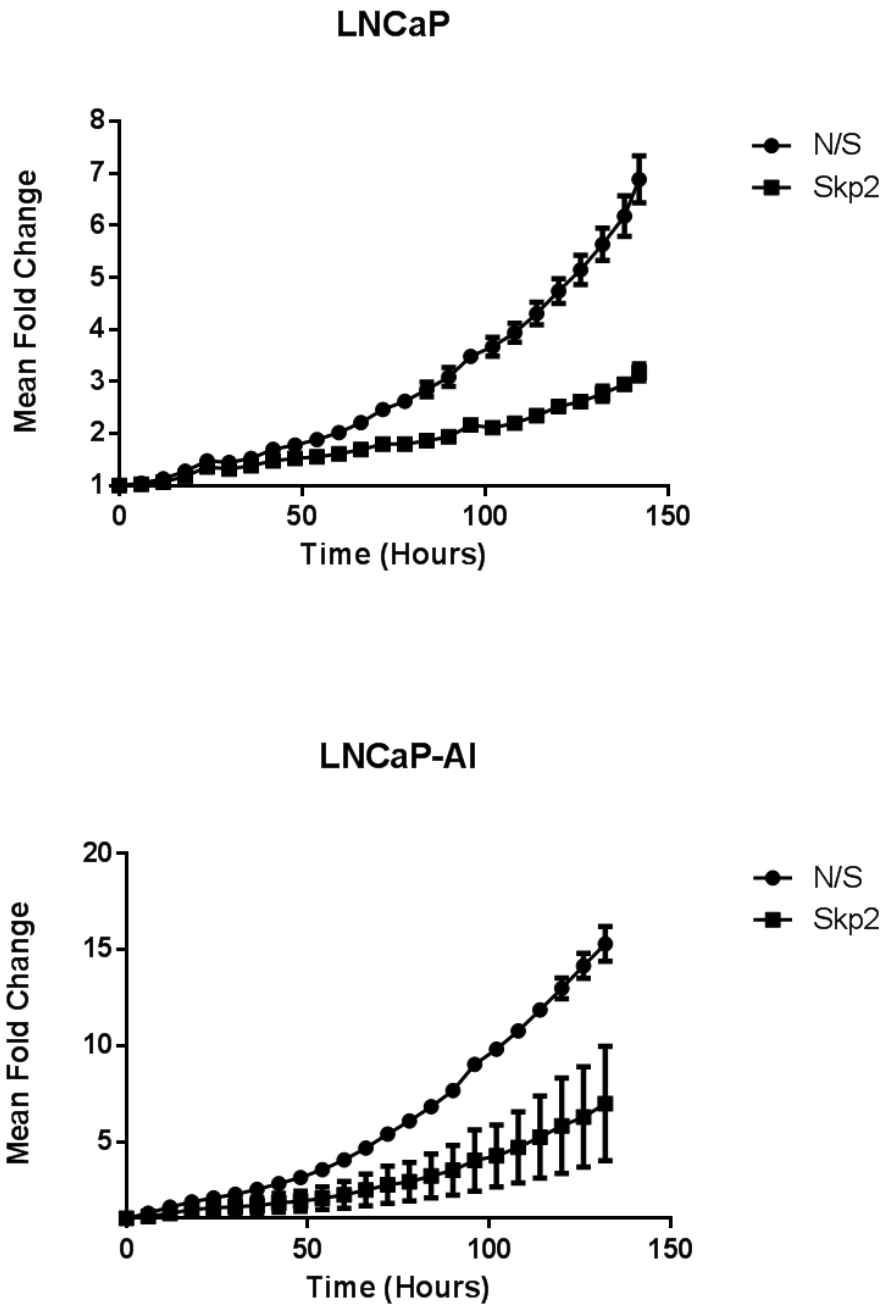


Figure 5-5: Skp2 suppression downregulates cell growth. LNCaP and LNCaP-AI cells were either transfected with non-silencing (N/S) or Skp2 siRNA in their native media. Cell growth (relative confluency) was then monitored using the IncuCyte system. Data are a mean of two independent experiments, and error bars represent SEM.

5.3.6 *Skp2* knockdown causes G1 cell cycle arrest in PC cell lines

As the role of Skp2 in promoting cell proliferation is mainly mediated by facilitating G1 to S phase transition, its effect on cell cycle was analysed in more detail. LNCaP and LNCaP-AI cells were transfected with Skp2 siRNA in their native growth culture. Following 72 hours incubation, the cells were stained with propidium iodide and subjected to flow cytometry.

In response to Skp2 knockdown, there was a clear increase in the percentage of cells in G1 for both cell lines, with a reciprocal decrease in the percentage of cells undergoing DNA replication in S phase, and in the G2/M phase of the cell cycle (Figure 5.6). Additionally, Skp2 depletion subtly increased the subG1 population, indicative of apoptotic/necrotic cells. This finding is in line with the role of Skp2 in regulating cell cycle progression, as well as, modulating apoptosis (Harada *et al.*, 2005; Lee and McCormick, 2005). These siRNA results are also consistent with previous published data that Skp2 depletion blocks cell cycle progression in G1-S transition (Carrano *et al.*, 1999).

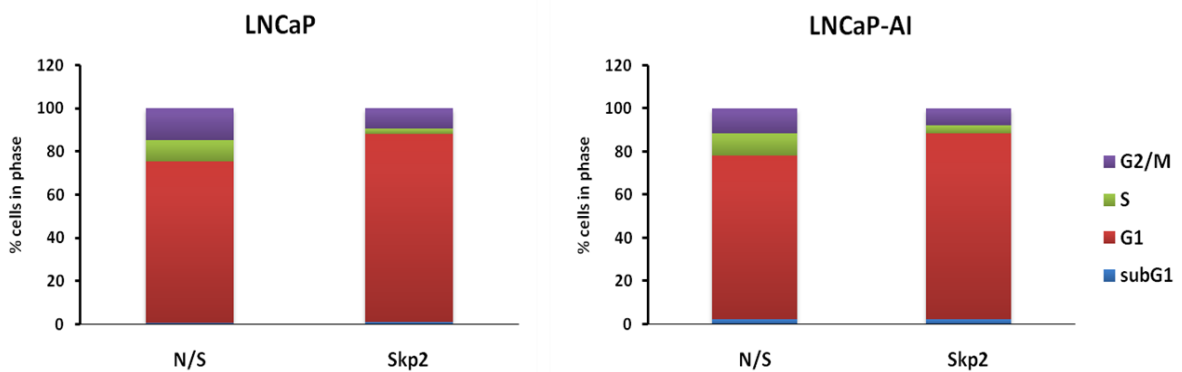


Figure 5-6: Skp2 depletion induces G1 cell cycle arrest in PC cell lines. LNCaP and LNCaP-AI cells grown in their native media were reverse transfected with either 25 nM non-silencing (N/S) or Skp2 siRNA. Following 72 hours post transfection, cells were subject to cell cycle analysis using propidium iodide based flow cytometry, for one repeat, n=1.

5.3.7 Determining the role of Skp2 in AR-mediated protein expression

Having validated the Skp2 siRNA, the role of Skp2 in regulating AR activity was investigated. As such AR transcriptional activity was determined by Western blotting for representative AR target genes, PSA and ATAD2. Although less well defined, the expression of ATAD2 is known to be activated by androgens through induction of AR binding to ARE within the ATAD2 distal enhancer region (Zou *et al.*, 2009; Altintas *et al.*, 2012). For this purpose, LNCaP and LNCaP-AI cells were either transfected with Skp2 or non-silencing control siRNA in steroid-depleted conditions for 72 hours. The cells were then stimulated with 10 nM DHT for various time points, followed by Western blot analysis.

Figure 5.7 demonstrates that in the control androgen-sensitive LNCaP cells, DHT treatment resulted in an up-regulation of PSA expression, which was not affected following Skp2 depletion. Similarly, the protein expression of ATAD2 was induced upon DHT stimulation when transfected with non-silencing control siRNA. Interestingly however, Skp2 knockdown led to the down-regulation of ATAD2 protein. Furthermore, the reduction was evident in the absence of supplemented androgens (0 hour DHT); prior to induced AR signalling, suggesting basal transcription of ATAD2 is affected. In line with the data for the LNCaP cells, ATAD2 protein expression was also increased following DHT stimulation in the LNCaP-AI non-silencing siRNA control cells. Skp2 depletion, similarly to the results in LNCaP cells, caused a reduction in ATAD2 protein in LNCaP-AI cells. As expected, the low level expression of PSA protein in LNCaP-AI cells explained the lack of PSA detected by western blotting in this cell line.

Moreover, consistent with the previous data (Figure 5.2), Skp2 protein expression was up-regulated in the control LNCaP cells with DHT stimulation, but remained unchanged in the LNCaP-AI cells when taking α -tubulin levels into account. Furthermore, the AR protein expression increased after androgenic stimulation in both cell lines as observed previously (Figure 5.1) and was not affected when Skp2 was inhibited.

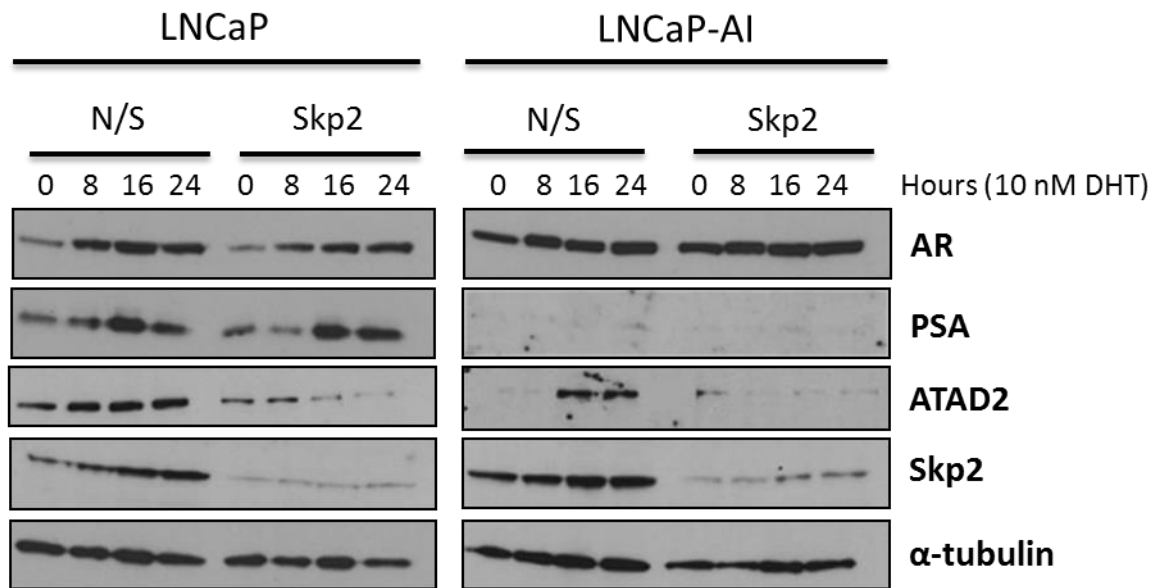


Figure 5-7: Skp2 depletion differentially affects AR-mediated gene expression. LNCaP and LNCaP-AI cells were reverse transfected with 25 nM siRNA either against Skp2 or the non-silencing (N/S) control for 72 hours whilst being cultured in steroid-depleted media (SDM). Cells were then treated with 10 nM DHT for the indicated time points before being collected for Western blot analysis for AR, PSA, ATAD2, Skp2 and the loading control α -tubulin. This is a representative blot of three independent repeats.

5.3.8 Assessing the effect of Skp2 depletion on AR-regulated gene expression

Skp2 knockdown led to a differential regulation of PSA and ATAD2 protein expression. Moreover, in the LNCaP cells, the reduction in ATAD2 protein in the absence of androgenic stimulation indicated that this could be due to Skp2 depletion altering ATAD2 basal transcription (Figure 5-7). Therefore, in order to further validate that Skp2 differentially affects AR-regulated gene expression, and also to determine whether it occurs at the basal transcription level, the AR transcriptional activity was assessed using qRT-PCR. As such, expression of additional AR-regulated genes including KLK2 and TMPRSS2 was examined. As the effect on ATAD2 was similar in both LNCaP and LNCaP-AI cell lines, this experiment was only performed in the LNCaP cells.

In keeping with being AR target genes, PSA, KLK2, TMPRSS2 and ATAD2 mRNA levels were all up-regulated by 2.4, 6.7, 5.7 and 2 fold respectively following 8 hours DHT stimulation. They further increased their expression at 16 hours post DHT treatment to 7.2, 19, 10.8 and 2.5 fold respectively, which were then maintained up to 24 hours of DHT treatment in the control non-silencing siRNA transfected cells (Figure 5.8). On the other hand, whilst TMPRSS2 was not influenced, the transactivation of PSA was induced to a greater extent (4.6 fold) and less so for KLK2 (7 fold) following Skp2 depletion post 8 hours DHT treatment. However, the mRNA expression of KLK2 and TMPRSS2 genes was reduced compared to non-silencing cells at 16 and 24 hours DHT treatment in the absence of Skp2 (Figure 5.8). This may imply that the AR requires Skp2 at later stages of its transcriptional activity at KLK2 and TMPRSS2 gene promoters. In a stark contrast, ATAD2 levels were reduced by almost 50% in the absence of DHT stimulation when Skp2 was depleted, implying that basal transcription of ATAD2 is inhibited. However, following DHT treatment, ATAD2 was still up-regulated with a similar magnitude as control cells. In line with the previous data (Figure 5.3), DHT did not affect Skp2 mRNA, and Skp2 siRNA knockdown efficiently inhibited Skp2 transcription (Figure 5.8). Overall, Skp2-mediated regulation of AR transcriptional activity appears complex as it causes a different outcome for different AR-target genes.

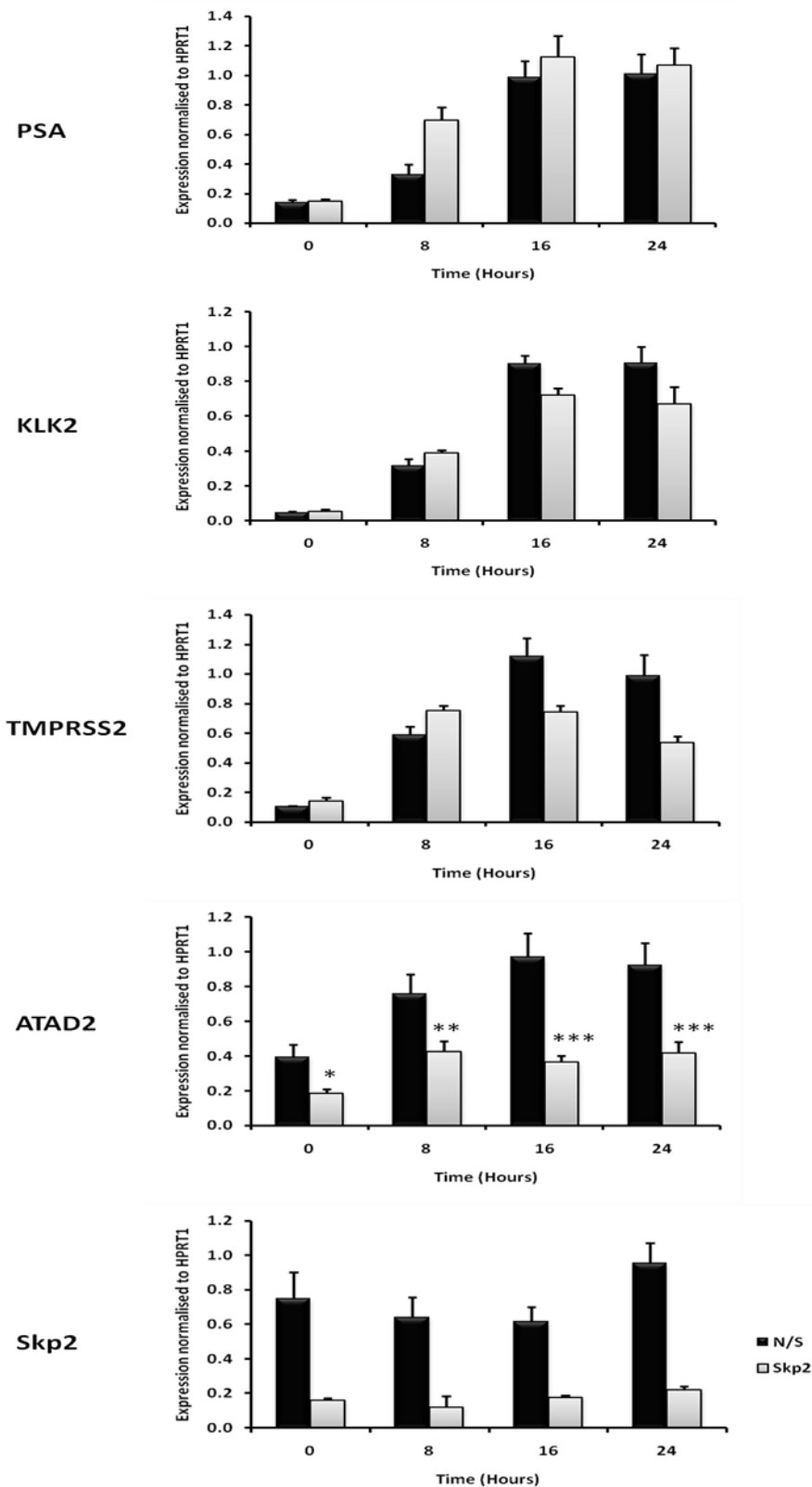


Figure 5-8: Skp2 depletion does not affect classical AR-mediated gene expression. LNCaP cells were reverse transfected with 25 nM Skp2 or the control non-silencing (N/S) siRNA while being cultured in steroid-depleted media (SDM). Following 72 hours post transfection, cells were stimulated with 10 nM DHT for the indicated time points before being subject to gene expression analysis by QRT-PCR. Data are normalised to the control gene HPRT1. Graph represents the mean from three independent repeats and error bars depict SEM. * represent a p-value <0.05, ** p < 0.01 and *** p < 0.001.

5.3.9 *Skp2 depletion does not affect protein AR levels*

Skp2 has previously been reported as an E3 ligase for the AR where it has been shown to ubiquitinate and target the AR for proteasomal degradation, leading to reduced AR protein level and transcriptional activity (Li *et al.*, 2014a). However, this cannot explain the data shown in (Figure 5.8) as Skp2 depletion would generally be expected to cause an up-regulation of AR-target genes. In contrast, Skp2 mRNA suppression caused a down-regulation of ATAD2 at the basal transcriptional level and reduced DHT-induced KLK2 and TMPRSS2 transcription. In order to elucidate the mechanism by which Skp2 knockdown causes decreased AR activity, the effect of Skp2 on AR protein level was investigated. As there is controversy in the literature regarding the regulation of AR stability by Skp2, three different siRNA oligonucleotides were utilised in LNCaP and LNCaP-AI cell lines grown in their native media, to silence Skp2 for 72 hours after which AR protein levels were determined. Figure 5.9A demonstrates that Skp2 inhibition did not alter AR expression. This finding is in agreement with earlier results where Skp2 knockdown in steroid-depleted conditions followed by androgenic stimulation did not change AR levels (Figure 5.7).

At the time this work was being performed, another study by Li *et al.* (Li *et al.*, 2014a) was published which showed Skp2 negatively regulates AR activity where Skp2 inhibition led to restoration of the AR protein expression in PC3 and DU145 AR-negative cell lines. As this is an observation at the other end of the spectrum to the data reported here, this experiment was repeated with the same experimental conditions stated in the paper, alongside our experimental conditions in PC3 cells, as well as, CWR22RV1 cells, the latter cell line expresses both a full-length mutant AR and a shorter constitutively active isoform of AR lacking the ligand binding domain (AR-V). However, in keeping with previous observations in this thesis, Skp2 depletion did not alter AR levels and was not able to restore AR expression in PC3 cells in either of the experimental conditions despite a clear up-regulation of p27 protein levels (Figure 5.9B). Interestingly, in the CWR22RV1 cell line, despite unaffected full-length AR levels, Skp2 knockdown did cause a small reduction in the shorter AR-V isoform, suggesting Skp2 may differentially regulate AR isoforms.

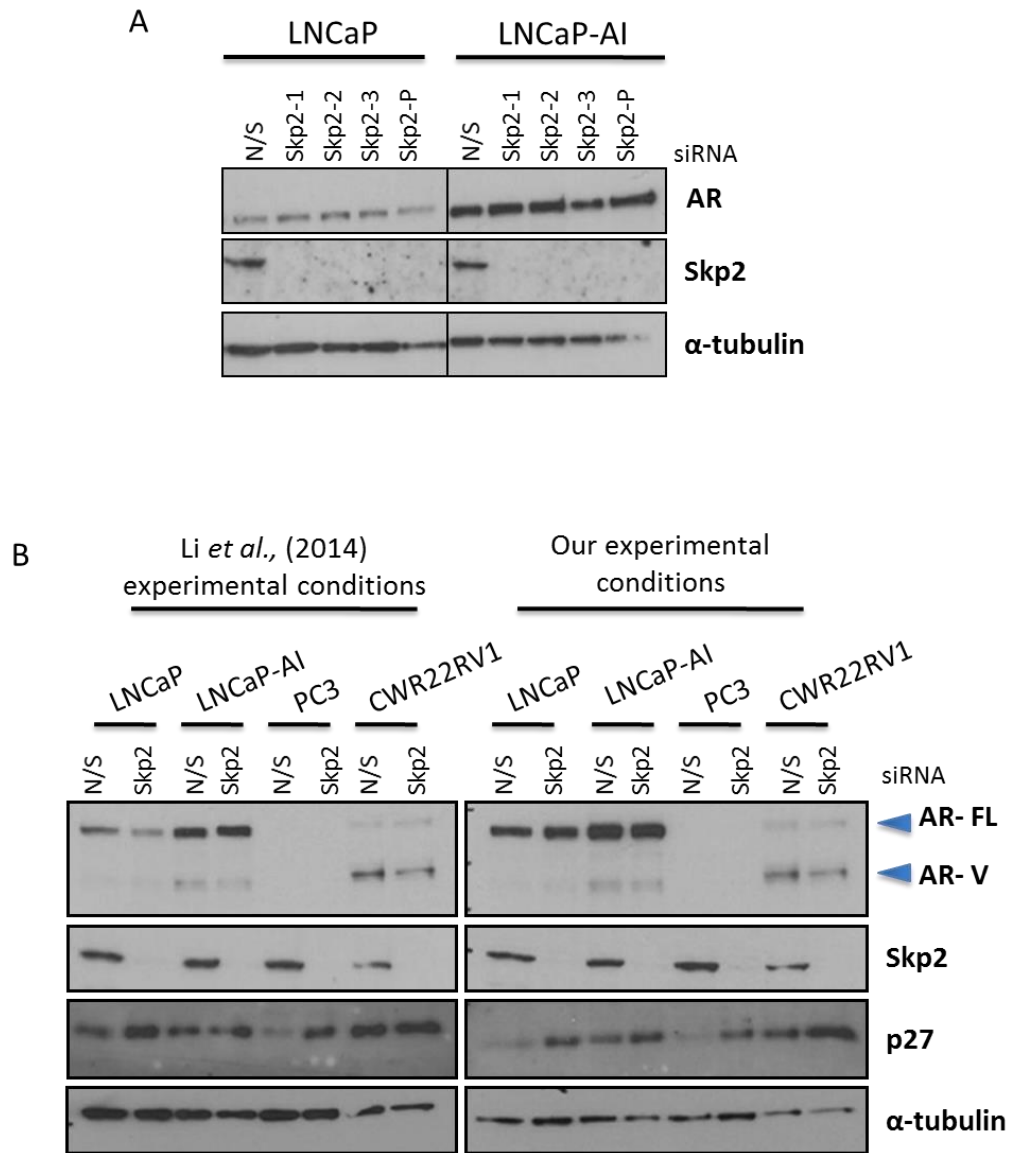


Figure 5-9: AR level is not altered by Skp2 depletion. Western blots of AR (FL, full-length and V, variant), Skp2, p27 and the loading control α -tubulin for (A) LNCaP and LNCaP-AI cells grown in their native media while reverse transfected with 25 nM of either three of the Skp2 siRNAs, combined pool of the three Skp2 siRNAs or the non-silencing control siRNA for 72 hours before being subject to Western blotting. (B) Direct comparison of the effect of Skp2 knockdown on AR level between Li *et al.*, (2014) and our experimental conditions. PC cell lines were reverse transfected using 10 nM siRNA for 48 hours and 25 nM for 72 hours under Li's and our experimental conditions, respectively.

5.3.10 *Skp2 protein forms a complex with the AR*

Although Skp2 was found to not regulate AR levels, it was speculated that Skp2 may modulate AR transcriptional activity independently of AR ubiquitination through an alternative mechanism which may require interacting with the AR. In order to establish if Skp2 and AR are found in a complex, immunoprecipitation was performed in LNCaP cells grown in their native media to pull down endogenous Skp2, followed by AR detection in the immunoprecipitated samples.

Interestingly, Skp2 was found to be in a complex with AR as AR was detected following Skp2 immunoprecipitation but not in the negative IgG or the antibody only control lanes (Figure 5.10). However, this experiment was conducted only once and unfortunately the Western blot for Skp2 was not particularly clear to demonstrate successful Skp2 immunoprecipitation. The co-immunoprecipitation of AR did however suggest the possibility that Skp2 binding to the AR may perturb AR signalling.

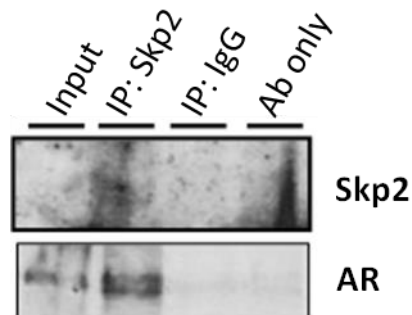


Figure 5-10: Skp2 and AR are found in a complex. Immunoprecipitation was performed under non-denaturing conditions with either 2 μ g anti-Skp2 or the negative control IgG antibody. Antibody control (Ab only) is a lysate-free sample control. Samples were subject to Western blot for Skp2 and AR. The experiment was conducted once.

5.3.11 *Skp2 does not affect AR localisation*

In addition to its ubiquitin ligase activity, Skp2 has also been reported to act independently of its SCF complex where it has been shown to regulate its substrates by sequestering them (Kitagawa *et al.*, 2008). AR translocates to the nucleus upon binding androgen to activate gene transcription. Therefore, it was hypothesised that cytoplasmic Skp2 may retard AR localisation to the nucleus following androgenic stimulation with DHT. To investigate this further, LNCaP cells were simultaneously starved in SDM and transfected with siRNA for 72 hours, followed by DHT stimulation for 2 hours prior to undergoing nuclear-cytoplasmic fractionation to compare AR subcellular localisation in response to DHT in the presence and absence of Skp2.

As expected, the AR was translocated to the nucleus following DHT stimulation in the control non-silencing siRNA transfected cells. However, despite initial indications, Skp2 silencing did not alter AR localisation (Figure 5.11A). Surprisingly, Skp2 was found to be almost exclusively cytoplasmic which was unexpected as Skp2 has previously been reported to be predominantly nuclear, though present in both compartments (Signoretto *et al.*, 2002; Radke *et al.*, 2005; Gao *et al.*, 2009).

This observation could possibly be explained by the fact that Skp2 localisation has previously not been characterised under steroid deprivation as was the case in our experimental conditions. Moreover, the fractionation method utilised may underlie the lack of Skp2 detection in the nuclear compartment, as an insoluble pellet comprising protein that are tightly bound to the chromatin is left behind following removal of the cytoplasmic and nuclear extracts. Recently, Skp2 has been shown to ubiquitinate macroH2A1 (mH2A1), a member of H2A family, for degradation (Xu *et al.*, 2015), indicating that Skp2 may have not been completely solubilised while being associated with mH2A and was consequently discarded as part of the insoluble pellet.

Therefore, the insoluble pellet which consists of cellular debris but mostly chromatin was re-suspended in SDS sample buffer and subjected to Western blotting. Interestingly, Skp2 was indeed found to be present in the chromatin-containing fraction (Figure 5.11B). However, it would have been more prudent to use a histone marker as a control to confirm the presence of histones in this fraction rather than PARP. Moreover, ideally, Skp2 localisation should be characterised in LNCaP cells when grown in their native media rather than in steroid depleted conditions as LNCaP cells are dependent on androgens for growth and survival and slowed growth due to starvation may in turn affect Skp2 levels as well as localisation. Consistently, Skp2 levels were found to decrease upon culturing LNCaP in SDM.

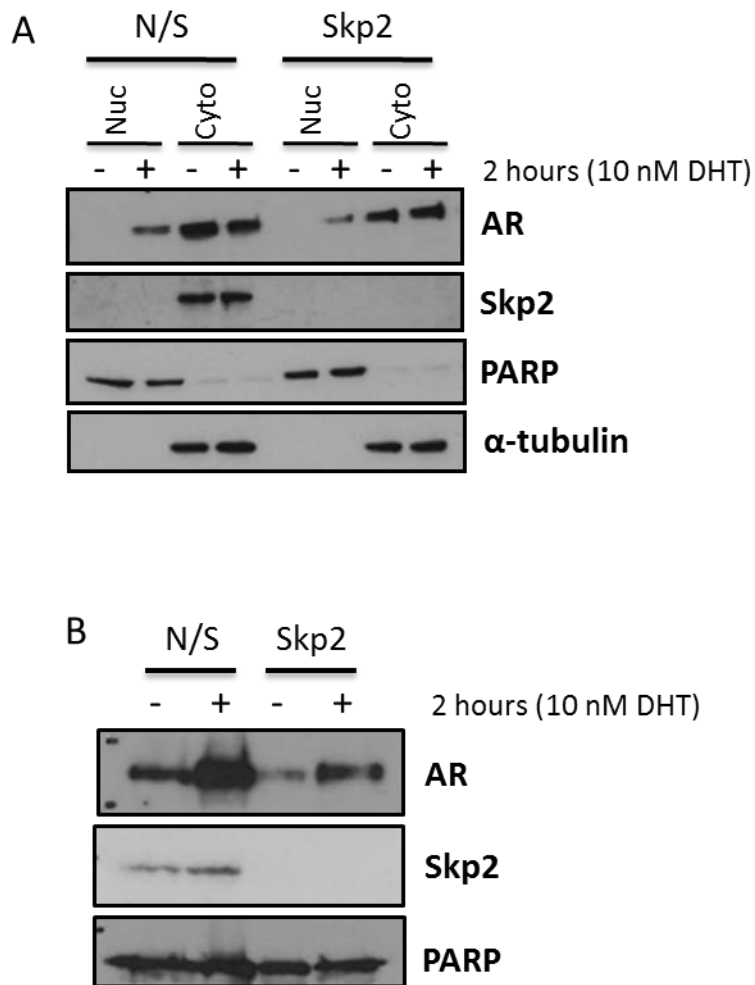


Figure 5-11: Skp2 depletion does not alter AR nuclear translocation upon androgenic stimulation. (A) LNCaP cells were reverse transfected in steroid-depleted media (SDM) for 72 hours. Cells were then stimulated with 10 nM DHT for 2 hours prior to being subject to cellular fractionation using the NE-PER™ nuclear and cytoplasmic extraction kit (Thermo Scientific) into the nuclear (Nuc) and cytoplasmic (Cyto) samples. (B) The remaining insoluble pellet (chromatin fraction) was re-suspended in SDS sample buffer and Western blot was performed on the samples for AR, Skp2, the nuclear and cytoplasmic controls PARP1/2 and α -tubulin, respectively.

5.3.12 Skp2 does not influence AR phosphorylation at serine 81

As previously mentioned, p27 is a cell cycle inhibitor which functions through regulating cyclin-cyclin dependent kinase (cyclin/CDK) complexes. Skp2 suppression led to up-regulation of p27 and reduced transcriptional activity of AR at some AR target genes without affecting AR levels and localisation. As AR is phosphorylated by cyclin/CDKs at serine 81 (pS81-AR) upon binding androgen to regulate AR ability to bind chromatin and gene transcription, it was hypothesised that Skp2 suppression may perturb phosphorylation of AR at serine 81. To this end, LNCaP and LNCaP-AI cells were transfected in SDM for 72 hours and then stimulated with DHT, followed by Western blot analysis.

It was observed that Skp2 depletion did not alter the overall phosphorylation level of AR at serine 81 (Figure 5.12). Although, this is difficult to accurately visualise in the LNCaP cell line because AR levels are dependent on androgens in these cells as seen by total AR being down-regulated to very low levels following growth in SDM which was then increased following DHT treatment. The considerable change in total AR levels between androgen stimulated and vehicle treated cells in both non-silencing and Skp2 siRNA arms is therefore the principle underlying reason for the changes observed in pS81-AR level which reflect total AR levels. However, the failure to alter pS81-AR levels in combined response to DHT treatment and Skp2 depletion is apparent in the LNCaP-AI cells as these cells are androgen-independent with their AR protein expression being sustained when androgen is depleted, undergoing only subtle changes in overall levels in response to androgen treatment. Under androgen deprived conditions, AR phosphorylation was almost undetectable despite high levels of the AR in LNCaP-AI cells, as expected. However, following DHT treatment, there was a strong induction of AR phosphorylation on serine 81 which occurred to a similar extent when Skp2 was depleted.

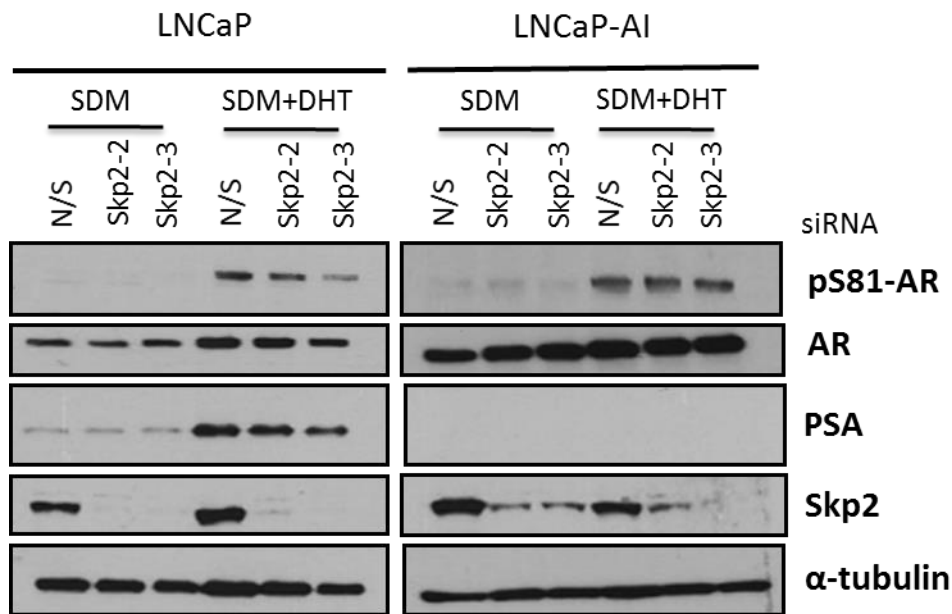


Figure 5-12: AR phosphorylation at serine 81 is not influenced upon Skp2 suppression. LNCaP and LNCaP-AI cells underwent reverse transfection using 25 nM siRNA whilst simultaneously starved in steroid-depleted media (SDM) for 72 hours. They were then treated with 10 nM DHT for 8 hours prior to collection for Western blotting to analyse AR phosphorylation at serine 81 (pS81-AR), AR, PSA, Skp2 and α -tubulin.

5.3.13 Skp2 over-expression does not affect AR transcriptional activity

It was determined that Skp2 did not influence AR level, localisation and phosphorylation on serine 81, all of which are important in regulating AR transcriptional activity. However, as Skp2 depletion led to reduced ATAD2 basal transcription, it was questioned whether Skp2 may act as a transcriptional cofactor for AR. For this purpose, transient transfection of a luciferase gene reporter was applied in an assay to determine AR activity. HEK293T cells were initially transfected with AR and an AR-responsive luciferase reporter, which consists of three androgen responsive elements (ARE) upstream of a luciferase reporter. Upon binding of the ectopically expressed AR to the AREs, it can promote active transcription of the luciferase gene which is therefore reflective of the activity of the AR. This transcriptional activity can in turn be altered depending on the presence of activating ligand and AR co-regulatory proteins. Briefly, cells were seeded in steroid-depleted media before being transfected for 48 hours, with 10 nM DHT added in the final 24 hours of incubation period.

As expected, luciferase activity was up-regulated by 2.1 fold upon addition of 10 nM DHT, indicating increased AR activity (Figure 5.13). Although this fold increase was substantially lower than expected. However, co-expression of Skp2 had no additional effect on the activity of AR and so the experiment was terminated with one repeat.

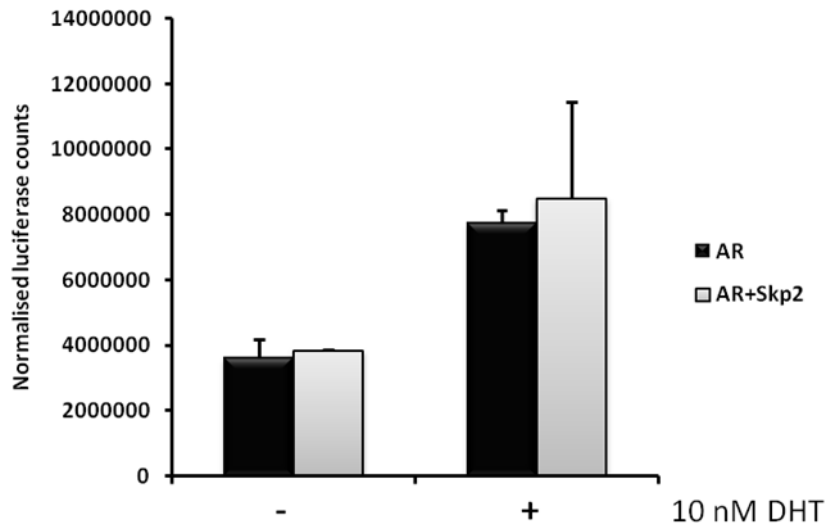


Figure 5-13: Over-expression of Skp2 does not enhance AR transcriptional activity. HEK293T cells were transfected with AR, ARE3-luc, pCMV- β -gal for normalisation either in the absence or presence of Skp2 construct. Following 24 hours incubation in steroid-depleted media (SDM), cells were treated with 10 nM DHT and were incubated for a further 24 hour period prior to performing the luciferase assay. Each reading is the mean of triplicate wells. Data was normalised using β -galactosidase activity.

5.4 Discussion

The aberrant elevation of Skp2 is recognised to contribute to the initiation and progression of different cancers, including PC. This is due to the diverse range of substrates that are regulated by Skp2; hence, placing Skp2 as a critical player in various important cellular processes (Guo *et al.*, 1997; Von Der Lehr *et al.*, 2003; Moro *et al.*, 2006; Chan *et al.*, 2010). The altered regulation of AR signalling by Skp2 has been suggested to be a possible underlying mechanism in prostate tumourigenesis; however, this has remained unclear due to the controversial literature to date. In Chapter 4, it was demonstrated that Skp2 regulates the mono-ubiquitination of KMT5A, where KMT5A has recently been identified as a novel co-activator of AR in CRPC cell line models. Although this suggested that Skp2 could potentially influence the AR through mono-ubiquitination of KMT5A, Skp2 could also exert its effect independently of KMT5A. Therefore, the aim of this chapter was to conduct an independent set of research experiments to determine the importance of Skp2 in AR signalling, addressing both the lack of previous detailed investigations and exploring different avenues of AR regulation by Skp2. Moreover, it aimed to determine whether Skp2 is under the androgenic-AR regulation in androgen dependent and independent cell lines.

The androgenic modulation of Skp2 could be an important underlying mechanism in Skp2 regulation considering the fact that it is frequently concomitantly overexpressed with the AR in CRPC. Moreover, it has been found that the ADT-mediated downregulation of AR leads to senescence as a result of Skp2 suppression (Pernicová *et al.*, 2011). Therefore, in this chapter, the effect of androgenic stimulation on protein and transcript level of Skp2 was determined, which has been an area of controversy to date. As already alluded to, the discrepancy in the literature with regards to androgen-AR regulation of Skp2 and vice versa, could be due to the use of different PC cell lines exhibiting different sensitivity to androgens, the limited number of AR-target genes studied, insufficient range of time points and either missing protein or mRNA data, all of which have been addressed to some extent in this part of the work.

It was found that Skp2 is not subject to direct regulation by the AR as androgenic stimulation only led to changes in Skp2 protein expression after a prolonged 48 hours exposure to DHT, compared to PSA which responded within 8 hours post DHT treatment (Figure 5.1). This was later confirmed at the transcriptional level which further validated Skp2 as not being a direct target of the AR as DHT had no effect on Skp2 mRNA level in either LNCaP or LNCaP-AI cell lines, whilst PSA was clearly induced (Figure 5.3). This finding is in line with the fact that the Skp2 promoter does not contain any identifiable AREs. The Skp2 protein however responded differently between the androgen-dependent and independent cell lines, LNCaP and

LNCaP-AI. Whereas Skp2 was up-regulated with DHT treatment in LNCaP cells, it was down-regulated following DHT treatment in LNCaP-AI cells (Figure 5.1 and Figure 5.2). This may be of relevance in the treatment of CRPC where Skp2 is suggested to be a promising therapeutic target, should ADT be utilised to also suppress Skp2 expression. Consistent with the data presented herein, Chuu *et al* (Kokontis *et al.*, 2014) reported Skp2 protein suppression by synthetic androgen, R1881, at physiological concentration of 10 nM in the LNCaP 104-R2 cell line representative of late stage CRPC. Conversely, in the androgen-dependent LNCaP 104 cells, sub-physiological concentration of R1881 induced Skp2 protein expression. However, this was observed following 96 hours of R1881 treatment which was the only time point used in this study. Nonetheless, it does demonstrate the slow kinetics of Skp2 response to androgen in line with the data presented here, further supporting the argument that Skp2 is not directly regulated by the AR. Furthermore, Wang *et al* (Wang *et al.*, 2008a) reported Skp2 is up-regulated with androgen at both mRNA and protein levels in LNCaP cells. Although, Skp2 protein response to androgen was observed at 24 hours, occurring with faster kinetics compared to its mRNA expression where changes were observed after 72 hours, indicating a secondary effect on Skp2 transcription rather than being a direct effect of the androgen-AR signalling. Consistently, the androgen-AR was shown to be responsible for the increased Skp2 protein stability mediated through the D-box degron in Skp2 N-terminus. These observations however contrast that of Jiang *et al* (Jiang *et al.*, 2012) who showed Skp2 expression is down-regulated by R1881 treatment at physiological and higher concentrations in LNCaP cells. Although the same group reported the changes in Skp2 expression is at the level of transcription, this was only evident following 12 hours of androgenic stimulation.

Deregulated Skp2 function promotes cell transformation and Skp2 has been reported to mediate androgen-dependent proliferation of PC cells. Supporting this statement, experiments in LNCaP and LNCaP-AI cells showed that Skp2 depletion caused a dramatic inhibition of cell growth, reducing cell proliferation by almost 50% (Figure 5.5) which was associated with an accumulation of cells in G1 phase of the cell cycle (Figure 5.6). Given the impact of Skp2 knockdown on cell growth, its effect on AR transcriptional activity was then investigated. As Skp2 was found to be expressed in an opposing manner following androgen treatment between LNCaP and LNCaP-AI cells, it suggested Skp2 expression changes may differentially alter AR activity in these cells. Whilst, PSA protein expression which could only be detected in the LNCaP cells was not affected, Skp2 depletion led to reduced protein levels of ATAD2 in both cell lines tested (Figure 5.7). Although there was no differences in the cell lines, data indicated that Skp2 differentially regulates AR-target genes and to further confirm it, mRNA level of

PSA and ATAD2, as well as additional AR target genes, KLK2 and TMPRSS2 were examined. In contrast with the protein expression data, Skp2 suppression induced PSA transcription. Interestingly, Skp2 knockdown led to reduced transcription of KLK2 and TMPRSS2 at later time points of 16 and 24 hours with DHT treatment, it caused a significant reduction in ATAD2 transcription under steroid-depleted conditions. Although, there was no overall change in the level of ATAD2 mRNA induction following DHT stimulation (Figure 5.8). This implied that Skp2 regulation may only be applicable to a subset of AR-regulated genes, where Skp2 functions in a promoter dependent manner. Unfortunately most of the reports on the role of Skp2 in regulating AR signalling have drawn conclusions based on one AR-target gene, PSA, without including different time points, with the data obtained being inconsistent between studies. For example, whilst Wang *et al* (Wang *et al.*, 2008a) showed Skp2 knockdown is unable to affect PSA expression, Li *et al* (Li *et al.*, 2014a) showed Skp2 depletion enhances AR-mediated expression of PSA. Lacking time course experiments to monitor AR transcriptional activity of course is a major flaw as AR transcription is known to occur in a cyclical manner (Felten *et al.*, 2013) and the published data therefore does not undermine the data presented here.

ATAD2, also known as ANCCA, is a member of the AAA+ ATPase family of bromodomain-containing proteins and is up-regulated in many solid human tumours, including androgen dependent and independent prostate tumours. It has been identified as a co-activator of several transcription factors such as the AR, ER and Myc. Down-regulation of ATAD2 by Skp2 depletion is reported herein for the first time. ATAD2 itself is regulated directly by AR and is an androgen-responsive gene (Zou *et al.*, 2009; Altintas *et al.*, 2012). It therefore became of great interest to try to elucidate the underlying mechanism that modulated AR transcriptional activity. It was hypothesised that Skp2 may influence AR protein levels as it has been reported to act as an E3 ligase for AR (Li *et al.*, 2014a). Although this would be unlikely as such a mechanism leads to attenuated transcription of all AR-target genes. Yet again, this a controversial area where Skp2 has been demonstrated to ubiquitinate the AR and mark it for proteasomal destruction (Li *et al.*, 2014a). Furthermore, Skp2 inhibition using both siRNA and shRNA led to restoration of AR protein expression in PC3 and DU145 cell lines which are widely demonstrated to lack any AR protein (Li *et al.*, 2014a). In contrast, Skp2 has also been shown to not have an effect on the AR (Wang *et al.*, 2008a). As such, three different siRNA oligonucleotides against Skp2 and additionally a pool of combined siRNAs was utilised in different PC lines to determine AR levels following Skp2 depletion. Overall, no appreciable change in AR protein level was found (Figure 5.9). Despite, highly efficient knockdown of

Skp2 achieved here compared to the poorer Skp2 depletion achieved by Li *et al* (2014), AR upregulation was not observed when evaluated in the PC3 and CWR22RV1 cell lines under similar experimental conditions. Consistent with the general studies on PC3 cell line, no detectable AR was evident under any condition applied.

Skp2 can also act independently of its SCF ligase complex, for example in regulating p53 where Skp2 sequesters p300 to prevent p300-mediated acetylation of p53 and consequently inhibits p53 transcriptional activity without interacting with p53 or affecting its expression (Kitagawa *et al.*, 2008). It was therefore hypothesised that cytoplasmic Skp2 may sequester AR and abrogate AR shuttling into the nucleus. Interestingly, although Skp2 was found to be in a complex with AR (Figure 5.10), it did not affect AR localisation upon DHT treatment (Figure 5.11). This however was not surprising as such a mechanism would lead to a global/general reduction in AR-regulated gene expression rather than of a specific gene. Although, it would have also been preferable to test that a well-established AR interacting partner could be detected by this immunoprecipitation experiment, as a positive control. Unexpectedly, Skp2 was found to be cytoplasmic in these experiments which may be a consequence of the starvation of cells in steroid-depleted media causing a cell cycle arrest, as Skp2 is predominantly nuclear in dividing cells. However, cytoplasmic Skp2 has been observed in many clinical tumour samples (Radke *et al.*, 2005) and Akt-mediated phosphorylation of Skp2 has been suggested as an underlying mechanism to protect Skp2 from degradation by Cdh-1 (Gao *et al.*, 2009). Cytoplasmic Skp2 has been found to regulate cell migration independently of its ability to regulate p27 ubiquitination and degradation. Consistently, Skp2 in the cytoplasm was shown not to interact with CUL1 and Skp1, or induce p27 ubiquitination. Importantly though, Skp2 was shown to be present in the chromatin containing fraction (Figure 5.11B), consistent with its recently published role in modulating the histone modification H3K4me3 through JARID1B regulation (Lu *et al.*, 2015).

Having demonstrated Skp2 knockdown promoted up-regulation of p27 levels, in keeping with its inverse correlation in PC, it was then speculated that increased p27 inhibits cyclin/CDK complex activity responsible for phosphorylation of AR on serine 81 and consequently would attenuate AR binding to chromatin. However, there was no change in DHT-induced AR phosphorylation with Skp2 depletion after 6 hours of treatment (Figure 5.12). Skp2 has previously been reported to act as a co-factor to activate c-Myc target genes (Kim *et al.*, 2003). Therefore, the ability of Skp2 to act as a co-regulator for AR was investigated in an effort to elucidate its mechanism of action in down-regulating ATAD2 basal transcription. Then again, it did not alter the activity of AR (Figure 5.13). It would have been prudent to perform this

experiment using AR binding sequence obtained from the ATAD2 distal enhancer region as Skp2 caused a significant reduction for ATAD2 only.

The fact that none of the AR related mechanisms tested were affected by Skp2 depletion suggests ATAD2 may be subject to direct regulation by Skp2, independently of the AR. Alternatively, Skp2 could be modulating AR recruitment specifically at the ATAD2 promoter. DHT-induced AR recruitment at the TMPRSS2 and PSA was examined but it did not show any change following Skp2 depletion (data not shown), which was expected as the transcription of these genes were not significantly affected upon Skp2 suppression. Again, these experiments should also have been performed by examining recruitment at the ATAD2 promoter region.

ATAD2 is currently an area of high interest for therapeutic targeting. We have reported here for the first time that ATAD2 could be under the regulation of Skp2 which could in turn provide a new pathway for therapeutic intervention. Importantly, considering that fact that Skp2 is suggested as a promising novel target in CRPC, with small molecule inhibitors being developed to inhibit the activity of Skp2, it is critical to have an appropriate biomarker to measure the outcome of Skp2-targetted therapy. PSA screening is often used to monitor the development and progression of PC. One important finding from this work is that PSA is not a suitable biomarker for therapies against Skp2. Interestingly, however, our data implies ATAD2 may be a potential biomarker for such a therapy. Taken together, our data suggests Skp2 is not a direct target of the AR. Furthermore, the effect of Skp2 silencing on proliferation is not due to its role as a regulator of AR signalling.

6 Discussion

Currently the AR is regarded as a key therapeutic target in the treatment of advanced PC, where therapies aim to reduce the AR activity. Although initially successful, AR-targeted therapies fail through a plethora of mechanisms including: AR amplification, AR mutations, expression of AR splice variants, increased intratumoural steroidogenesis and altered expression of AR co-regulators. Ultimately, these mechanisms lead to restoration of AR activity, rendering the AR-targeted therapies ineffective. This results in the emergence of the more aggressive CRPC (Chan and Dehm, 2014). Therefore, exploiting the regulatory mechanisms that modulate the AR by targeting AR regulatory proteins to indirectly inhibit AR function may provide a possible solution to existing treatment limitations.

The AR is regulated by numerous co-regulatory proteins and it is becoming evident that one large class are the lysine methyltransferase enzymes, whereby deregulation of these proteins has been shown to cause aberrant AR activity in PC. In addition to mediating histone modifications to regulate chromatin-related functions, these enzymes, for example SET9, have also been shown to directly methylate non-histone proteins including the AR, causing enhanced AR transcriptional activity (Gaughan *et al.*, 2011; Ko *et al.*, 2011).

To identify methyltransferases and opposing demethylases that are important in AR regulation, an siRNA screen was previously undertaken. Results from the screen identified SET8/KMT5A as a novel regulatory AR protein that functions to repress AR activity in the LNCaP cells. Interestingly, in the castrate and drug-resistant PC cell line, LNCaP-AI, KMT5A was found to act in an opposite manner where it functioned as an AR co-activator (Coffey *et al.*, unpublished data). The activity of KMT5A is tightly regulated primarily through PTMs, including ubiquitination, which ensures precise KMT5A protein levels in a cell cycle-dependent manner. The aim of this project was to investigate and validate a novel PTM of KMT5A which could potentially be exploited to indirectly target the AR.

Results from Chapter 3 identified mono-ubiquitination as a novel PTM of KMT5A. Mono-ubiquitinated KMT5A was found as the predominant form of modified KMT5A in several PC cell lines. Subsequently, KMT5A C-terminus which comprises the SET-domain responsible for KMT5A enzymatic activity was shown to undergo mono-ubiquitination. Despite strenuous efforts to identify the site of mono-ubiquitination, a specific lysine residue could not be identified. Instead the site responsible for mono-ubiquitination was narrowed down to a specific region (amino acid 310-330) within the C-terminus. Moreover, similarly, mono-ubiquitinated KMT5A has also been consistently observed in breast cancer cell lines, although the nature of

this form of KMT5A was not known at all and only became evident following the work conducted here (personal communication, Dr Fabio Pittella Silva, Memorial Sloane Kettering Cancer Centre, USA).

The impact of mono-ubiquitination on KMT5A could be important as KMT5A is being considered as a therapeutic target. Mono-ubiquitination is associated with non-proteolytic functions and has been extensively shown to regulate the function of many proteins. For example, mono-ubiquitination of SETDB1 in its SET-insertion domain is essential for its enzymatic activity where the conjugated mono-ubiquitin is actively protected from de-ubiquitination (Sun and Fang, 2016). Moreover, mono-ubiquitin conjugation may result in a conformational change in the protein structure. Similarly, should mono-ubiquitination alter the enzymatic activity or structure of KMT5A, this may subsequently influence the efficacy of the small molecule inhibitors being developed against the enzymatic activity of unmodified KMT5A.

KMT5A is over-expressed in many types of cancer including bladder cancer, non-small cell lung carcinoma (NSCLC), small cell lung carcinoma (SCLC), chronic myelogenous leukaemia, hepatocellular carcinoma, and pancreatic cancer (Takawa *et al.*, 2012). However, the underlying mechanisms leading to KMT5A over-expression has not been fully investigated and has remained largely unknown. So far, only the presence of multiple single-nucleotide polymorphisms in the 3'UTR of KMT5A mRNA has been shown to cause KMT5A up-regulation. Furthermore, KMT5A over-expression was also shown in PC compared to benign samples (Coffey *et al.*, unpublished data). Interestingly data from this work implied mono-ubiquitinated KMT5A is a stable form of this protein that may be causing its prominent expression. Increased KMT5A stability could potentially be an underlying mechanism for its up-regulated levels. It is therefore essential to further interrogate the stability of unmodified and mono-ubiquitinated KMT5A in a number of PC cell lines. Moreover, the mono-ubiquitin deficient and competent KMT5A constructs generated could also provide an additional tool to determine the role of mono-ubiquitination in KMT5A protein stability.

The high expression of KMT5A is positively associated with metastasis, poor overall and disease free survival in breast cancer patients (Yang *et al.*, 2012; Liu *et al.*, 2016). Consistently, hepatocellular carcinoma and SCLC patients with lower KMT5A expression had longer survival time (Ding *et al.*, 2012; Guo *et al.*, 2012). In addition, high KMT5A expression is associated with an early age of breast cancer onset, whilst its low expression contributes to a

lower risk of epithelial ovarian cancer (Song *et al.*, 2009; Wang *et al.*, 2012). However, the clinical significance of mono-ubiquitinated KMT5A is not known.

Moreover, despite the up-regulated KMT5A expression in PC tissue, the molecular form of the KMT5A protein is not known. It is therefore of great value to distinguish between the unmodified and mono-ubiquitinated forms of KMT5A using antibodies specific to mono-ubiquitinated KMT5A and perform staining on tissue microarrays (TMA) containing samples from patients with BPH and PC. Currently there is an acute lack of prognostic and therapeutic biomarkers in PC. Although, the currently used PSA monitoring is useful as part of the diagnostic repertoire and as an indicator of PC recurrence, it is not a cancer specific marker but pertinent to monitoring tumour burden. This method has led to diagnosis and overtreatment of PC (Shtivelman *et al.*, 2014). It would therefore be useful to ascertain whether mono-ubiquitinated KMT5A could be used as a potential biomarker by assessing its expression in association with Gleason grade, response to therapy, time to relapse or overall survival. Unfortunately, the current lack of an antibody to detect the mono-ubiquitinated form of KMT5A hinders such investigations.

Work in Chapter 4 focussed on characterising the cell cycle control of KMT5A mono-ubiquitination and conversely, the role of mono-ubiquitinated KMT5A on the cell cycle and cell growth. It was revealed that similar to its other PTMs, mono-ubiquitination of KMT5A is subject to dynamic changes during the cell cycle, being at its highest level in S phase despite minimal levels of unmodified KMT5A. Conversely, mono-ubiquitinated KMT5A was at its lowest level in G2/M phase, whilst, unmodified KMT5A was at its peak. Furthermore, the data suggested a positive association between cell proliferation and levels of KMT5A mono-ubiquitination. Interestingly, the mono-ubiquitin conjugated form of KMT5A was found to be exclusively cytoplasmic. The subcellular localisation of proteins has been linked with tumour aggressiveness, for example the DNA repair APE1 enzyme has been observed to be present at higher concentrations in the cytoplasm of colorectal carcinoma cells compared to normal cells (Kakolyriset *et al.*, 1997). It would therefore be useful to also determine mono-ubiquitinated KMT5A tissue localisation.

The physiological role of mono-ubiquitinated KMT5A is still an open question and is something that will require substantial research in the future. Firstly, it is critical to identify the effect of mono-ubiquitination on KMT5A enzymatic activity. As such, mono-ubiquitination has been shown to cause activation of the substrate protein in many instances (van der Horst *et al.*, 2006; Sun and Fang, 2016). Interestingly, the cytoplasmic localisation of mono-ubiquitin

conjugated KMT5A suggests this form of KMT5A is involved in the regulation of non-histone proteins. It became questionable if pathways leading to KMT5A mono-ubiquitination could potentially be targeted therapeutically in PC, should mono-ubiquitinated KMT5A have a clinical significance, as mono-ubiquitinated KMT5A was exclusively cytoplasmic. Consistently, KMT5A plays a role in various cellular processes and in addition to H4K20 methylation, it methylates non-histone proteins such as p53 and Numb, resulting in a decrease in apoptosis (Shi *et al.*, 2007; Dhami *et al.*, 2013). Furthermore, it positively regulates the activity of Twist in promoting EMT in breast cancer (Yang *et al.*, 2012). In support of the speculation here, recently presented work at the American Association for Cancer Research (AACR) 2016 had identified novel substrates for KMT5A (Silva *et al.*, 2016). Intriguingly, almost half of the substrates were found to be cytoplasmic proteins. Although puzzled by their finding, based on the assumption that KMT5A is a nuclear protein, it is now evident that this could be due to the presence of the mono-ubiquitinated form of KMT5A. Secondly, it is of utmost importance to identify the substrates of mono-ubiquitinated KMT5A. These could be determined by mono-ubiquitinated KMT5A immunoprecipitation and mass spectrometry studies. Subsequently, identified proteins which have a role in PC development could be investigated. In contrast to its unmodified form, mono-ubiquitinated KMT5A was no longer considered to directly regulate the AR in the nucleus, however it may alternatively regulate PC independently of AR signalling. Identification of mono-ubiquitinated KMT5A substrates could therefore enable the discovery of additional as yet unidentified pathways in which it participates. Nonetheless, mono-ubiquitinated KMT5A could affect the cytoplasmic AR. The role of KMT5A mono-ubiquitination however suggested that it signals for KMT5A translocation out of the nucleus as an additional mechanism to lower the levels of nuclear KMT5A during S phase to enable proper cell cycle progression.

Despite the prominent existence of mono-ubiquitinated KMT5A, nothing is known about the key regulatory enzymes that regulate this modification and is another area requiring research. Additionally, it has not yet been examined if the mono-ubiquitination of KMT5A is dependent on a specific phosphorylation state of KMT5A. In line with this notion, cell cycle-specific phosphorylation of KMT5A has been reported which regulates KMT5A binding to chromatin and its stability by the APC^{Ch1} complex (Wu *et al.*, 2010). Work in Chapter 4 also demonstrated that Skp2 promotes the mono-ubiquitination of KMT5A which was not associated with protein turnover. Skp2 up-regulation during G1 phase and even further elevation in S phase was concomitant with the increased KMT5A mono-ubiquitination. Given the frequent over-expression of Skp2 in PC, coupled with up-regulated KMT5A levels, it is possible that a Skp2-

KMT5A mono-ubiquitination axis could be of clinical significance in PC. However, the enzyme responsible for the basal KMT5A mono-ubiquitination remains unknown.

Skp2 is known to play a dynamic role in the regulation of multiple cellular pathways. As Skp2 was shown to promote KMT5A mono-ubiquitination, its role in AR signalling was independently investigated. In Chapter 5, Skp2 was shown to not be a direct target of the androgen-AR signalling cascade. Furthermore, the regulation of the AR signalling itself by Skp2 seemed more complex than what has been reported. Overall, despite the substantial reduction in PC cell growth following Skp2 depletion, Skp2 did not regulate the AR and the expression of its target genes, except ATAD2. However, data implicated Skp2 to be a direct regulator of ATAD2. Interestingly, the data revealed that PSA is an unsuitable marker for Skp2-targetted therapies, whereas ATAD2 could potentially be a novel marker for Skp2 therapeutics. However, a great deal more research needs to be conducted to interrogate the underlying mechanism.

In conclusion, this study identified mono-ubiquitination as a novel PTM of KMT5A which functions as an additional mechanism to regulate precise KMT5A levels during S phase. The identification of this PTM aids our understanding of KMT5A regulation by mono-ubiquitin conjugation. Although, this form of KMT5A is unlikely to directly regulate AR transcriptional activity in the nucleus, it could influence other signalling cascades to indirectly affect PC. Moreover, the up-regulation of KMT5A mono-ubiquitination by Skp2 could promote a rapid localisation of KMT5A into the cytoplasm to ensure timely progression of the cell cycle. Additionally, although Skp2 depletion reduces cell growth, it is not through the direct regulation of AR signalling.

7 References

- Abbas, T., Shibata, E., Park, J., Jha, S., Karnani, N. and Dutta, A. (2010) 'CRL4Cdt2 regulates cell proliferation and histone gene expression by targeting PR-Set7/Set8 for degradation', *Molecular Cell*, 40(1), pp. 9-21.
- Abbas, T., Sivaprasad, U., Terai, K., Amador, V., Pagano, M. and Dutta, A. (2008) 'PCNA-dependent regulation of p21 ubiquitylation and degradation via the CRL4Cdt2 ubiquitin ligase complex', *Genes and Development*, 22(18), pp. 2496-2506.
- Abeshouse, A., Ahn, J., Akbani, R., Ally, A., Amin, S., Andry, Christopher D., Annala, M., Aprikian, A., Armenia, J., Arora, A., Auman, J.T., Balasundaram, M., Balu, S., Barbieri, Christopher E., Bauer, T., Benz, Christopher C., Bergeron, A., Beroukhim, R., Berrios, M., Bivol, A., Bodenheimer, T., Boice, L., Bootwalla, Moiz S., Borges dos Reis, R., Boutros, Paul C., Bowen, J., Bowlby, R., Boyd, J., Bradley, Robert K., Breggia, A., Brimo, F., Bristow, Christopher A., Brooks, D., Broom, Bradley M., Bryce, Alan H., Bubley, G., Burks, E., Butterfield, Yaron S.N., Button, M., Canes, D., Carlotti, Carlos G., Carlsen, R., Carmel, M., Carroll, Peter R., Carter, Scott L., Cartun, R., Carver, Brett S., Chan, June M., Chang, Matthew T., Chen, Y., Cherniack, Andrew D., Chevalier, S., Chin, L., Cho, J., Chu, A., Chuah, E., Chudamani, S., Cibulskis, K., Ciriello, G., Clarke, A., Cooperberg, Matthew R., Corcoran, Niall M., Costello, Anthony J., Cowan, J., Crain, D., Curley, E., David, K., Demchok, John A., Demichelis, F., Dhalla, N., Dhir, R., Doueik, A., Drake, B., Dvinge, H., Dyakova, N., Felau, I., Ferguson, Martin L., Frazer, S., Freedland, S., Fu, Y., Gabriel, Stacey B., Gao, J., Gardner, J., Gastier-Foster, Julie M., Gehlenborg, N., Gerken, M., Gerstein, Mark B., Getz, G., Godwin, Andrew K., Gopalan, A., Graefen, M., Graim, K., Gribbin, T., Guin, R., Gupta, M., Hadjipanayis, A., Haider, S., Hamel, L., Hayes, D.N., Heiman, David I., et al. (2015) 'The Molecular Taxonomy of Primary Prostate Cancer', *Cell*, 163(4), pp. 1011-1025.
- Al-Hakim, A.K., Zagorska, A., Chapman, L., Deak, M., Peggie, M. and Alessi, D.R. (2008) 'Control of AMPK-related kinases by USP9X and atypical Lys 29/Lys33-linked polyubiquitin chains', *Biochemical Journal*, 411(2), pp. 249-260.
- Altintas, D.M., Shukla, M.S., Goutte-Gattat, D., Angelov, D., Rouault, J.P., Dimitrov, S. and Samarut, J. (2012) 'Direct cooperation between androgen receptor and E2F1 reveals a common regulation mechanism for androgen-responsive genes in prostate cells', *Molecular Endocrinology*, 26(9), pp. 1531-1541.
- Arias, E.E. and Walter, J.C. (2005) 'Replication-dependent destruction of Cdt1 limits DNA replication to a single round per cell cycle in *Xenopus* egg extracts', *Genes and Development*, 19(1), pp. 114-126.
- Arora, V.K., Schenkein, E., Murali, R., Subudhi, S.K., Wongvipat, J., Balbas, M.D., Shah, N., Cai, L., Efstathiou, E., Logothetis, C., Zheng, D. and Sawyers, C.L. (2013) 'Glucocorticoid receptor confers resistance to antiandrogens by bypassing androgen receptor blockade', *Cell*, 155(6), pp. 1309-1322.
- Balaji, K.C., Rabbani, F., Tsai, H., Bastar, A. and Fair, W.R. (1999) 'Effect of neoadjuvant hormonal therapy on prostatic intraepithelial neoplasia and its prognostic significance', *Journal of Urology*, 162(3 D), pp. 753-757.
- Balk, S.P., Ko, Y.J. and Bubley, G.J. (2003) 'Biology of prostate-specific antigen', *Journal of Clinical Oncology*, 21(2), pp. 383-391.
- Barbieri, C.E., Baca, S.C., Lawrence, M.S., Demichelis, F., Blattner, M., Theurillat, J.P., White, T.A., Stojanov, P., Van Allen, E., Stransky, N., Nickerson, E., Chae, S.S., Boysen, G., Auclair,

- D., Onofrio, R.C., Park, K., Kitabayashi, N., MacDonald, T.Y., Sheikh, K., Vuong, T., Guiducci, C., Cibulskis, K., Sivachenko, A., Carter, S.L., Saksena, G., Voet, D., Hussain, W.M., Ramos, A.H., Winckler, W., Redman, M.C., Ardlie, K., Tewari, A.K., Mosquera, J.M., Rupp, N., Wild, P.J., Moch, H., Morrissey, C., Nelson, P.S., Kantoff, P.W., Gabriel, S.B., Golub, T.R., Meyerson, M., Lander, E.S., Getz, G., Rubin, M.A. and Garraway, L.A. (2012) 'Exome sequencing identifies recurrent SPOP, FOXA1 and MED12 mutations in prostate cancer', *Nature Genetics*, 44(6), pp. 685-689.
- Barrie, S.E., Potter, G.A., Goddard, P.M., Haynes, B.P., Dowsett, M. and Jarman, M. (1994) 'Pharmacology of novel steroidal inhibitors of cytochrome P45017 α (17 α -hydroxylase/C17-20 lyase)', *Journal of Steroid Biochemistry and Molecular Biology*, 50(5-6), pp. 267-273.
- Barski, A., Cuddapah, S., Cui, K., Roh, T.Y., Schones, D.E., Wang, Z., Wei, G., Chepelev, I. and Zhao, K. (2007) 'High-Resolution Profiling of Histone Methylations in the Human Genome', *Cell*, 129(4), pp. 823-837.
- Bartel, D.P. (2004) 'MicroRNAs: Genomics, Biogenesis, Mechanism, and Function', *Cell*, 116(2), pp. 281-297.
- Bechis, S.K., Otsetov, A.G., Ge, R. and Olumi, A.F. (2014) 'Personalized medicine for the management of benign prostatic hyperplasia', *Journal of Urology*, 192(1), pp. 16-23.
- Ben-Izhak, O., Lahav-Baratz, S., Meretyk, S., Ben-Eliezer, S., Sabo, E., Dirnfeld, M., Cohen, S. and Ciechanover, A. (2003) 'Inverse relationship between Skp2 ubiquitin ligase and the cyclin dependent kinase inhibitor p27Kip1 in prostate cancer', *Journal of Urology*, 170(1), pp. 241-245.
- Bennett, N.C., Gardiner, R.A., Hooper, J.D., Johnson, D.W. and Gobe, G.C. (2010) 'Molecular cell biology of androgen receptor signalling', *International Journal of Biochemistry and Cell Biology*, 42(6), pp. 813-827.
- Berndsen, C.E. and Wolberger, C. (2014) 'New insights into ubiquitin E3 ligase mechanism', *Nature Structural and Molecular Biology*, 21(4), pp. 301-307.
- Bettendorf, O., Schmidt, H., Staebler, A., Grobholz, R., Heinecke, A., Boecker, W., Hertle, L. and Semjonow, A. (2008) 'Chromosomal imbalances, loss of heterozygosity, and immunohistochemical expression of TP53, RB1, and PTEN in intraductal cancer, intraepithelial neoplasia, and invasive adenocarcinoma of the prostate', *Genes Chromosomes and Cancer*, 47(7), pp. 565-572.
- Bokser, L., Zarandi, M. and Schally, A.V. (1990) 'Evaluation of in vitro biological activity of new agmatine analogs of growth hormone-releasing hormone (GH-RH)', *Life Sciences*, 46(14), pp. 999-1005.
- Bostwick, D.G. (2000) 'Prostatic intraepithelial neoplasia', *Current urology reports*, 1(1), pp. 65-70.
- Botuyan, M.V., Lee, J., Ward, I.M., Kim, J.E., Thompson, J.R., Chen, J. and Mer, G. (2006) 'Structural Basis for the Methylation State-Specific Recognition of Histone H4-K20 by 53BP1 and Crb2 in DNA Repair', *Cell*, 127(7), pp. 1361-1373.
- Boutet, S.C., Disatnik, M.H., Chan, L.S., Iori, K. and Rando, T.A. (2007) 'Regulation of Pax3 by Proteasomal Degradation of Monoubiquitinated Protein in Skeletal Muscle Progenitors', *Cell*, 130(2), pp. 349-362.

- Brady, M.E., Ozanne, D.M., Gaughan, L., Waite, I., Cook, S., Neal, D.E. and Robson, C.N. (1999) 'Tip60 is a nuclear hormone receptor coactivator', *Journal of Biological Chemistry*, 274(25), pp. 17599-17604.
- Brawley, O.W., Knopf, K. and Merrill, R. (1998a) 'The epidemiology of prostate cancer Part I: Descriptive epidemiology', *Seminars in Urologic Oncology*, 16(4), pp. 187-192.
- Brawley, O.W., Knopf, K. and Thompson, I. (1998b) 'The epidemiology of prostate cancer Part II: The risk factors', *Seminars in Urologic Oncology*, 16(4), pp. 193-201.
- Bremm, A., Moniz, S., Mader, J., Rocha, S. and Komander, D. (2014) 'Cezanne (OTUD7B) regulates HIF-1 α homeostasis in a proteasome-independent manner', *EMBO Reports*, 15(12), pp. 1268-1277.
- Brinkmann, A.O., Jenster, G., Ris-Stalpers, C., Van Der Korput, H., Brüggewirth, H., Boehmer, A. and Trapman, J. (1996) 'Molecular basis of androgen insensitivity', *Steroids*, 61(4), pp. 172-175.
- Brustel, J., Tardat, M., Kirsh, O., Grimaud, C. and Julien, E. (2011) 'Coupling mitosis to DNA replication: The emerging role of the histone H4-lysine 20 methyltransferase PR-Set7', *Trends in Cell Biology*, 21(8), pp. 452-460.
- Brzovic, P.S., Rajagopal, P., Hoyt, D.W., King, M.C. and Klevit, R.E. (2001) 'Structure of a BRCA1-BARD1 heterodimeric RING-RING complex', *Nature Structural Biology*, 8(10), pp. 833-837.
- Bubley, G.J. (2001) 'Is the flare phenomenon clinically significant?', *Urology*, 58(2 SUPPL. 1), pp. 5-9.
- Buchanan, G., Yang, M., Cheong, A., Harris, J.M., Irvine, R.A., Lambert, P.F., Moore, N.L., Raynor, M., Neufing, P.J., Coetzee, G.A. and Tilley, W.D. (2004) 'Structural and functional consequences of glutamine tract variation in the androgen receptor', *Human Molecular Genetics*, 13(16), pp. 1677-1692.
- Busso, C.S., Iwakuma, T. and Izumi, T. (2009) 'Ubiquitination of mammalian AP endonuclease (APE1) regulated by the p53-MDM2 signaling pathway', *Oncogene*, 28(13), pp. 1616-1625.
- Calvo, A., Xiao, N., Kang, J., Best, C.J.M., Leiva, I., Emmert-Buck, M.R., Jorcyk, C. and Green, J.E. (2002) 'Alterations in gene expression profiles during prostate cancer progression: Functional correlations to tumorigenicity and down-regulation of selenoprotein-P in mouse and human tumors', *Cancer Research*, 62(18), pp. 5325-5335.
- Campbell, S.J., Edwards, R.A., Leung, C.C.Y., Neculai, D., Hodge, C.D., Dhe-Paganon, S. and Glover, J.N.M. (2012) 'Molecular insights into the function of RING finger (RNF)-containing proteins hRNF8 and hRNF168 in Ubc13/Mms2-dependent ubiquitylation', *Journal of Biological Chemistry*, 287(28), pp. 23900-23910.
- Carrano, A.C., Eytan, E., Hershko, A. and Pagano, M. (1999) 'SKP2 is required for ubiquitin-mediated degradation of the CDK inhibitor p27', *Nature Cell Biology*, 1(4), pp. 193-199.
- Catzavelos, C., Bhattacharya, N., Ung, Y.C., Wilson, J.A., Roncari, L., Sandhu, C., Shaw, P., Yeger, H., Morava-Protzner, I., Kapusta, L., Franssen, E., Pritchard, K.I. and Slingerland, J.M. (1997) 'Decreased levels of the cell-cycle inhibitor p27(Kip1) protein: Prognostic implications in primary breast cancer', *Nature Medicine*, 3(2), pp. 227-230.

Centore, R.C., Havens, C.G., Manning, A.L., Li, J.M., Flynn, R.L., Tse, A., Jin, J., Dyson, N.J., Walter, J.C. and Zou, L. (2010) 'CRL4Cdt2-mediated destruction of the histone methyltransferase Set8 prevents premature chromatin compaction in S phase', *Molecular Cell*, 40(1), pp. 22-33.

Chamberlain, N.L., Driver, E.D. and Miesfeld, R.L. (1994) 'The length and location of CAG trinucleotide repeats in the androgen receptor N-terminal domain affect transactivation function', *Nucleic Acids Research*, 22(15), pp. 3181-3186.

Chan, C.H., Lee, S.W., Li, C.F., Wang, J., Yang, W.L., Wu, C.Y., Wu, J., Nakayama, K.I., Kang, H.Y., Huang, H.Y., Hung, M.C., Pandolfi, P.P. and Lin, H.K. (2010) 'Deciphering the transcriptional complex critical for RhoA gene expression and cancer metastasis', *Nature Cell Biology*, 12(5), pp. 457-467.

Chan, S.C. and Dehm, S.M. (2014) 'Constitutive activity of the androgen receptor' *Advances in Pharmacology* [Article]. pp. 327-366. Available at: <https://www.scopus.com/inward/record.uri?eid=2-s2.0-84902138299&partnerID=40&md5=2dc4b9eb31c2b487400ab09877f042f5>.

Chang, K.H., Li, R., Papari-Zareei, M., Watumull, L., Zhao, Y.D., Auchus, R.J. and Sharifi, N. (2011) 'Dihydrotestosterone synthesis bypasses testosterone to drive castration-resistant prostate cancer', *Proceedings of the National Academy of Sciences of the United States of America*, 108(33), pp. 13728-13733.

Chastagner, P., Israël, A. and Brou, C. (2006) 'Itch/AIP4 mediates Deltex degradation through the formation of K29-linked polyubiquitin chains', *EMBO Reports*, 7(11), pp. 1147-1153.

Chau, V., Tobias, J.W., Bachmair, A., Marriott, D., Ecker, D.J., Gonda, D.K. and Varshavsky, A. (1989) 'A multiubiquitin chain is confined to specific lysine in a targeted short-lived protein', *Science*, 243(4898), pp. 1576-1583.

Chen, J., Chen, S., Saha, P. and Dutta, A. (1996) 'p21Cip1/Waf1 disrupts the recruitment of human Fen1 by proliferating-cell nuclear antigen into the DNA replication complex', *Proceedings of the National Academy of Sciences of the United States of America*, 93(21), pp. 11597-11602.

Chernov, M.V., Bean, L.J.H., Lerner, N. and Stark, G.R. (2001) 'Regulation of Ubiquitination and Degradation of p53 in Unstressed Cells through C-terminal Phosphorylation', *Journal of Biological Chemistry*, 276(34), pp. 31819-31824.

Chiu, Y.H., Sun, Q. and Chen, Z.J. (2007) 'E1-L2 Activates Both Ubiquitin and FAT10', *Molecular Cell*, 27(6), pp. 1014-1023.

Christiaens, V., Bevan, C.L., Callewaert, L., Haelens, A., Verrijdt, G., Rombauts, W. and Claessens, F. (2002) 'Characterization of the two coactivator-interacting surfaces of the androgen receptor and their relative role in transcriptional control', *Journal of Biological Chemistry*, 277(51), pp. 49230-49237.

Ciechanover, A., Heller, H., Katz-Etzion, R. and Hershko, A. (1981) 'Activation of the heat-stable polypeptide of the ATP-dependent proteolytic system', *Proceedings of the National Academy of Sciences of the United States of America*, 78(2 II), pp. 761-765.

Claessens, F., Denayer, S., Van Tilborgh, N., Kerkhofs, S., Helsen, C. and Haelens, A. (2008) 'Diverse roles of androgen receptor (AR) domains in AR-mediated signaling', *Nuclear receptor signaling*, 6.

- Congdon, L.M., Houston, S.I., Veerappan, C.S., Spektor, T.M. and Rice, J.C. (2010) 'PR-Set7-mediated monomethylation of histone H4 lysine 20 at specific genomic regions induces transcriptional repression', *Journal of Cellular Biochemistry*, 110(3), pp. 609-619.
- Conze, D.B., Wu, C.J., Thomas, J.A., Landstrom, A. and Ashwell, J.D. (2008) 'Lys63-linked polyubiquitination of IRAK-1 is required for interleukin-1 receptor- and toll-like receptor-mediated NF- κ B activation', *Molecular and Cellular Biology*, 28(10), pp. 3538-3547.
- Couture, J.F., Collazo, E., Brunzelle, J.S. and Trievel, R.C. (2005) 'Structural and functional analysis of SET8, a histone H4 Lys-20 methyltransferase', *Genes and Development*, 19(12), pp. 1455-1465.
- Craft, N., Shostak, Y., Carey, M. and Sawyers, C.L. (1999) 'A mechanism for hormone-independent prostate cancer through modulation of androgen receptor signaling by the HER-2/neu tyrosine kinase', *Nature Medicine*, 5(3), pp. 280-285.
- Culig, Z., Hobisch, A., Cronauer, M.V., Radmayr, R., Bartsch, G., Klocker, H., Hittmair, A. and Trapman, J. (1994) 'Androgen Receptor Activation in Prostatic Tumor Cell Lines by Insulin-like Growth Factor-I, Keratinocyte Growth Factor, and Epidermal Growth Factor', *Cancer Research*, 54(20), pp. 5474-5478.
- Dehm, S.M., Schmidt, L.J., Heemers, H.V., Vessella, R.L. and Tindall, D.J. (2008) 'Splicing of a novel androgen receptor exon generates a constitutively active androgen receptor that mediates prostate cancer therapy resistance', *Cancer Research*, 68(13), pp. 5469-5477.
- Demuc, A., Bosch-Comas, A., González-Duarte, R. and Marfany, G. (2009) 'The UBA-UIM domains of the USP25 regulate the enzyme ubiquitination state and modulate substrate recognition', *PLoS ONE*, 4(5).
- Deveraux, Q., Ustrell, V., Pickart, C. and Rechsteiner, M. (1994) 'A 26 S protease subunit that binds ubiquitin conjugates', *Journal of Biological Chemistry*, 269(10), pp. 7059-7061.
- Dhami, G., Liu, H., Galka, M., Voss, C., Wei, R., Muranko, K., Kaneko, T., Cregan, S., Li, L. and Li, S.C. (2013) 'Dynamic Methylation of Numb by Set8 Regulates Its Binding to p53 and Apoptosis', *Molecular Cell*, 50(4), pp. 565-576.
- Dimova, N.V., Hathaway, N.A., Lee, B.H., Kirkpatrick, D.S., Berkowitz, M.L., Gygi, S.P., Finley, D. and King, R.W. (2012) 'APC/C-mediated multiple monoubiquitylation provides an alternative degradation signal for cyclin B1', *Nature Cell Biology*, 14(2), pp. 168-176.
- Ding, C., Li, R., Peng, J., Li, S. and Guo, Z. (2012) 'A polymorphism at the miR-502 binding site in the 3' untranslated region of the SET8 gene is associated with the outcome of small-cell lung cancer', *Experimental and Therapeutic Medicine*, 3(4), pp. 689-692.
- Driskell, I., Oda, H., Blanco, S., Nascimento, E., Humphreys, P. and Frye, M. (2012) 'The histone methyltransferase Setd8 acts in concert with c-Myc and is required to maintain skin', *EMBO Journal*, 31(3), pp. 616-629.
- Duff, J. and McEwan, I.J. (2005) 'Mutation of histidine 874 in the androgen receptor ligand-binding domain leads to promiscuous ligand activation and altered p160 coactivator interactions', *Molecular Endocrinology*, 19(12), pp. 2943-2954.
- Dulev, S., Tkach, J., Lin, S. and Batada, N.N. (2014) 'SET8 methyltransferase activity during the DNA double-strand break response is required for recruitment of 53BP1', *EMBO Reports*, 15(11), pp. 1163-1174.

- Durcan, T.M., Tang, M.Y., Pérusse, J.R., Dashti, E.A., Aguilera, M.A., McLelland, G.L., Gros, P., Shaler, T.A., Faubert, D., Coulombe, B. and Fon, E.A. (2015) 'USP8 regulates mitophagy by removing K6-linked ubiquitin conjugates from parkin', *EMBO Journal*.
- Dynek, J.N., Goncharov, T., Dueber, E.C., Fedorova, A.V., Izrael-Tomasevic, A., Phu, L., Helgason, E., Fairbrother, W.J., Deshayes, K., Kirkpatrick, D.S. and Vucic, D. (2010) 'C-IAP1 and UbcH5 promote K11-linked polyubiquitination of RIP1 in TNF signalling', *EMBO Journal*, 29(24), pp. 4198-4209.
- Elia, A.E.H., Boardman, A.P., Wang, D.C., Huttlin, E.L., Everley, R.A., Dephoure, N., Zhou, C., Koren, I., Gygi, S.P. and Elledge, S.J. (2015) 'Quantitative Proteomic Atlas of Ubiquitination and Acetylation in the DNA Damage Response', *Molecular Cell*, 59(5), pp. 867-881.
- Fang, D. and Kerppola, T.K. (2004) 'Ubiquitin-mediated fluorescence complementation reveals that Jun ubiquitinated by Itch/AIP4 is localized to lysosomes', *Proceedings of the National Academy of Sciences of the United States of America*, 101(41), pp. 14782-14787.
- Fang, J., Feng, Q., Ketel, C.S., Wang, H., Cao, R., Xia, L., Erdjument-Bromage, H., Tempst, P., Simon, J.A. and Zhang, Y. (2002) 'Purification and functional characterization of SET8, a nucleosomal histone H4-lysine 20-specific methyltransferase', *Current Biology*, 12(13), pp. 1086-1099.
- Fei, C., Li, Z., Li, C., Chen, Y., Chen, Z., He, X., Mao, L., Wang, X., Zeng, R. and Li, L. (2013) 'Smurf1-mediated lys29-linked nonproteolytic polyubiquitination of axin negatively regulates wnt/ β -catenin signaling', *Molecular and Cellular Biology*, 33(20), pp. 4095-4105.
- Feilotter, H.E., Nagai, M.A., Boag, A.H., Eng, C. and Mulligan, L.M. (1998) 'Analysis of PTEN and the 10q23 region in primary prostate carcinomas', *Oncogene*, 16(13), pp. 1743-1748.
- Feldman, B.J. and Feldman, D. (2001) 'The development of androgen-independent prostate cancer', *Nature Reviews Cancer*, 1(1), pp. 34-45.
- Felten, A., Brinckmann, D., Landsberg, G. and Scheidtmann, K.H. (2013) 'Zipper-interacting protein kinase is involved in regulation of ubiquitination of the androgen receptor, thereby contributing to dynamic transcription complex assembly', *Oncogene*, 32(41), pp. 4981-4988.
- Fraga, M.F., Ballestar, E., Villar-Garea, A., Boix-Chornet, M., Espada, J., Schotta, G., Bonaldi, T., Haydon, C., Ropero, S., Petrie, K., Iyer, N.G., Pérez-Rosado, A., Calvo, E., Lopez, J.A., Cano, A., Calasanz, M.J., Colomer, D., Piris, M.Á., Ahn, N., Imhof, A., Caldas, C., Jenuwein, T. and Esteller, M. (2005) 'Loss of acetylation at Lys16 and trimethylation at Lys20 of histone H4 is a common hallmark of human cancer', *Nature Genetics*, 37(4), pp. 391-400.
- Freedman, L.P. (1992) 'Anatomy of the steroid receptor zinc finger region', *Endocrine Reviews*, 13(2), pp. 129-145.
- Frescas, D. and Pagano, M. (2008) 'Deregulated proteolysis by the F-box proteins SKP2 and β -TrCP: Tipping the scales of cancer', *Nature Reviews Cancer*, 8(6), pp. 438-449.
- Frick, J. and Aulitzky, W. (1991) 'Physiology of the prostate', *Infection*, 19(3 Supplement).
- Fuchs, S.Y., Dolan, L., Davis, R.J. and Ronai, Z. (1996) 'Phosphorylation-dependent targeting of c-Jun ubiquitination by Jun N-kinase', *Oncogene*, 13(7), pp. 1531-1535.

- Gao, D., Inuzuka, H., Tseng, A., Chin, R.Y., Toker, A. and Wei, W. (2009) 'Phosphorylation by Akt1 promotes cytoplasmic localization of Skp2 and impairs APC^{Cdh1}-mediated Skp2 destruction', *Nature Cell Biology*, 11(4), pp. 397-408.
- Gao, W., Bohl, C.E. and Dalton, J.T. (2005) 'Chemistry and structural biology of androgen receptor', *Chemical Reviews*, 105(9), pp. 3352-3370.
- Gatti, M., Pinato, S., Maiolica, A., Rocchio, F., Prato, M., Aebersold, R. and Penengo, L. (2015) 'RNF168 promotes noncanonical K27ubiquitination to signal DNA damage', *Cell Reports*, 10(2), pp. 226-238.
- Gaughan, L., Brady, M.E., Cook, S., Neal, D.E. and Robson, C.N. (2001) 'Tip60 Is a Co-activator Specific for Class I Nuclear Hormone Receptors', *Journal of Biological Chemistry*, 276(50), pp. 46841-46848.
- Gaughan, L., Logan, I.R., Cook, S., Neal, D.E. and Robson, C.N. (2002) 'Tip60 and histone deacetylase 1 regulate androgen receptor activity through changes to the acetylation status of the receptor', *Journal of Biological Chemistry*, 277(29), pp. 25904-25913.
- Gaughan, L., Stockley, J., Wang, N., McCracken, S.R.C., Treumann, A., Armstrong, K., Shaheen, F., Watt, K., McEwan, I.J., Wang, C., Pestell, R.G. and Robson, C.N. (2011) 'Regulation of the androgen receptor by SET9-mediated methylation', *Nucleic Acids Research*, 39(4), pp. 1266-1279.
- Gioeli, D., Ficarro, S.B., Kwiek, J.J., Aaronson, D., Hancock, M., Catling, A.D., White, F.M., Christian, R.E., Settlege, R.E., Shabanowitz, J., Hunt, D.F. and Weber, M.J. (2002) 'Androgen receptor phosphorylation. Regulation and identification of the phosphorylation sites', *Journal of Biological Chemistry*, 277(32), pp. 29304-29314.
- Girish, T.S., McGinty, R.K. and Tan, S. (2016) 'Multivalent interactions by the set8 histone methyltransferase with its nucleosome substrate', *Journal of Molecular Biology*, 428(8), pp. 1531-1543.
- Goldenberg, S.L. and Bruchovsky, N. (1991) 'Use of cyproterone acetate in prostate cancer', *Urologic Clinics of North America*, 18(1), pp. 111-122.
- Goodwin, J.F., Schiewer, M.J., Dean, J.L., Schrecengost, R.S., de Leeuw, R., Han, S., Ma, T., Den, R.B., Dicker, A.P., Feng, F.Y. and Knudsen, K.E. (2013) 'A hormone-DNA repair circuit governs the response to genotoxic insult', *Cancer Discovery*, 3(11), pp. 1254-1271.
- Goren, A., Tabib, A., Hecht, M. and Cedar, H. (2008) 'DNA replication timing of the human β -globin domain is controlled by histone modification at the origin', *Genes and Development*, 22(10), pp. 1319-1324.
- Grasso, C.S., Wu, Y.M., Robinson, D.R., Cao, X., Dhanasekaran, S.M., Khan, A.P., Quist, M.J., Jing, X., Lonigro, R.J., Brenner, J.C., Asangani, I.A., Ateeq, B., Chun, S.Y., Siddiqui, J., Sam, L., Anstett, M., Mehra, R., Prensner, J.R., Palanisamy, N., Ryslik, G.A., Vandin, F., Raphael, B.J., Kunju, L.P., Rhodes, D.R., Pienta, K.J., Chinnaiyan, A.M. and Tomlins, S.A. (2012) 'The mutational landscape of lethal castration-resistant prostate cancer', *Nature*, 487(7406), pp. 239-243.
- Gregory, C.W., He, B., Johnson, R.T., Ford, O.H., Mohler, J.L., French, F.S. and Wilson, E.M. (2001) 'A mechanism for androgen receptor-mediated prostate cancer recurrence after androgen deprivation therapy', *Cancer Research*, 61(11), pp. 4315-4319.

- Groettrup, M., Pelzer, C., Schmidtke, G. and Hofmann, K. (2008) 'Activating the ubiquitin family: UBA6 challenges the field', *Trends in Biochemical Sciences*, 33(5), pp. 230-237.
- Grompe, M. and D'Andrea, A. (2001) 'Fanconi anemia and DNA repair', *Human Molecular Genetics*, 10(20), pp. 2253-2259.
- Gstaiger, M., Jordan, R., Lim, M., Catzavelos, C., Mestan, J., Slingerland, J. and Krek, W. (2001) 'Skp2 is oncogenic and overexpressed in human cancers', *Proceedings of the National Academy of Sciences of the United States of America*, 98(9), pp. 5043-5048.
- Guo, Y., Sklar, G.N., Borkowski, A. and Kyprianou, N. (1997) 'Loss of the cyclin-dependent kinase inhibitor p27(Kip1) protein in human prostate cancer correlates with tumor grade', *Clinical Cancer Research*, 3(12 I), pp. 2269-2274.
- Guo, Z., Wu, C., Wang, X., Wang, C., Zhang, R. and Shan, B. (2012) 'A polymorphism at the miR-502 binding site in the 3'-untranslated region of the histone methyltransferase SET8 is associated with hepatocellular carcinoma outcome', *International Journal of Cancer*, 131(6), pp. 1318-1322.
- Guo, Z., Yang, X., Sun, F., Jiang, R., Linn, D.E., Chen, H., Chen, H., Kong, X., Melamed, J., Tepper, C.G., Kung, H.J., Brodie, A.M.H., Edwards, J. and Qiu, Y. (2009) 'A novel androgen receptor splice variant is up-regulated during prostate cancer progression and promotes androgen depletion-resistant growth', *Cancer Research*, 69(6), pp. 2305-2313.
- Haelens, A., Tanner, T., Denayer, S., Callewaert, L. and Claessens, F. (2007) 'The hinge region regulates DNA binding, nuclear translocation, and transactivation of the androgen receptor', *Cancer Research*, 67(9), pp. 4514-4523.
- Haelens, A., Verrijdt, G., Callewaert, L., Christiaens, V., Schauwaers, K., Peeters, B., Rombauts, W. and Claessens, F. (2003) 'DNA recognition by the androgen receptor: Evidence for an alternative DNA-dependent dimerization, and an active role of sequences flanking the response element on transactivation', *Biochemical Journal*, 369(1), pp. 141-151.
- Haglund, K., Sigismund, S., Polo, S., Szymkiewicz, I., Di Fiore, P.P. and Dikic, I. (2003) 'Multiple monoubiquitination of RTKs is sufficient for their endocytosis and degradation', *Nature Cell Biology*, 5(5), pp. 461-466.
- Hanahan, D. and Weinberg, R.A. (2000) 'The hallmarks of cancer', *Cell*, 100(1), pp. 57-70.
- Harada, K., Supriatno, Kawashima, Y., Itashiki, Y., Yoshida, H. and Sato, M. (2005) 'Down-regulation of S-phase kinase associated protein 2 (Skp2) induces apoptosis in oral cancer cells', *Oral Oncology*, 41(6), pp. 623-630.
- Havens, C.G. and Walter, J.C. (2009) 'Docking of a Specialized PIP Box onto Chromatin-Bound PCNA Creates a Degron for the Ubiquitin Ligase CRL4Cdt2', *Molecular Cell*, 35(1), pp. 93-104.
- Hay-Koren, A., Caspi, M., Zilberberg, A. and Rosin-Arbesfeld, R. (2011) 'The EDD E3 ubiquitin ligase ubiquitinates and up-regulates β -catenin', *Molecular Biology of the Cell*, 22(3), pp. 399-411.
- Heemers, H.V., Schmidt, L.J., Kidd, E., Raclaw, K.A., Regan, K.M. and Tindall, D.J. (2010) 'Differential regulation of steroid nuclear receptor coregulator expression between normal and neoplastic prostate epithelial cells', *Prostate*, 70(9), pp. 959-970.

- Heidenreich, A., Bastian, P.J., Bellmunt, J., Bolla, M., Joniau, S., Van Der Kwast, T., Mason, M., Matveev, V., Wiegel, T., Zattoni, F. and Mottet, N. (2014) 'EAU guidelines on prostate cancer. Part II: Treatment of advanced, relapsing, and castration-resistant prostate cancer', *European Urology*, 65(2), pp. 467-479.
- Hershko, D., Bornstein, G., Ben-Izhak, O., Carrano, A., Pagano, M., Krausz, M.M. and Hershko, A. (2001) 'Inverse relation between levels of p27Kip1 and of its ubiquitin ligase subunit Skp2 in colorectal carcinomas', *Cancer*, 91(9), pp. 1745-1751.
- Hibbert, R.G., Huang, A., Boelens, R. and Sixma, T.K. (2011) 'E3 ligase Rad18 promotes monoubiquitination rather than ubiquitin chain formation by E2 enzyme Rad6', *Proceedings of the National Academy of Sciences of the United States of America*, 108(14), pp. 5590-5595.
- Horszewicz, J.S., Leong, S.S., Chu, T.M., Wajzman, Z.L., Friedman, M., Papsidero, L., Kim, U., Chai, L.S., Kakati, S., Arya, S.K. and Sandberg, A.A. (1980) 'The LNCaP cell line--a new model for studies on human prostatic carcinoma', *Progress in clinical and biological research*, 37, pp. 115-132.
- Houston, S.I., McManus, K.J., Adams, M.M., Sims, J.K., Carpenter, P.B., Hendzel, M.J. and Rice, J.C. (2008) 'Catalytic function of the PR-Set7 histone H4 lysine 20 monomethyltransferase is essential for mitotic entry and genomic stability', *Journal of Biological Chemistry*, 283(28), pp. 19478-19488.
- Hsing, A.W. and Chokkalingam, A.P. (2006) 'Prostate cancer epidemiology', *Frontiers in Bioscience*, 11(2 P.1199-1590), pp. 1388-1413.
- Huang, D.T., Hunt, H.W., Zhuang, M., Ohi, M.D., Holton, J.M. and Schulman, B.A. (2007a) 'Basis for a ubiquitin-like protein thioester switch toggling E1-E2 affinity', *Nature*, 445(7126), pp. 394-398.
- Huang, H., Jeon, M.S., Liao, L., Yang, C., Elly, C., Yates, J.R. and Liu, Y.C. (2010) 'K33-Linked polyubiquitination of T cell receptor- ζ regulates proteolysis-independent T cell signaling', *Immunity*, 33(5), p. 830.
- Huang, J., Wu, C., Di Sant'Agnese, P.A., Yao, J.L., Cheng, L. and Na, Y. (2007b) 'Function and molecular mechanisms of neuroendocrine cells in prostate cancer', *Analytical and Quantitative Cytology and Histology*, 29(3), pp. 128-138.
- Huen, M.S.Y., Grant, R., Manke, I., Minn, K., Yu, X., Yaffe, M.B. and Chen, J. (2007) 'RNF8 Transduces the DNA-Damage Signal via Histone Ubiquitylation and Checkpoint Protein Assembly', *Cell*, 131(5), pp. 901-914.
- Huen, M.S.Y., Sy, S.M.H., Van Deursen, J.M. and Chen, J. (2008) 'Direct interaction between SET8 and proliferating cell nuclear antigen couples H4-K20 methylation with DNA replication', *Journal of Biological Chemistry*, 283(17), pp. 11073-11077.
- Huggins, C. and Neal, W. (1942) 'COAGULATION AND LIQUEFACTION OF SEMEN: PROTEOLYTIC ENZYMES AND CITRATE IN PROSTATIC FLUID', *The Journal of Experimental Medicine*, 76(6), pp. 527-541.
- Huibregtse, J.M., Scheffner, M., Beaudenon, S. and Howley, P.M. (1995) 'A family of proteins structurally and functionally related to the E6-AP ubiquitin-protein ligase', *Proceedings of the National Academy of Sciences of the United States of America*, 92(7), pp. 2563-2567.

- Iizuka, M., Matsui, T., Takisawa, H. and Smith, M.M. (2006) 'Regulation of replication licensing by acetyltransferase Hbo1', *Molecular and Cellular Biology*, 26(3), pp. 1098-1108.
- Ikeda, F., Deribe, Y.L., Skånland, S.S., Stieglitz, B., Grabbe, C., Franz-Wachtel, M., Van Wijk, S.J.L., Goswami, P., Nagy, V., Terzic, J., Tokunaga, F., Androulidaki, A., Nakagawa, T., Pasparakis, M., Iwai, K., Sundberg, J.P., Schaefer, L., Rittinger, K., MacEk, B. and Dikic, I. (2011) 'SHARPIN forms a linear ubiquitin ligase complex regulating NF- κ B activity and apoptosis', *Nature*, 471(7340), pp. 637-641.
- Iwai, K. and Tokunaga, F. (2009) 'Linear polyubiquitination: A new regulator of NF- κ B activation', *EMBO Reports*, 10(7), pp. 706-713.
- Jackson, P.K., Eldridge, A.G., Freed, E., Furstenthal, L., Hsu, J.Y., Kaiser, B.K. and Reimann, J.D.R. (2000) 'The lore of the RINGS: Substrate recognition and catalysis by ubiquitin ligases', *Trends in Cell Biology*, 10(10), pp. 429-439.
- Jenster, G., Van der Korput, H.A.G.M., Trapman, J. and Brinkmann, A.O. (1995) 'Identification of two transcription activation units in the N-terminal domain of the human androgen receptor', *Journal of Biological Chemistry*, 270(13), pp. 7341-7346.
- Jenster, G., Van der Korput, H.A.G.M., Van Vroonhoven, C., Van der Kwast, T.H., Trapman, J. and Brinkmann, A.O. (1991) 'Domains of the human androgen receptor involved in steroid binding, transcriptional activation, and subcellular localization', *Molecular Endocrinology*, 5(10), pp. 1396-1404.
- Jiang, J., Pan, Y., Regan, K.M., Wu, C., Zhang, X., Tindall, D.J. and Huang, H. (2012) 'Androgens repress expression of the f-box protein Skp2 via p107 dependent and independent mechanisms in LNCaP prostate cancer cells', *Prostate*, 72(2), pp. 225-232.
- Jin, J., Li, X., Gygi, S.P. and Harper, J.W. (2007) 'Dual E1 activation systems for ubiquitin differentially regulate E2 enzyme charging', *Nature*, 447(7148), pp. 1135-1138.
- Jørgensen, S., Elvers, I., Trelle, M.B., Menzel, T., Eskildsen, M., Jensen, O.N., Helleday, T., Helin, K. and Sørensen, C.S. (2007) 'The histone methyltransferase SET8 is required for S-phase progression', *Journal of Cell Biology*, 179(7), pp. 1337-1345.
- Jørgensen, S., Eskildsen, M., Fugger, K., Hansen, L., Larsen, M.S.Y., Kousholt, A.N., Syljuåsen, R.G., Trelle, M.B., Jensen, O.N., Helin, K. and Sørensen, C.S. (2011) 'SET8 is degraded via PCNA-coupled CRL4(CDT2) ubiquitylation in S phase and after UV irradiation', *Journal of Cell Biology*, 192(1), pp. 43-54.
- Ju, D. and Xie, Y. (2006) 'Identification of the preferential ubiquitination site and ubiquitin-dependent degradation signal of Rpn4', *Journal of Biological Chemistry*, 281(16), pp. 10657-10662.
- Kahl, P., Gullotti, L., Heukamp, L.C., Wolf, S., Friedrichs, N., Vorreuther, R., Solleder, G., Bastian, P.J., Ellinger, J., Metzger, E., Schüle, R. and Buettner, R. (2006) 'Androgen receptor coactivators lysine-specific histone demethylase 1 and four and a half LIM domain protein 2 predict risk of prostate cancer recurrence', *Cancer Research*, 66(23), pp. 11341-11347.
- Kalakonda, N., Fischle, W., Bocconi, P., Gurvich, N., Hoya-Arias, R., Zhao, X., Miyata, Y., MacGrogan, D., Zhang, J., Sims, J.K., Rice, J.C. and Nimer, S.D. (2008) 'Histone H4 lysine 20 monomethylation promotes transcriptional repression by L3MBTL1', *Oncogene*, 27(31), pp. 4293-4304.

- Karachentsev, D., Sarma, K., Reinberg, D. and Steward, R. (2005) 'PR-Set7-dependent methylation of histone H4 Lys 20 functions in repression of gene expression and is essential for mitosis', *Genes and Development*, 19(4), pp. 431-435.
- Kerscher, O., Felberbaum, R. and Hochstrasser, M. 22 (2006) 'Modification of proteins by ubiquitin and ubiquitin-like proteins' *Annual Review of Cell and Developmental Biology* [Review]. pp. 159-180. Available at: <https://www.scopus.com/inward/record.uri?eid=2-s2.0-33749346301&partnerID=40&md5=5082e3a4c25f53f374e2abb6dfbecfc0>.
- Kim, S.Y., Herbst, A., Tworowski, K.A., Salghetti, S.E. and Tansey, W.P. (2003) 'Skp2 regulates Myc protein stability and activity', *Molecular Cell*, 11(5), pp. 1177-1188.
- Kim, W., Bennett, E., Huttlin, E., Guo, A., Li, J., Possemato, A., Sowa, M., Rad, R., Rush, J., Comb, M., Harper, J.W. and Gygi, S. (2011) 'Systematic and quantitative assessment of the ubiquitin-modified proteome', *Molecular Cell*, 44(2), pp. 325-340.
- Kim, Y., Starostina, N.G. and Kipreos, E.T. (2008) 'The CRL4Cdt2 ubiquitin ligase targets the degradation of p21Cip1 to control replication licensing', *Genes and Development*, 22(18), pp. 2507-2519.
- Kirisako, T., Kamei, K., Murata, S., Kato, M., Fukumoto, H., Kanie, M., Sano, S., Tokunaga, F., Tanaka, K. and Iwai, K. (2006) 'A ubiquitin ligase complex assembles linear polyubiquitin chains', *EMBO Journal*, 25(20), pp. 4877-4887.
- Kitagawa, M., Lee, S.H. and McCormick, F. (2008) 'Skp2 Suppresses p53-Dependent Apoptosis by Inhibiting p300', *Molecular Cell*, 29(2), pp. 217-231.
- Klotz, L. (2013) 'Active surveillance for prostate cancer: Overview and update', *Current Treatment Options in Oncology*, 14(1), pp. 97-108.
- Ko, S., Ahn, J., Song, C.S., Kim, S., Knapczyk-Stwora, K. and Chatterjee, B. (2011) 'Lysine methylation and functional modulation of androgen receptor by set9 methyltransferase', *Molecular Endocrinology*, 25(3), pp. 433-444.
- Kohlmaier, A., Savarese, F., Lachner, M., Martens, J., Jenuwein, T. and Wutz, A. (2004) 'A chromosomal memory triggered by Xist regulates histone methylation in X inactivation', *PLoS Biology*, 2(7).
- Koivisto, P., Visakorpi, T. and Kallioniemi, O.P. (1996) 'Androgen receptor gene amplification: A novel molecular mechanism for endocrine therapy resistance in human prostate cancer', *Scandinavian Journal of Clinical and Laboratory Investigation, Supplement*, 56(226), pp. 57-64.
- Kokontis, J.M., Lin, H.P., Jiang, S.S., Lin, C.Y., Fukuchi, J., Hiipakka, R.A., Chung, C.J., Chan, T.M., Liao, S., Chang, C.H. and Chuu, C.P. (2014) 'Correction: Androgen suppresses the proliferation of androgen receptor-positive castration-resistant prostate cancer cells via inhibition of Cdk2, CyclinA, and Skp2 (PLoS ONE (2014) 9, 10 (e109170) DOI: 10.1371/journal.pone.0109170)', *PLoS ONE*, 9(10).
- Komander, D., Clague, M.J. and Urbé, S. (2009) 'Breaking the chains: Structure and function of the deubiquitinases', *Nature Reviews Molecular Cell Biology*, 10(8), pp. 550-563.
- Komander, D. and Rape, M. 81 (2012) 'The ubiquitin code' *Annual Review of Biochemistry* [Article]. pp. 203-229. Available at: <https://www.scopus.com/inward/record.uri?eid=2-s2.0-84861877407&partnerID=40&md5=a2e745ff0c398b7956ae2ce4d2cad4a5>.

- Korpai, M., Korn, J.M., Gao, X., Rakiec, D.P., Ruddy, D.A., Doshi, S., Yuan, J., Kovats, S.G., Kim, S., Cooke, V.G., Monahan, J.E., Stegmeier, F., Roberts, T.M., Sellers, W.R., Zhou, W. and Zhu, P. (2013) 'An F876I mutation in androgen receptor confers genetic and phenotypic resistance to MDV3100 (Enzalutamide)', *Cancer Discovery*, 3(9), pp. 1030-1043.
- Kuiper, G.G.J.M., Faber, P.W., Van Rooij, H.C.J., Van der Korput, J.A.G.M., Ris-Stalpers, C., Klaassen, P., Trapman, J. and Brinkmann, A.O. (1989) 'Structural organization of the human androgen receptor gene', *Journal of Molecular Endocrinology*, 2(3).
- Kumar, V.L. and Majumder, P.K. (1995) 'Prostate gland: Structure, functions and regulation', *International Urology and Nephrology*, 27(3), pp. 231-243.
- Latres, E., Chiarle, R., Schulman, B.A., Pavletich, N.P., Pellicer, A., Inghirami, G. and Pagano, M. (2001) 'Role of the F-box protein Skp2 in lymphomagenesis', *Proceedings of the National Academy of Sciences of the United States of America*, 98(5), pp. 2515-2520.
- Lauwers, E., Jacob, C. and Andre, B. (2009) 'K63-linked ubiquitin chains as a specific signal for protein sorting into the multivesicular body pathway', *Journal of Cell Biology*, 185(3), pp. 493-502.
- Lee, I. and Schindelin, H. (2008) 'Structural Insights into E1-Catalyzed Ubiquitin Activation and Transfer to Conjugating Enzymes', *Cell*, 134(2), pp. 268-278.
- Lee, S.H. and McCormick, F. (2005) 'Downregulation of Skp2 and p27/Kip1 synergistically induces apoptosis in T98G glioblastoma cells', *Journal of Molecular Medicine*, 83(4), pp. 296-307.
- Lee, S.W., Li, C.F., Jin, G., Cai, Z., Han, F., Chan, C.H., Yang, W.L., Li, B.K., Rezaeian, A., Li, H.Y., Huang, H.Y. and Lin, H.K. (2015) 'Skp2-Dependent Ubiquitination and Activation of LKB1 Is Essential for Cancer Cell Survival under Energy Stress', *Molecular Cell*, 57(6), pp. 1022-1033.
- Li, B., Lu, W., Yang, Q., Yu, X., Matusik, R.J. and Chen, Z. (2014a) 'Skp2 regulates androgen receptor through ubiquitin-mediated degradation independent of akt/mTOR pathways in prostate cancer', *Prostate*, 74(4), pp. 421-432.
- Li, H., Fischle, W., Wang, W., Duncan, E.M., Liang, L., Murakami-Ishibe, S., Allis, C.D. and Patel, D.J. (2007) 'Structural Basis for Lower Lysine Methylation State-Specific Readout by MBT Repeats of L3MBTL1 and an Engineered PHD Finger', *Molecular Cell*, 28(4), pp. 677-691.
- Li, L., Chang, W., Yang, G., Ren, C., Park, S., Karantanos, T., Karanika, S., Wang, J., Yin, J., Shah, P.K., Takahiro, H., Dobashi, M., Zhang, W., Efstathiou, E., Maity, S.N., Aparicio, A.M., Li Ning Tapia, E.M., Troncoso, P., Broom, B., Xiao, L., Lee, H.S., Lee, J.S., Corn, P.G., Navone, N. and Thompson, T.C. (2014b) 'Targeting poly(ADP-ribose) polymerase and the c-Myc-regulated DNA damage response pathway in castration-resistant prostate cancer', *Science Signaling*, 7(326).
- Li, M., Brooks, C.L., Wu-Baer, F., Chen, D., Baer, R. and Gu, W. (2003) 'Mono- Versus Polyubiquitination: Differential Control of p53 Fate by Mdm2', *Science*, 302(5652), pp. 1972-1975.
- Li, Y., Sun, L., Zhang, Y., Wang, D., Wang, F., Liang, J., Gui, B. and Shang, Y. (2011a) 'The histone modifications governing TFF1 transcription mediated by estrogen receptor', *J Biol Chem*, 286(16), pp. 13925-36.

- Li, Y., Sun, X.X., Elferich, J., Shinde, U., David, L.L. and Dai, M.S. (2014c) 'Monoubiquitination is critical for ovarian tumor domain-containing ubiquitin aldehyde binding protein 1 (Otub1) to suppress UbcH5 enzyme and Stabilize p53 protein', *Journal of Biological Chemistry*, 289(8), pp. 5097-5108.
- Li, Z., Nie, F., Wang, S. and Li, L. (2011b) 'Histone H4 Lys 20 monomethylation by histone methylase SET8 mediates Wnt target gene activation', *Proceedings of the National Academy of Sciences of the United States of America*, 108(8), pp. 3116-3123.
- Lieber, M.R. (1997) 'The FEN-1 family of structure-specific nucleases in eukaryotic DNA replication, recombination and repair', *BioEssays*, 19(3), pp. 233-240.
- Lilja, H., Abrahamsson, P.A. and Lundwall, A. (1989) 'Semenogelin, the predominant protein in human semen. Primary structure and identification of closely related proteins in the male accessory sex glands and on the spermatozoa', *Journal of Biological Chemistry*, 264(3), pp. 1894-1900.
- Lin, H.K., Chen, Z., Wang, G., Nardella, C., Lee, S.W., Chan, C.H., Yang, W.L., Wang, J., Egia, A., Nakayama, K.I., Cordon-Cardo, C., Teruya-Feldstein, J. and Pandolfi, P.P. (2010) 'Skp2 targeting suppresses tumorigenesis by Arf-p53-independent cellular senescence', *Nature*, 464(7287), pp. 374-379.
- Liu, B., Zhang, X., Song, F., Zheng, H., Zhao, Y., Li, H., Zhang, L., Yang, M., Zhang, W. and Chen, K. (2016) 'MiR-502/SET8 regulatory circuit in pathobiology of breast cancer', *Cancer Letters*, 376(2), pp. 259-267.
- Liu, W., Tanasa, B., Tyurina, O.V., Zhou, T.Y., Gassmann, R., Liu, W.T., Ohgi, K.A., Benner, C., Garcia-Bassets, I., Aggarwal, A.K., Desai, A., Dorrestein, P.C., Glass, C.K. and Rosenfeld, M.G. (2010) 'PHF8 mediates histone H4 lysine 20 demethylation events involved in cell cycle progression', *Nature*, 466(7305), pp. 508-512.
- Locke, J.A., Guns, E.S., Lubik, A.A., Adomat, H.H., Hendy, S.C., Wood, C.A., Ettinger, S.L., Gleave, M.E. and Nelson, C.C. (2008) 'Androgen Levels increase by intratumoral de novo steroidogenesis during progression of castration-resistant prostate cancer', *Cancer Research*, 68(15), pp. 6407-6415.
- Lonergan, P. and Tindall, D. (2011) 'Androgen receptor signaling in prostate cancer development and progression', *Journal of Carcinogenesis*, 10.
- Lu, W., Liu, S., Li, B., Xie, Y., Adhiambo, C., Yang, Q., Ballard, B.R., Nakayama, K.I., Matusik, R.J. and Chen, Z. (2015) 'SKP2 inactivation suppresses prostate tumorigenesis by mediating JARID1B ubiquitination', *Oncotarget*, 6(2), pp. 771-788.
- Lu, X., Simon, M.D., Chodaparambil, J.V., Hansen, J.C., Shokat, K.M. and Luger, K. (2008) 'The effect of H3K79 dimethylation and H4K20 trimethylation on nucleosome and chromatin structure', *Nature Structural and Molecular Biology*, 15(10), pp. 1122-1124.
- Lubahn, D.B., Joseph, D.R., Sullivan, P.M., Willard, H.F., French, F.S. and Wilson, E.M. (1988) 'Cloning of human androgen receptor complementary DNA and localization to the X chromosome', *Science*, 240(4850), pp. 327-330.
- MacDonald, C., Buchkovich, N.J., Stringer, D.K., Emr, S.D. and Piper, R.C. (2012) 'Cargo ubiquitination is essential for multivesicular body intraluminal vesicle formation', *EMBO Reports*, 13(4), pp. 331-338.

- Mamillapalli, R., Gavrilova, N., Mihaylova, V.T., Tsvetkov, L.M., Wu, H., Zhang, H. and Sun, H. (2001) 'PTEN regulates the ubiquitin-dependent degradation of the CDK inhibitor p27KIP1 through the ubiquitin E3 ligase SCF^{SKP2}', *Current Biology*, 11(4), pp. 263-267.
- Mashtalir, N., Daou, S., Barbour, H., Sen, N.N., Gagnon, J., Hammond-Martel, I., Dar, H.H., Therrien, M. and Affar, E.B. (2014) 'Autodeubiquitination protects the tumor suppressor BAP1 from cytoplasmic sequestration mediated by the atypical ubiquitin ligase UBE2O', *Molecular Cell*, 54(3), pp. 392-406.
- Matsumoto, M.L., Wickliffe, K.E., Dong, K.C., Yu, C., Bosanac, I., Bustos, D., Phu, L., Kirkpatrick, D.S., Hymowitz, S.G., Rape, M., Kelley, R.F. and Dixit, V.M. (2010) 'K11-linked polyubiquitination in cell cycle control revealed by a K11 linkage-specific antibody', *Molecular Cell*, 39(3), pp. 477-484.
- McCracken, S.R.C., Durkan, G.C., Pickard, R.S. and Robson, C.N. (2010) 'Diagnosis and management of prostate cancer in the older man', *Reviews in Clinical Gerontology*, 20(3), pp. 193-204.
- McLaughlin, P.W., Troyer, S., Berri, S., Narayana, V., Meirowitz, A., Roberson, P.L. and Montie, J. (2005) 'Functional anatomy of the prostate: Implications for treatment planning', *International Journal of Radiation Oncology Biology Physics*, 63(2), pp. 479-491.
- McNeal, J. (1990) 'Pathology of benign prostatic hyperplasia. Insight into etiology', *Urologic Clinics of North America*, 17(3), pp. 477-486.
- McNeal, J.E. (1981) 'The zonal anatomy of the prostate', *Prostate*, 2(1), pp. 35-49.
- McNeal, J.E. (1988) 'Normal histology of the prostate', *American Journal of Surgical Pathology*, 12(8), pp. 619-633.
- McVary, K.T. (2006) 'BPH: Epidemiology and comorbidities', *American Journal of Managed Care*, 12(SUPPL. 5).
- Metzger, E., Wissmann, M. and Schüle, R. (2006) 'Histone demethylation and androgen-dependent transcription', *Current Opinion in Genetics and Development*, 16(5), pp. 513-517.
- Metzger, E., Wissmann, M., Yin, N., Müller, J.M., Schneider, R., Peters, A.H.F.M., Günther, T., Buettner, R. and Schüle, R. (2005) 'LSD1 demethylates repressive histone marks to promote androgen-receptor-dependent transcription', *Nature*, 437(7057), pp. 436-439.
- Miller, D.C., Hafez, K.S., Stewart, A., Montie, J.E. and Wei, J.T. (2003) 'Prostate carcinoma presentation, diagnosis, and staging: An update from the National Cancer Data Base', *Cancer*, 98(6), pp. 1169-1178.
- Min, J., Allali-Hassani, A., Nady, N., Qi, C., Ouyang, H., Liu, Y., MacKenzie, F., Vedadi, M. and Arrowsmith, C.H. (2007) 'L3MBTL1 recognition of mono- and dimethylated histones', *Nature Structural and Molecular Biology*, 14(12), pp. 1229-1230.
- Miotto, B. and Struhl, K. (2008) 'HBO1 histone acetylase is a coactivator of the replication licensing factor Cdt1', *Genes and Development*, 22(19), pp. 2633-2638.
- Miotto, B. and Struhl, K. (2010) 'HBO1 Histone Acetylase Activity Is Essential for DNA Replication Licensing and Inhibited by Geminin', *Molecular Cell*, 37(1), pp. 57-66.
- Moras, D. and Gronemeyer, H. (1998) 'The nuclear receptor ligand-binding domain: Structure and function', *Current Opinion in Cell Biology*, 10(3), pp. 384-391.

- Moro, L., Arbini, A.A., Marra, E. and Greco, M. (2006) 'Up-regulation of Skp2 after prostate cancer cell adhesion to basement membranes results in BRCA2 degradation and cell proliferation', *Journal of Biological Chemistry*, 281(31), pp. 22100-22107.
- Mottet, N., Clarke, N., De Santis, M., Zattoni, F., Morote, J. and Joniau, S. (2015) 'Implementing newer agents for the management of castrate-resistant prostate cancer: What is known and what is needed?', *BJU International*, 115(3), pp. 364-372.
- Nguyen, P.L., Lin, D.I., Lei, J., Fiorentino, M., Mueller, E., Weinstein, M.H., Pagano, M. and Loda, M. (2011) 'The impact of Skp2 overexpression on recurrence-free survival following radical prostatectomy', *Urologic Oncology: Seminars and Original Investigations*, 29(3), pp. 302-308.
- Nishioka, K., Rice, J.C., Sarma, K., Erdjument-Bromage, H., Werner, J., Wang, Y., Chuikov, S., Valenzuela, P., Tempst, P., Steward, R., Lis, J.T., Allis, C.D. and Reinberg, D. (2002) 'PR-Set7 is a nucleosome-specific methyltransferase that modifies lysine 20 of histone H4 and is associated with silent Chromatin', *Molecular Cell*, 9(6), pp. 1201-1213.
- Nishitani, H., Shiomi, Y., Iida, H., Michishita, M., Takami, T. and Tsurimoto, T. (2008) 'CDK inhibitor p21 is degraded by a proliferating cell nuclear antigen-coupled Cul4-DDB1Cdt2 pathway during S phase and after UV irradiation', *Journal of Biological Chemistry*, 283(43), pp. 29045-29052.
- Noordzij, M.A., van Steenbrugge, G.J., van der Kwast, T.H. and Schröder, F.H. (1995) 'Neuroendocrine cells in the normal, hyperplastic and neoplastic prostate', *Urological Research*, 22(6), pp. 333-341.
- Oda, H., Hübner, M.R., Beck, D.B., Vermeulen, M., Hurwitz, J., Spector, D.L. and Reinberg, D. (2010) 'Regulation of the Histone H4 Monomethylase PR-Set7 by CRL4Cdt2-Mediated PCNA-Dependent Degradation during DNA Damage', *Molecular Cell*, 40(3), pp. 364-376.
- Oda, H., Okamoto, I., Murphy, N., Chu, J., Price, S.M., Shen, M.M., Torres-Padilla, M.E., Heard, E. and Reinberg, D. (2009) 'Monomethylation of histone H4-lysine 20 is involved in chromosome structure and stability and is essential for mouse development', *Molecular and Cellular Biology*, 29(8), pp. 2278-2295.
- Panier, S. and Boulton, S.J. (2014) 'Double-strand break repair: 53BP1 comes into focus', *Nature Reviews Molecular Cell Biology*, 15(1), pp. 7-18.
- Paulsen, R.D., Soni, D.V., Wollman, R., Hahn, A.T., Yee, M.C., Guan, A., Hesley, J.A., Miller, S.C., Cromwell, E.F., Solow-Cordero, D.E., Meyer, T. and Cimprich, K.A. (2009) 'A Genome-wide siRNA Screen Reveals Diverse Cellular Processes and Pathways that Mediate Genome Stability', *Molecular Cell*, 35(2), pp. 228-239.
- Pelzer, C., Kassner, I., Matentzoglou, K., Singh, R.K., Wollscheid, H.P., Scheffner, M., Schmidtke, G. and Groettrup, M. (2007) 'UBE1L2, a novel E1 enzyme specific for ubiquitin', *Journal of Biological Chemistry*, 282(32), pp. 23010-23014.
- Peng, J., Schwartz, D., Elias, J.E., Thoreen, C.C., Cheng, D., Marsischky, G., Roelofs, J., Finley, D. and Gygi, S.P. (2003) 'A proteomics approach to understanding protein ubiquitination', *Nature Biotechnology*, 21(8), pp. 921-926.
- Pernicová, Z., Slabáková, E., Kharaihvili, G., Bouchal, J., Král, M., Kunická, Z., Machala, M., Kozubík, A. and Souček, K. (2011) 'Androgen depletion induces senescence in prostate cancer cells through down-regulation of Skp2', *Neoplasia*, 13(6), pp. 526-536.

- Pesavento, J.J., Yang, H., Kelleher, N.L. and Mizzen, C.A. (2008) 'Certain and progressive methylation of histone H4 at lysine 20 during the cell cycle', *Molecular and Cellular Biology*, 28(1), pp. 468-486.
- Pickart, C.M. (2000) 'Ubiquitin in chains', *Trends in Biochemical Sciences*, 25(11), pp. 544-548.
- Pickart, C.M. and Fushman, D. (2004) 'Polyubiquitin chains: Polymeric protein signals', *Current Opinion in Chemical Biology*, 8(6), pp. 610-616.
- Pilch, D.R., Sedelnikova, O.A., Redon, C., Celeste, A., Nussenzweig, A. and Bonner, W.M. (2003) 'Characteristics of γ -H2AX foci at DNA double-strand breaks sites', *Biochemistry and Cell Biology*, 81(3), pp. 123-129.
- Pinheiro, L.C. and Martins Pisco, J. (2012) 'Treatment of Benign Prostatic Hyperplasia', *Techniques in Vascular and Interventional Radiology*, 15(4), pp. 256-260.
- Porter, P.L., Malone, K.E., Heagerty, P.J., Alexander, G.M., Gatti, L.A., Firpo, E.J., Daling, J.R. and Roberts, J.M. (1997) 'Expression of cell-cycle regulators p27(Kip1) and cyclin E, alone and in combination, correlate with survival in young breast cancer patients', *Nature Medicine*, 3(2), pp. 222-225.
- Powell, S.M., Christiaens, V., Voulgaraki, D., Waxman, J., Claessens, F. and Bevan, C.L. (2004) 'Mechanisms of androgen receptor signalling via steroid receptor coactivator-1 in prostate', *Endocrine-Related Cancer*, 11(1), pp. 117-130.
- Qi, H.H., Sarkissian, M., Hu, G.Q., Wang, Z., Bhattacharjee, A., Gordon, D.B., Gonzales, M., Lan, F., Ongusaha, P.P., Huarte, M., Yaghi, N.K., Lim, H., Garcia, B.A., Brizuela, L., Zhao, K., Roberts, T.M. and Shi, Y. (2010) 'Histone H4K20/H3K9 demethylase PHF8 regulates zebrafish brain and craniofacial development', *Nature*, 466(7305), pp. 503-507.
- Radke, S., Pirkmaier, A. and Germain, D. (2005) 'Differential expression of the F-box proteins Skp2 and Skp2B in breast cancer', *Oncogene*, 24(21), pp. 3448-3458.
- Ramachandran, S., Haddad, D., Li, C., Le, M.X., Ling, A.K., So, C.C., Nepal, R.M., Gommerman, J.L., Yu, K., Ketela, T., Moffat, J. and Martin, A. (2016) 'The SAGA Deubiquitination Module Promotes DNA Repair and Class Switch Recombination through ATM and DNAPK-Mediated γ H2AX Formation', *Cell Reports*, 15(7), pp. 1554-1565.
- Ramos, C.G., Carvahal, G.F., Mager, D.E., Haberer, B. and Catalona, W.J. (1999) 'The effect of high grade prostatic intraepithelial neoplasia on serum total and percentage of free prostate specific antigen levels', *Journal of Urology*, 162(5), pp. 1587-1590.
- Ray, S., Zhao, Y., Jamaluddin, M., Edeh, C.B., Lee, C. and Brasier, A.R. (2014) 'Inducible STAT3 NH2 terminal mono-ubiquitination promotes BRD4 complex formation to regulate apoptosis', *Cellular Signalling*, 26(7), pp. 1445-1455.
- Remus, D. and Diffley, J.F. (2009) 'Eukaryotic DNA replication control: Lock and load, then fire', *Current Opinion in Cell Biology*, 21(6), pp. 771-777.
- Rice, J.C., Nishioka, K., Sarma, K., Steward, R., Reinberg, D. and David Allis, C. (2002) 'Mitotic-specific methylation of histone H4 Lys 20 follows increased PR-Set7 expression and its localization to mitotic chromosomes', *Genes and Development*, 16(17), pp. 2225-2230.
- Rick, F.G., Block, N.L. and Schally, A.V. (2013) 'Agonists of luteinizing hormone-releasing hormone in prostate cancer', *Expert Opinion on Pharmacotherapy*, 14(16), pp. 2237-2247.

Robbins, C.M., Tembe, W.A., Baker, A., Sinari, S., Moses, T.Y., Beckstrom-Sternberg, S., Beckstrom-Sternberg, J., Barrett, M., Long, J., Chinnaiyan, A., Lowey, J., Suh, E., Pearson, J.V., Craig, D.W., Agus, D.B., Pienta, K.J. and Carpten, J.D. (2011) 'Copy number and targeted mutational analysis reveals novel somatic events in metastatic prostate tumors', *Genome Research*, 21(1), pp. 47-55.

Sack, J.S., Kish, K.F., Wang, C., Attar, R.M., Kiefer, S.E., An, Y., Wu, G.Y., Scheffler, J.E., Salvati, M.E., Krystek S.R, Jr., Weinmann, R. and Einspahr, H.M. (2001) 'Crystallographic structures of the ligand-binding domains of the androgen receptor and its T877A mutant complexed with the natural agonist dihydrotestosterone', *Proceedings of the National Academy of Sciences of the United States of America*, 98(9), pp. 4904-4909.

Sahu, B., Laakso, M., Pihlajamaa, P., Ovaska, K., Sinielnikov, I., Hautaniemi, S. and Jänne, O.A. (2013) 'FoxA1 specifies unique androgen and glucocorticoid receptor binding events in prostate cancer cells', *Cancer Research*, 73(5), pp. 1570-1580.

Sakaguchi, A. and Steward, R. (2007) 'Aberrant monomethylation of histone H4 lysine 20 activates the DNA damage checkpoint in *Drosophila melanogaster*', *Journal of Cell Biology*, 176(2), pp. 155-162.

Sanders, S.L., Portoso, M., Mata, J., Bähler, J., Allshire, R.C. and Kouzarides, T. (2004) 'Methylation of histone H4 lysine 20 controls recruitment of Crb2 to sites of DNA damage', *Cell*, 119(5), pp. 603-614.

Scheffner, M. and Kumar, S. (2014) 'Mammalian HECT ubiquitin-protein ligases: Biological and pathophysiological aspects', *Biochimica et Biophysica Acta - Molecular Cell Research*, 1843(1), pp. 61-74.

Schotta, G., Lachner, M., Sarma, K., Ebert, A., Sengupta, R., Reuter, G., Reinberg, D. and Jenuwein, T. (2004) 'A silencing pathway to induce H3-K9 and H4-K20 trimethylation at constitutive heterochromatin', *Genes and Development*, 18(11), pp. 1251-1262.

Schulman, B.A., Carrano, A.C., Jeffrey, P.D., Bowen, Z., Kinnucan, E.R.E., Finnin, M.S., Elledge, S.J., Harper, J.W., Pagano, M. and Pavletich, N.P. (2000) 'Insights into SCF ubiquitin ligases from the structure of the Skp1-Skp2 complex', *Nature*, 408(6810), pp. 381-386.

Shah, R.B. and Zhou, M. (2012) *In Prostate Biopsy Interpretation: Illustrated Guide*.

Shang, F., Deng, G., Liu, Q., Guo, W., Haas, A.L., Crosas, B., Finley, D. and Taylor, A. (2005) 'Lys6-modified ubiquitin inhibits ubiquitin-dependent protein degradation', *Journal of Biological Chemistry*, 280(21), pp. 20365-20374.

Shen, M.M. and Abate-Shen, C. (2010) 'Molecular genetics of prostate cancer: New prospects for old challenges', *Genes and Development*, 24(18), pp. 1967-2000.

Shi, D., Pop, M.S., Kulikov, R., Love, I.M., Kung, A. and Grossman, S.R. (2009) 'CBP and p300 are cytoplasmic E4 polyubiquitin ligases for p53', *Proceedings of the National Academy of Sciences of the United States of America*, 106(38), pp. 16275-16280.

Shi, X., Kachirskaja, I., Yamaguchi, H., West, L.E., Wen, H., Wang, E.W., Dutta, S., Appella, E. and Gozani, O. (2007) 'Modulation of p53 Function by SET8-Mediated Methylation at Lysine 382', *Molecular Cell*, 27(4), pp. 636-646.

Shtivelman, E., Beer, T.M. and Evans, C.P. (2014) 'Molecular pathways and targets in prostate cancer', *Oncotarget*, 5(17), pp. 7217-7259.

- Signoretti, S., Marcotullio, L.D., Richardson, A., Ramaswamy, S., Isaac, B., Rue, M., Monti, F., Loda, M. and Pagano, M. (2002) 'Oncogenic role of the ubiquitin ligase subunit Skp2 in human breast cancer', *Journal of Clinical Investigation*, 110(5), pp. 633-641.
- Silva, F.P., Blum, G., Senevirathne, C. and Luo, M. (2016) 'Substrate profiling for SETD8 reveals novel protein targets involved in DNA replication and DNA damage response', *Proceedings of the 107th Annual Meeting of the American Association for Cancer Research*, 76(14), p. 4521.
- Silva, G.M., Finley, D. and Vogel, C. (2015) 'K63 polyubiquitination is a new modulator of the oxidative stress response', *Nature Structural and Molecular Biology*, 22(2), pp. 116-123.
- Sims, J.K. and Rice, J.C. (2008) 'PR-set7 establishes a repressive trans-tail histone code that regulates differentiation', *Molecular and Cellular Biology*, 28(14), pp. 4459-4468.
- Smith, D.F. and Toft, D.O. (2008) 'The intersection of steroid receptors with molecular chaperones: Observations and questions', *Molecular Endocrinology*, 22(10), pp. 2229-2240.
- Song, F., Zheng, H., Liu, B., Wei, S., Dai, H., Zhang, L., Calin, G.A., Hao, X., Wei, Q., Zhang, W. and Chen, K. (2009) 'An miR-502-binding site single-nucleotide polymorphism in the 3'-untranslated region of the SET8 gene is associated with early age of breast cancer onset', *Clinical Cancer Research*, 15(19), pp. 6292-6300.
- Spektor, T.M., Congdon, L.M., Veerappan, C.S. and Rice, J.C. (2011) 'The UBC9 E2 SUMO conjugating enzyme binds the PR-Set7 histone methyltransferase to facilitate target gene repression', *PLoS One*, 6(7), p. e22785.
- Spence, J., Gali, R.R., Dittmar, G., Sherman, F., Karin, M. and Finley, D. (2000) 'Cell cycle-regulated modification of the ribosome by a variant multiubiquitin chain', *Cell*, 102(1), pp. 67-76.
- Steketee, K., Timmerman, L., Ziel-Van Der Made, A.C.J., Doesburg, P., Brinkmann, A.O. and Trapman, J. (2002) 'Broadened ligand responsiveness of androgen receptor mutants obtained by random amino acid substitution of H874 and mutation hot spot T877 in prostate cancer', *International Journal of Cancer*, 100(3), pp. 309-317.
- Stukenberg, P.T., Lustig, K.D., McGarry, T.J., King, R.W., Kuang, J. and Kirschner, M.W. (1997) 'Systematic identification of mitotic phosphoproteins', *Current Biology*, 7(5), pp. 338-348.
- Sun, L. and Fang, J. (2016) 'E3-Independent Constitutive Monoubiquitination Complements Histone Methyltransferase Activity of SETDB1', *Molecular Cell*, 62(6), pp. 958-966.
- Sutterlüty, H., Chatelain, E., Marti, A., Wirbelauer, C., Senften, M., Müller, U. and Krek, W. (1999) 'p45SKP2 promotes p27Kip1 degradation and induces S phase in quiescent cells', *Nature Cell Biology*, 1(4), pp. 207-214.
- Suzuki, H., Akakura, K., Komiya, A., Aida, S., Akimoto, S. and Shimazaki, J. (1996) 'Codon 877 mutation in the androgen receptor gene in advanced prostate cancer: Relation to antiandrogen withdrawal syndrome', *Prostate*, 29(3), pp. 153-158.
- Takawa, M., Cho, H.S., Hayami, S., Toyokawa, G., Kogure, M., Yamane, Y., Iwai, Y., Maejima, K., Ueda, K., Masuda, A., Dohmae, N., Field, H.I., Tsunoda, T., Kobayashi, T., Akasu, T., Sugiyama, M., Ohnuma, S., Atomi, Y., Ponder, B.A., Nakamura, Y. and Hamamoto,

- R. (2012) 'Histone lysine methyltransferase SETD8 promotes carcinogenesis by deregulating PCNA expression', *Cancer Res*, 72(13), pp. 3217-27.
- Talasz, H., Lindner, H.H., Sarg, B. and Helliger, W. (2005) 'Histone H4-lysine 20 monomethylation is increased in promoter and coding regions of active genes and correlates with hyperacetylation', *Journal of Biological Chemistry*, 280(46), pp. 38814-38822.
- Tanner, T., Claessens, F. and Haelens, A. 1030 (2004) 'The hinge region of the androgen receptor plays a role in proteasome-mediated transcriptional activation' *Annals of the New York Academy of Sciences* [Conference Paper]. pp. 587-592. Available at: <https://www.scopus.com/inward/record.uri?eid=2-s2.0-15044349502&partnerID=40&md5=927fbf6fd3b2971610f1136080d92ff5>.
- Tardat, M., Brustel, J., Kirsh, O., Lefevbre, C., Callanan, M., Sardet, C. and Julien, E. (2010) 'The histone H4 Lys 20 methyltransferase PR-Set7 regulates replication origins in mammalian cells', *Nature Cell Biology*, 12(11), pp. 1086-1093.
- Tardat, M., Murr, R., Herceg, Z., Sardet, C. and Julien, E. (2007) 'PR-Set7-dependent lysine methylation ensures genome replication and stability through S phase', *Journal of Cell Biology*, 179(7), pp. 1413-1426.
- Terrell, J., Shih, S., Dunn, R. and Hicke, L. (1998) 'A function for monoubiquitination in the internalization of a G protein-coupled receptor', *Molecular Cell*, 1(2), pp. 193-202.
- Thomas, J.A., Gerber, L., Moreira, D.M., Hamilton, R.J., Bañez, L.L., Castro-Santamaria, R., Andriole, G.L., Isaacs, W.B., Xu, J. and Freedland, S.J. (2012) 'Prostate cancer risk in men with prostate and breast cancer family history: Results from the REDUCE study (R1)', *Journal of Internal Medicine*, 272(1), pp. 85-92.
- Tomlins, S.A., Rhodes, D.R., Perner, S., Dhanasekaran, S.M., Mehra, R., Sun, X.W., Varambally, S., Cao, X., Tchinda, J., Kuefer, R., Lee, C., Montie, J.E., Shah, R.B., Pienta, K.J., Rubin, M.A. and Chinnaiyan, A.M. (2005) 'Recurrent fusion of TMPRSS2 and ETS transcription factor genes in prostate cancer', *Science*, 310(5748), pp. 644-648.
- Tran, C., Ouk, S., Clegg, N.J., Chen, Y., Watson, P.A., Arora, V., Wongvipat, J., Smith-Jones, P.M., Yoo, D., Kwon, A., Wasielewska, T., Welsbie, D., Chen, C.D., Higano, C.S., Beer, T.M., Hung, D.T., Scher, H.I., Jung, M.E. and Sawyers, C.L. (2009) 'Development of a second-generation antiandrogen for treatment of advanced prostate cancer', *Science*, 324(5928), pp. 787-790.
- Trojer, P., Li, G., Sims Iii, R.J., Vaquero, A., Kalakonda, N., Boccuni, P., Lee, D., Erdjument-Bromage, H., Tempst, P., Nimer, S.D., Wang, Y.H. and Reinberg, D. (2007) 'L3MBTL1, a Histone-Methylation-Dependent Chromatin Lock', *Cell*, 129(5), pp. 915-928.
- Tsvetkov, L.M., Yeh, K.H., Lee, S.J., Sun, H. and Zhang, H. (1999) 'p27(Kip1) ubiquitination and degradation is regulated by the SCF(Skp2) complex through phosphorylated Thr187 in p27', *Current Biology*, 9(12), pp. 661-664.
- Tut, T.G., Ghadessy, F.J., Trifiro, M.A., Pinsky, L. and Yong, E.L. (1997) 'Long polyglutamine tracts in the androgen receptor are associated with reduced trans-activation, impaired sperm production, and male infertility', *Journal of Clinical Endocrinology and Metabolism*, 82(11), pp. 3777-3782.
- Tuxhorn, J.A., Ayala, G.E. and Rowley, D.R. (2001) 'Reactive stroma in prostate cancer progression', *Journal of Urology*, 166(6), pp. 2472-2483.

Tuzon, C.T., Spektor, T., Kong, X., Congdon, L.M., Wu, S., Schotta, G., Yokomori, K. and Rice, J.C. (2014) 'Concerted Activities of Distinct H4K20 Methyltransferases at DNA Double-Strand Breaks Regulate 53BP1 Nucleation and NHEJ-Directed Repair', *Cell Reports*, 8(2), pp. 430-438.

Ueda, T., Bruchovsky, N. and Sadar, M.D. (2002) 'Activation of the androgen receptor N-terminal domain by interleukin-6 via MAPK and STAT3 signal transduction pathways', *Journal of Biological Chemistry*, 277(9), pp. 7076-7085.

Vakoc, C.R., Sachdeva, M.M., Wang, H. and Blobel, G.A. (2006) 'Profile of histone lysine methylation across transcribed mammalian chromatin', *Molecular and Cellular Biology*, 26(24), pp. 9185-9195.

van de Wijngaart, D.J., Dubbink, H.J., van Royen, M.E., Trapman, J. and Jenster, G. (2012) 'Androgen receptor coregulators: Recruitment via the coactivator binding groove', *Molecular and Cellular Endocrinology*, 352(1-2), pp. 57-69.

van der Horst, A., de Vries-Smits, A.M.M., Brenkman, A.B., van Triest, M.H., van den Broek, N., Colland, F., Maurice, M.M. and Burgering, B.M.T. (2006) 'FOXO4 transcriptional activity is regulated by monoubiquitination and USP7/HAUSP', *Nature Cell Biology*, 8(10), pp. 1064-1073.

Van Duijn, P.W. and Trapman, J. (2006) 'PI3K/Akt signaling regulates p27kip1 expression via Skp2 in PC3 and DU145 prostate cancer cells, but is not a major factor in p27kip1 regulation in LNCaP and PC346 cells', *Prostate*, 66(7), pp. 749-760.

Vijay-kumar, S., Bugg, C.E. and Cook, W.J. (1987) 'Structure of ubiquitin refined at 1.8 Å resolution', *Journal of Molecular Biology*, 194(3), pp. 531-544.

Villamil, M.A., Liang, Q. and Zhuang, Z. (2013) 'The WD40-Repeat Protein-Containing Deubiquitinase Complex: Catalysis, Regulation, and Potential for Therapeutic Intervention', *Cell Biochemistry and Biophysics*, 67(1), pp. 111-126.

Visakorpi, T., Hyytinen, E., Koivisto, P., Tanner, M., Keinänen, R., Palmberg, C., Palotie, A., Tammela, T., Isola, J. and Kallioniemi, O.P. (1995) 'In vivo amplification of the androgen receptor gene and progression of human prostate cancer', *Nature Genetics*, 9(4), pp. 401-406.

Von Der Lehr, N., Johansson, S., Wu, S., Bahram, F., Castell, A., Cetinkaya, C., Hydbring, P., Weidung, I., Nakayama, K., Nakayama, K.I., Söderberg, O., Kerppola, T.K. and Larsson, L.G. (2003) 'The F-box protein Skp2 participates in c-Myc proteosomal degradation and acts as a cofactor for c-Myc-regulated transcription', *Molecular Cell*, 11(5), pp. 1189-1200.

Wakabayashi, K.I., Okamura, M., Tsutsumi, S., Nishikawa, N.S., Tanaka, T., Sakakibara, I., Kitakami, J.I., Ihara, S., Hashimoto, Y., Hamakubo, T., Kodama, T., Aburatani, H. and Sakai, J. (2009) 'The peroxisome proliferator-activated receptor γ /retinoid X receptor α heterodimer targets the histone modification enzyme PR-Set7/Setd8 gene and regulates adipogenesis through a positive feedback loop', *Molecular and Cellular Biology*, 29(13), pp. 3544-3555.

Wang, C., Guo, Z., Wu, C., Li, Y. and Kang, S. (2012) 'A polymorphism at the miR-502 binding site in the 3' untranslated region of the SET8 gene is associated with the risk of epithelial ovarian cancer', *Cancer Genetics*, 205(7-8), pp. 373-376.

Wang, H., Cao, R., Xia, L., Erdjument-Bromage, H., Borchers, C., Tempst, P. and Zhang, Y. (2001) 'Purification and functional characterization of a histone H3-lysine 4-specific methyltransferase', *Molecular Cell*, 8(6), pp. 1207-1217.

- Wang, H., Sun, D., Ji, P., Mohler, J. and Zhu, L. (2008a) 'An AR-Skp2 pathway for proliferation of androgen-dependent prostate-cancer cells', *Journal of Cell Science*, 121(15), pp. 2578-2587.
- Wang, Q., Li, W., Zhang, Y., Yuan, X., Xu, K., Yu, J., Chen, Z., Beroukhim, R., Wang, H., Lupien, M., Wu, T., Regan, M.M., Meyer, C.A., Carroll, J.S., Manrai, A.K., Jänne, O.A., Balk, S.P., Mehra, R., Han, B., Chinnaiyan, A.M., Rubin, M.A., True, L., Fiorentino, M., Fiore, C., Loda, M., Kantoff, P.W., Liu, X.S. and Brown, M. (2009) 'Androgen Receptor Regulates a Distinct Transcription Program in Androgen-Independent Prostate Cancer', *Cell*, 138(2), pp. 245-256.
- Wang, Q., Liu, X., Cui, Y., Tang, Y., Chen, W., Li, S., Yu, H., Pan, Y. and Wang, C. (2014) 'The E3 Ubiquitin ligase AMFR and INSIG1 bridge the activation of TBK1 kinase by modifying the adaptor STING', *Immunity*, 41(6), pp. 919-933.
- Wang, Z., Dai, X., Zhong, J., Inuzuka, H., Wan, L., Li, X., Wang, L., Ye, X., Sun, L., Gao, D., Zou, L. and Wei, W. (2015) 'SCF β -TRCP promotes cell growth by targeting PR-Set7/Set8 for degradation', *Nature Communications*, 6.
- Wang, Z., Zang, C., Rosenfeld, J.A., Schones, D.E., Barski, A., Cuddapah, S., Cui, K., Roh, T.Y., Peng, W., Zhang, M.Q. and Zhao, K. (2008b) 'Combinatorial patterns of histone acetylations and methylations in the human genome', *Nature Genetics*, 40(7), pp. 897-903.
- Ward, I., Kim, J.E., Minn, K., Chini, C.C., Mer, G. and Chen, J. (2006) 'The tandem BRCT domain of 53BP1 is not required for its repair function', *Journal of Biological Chemistry*, 281(50), pp. 38472-38477.
- Weissman, A.M. (2001) 'Themes and variations on ubiquitylation', *Nature Reviews Molecular Cell Biology*, 2(3), pp. 169-178.
- Wenzel, D.M. and Klevit, R.E. (2012) 'Following Ariadne's thread: A new perspective on RBR ubiquitin ligases', *BMC Biology*, 10.
- Wu-Baer, F., Lagrazon, K., Yuan, W. and Baer, R. (2003) 'The BRCA1/BARD1 heterodimer assembles polyubiquitin chains through an unconventional linkage involving lysine residue K6 of ubiquitin', *Journal of Biological Chemistry*, 278(37), pp. 34743-34746.
- Wu, S. and Rice, J.C. (2011) 'A new regulator of the cell cycle: The PR-Set7 histone methyltransferase', *Cell Cycle*, 10(1), pp. 68-72.
- Wu, S., Wang, W., Kong, X., Congdon, L.M., Yokomori, K., Kirschner, M.W. and Rice, J.C. (2010) 'Dynamic regulation of the PR-Set7 histone methyltransferase is required for normal cell cycle progression', *Genes and Development*, 24(22), pp. 2531-2542.
- Xiao, B., Jing, C., Kelly, G., Walker, P.A., Muskett, F.W., Frenkiel, T.A., Martin, S.R., Sarma, K., Reinberg, D., Gamblin, S.J. and Wilson, J.R. (2005) 'Specificity and mechanism of the histone methyltransferase Pr-Set7', *Genes and Development*, 19(12), pp. 1444-1454.
- Xiao, B., Wilson, J.R. and Gamblin, S.J. (2003) 'SET domains and histone methylation', *Current Opinion in Structural Biology*, 13(6), pp. 699-705.
- Xin, L. (2013) 'Cells of origin for cancer: An updated view from prostate cancer', *Oncogene*, 32(32), pp. 3655-3663.
- Xu, D., Li, C.F., Zhang, X., Gong, Z., Chan, C.H., Lee, S.W., Jin, G., Rezaeian, A.H., Han, F., Wang, J., Yang, W.L., Feng, Z.Z., Chen, W., Wu, C.Y., Wang, Y.J., Chow, L.P., Zhu, X.F.,

- Zeng, Y.X. and Lin, H.K. (2015) 'Skp2-MacroH2A1-CDK8 axis orchestrates G2/M transition and tumorigenesis', *Nature Communications*, 6.
- Xu, P., Duong, D.M., Seyfried, N.T., Cheng, D., Xie, Y., Robert, J., Rush, J., Hochstrasser, M., Finley, D. and Peng, J. (2009) 'Quantitative Proteomics Reveals the Function of Unconventional Ubiquitin Chains in Proteasomal Degradation', *Cell*, 137(1), pp. 133-145.
- Xu, P. and Peng, J. (2006) 'Dissecting the ubiquitin pathway by mass spectrometry', *Biochimica et Biophysica Acta - Proteins and Proteomics*, 1764(12), pp. 1940-1947.
- Yagoda, A. and Petrylak, D. (1993) 'Cytotoxic chemotherapy for advanced hormone-resistant prostate cancer', *Cancer*, 71(3 SUPPL.), pp. 1098-1109.
- Yang, F., Sun, L., Li, Q., Han, X., Lei, L., Zhang, H. and Shang, Y. (2012) 'SET8 promotes epithelial-mesenchymal transition and confers TWIST dual transcriptional activities', *EMBO Journal*, 31(1), pp. 110-123.
- Yang, G., Ayala, G., De Marzo, A., Tian, W., Frolov, A., Wheeler, T.M., Thompson, T.C. and Harper, J.W. (2002) 'Elevated Skp2 protein expression in human prostate cancer: Association with loss of the cyclin-dependent kinase inhibitor p27 and PTEN and with reduced recurrence-free survival', *Clinical Cancer Research*, 8(11), pp. 3419-3426.
- Yang, H., Pesavento, J.J., Starnes, T.W., Cryderman, D.E., Wallrath, L.L., Kelleher, N.L. and Mizzen, C.A. (2008) 'Preferential dimethylation of histone H4 lysine 20 by Suv4-20', *Journal of Biological Chemistry*, 283(18), pp. 12085-12092.
- Yao, L., Li, Y., Du, F., Han, X., Li, X., Niu, Y., Ren, S. and Sun, Y. (2014) 'Histone H4 Lys 20 methyltransferase SET8 promotes androgen receptor-mediated transcription activation in prostate cancer', *Biochemical and Biophysical Research Communications*, 450(1), pp. 692-696.
- Ye, Y. and Rape, M. (2009) 'Building ubiquitin chains: E2 enzymes at work', *Nature Reviews Molecular Cell Biology*, 10(11), pp. 755-764.
- Yin, L., Yu, V.C., Zhu, G. and Chang, D.C. (2008) 'SET8 plays a role in controlling G1/S transition by blocking lysine acetylation in histone through binding to H4 N-terminal tail', *Cell Cycle*, 7(10), pp. 1423-1432.
- Yin, Y., Liu, C., Tsai, S.N., Zhou, B., Ngai, S.M. and Zhu, G. (2005) 'SET8 recognizes the sequence RHRK20VLRDN within the N terminus of histone H4 and mono-methylates lysine 20', *Journal of Biological Chemistry*, 280(34), pp. 30025-30031.
- Yu, N., Huangyang, P., Yang, X., Han, X., Yan, R., Jia, H., Shang, Y. and Sun, L. (2013) 'MicroRNA-7 suppresses the invasive potential of breast cancer cells and sensitizes cells to DNA damages by targeting histone methyltransferase SET8', *Journal of Biological Chemistry*, 288(27), pp. 19633-19642.
- Yuan, W.C., Lee, Y.R., Lin, S.Y., Chang, L.Y., Tan, Y.P., Hung, C.C., Kuo, J.C., Liu, C.H., Lin, M.Y., Xu, M., Chen, Z.J. and Chen, R.H. (2014) 'K33-Linked Polyubiquitination of Coronin 7 by Cul3-KLHL20 Ubiquitin E3 Ligase Regulates Protein Trafficking', *Molecular Cell*, 54(4), pp. 586-600.
- Zhang, H., Kobayashi, R., Galaktionov, K. and Beach, D. (1995) 'p19skp1 and p45skp2 are essential elements of the cyclin A-CDK2 S phase kinase', *Cell*, 82(6), pp. 915-925.

Zheng, L., Dai, H., Qiu, J., Huang, Q. and Shen, B. (2007) 'Disruption of the FEN-1/PCNA interaction results in DNA replication defects, pulmonary hypoplasia, pancytopenia, and newborn lethality in mice', *Molecular and Cellular Biology*, 27(8), pp. 3176-3186.

Zhou, H., Wertz, I., O'Rourke, K., Ultsch, M., Seshagir, S., Eby, M., Xiao, W. and Dixit, V.M. (2004) 'Bcl10 activates the NF- κ B pathway through ubiquitination of NEMO', *Nature*, 427(6970), pp. 167-171.

Zhu, B., Yan, K., Li, L., Lin, M., Zhang, S., He, Q., Zheng, D., Yang, H. and Shao, G. (2015) 'K63-linked ubiquitination of FANCG is required for its association with the Rap80-BRCA1 complex to modulate homologous recombination repair of DNA interstrand crosslinks', *Oncogene*, 34(22), pp. 2867-2878.

Zou, J.X., Guo, L., Revenko, A.S., Tepper, C.G., Gemo, A.T., Kung, H.J. and Chen, H.W. (2009) 'Androgen-induced coactivator ANCCA mediates specific Androgen receptor signaling in prostate cancer', *Cancer Research*, 69(8), pp. 3339-3346.